AVERTISSEMENT

Ce document est le fruit d'un long travail approuvé par le jury de soutenance et mis à disposition de l'ensemble de la communauté universitaire élargie.

Il est soumis à la propriété intellectuelle de l'auteur. Ceci implique une obligation de citation et de référencement lors de l'utilisation de ce document.

D'autre part, toute contrefaçon, plagiat, reproduction illicite encourt une poursuite pénale.

Contact : ddoc-theses-contact@univ-lorraine.fr

LIENS

Code de la Propriété Intellectuelle. articles L 122. 4
Code de la Propriété Intellectuelle. articles L 335.2- L 335.10
http://www.cfcopies.com/V2/leg/leg_droi.php
http://www.culture.gouv.fr/culture/infos-pratiques/droits/protection.htm

UNIVERSITÉ DE LORRAINE

École doctorale IAEM Lorraine

Améliorer la Coordination Motrice dans les Interactions Homme-Robot avec des Contrôleurs Bio-inspirés

Improving Motor Coordination in Human-Robot Interactions using Bio-inspired Controllers

THÈSE

présentée et soutenue publiquement le 17 Juin 2020

pour l'obtention du

Doctorat de l'Université de Lorraine

(mention informatique)

par

Melanie Jouaiti

Composition du jury

Rapporteurs :	Peter Ford Dominey	Directeur de recherche CNRS, INSERM, France
	Mohamed Chetouani	Professeur, UPMC, France
Examinateurs :	Tamim Asfour	Professeur, Karlsruhe Institute of Technology, Germany
	Christine Chevallereau	Directrice de recherche CNRS, LS2N, France
	Dominique Martinez	Directeur de recherche CNRS, Loria, France
	Emmanuelle Tognoli	Professeure, Florida Atlantic University, USA
Directeur de thèse :	François Charpillet	Directeur de recherche, Inria Grand-Est, France

Laboratoire Lorrain de Recherche en Informatique et ses Applications — UMR 7503

Mis en page avec la classe thesul.

Remerciements

I thank the members of the jury for accepting to be part of the defense committee. I thank Mohamed Chetouani and Peter Ford Dominey for their reports and Emmanuelle Tognoli for her thorough reading and extensive comments.

This thesis would not have taken place without one person who believed in me when nobody (not even I) did. So my first thanks naturally go to Prof. Tamim Asfour, who welcomed me with open arms into the world of robotics and showed me that I am worth something. For this, I am eternally grateful.

I thank my family for their support in these difficult years, especially my mom who also proof-read every single paper and this thesis, as well.

I thank François Charpillet for always seeing the best in me, for always offering his help and for fighting with me to make things right. I also thank his wife Gisèle for her understanding in difficult times and for dinner invitations.

I thank Dominique Martinez for insane discussions, for his unwavering support, for giving me my daily dose of laughter, for being my occasional driver and all my acquired knowledge about moths and cable robots.

François, Dominique, I wouldn't have made it through without you.

I thank Rémi Pannequin for his convoluted explanations that taught me that *everything is possible* and the subsequent headaches... You may be surrounded by idiots but remember Scar dies at the hand of those same idiots in the end. We will get you one day!

I thank Adrien Guénard for his "pro-activity", his constant willingness to help and for being my PhD student for a while.

I thank Dominique Mery for being my thesis committee and for his help and support when I needed it.

I thank Eloise Zehnder who willingly agreed to help me and her involvement in my experiment even though it had little to do with her thesis.

I thank Pr. Carmen Schroder, Dr. Agnes Gras and Dr. Jean-Luc Hennecon who agreed to let me perform my experiments at Strasbourg hospital. I thank all the educators and children who welcomed me warmly and made me a part of their routine. I loved spending those ten days with you.

Next to last but certainly not least, a huge thanks to Antoinette Courrier and Helene Cavallini for going above and beyond in helping me with my most challenging/unusual/weird requests. Sending that robot to Strasbourg was quite an adventure/hassle but you made it so much easier.

Last, I always promised I'd dedicate this thesis to Dr. Philippe Chabert. So here's to you. It was my unparalleled pleasure to prove you wrong.

To Papy.
To my Mom who got me there.

Résumé français

Contexte

Le domaine des interactions homme-robot (IHR) est multidisciplinaire, à l'intersection entre la robotique, l'informatique et les sciences cognitives. Ce champ de recherche repose sur la compréhension, la conception et l'évaluation de systèmes robotiques en interaction avec des humains. Les interactions impliquent une forme de communication qui peut être verbale, gestuelle, émotionnelle ou sensorielle. Cette thèse se focalise uniquement sur l'aspect gestuel des interactions, c'est-à-dire sur la coordination motrice. La synchronie est omniprésente dans les systèmes biologiques, de la bactérie à l'humain. Pour les humains, les interactions physiques et sociales induisent de la communication gestuelle qui repose sur des mécanismes et des mouvements rythmiques. [Paxton and Dale, 2017, Gueugnon et al., 2016, Nessler and Gilliland, 2009, Ellamil et al., 2016]. La synchronie se trouve donc à la genèse des interactions interpersonnelles et affecte inconsciemment les personnes au niveau social, mais également au niveau comportemental [Delaherche et al., 2012]. La synchronie est inhérente aux interactions homme-homme et des études ont montré qu'une adaptation est attendue de la part des robots par les humains, au risque d'éprouver une gêne lors de l'interaction. En effet, les études en IHR confirment que les humains ne peuvent résister à la coordination non-intentionnelle avec un robot qui fait des mouvements à une fréquence constante qui n'est pas très éloignée de la leur [Hasnain et al., 2013, Lorenz et al., 2013]. Cependant, la coordination peut échouer si les fréquences sont trop différentes. Les humains apprécient plus l'interaction quand l'interaction est bilatérale. Alors que la robotique est un sujet populaire, embelli par les films, la littérature et les médias, nos attentes ont également tendance à augmenter déraisonnablement. Pour être honnête, nous sommes à peu près aussi loin des robots qui prennent le contrôle du monde que des robots qui se comportent de façon socialement acceptable.

Historiquement, les roboticiens aiment s'inspirer de la nature: de la fourmi du désert à l'hexapode, de l'humain au robot humanoïde... L'humain est, naturellement, également la source d'inspiration de cette thèse. La génération de mouvements en robotique a une forte inspiration biologique et vise à paraître plus humaine. Au cours des années, les contrôleurs bio-inspirés ont été développés, notamment les contrôleurs CPG (Central Pattern Generators) [Ijspeert, 2008, Yu et al., 2014]. Les CPGs [Brown, 1912, Holst, 1935] se trouvent dans la moelle épinière des vertébrés [Grillner and Wallen, 1985] et chez certains invertébrés [Marder et al., 2005, Selverston, 2005], ils sont responsables de la génération de comportements rythmiques, tels que la marche, la mastication, la respiration... Les CPGs sont des structures polyvalentes qui sont organisées en réseaux. Ils peuvent générer, à la fois, des mouvements rythmiques et discrets (non-rythmiques). Cependant, en robotique, alors que les CPGs ont été utilisés de façon prédominante pour la locomotion robotique, ils apparaissent très rarement pour les interactions homme-robot et jamais pour des mouvements discrets. Les CPGs peuvent être dotés de capacités adaptatives afin que le comportement du CPG évolue de façon appropriée. Les contrôleurs adaptatifs permettraient

donc d'améliorer la coordination motrice des robots et donc, en retour, mener à des interactions bilatérales plus naturelles.

Cependant, les interactions resteront compliquées et unilatérales si l'humain a des déficits moteurs. Il est établi qu'un signal auditif rythmique est un outil efficace pour la réhabilitation motrice pour des pathologies telles que Parkinson ou les AVC. En effet, les personnes avec des problèmes neurologiques conservent leur capacité de synchronisation [LaGasse and Hardy, 2013]. Un signal rythmique active les neurones moteurs via les voies reticulospinales, activant le système moteur ce qui mène à une synchronisation motrice rapide avec un signal rythmique externe [Thaut et al., 1999].

Les troubles de la coordination affectent 5 à 6% des enfants entre 5 et 11 ans. Ce pourcentage augmente jusqu'à 79% pour les enfants autistes [Kopp et al., 2010, Peña de Moraes et al., 2017]. Les enfants autistes sont particulièrement connus pour leurs troubles de la communication mais bien que prédominants, les troubles moteurs restent un aspect négligé de l'autisme, surtout en thérapie assistée par robot. De plus, les troubles moteurs sont directement corrélés avec la sévérité de l'autisme [MacDonald et al., 2014, Dziuk et al., 2007], cette problématique devrait donc bénéficier d'un peu plus d'attention. Par ailleurs, en considérant le coût élevé de la thérapie et le manque de thérapeutes, un grand nombre d'enfants autistes ne peuvent pas bénéficier de soins appropriés. La thérapie assistée par robot pourrait donc être une bonne alternative car les enfants autistes réagissent favorablement aux robots [Diehl et al., 2012, Desideri, 2017, Costescu et al., 2014, Breazeal, 2011] et encore plus favorablement dans le cas d'actes moteurs [Pierno et al., 2008]. Puisque les enfants autistes ont des interactions sociales plus limitées, ils ont moins d'opportunités d'imitation qui est une part essentielle du développement de l'enfant. Les robots pourraient aider les enfants à améliorer leurs interactions sociales, l'imitation et la coordination. Le but de la thérapie par robot ne doit, bien entendu, pas être de remplacer l'humain mais de recommander une approche à petite dose où le robot peut être employé comme un outil ou un médiateur pour aider les enfants à développer de meilleurs aptitudes à l'interaction avec d'autres humains [Robins et al., 2005a, Goodrich et al., 2011].

1 Problématique

L'objectif de cette thèse est triple pour améliorer la coordination motrice dans les IHR. Le premier objectif consiste à observer et à comprendre les mécanismes de synchronisation chez l'humain. Deuxièmement, le but est de doter les robots de mécanismes de plasticité, en prenant l'humain comme inspiration, pour parvenir à réaliser de la coordination motrice. Pour rendre ces interactions aussi naturelles et agréables que possible, nous utilisons un contrôleur CPG bio-inspiré, plus particulièrement le modèle de Rowat-Selverston. Finalement, le troisième objectif consiste à utiliser des robots avec des capacités adaptatives pour améliorer la coordination motrice chez des enfants avec des troubles du développement de la coordination, tels que les enfants autistes.

Contributions

Partie I

Dans la première partie de cette thèse, nous rappelons le contexte de la synchronie qui est un aspect indissociable des interactions interpersonnelles. Puisque les humains apprécient plus un partenaire capable de s'adapter à eux, il parait pertinent de doter les robots de mécanismes

adaptatifs pour améliorer leur acceptabilité sociale. Par ailleurs, nous donnons un aperçu des différentes méthodes d'évaluation pour la coordination/synchronisation et la justesse d'imitation. Tout au long de cette thèse, nous utilisons différentes méthodes d'évaluation pour la coordination selon nos besoins.

En robotique, la plupart des méthodes pour l'adaptation ou l'imitation ne prennent pas la bio-inspiration en compte. Ceci est une malencontreuse négligence puisque des études ont montré que les humains acceptent plus facilement un robot qui réalise des mouvement biologiques [Kupferberg et al., 2011].

Un autre aspect intéressant est le fait que les moteurs de robot produisent du son quand ils bougent. Dans le cas des interactions rythmiques avec un robot, les humains reçoivent donc deux informations congruentes (visuelles et auditives) par rapport au même mouvement. Les adultes ont une dominance sensorielle auditive par rapport au visuel mais l'audition peut également sévèrement altérer la perception visuelle si les signaux sont spatialement et temporellement congruents. Étant donné le fonctionnement du traitement sensoriel chez l'humain, nous avons conçu une expérience pour vérifier si l'interférence de stimuli peut être perturbante lors d'une IHR [Jouaiti and Henaff, 2019e]. Cette étude confirme que la modalité auditive est la meilleure pour une interaction rythmique, bien que la modalité visuelle soit également tout à fait adéquate. En revanche, la combinaison des perceptions audiovisuelles d'une mouvement est perturbante pour l'interaction avec un robot. Ce résultat était prévisible puisque les informations auditives et visuelles émanant du robot sont congruentes, à la fois spatialement et temporellement et interfèrent donc entre elles dans le traitement sensoriel de l'humain. Ceci pourrait être un aspect important à considérer, particulièrement en robotique thérapeutique. Malheureusement, nous n'avons pas, à ce jour, trouvé de solutions efficaces pour enlever le son des moteurs de robot.

Ensuite, nous présentons également une étude observationnelle sur la coordination involontaire entre un enfant et un robot. Nous observons que, bien que les enfants soient soumis à la coordination involontaire, ils conservent tout de même leurs caractéristiques individuelles de mouvement, telles que le type de mouvement et l'amplitude. Ceci est la preuve directe de l'effet de maintenance. Ceci nous permet de conclure qu'un robot interagissant avec un humain doit être également capable de s'adapter, tout en conservant ses propres caractéristiques. Nous allons donc tenter de reproduire cela avec un contrôleur bio-inspiré doté de mécanismes de plasticité.

Partie II

Dans la seconde partie de cette thèse, nous nous efforçons de reproduire les mécanismes de synchronisation avec des robots. Le neurone de Rowat-Selverston fut introduit en 1993 par [Rowat and Selverston, 1993]. Cependant ce modèle de neurone demeure, à ce jour, sous-utilisé. Nous intégrons des mécanismes de plasticité hebbienne pour l'adaptation en fréquence [Jouaiti et al., 2018] en nous inspirant de [Righetti et al., 2006]. Nous dotons également le CPG de mécanismes de plasticité synaptique pour l'apprentissage de l'amplitude et des gains synaptiques [Jouaiti et al., 2018]. Ces règles sont ensuite adaptées pour considérer le mode discret du CPG puisque nous avons démontré que le CPG se comporte comme un contrôleur PID dans ce mode de fonctionnement [Jouaiti and Henaff, 2018a]. Puisque les mouvements sont rarement uniquement rythmiques ou discrets, mais usuellement une combinaison ou concaténation des deux, nous présentons un algorithme de classification et intégrons un dernier mécanismes de plasticité afin que le CPG puis passer automatiquement d'un mode à l'autre [Jouaiti and Henaff, 2019c]. Ces mécanismes d'adaptation ont pour but d'augmenter la polyvalence du CPG.

Par ailleurs, nous évaluons le contrôleur bio-inspiré théoriquement et expérimentalement. Tout d'abord, nous comparons le neurone de Rowat-Selverston avec le neurone de Matsuoka et

l'oscillateur de Hopf [Jouaiti and Henaff, 2019a]. Les trois oscillateurs sont évalués en fonction de leur intervalle d'entraînement et capacité de synchronisation lors d'une poignée de main simulée avec un robot Kinova. Des mécanismes de plasticités sont intégrés à chaque modèle et l'impact de ces mécanismes sur la dépense énergétique est estimé. L'intégration des mécanismes de plasticité n'a pas de réel impact sur la synchronisation, cependant, elle permet une réduction significative de la dépense énergétique et a un plus grand intervalle d'entraînement. L'oscillateur de Matsuoka s'est révélé être assez ardu à contrôler avec ses paramètres et a un intervalle d'entraînement très limité. Hopf se synchronise aussi bien (voire même mieux) que Rowat-Selverston et est très simple à contrôler mais il est moins polyvalent et il est moins aisé d'intégrer de nouveaux mécanismes adaptatifs. Régler les paramètres de Rowat-Selverston peut paraître plus complexe, au premier abord, avec un plus grand nombre de paramètres mais l'intégration de nouveaux mécanismes de plasticité est plus évidente. Il a également un large intervalle d'entraînement et une faible dépense énergétique. C'est le seul oscillateur capable de générer également des mouvements discrets.

De plus, nous montrons expérimentalement qu'un robot parvient à réaliser de la coordination motrice avec un partenaire humain grâce au signal visuel d'une main réalisant des mouvements rythmiques [Jouaiti and Henaff, 2018b, Jouaiti and Henaff, 2019b]. Le robot peut adapter sa fréquence, amplitude et type de mouvement selon le mouvement de l'humain. En revanche, le robot ne copie pas le mouvement mais s'adapte en fréquence et amplitude tout en conservant sa propre identité. Ceci est cohérent par rapport à l'effet de maintenance que nous avons pu observer dans la partie I de cette thèse dans notre étude de coordination involontaire.

Ensuite, nous décidons de réaliser des mouvements plus complexes à plusieurs articulations, ce qui nécessite un système de vision de l'état de l'art pour percevoir le mouvement humain. Nous avons donc utilisé OpenPose, que nous avons adapté avec coreML pour qu'il puisse fonctionner avec OSX sur une carte graphique AMD (Radeon pro Vega 20 4GB) [1]. Le programme gère également la détection multi-personnes. Le temps d'inférence est en moyenne 30 ms, ce qui permet un traitement en temps réel. L'estimation de pose 2D est également combiné avec un autre réseau de neurone qui permet de transformer la pose 2D en pose 3D. Cependant, ce réseau de neurone [Martinez et al., 2017] a été entraîné sur des poses relativement similaires et ne généralise pas forcément correctement. Par exemple, les bras tendus en avant ou vers le haut sont systématiquement associés à des poses erronées.

Grâce à ce système, nous comparons le contrôle par CPG avec un contrôle géométrique directe. Alors que les deux méthodes donnent des résultats équivalents pour les mouvements discrets, le CPG est bien meilleur pour des mouvements rythmiques grâce à sa capacité à s'adapter et à "anticiper" le mouvement. Il serait intéressant de comparer le CPG avec d'autres contrôleurs qui prennent en compte la dynamique du robot et qui pourraient être plus efficaces.

Nous validons ce travail dans une étude utilisateur pour évaluer l'influence du type de partenaire (humain, robot, agent virtuel | adaptatif ou non) sur la coordination, l'engagement et la perception de l'utilisateur. Les résultats préliminaires corroborent que le type de partenaire a une influence sur l'engagement et la coordination. De façon prévisible, les sujets sont plus coordonnés et engagés lorsqu'ils interagissent avec un humain adaptatif. En effet, l'adaptation unilatérale dans les IHR est ressentie comme gênante [Lorenz et al., 2013], mais les humains ont des attentes encore plus élevées pour les autres humains. Ceci confirme les résultats de [Lorenz et al., 2013, Hasnain et al., 2013] qui montrent qu'un partenaire humain non-adaptatif est ressenti comme non-naturel. L'engagement n'est pas aussi haut qu'espéré avec le robot non-adaptatif à cause de difficultés techniques qui ont frustré certains sujets. Les autres, en revanche, ont beaucoup apprécié l'interaction et se sont impliqués dans l'interaction avec le robot.

[1] https://github.com/mjouaiti/openPose-coreML

Les résultats du questionnaire ont également révélé que la plupart des sujets ont l'impression que les partenaires s'adaptent à eux dans les modes non-adaptatifs. Ceci illustre parfaitement la coordination involontaire puisque les sujets n'ont même pas conscience qu'ils s'adaptent.

Après avoir validé expérimentalement le contrôleur CPG et sachant que la thérapie par le rythme est une des plus efficaces puisque les personnes avec troubles neurologiques conservent des capacités de synchronisation intactes, nous dirigeons notre travail vers la réhabilitation motrice pour les enfants autistes.

Partie III

Dans la troisième partie de cette thèse, nous réalisons une revue systématique sur la réhabilitation motrice assistée par robot pour les enfants autistes. Nous constatons que la plupart des études thérapeutiques impliquant des robots se concentrent sur l'amélioration des compétences sociales et émotionnelles. Bien que ces compétences soient bien évidemment primordiales, les déficits moteurs ne devraient pas être négligés puisque les troubles du développement de la coordination sont une importante comorbidité de l'autisme et les troubles moteurs sont directement corrélés avec les sévérités de communication. Cependant, à ce jour, il y a très peu de bonne thérapie pour améliorer les troubles moteurs dans l'autisme. En effet, bien qu'il y ait une quantité significative de recherche en réhabilitation motrice pour d'autres pathologies telles que les AVC, Parkinson ou l'infirmité motrice cérébrale, ces études s'étendent rarement à l'autisme. Malgré des arguments indiscutables [Janzen and Thaut, 2018, Tryfon et al., 2017, LaGasse and Hardy, 2013, Jamey et al., 2019], la réhabilitation par le rythme est dramatiquement sous-représentée pour l'autisme. Il a, en effet, été observé que malgré des malformations du cervelet, les individus sont toujours capables d'entraînement moteur et de synchronisation. De plus, s'impliquer dans des courtes activités motrices rythmiques déclenche la plasticité cérébrale et implique des changements structurels et fonctionnels au niveau du cerveau [Luft et al., 2004]. Nous sommes donc convaincus que combiner l'efficacité de la réhabilitation par le rythme et l'implication des enfants autistes avec les robots est une perspective prometteuse.

Nous avons donc réalisé deux études observationelles avec des enfants autistes. La première étude reproduit l'étude de dominance sensorielle de la partie I mais avec des enfants neurotypiques et autistes. En raison de la pandémie de COVID-19, nous ne pouvons présenter que des résultats préliminaires qui montrent que les enfants autistes et neurotypiques se coordonnent mieux avec un signal visuel ou avec une combinaison audiovisuelle qu'avec un signal auditif. Cette prédominance de la vision par rapport à l'audition est cohérente avec des études sur le traitement sensoriel des enfants [Hermelin and O'connor, 1970, Hermelin and O'Connor, 1964, O'Connor, 1971, O'Connor and Hermelin, 1965]. Bien que cela doivent bien évidemment être confirmé avec un plus grand nombre d'enfant, ces résultats diffèrent de ceux des adultes. Alors que les adultes étaient perturbés dans leur coordination par la combinaison des perceptions audiovisuelles, cette combinaison semble, au contraire, renforcer l'interaction des enfants, surtout des enfants autistes, et mener à une meilleure coordination.

La seconde expérience est une étude pilote pour une étude clinique potentielle avec le CHRU de Strasbourg concernant la réhabilitation motrice avec le robot Pepper. Dans cette expérience, la méthode de contrôle par CPG est utilisée avec des enfants autistes. Le but principal est d'étudier la faisabilité en validant le contrôleur dans des conditions réelles mais également d'observer la réponse des enfants par rapport au robot. Ce premier essai, plutôt couronné de succès, mous permet également d'identifier d'autres besoins où le robot pourrait être utile. Par ailleurs, le robot est très populaire avec le personnel médical. Lorsque les enfants interagissent librement avec le robot, le personnel remarque que les enfants avec troubles de l'élocution produisent de

nombreux efforts pour se faire comprendre du robot. D'autre part, les enfants avec un problème d'espace personnel ne sont pas envahissant avec le robot et attendent patiemment leur tour pour parler. Cette étude pilote valide la méthode d'imitation bien qu'il y ait encore des problèmes avec l'estimation de pose pour certaines postures. Les enfants sont très enthousiastes à l'idée que le robot les imitent mais également de l'imiter. Ils sont également prêts à pardonner facilement au robot ses faiblesses "Il n'a pas encore appris ça".

Perspectives

La génération de mouvements ressemblant à l'humain est un aspect pertinent des interactions puisque plusieurs études affirment que les humains font preuve de plus d'acceptabilité pour un mouvement biologique que pour un mouvement artificiel [Perry et al., 2010, Kupferberg et al., 2011, Chaminade et al., 2005]. Puisque notre modèle de CPG est bio-inspiré, il serait très intéressant d'étudier la perception humaine du contrôle par CPG par rapport à un contrôle artificiel et à un mouvement biologique.

Par ailleurs, les interactions gestuelles peuvent avoir lieu avec ou sans contact. Dans le cas des interactions avec contact, un verrouillage mécanique a lieu et le robot est forcé physiquement de s'adapter à l'humain, contrairement aux interactions sans contact ou l'adaptation dépend uniquement du contrôleur. Dans cette thèse, nous avons presque exclusivement travaillé sur l'interaction sans contact.

De plus, l'étude pilote de Strasbourg a reçu de très bons retours de la part des enfants et du personnel médical. Cette étude pilote devrait donc être transformée en en étude au long terme pour évaluer exactement l'impact du robot sur les capacités motrices. [Yoo and Kim, 2018] a présenté une étude de réhabilitation par le rythme pour enfants autistes qui consistait en une tâche de battement de tambour entre un enfant et un expérimentateur. L'expérience était divisée en trois parties: premièrement, l'expérimentateur s'adaptait à l'enfant; deuxièmement, l'enfant devait s'adapter à l'expérimentateur; troisièmement, l'enfant s'adaptait à l'expérimentateur et la coordination était perturbée aléatoirement. Perturber la coordination mène à une meilleur conscience de soi [Mundy and Jarrold, 2010]. Ce protocole a permis d'améliorer la coordination et l'imitation pour les enfants autistes. Il serait très intéressant de répliquer cette expérience avec un robot et de comparer les résultats d'une traditionnelle thérapie par le rythme et ceux d'une thérapie par le rythme assistée par robot. Nous espérons sincèrement, qu'au long terme, ce travail se révélera utile pour la réhabilitation motrice d'enfants affectés par des troubles de la coordination.

D'autre part, comme nous avons pu le constater lors de notre étude pilote, le robot pourrait également être utilise pour améliorer d'autres compétences telles que l'élocution ou attendre son tour. Cette immersion à l'hôpital nous a permis de mieux comprendre les différents besoins et attentes de ces enfants. Cette étude a permis d'ouvrir de nouvelles perspectives pour aider ces enfants de façon concrète.

Contents

Résumé français **v**

1 Problématique vi

Glossary

Introduction **xxv**

1 Context xxv

2 Problematic xxvi

3 Contribution xxvi

4 Organisation xxvii

Part I Synchrony: From Interpersonal Interactions to Human-Robot Interactions **1**

Chapter 1 Synchrony in Interpersonal Interactions **3**

1.1 Synchrony, Coordination, Synchronisation... 3

1.1.1 Interpersonal Interactions 3

1.1.2 Imitation 4

1.1.3 Coordination Dynamics 5

1.1.4 Theoretical Model of Motor Coordination 6

1.2 Evaluation of the Interaction 7

1.2.1 Coordination 7

1.2.2 Similarity Measures 12

Chapter 2 Motor Coordination in Human Robot Interactions (HRI) 17
2.1 Synchronisation in HRI . . . 17
2.1.1 Adaptive Robots . . . 17
2.1.2 Of the Relevance of Synchronisation in HRI . . . 18
2.2 Motor Imitation . . . 19
2.2.1 Action Observation . . . 19
2.2.2 Action Representation . . . 20
2.2.3 Imitation in HRI . . . 21

Chapter 3 Observing Coordination in Human-Robot Interactions 23
3.1 The Sound of Actuators: Disturbance of Motor Coordination? . . . 23
3.1.1 Human Sensory Perception . . . 23
3.1.2 Experimental Protocol . . . 25
3.1.3 Results . . . 25
3.2 Involuntary Coordination in Children . . . 27
3.2.1 Experimental Protocol . . . 27
3.2.2 Results . . . 27

Part II The Bio-Inspired Controller 31

Chapter 4 Bio-inspired Control 33
4.1 The Anatomy of Human Movement . . . 33
4.1.1 Voluntary Movements . . . 33
4.1.2 Automatic Movements . . . 34
4.2 CPG Controllers . . . 36

Chapter 5 Extending the Rowat-Selverston CPG 39
5.1 The Rowat-Selverston CPG . . . 39
5.1.1 The Rowat-Selverston Oscillator . . . 39
5.1.2 The CPG Architecture . . . 40
5.2 Integrating the CPG with Adaptive Mechanisms . . . 43
5.2.1 Frequency Learning . . . 43

5.2.2 Neuronal Plasticity for Amplitude Learning . . . 44
5.2.3 Synaptic Plasticity for ϵ . . . 44
5.3 Discrete Operating Mode . . . 45
5.3.1 CPG Behaves like a PID Controller . . . 46
5.3.2 Redefining Plasticity . . . 47
5.4 Movement Classification . . . 48

Chapter 6 Evaluation of the CPG-Controller **51**
6.1 Comparative Study of Several Oscillators . . . 51
6.1.1 Oscillating Neuron Models . . . 51
6.1.2 An Overview of Parameter Tuning . . . 52
6.1.3 The Kasuga Control Architecture . . . 53
6.1.4 Entrainment Range . . . 53
6.1.5 Simulated Handshaking . . . 54
6.1.6 Results Without any Plasticity Mechanisms . . . 56
6.1.7 Results with Plasticity Mechanisms . . . 58
6.1.8 Power Consumption . . . 59
6.2 Motor Coordination with the CPG Controller . . . 61
6.2.1 Experimental Protocol . . . 61
6.2.2 CPG Architecture . . . 62
6.2.3 Experimental Results . . . 63
6.3 Comparison Between the CPG-Controller and Geometric Direct Control . . . 65
6.3.1 Direct Geometric Angular Control . . . 65
6.3.2 CPG Architecture . . . 66
6.3.3 Results . . . 67

Chapter 7 User Study: Influence of Adaptive Mechanisms on Engagement and Coordination **71**
7.1 Methods . . . 72
7.1.1 Study Overview . . . 72
7.1.2 Experiment Design . . . 72
7.1.3 Technical Setup . . . 73
7.1.4 Participants . . . 74
7.1.5 Materials . . . 74
7.2 Results . . . 78
7.2.1 NARS Results . . . 78
7.2.2 Do Different Types of Partners influence Coordination? . . . 78

7.2.3 Do Different Types of Partners influence Engagement? 79
7.2.4 Does Engagement correlate with Coordination? 80
7.2.5 Do Adaptive Abilities Improve Engagement or Coordination? 80

Part III Towards Robot-Assisted Motor Therapy for Autism 83

Chapter 8 Motor Coordination in Autism Spectrum Disorders (ASD) 85
8.1 Autism spectrum disorder 85
8.1.1 Social Interaction 86
8.1.2 Social Communication 86
8.1.3 Imagination 86
8.2 Motor Deficits in ASD 86
8.3 Robot-Assisted Therapy for Motor Rehabilitation in ASD 89
8.3.1 Coordination 89
8.3.2 Imitation 90
8.3.3 Fine Motor Skills 90
8.3.4 Sensorimotor Skills 91

Chapter 9 ASD Child-Robot Interactions: Pilot Studies 93
9.1 Sensory Dominance in ASD 93
9.1.1 Experimental Protocol 94
9.1.2 Results 95
9.2 Imitation with CPG Controllers in ASD 97
9.2.1 Experimental Protocol 97
9.2.2 Robot Imitation 98
9.2.3 Child Imitation 100
9.3 Conclusion 100

Discussion 103
3.1 Other Papers 108
3.2 Poster Presentations 108
3.3 Other Presentations 108

Appendices

Appendix A Mathematical Details for the Rowat-Selverston Neuron **109**
A.1 Van der Pol Form of Rowat-Selverston Neuron . . . 109
A.2 Recall of Righetti's Model for Dynamic Hebbian Learning into Van der Pol Oscillators . . . 111
A.3 Applying Dynamic Hebbian Learning to the Rowat-Selverston Neuron . . . 111

Appendix B Details on Comparing the Oscillator Models **113**
B.1 Coupling the Oscillatory Neurons . . . 113
B.1.1 Matsuoka Model . . . 113
B.1.2 Hopf Model . . . 114
B.1.3 Rowat-Selverston Model . . . 114
B.2 The Kasuga Control Architecture . . . 114
B.2.1 Matsuoka Model . . . 114
B.2.2 Hopf Model . . . 115
B.2.3 Rowat-Selverston Model . . . 116

Appendix C The Vision Processing System **117**
C.1 2D Pose Estimation Inference . . . 117
C.2 3D Pose Estimation Inference . . . 117
C.3 Angular Values Computation . . . 118

Appendix D Questionnaires **119**
D.1 NARS Questionnaire . . . 119
D.2 Technology Anxiety . . . 120
D.3 Acceptance of Assistive Social Agent . . . 120
D.4 Attrakdiff . . . 122
D.5 Technological familiarity . . . 122

Bibliography **125**

List of Figures

1 Thesis contributions xxviii

1.1 Illustration of HKB showing the potential field $V = -a\cos\Phi - b\cos 2\Phi$, i.e. the attractors of the system for varying values of b/a. The ratio b/a represents the effect of the oscillation frequency on the potential landscape. As the frequency increases (b/a decreases), the anti-phase mode becomes less stable. Below a given value for b/a, the potential becomes monostable. (Reproduced from [Monno et al., 2002]) 6

1.2 Artificial signals used to evaluate the coordination. They consist of $10s$ of sinusoidal signals in phase, $10s$ of sinusoidal signals in anti-phase, followed by $10s$ of sinusoidal signals with a phase difference of $\pi/2$ and $10s$ of sinusoidal signals with a factor of two between their frequencies, then steps occurring at the same time and finally delayed steps 7

1.3 Three correlation measures applied to the artificial signals. Left: Peak picking P_{xy} ($w = 100$); Middle: 1D cross-correlation S_{xy} ($w = 100$); Right: 2D lagged cross-correlation C_{xy} ($w = 100$) (The correlation strength is represented with different shades) 8

1.4 Cross-recurrence analysis applied to the theoretical signals in figure 1.2 ($\epsilon = 0.1$, $thresh = 10$) 9

1.5 Wavelet transform of each signal and their cross-wavelet transform 10

1.6 Phase Locking Value between the two theoretical signals 11

1.7 Synchrosqueezing of each theoretical signal and their cross-synchrosqueezing . . . 12

1.8 DTW on a series of examples. 1. DTW on similar step signals (DTW score = 0). 2. DTW on step signals with different amplitude (DTW score = 100). 3. DTW on step signals with different width (DWT score = 0). 4. DTW on step signals with different offsets (DWT score = 0) 14

3.1 Experimental setup. The robot is placed in front of the human and waves. The human waves back with his/her arm supported by a pillow. 26

3.2 Example of interaction with switch between anti-phase and phase 28

3.3 Example of interaction with short adaptation period 28

3.4 Example of interaction that would be best described as imitation, rather than intentional coordination 28

3.5 Superposed Synchrosqueezing for the 19 interactions. Top: Synchrosqueezing of the robot movement. Middle: Synchrosqueezing of the children's movements. Bottom: cross-synchrosqueezing between the robot and the children's movements. 30

4.1 Motor cortex. *Reproduced from [Botrel, 2018]* 33

4.2 Overview of the motor generation process in the human brain for voluntary movements 35

5.1 Current voltage I-V curves for the cellular membrane with various values of σ_f and A_f 40
5.2 Left: Intrinsic frequency of the oscillator depending on the values of σ_s, τ_m ($\tau_s = 10\tau_m$). $\sigma_f = 2.0$. Right: Evolution of the limit cycle in the phase plane. The limit cycle begins as relatively circular and, with varying σ_f, becomes increasingly sharp 41
5.3 Intrinsic modes of the Rowat-Selverston neuron. In blue: the oscillator output. In orange: the input signal when applicable, otherwise there is no input signal. A: Discrete adaptation ($\sigma_s = 2$, $\sigma_f = 0$, $\tau_m = 0.5$, $\tau_s = 5$). B: Damped oscillations ($\sigma_s = 2$, $\sigma_f = 1$, $\tau_m = 0.5$, $\tau_s = 5$). C: Endogenous bursting ($\sigma_s = 2$, $\sigma_f = 2$, $\tau_m = 0.5$, $\tau_s = 5$). D: Endogenous bursting ($\sigma_s = 2$, $\sigma_f = 4$, $\tau_m = 0.5$, $\tau_s = 5$). E: Post-inhibitory rebound ($\sigma_s = 2$, $\sigma_f = 4$, $\tau_m = 10$, $\tau_s = 6$). F: Plateau potential ($\sigma_s = 0$, $\sigma_f = 2$, $\tau_m = 1$, $\tau_s = 0.2$) 42
5.4 Generalised CPG architecture. When controlling a musculoskeletal model, the extensor and flexor muscles can be controlled independently with the CPG extensor and flexor outputs. This is, however, not the case for robots, so it has become common practice to subtract the outputs to obtain a single value 43
5.5 Evolution of σ_s according to various values of A_f (Left) and ϵ (Right) 44
5.6 Top: Rowat-Selverston CPG as originally defined when subjected to a $1Hz$ signal. Bottom: CPG endowed with the three plasticity mechanisms previously defined and the evolution of σ_s, ϵ and A_f 45
5.7 Evolution of the position (left) of a joint controlled by our CPG in discrete mode and the CPG output (right) for various values of ϵ. In red, $\epsilon = 5$; in blue, $\epsilon = 19$; in green, $\epsilon = 1$; in purple, $\epsilon = 0.5$. 47
5.8 In blue: input signal of the CPG; in orange: CPG output. Left: CPG without any learning rule. Right: CPG with the new learning rule 48
5.9 Example of classification result. In orange, the movement data, in blue, the classification result (1 for rhythmic and 0 for discrete) 49
5.10 Example of classification result. In blue, the CPG input, in magenta, the classification result (1 for rhythmic and 0 for discrete), in green the CPG output 50

6.1 Oscillatory cells integrated to the generalised Kasuga architecture. C_i, L_i, K_i, O_i are gains and $C_{i\{E,F\}}$ is the neuron cell for the joint i controlling the extensor or flexor and torque_i is the input. Note that one cell receives torque - |torque| as an input and the other -torque - |torque|; for a sinusoidal signal, this means that one cell is receiving the positive components of the signal and the other the negative ones. 54
6.2 Simulated robotic arm with the static ball inside its gripper. We control the ball kinematics. We consider a rigid mechanical link because we want to impose a force on the robot which cannot be influenced. We set the ball position repeatedly according to a sinusoidal signal. The time step is small enough so that the motion appears smooth 55
6.3 Response of the Matsuoka oscillator. In gray: CPG input, in black: CPG output for both joints 56
6.4 Response of the Hopf oscillator. In gray: CPG input, in black: CPG output for both joints 57

6.5 Response of the Rowat-Selverston oscillator. In gray: CPG input, in black: CPG output for both joints . . . 57
6.6 PLV for joint 2 (left), joint 3 (right). The vertical grey lines delimit each frequency range. The horizontal line indicates the reference for perfect coordination at 1.0 (See details in text) . . . 58
6.7 Response of the Matsuoka oscillator with time constant adaptation. In gray: CPG input, in black: CPG output for both joints . . . 59
6.8 Response of the Hopf oscillator with Frequency Learning. In gray: CPG input, in black: CPG output for both joints . . . 59
6.9 Response of the Rowat-Selverston oscillator with Frequency Learning. In gray: CPG input, in black: CPG output for both joints . . . 60
6.10 Response of the Rowat-Selverston oscillator with all the plasticity mechanisms. In gray: CPG input, in black: CPG output for both joints . . . 60
6.11 PLV for joint 2 (left), joint 3 (right). The vertical grey lines delimit each frequency range. The horizontal line indicates the reference for perfect coordination at 1.0 61
6.12 Left: arm joints for the Pepper robot (reproduced from Aldebaran). Right: CPG architecture. The shoulder pitch joint receives the vertical visual signal F_V as an input and its output is the input of the CPG controlling the elbow yaw joint; the shoulder roll joint receives the horizontal visual signal F_H as an input . . . 62
6.13 Top Left: phase portrait of the articular position, in green for the first part (before 15 s) and in blue for the second part. Top Right: in red, input of the Shoulder Roll (SR) CPG; in blue, output of the Shoulder Roll (SR) CPG. Bottom Left: σ_S for the Shoulder Roll joint (red), the Shoulder Pitch joint (blue), the Elbow Yaw joint (green). Bottom Right: in red, input of the Shoulder Pitch (SP) CPG; in blue, output of the Shoulder Pitch (SP) CPG . . . 64
6.14 Top Left: phase portrait of the articular position, in green for the first part (before 15 s) and in blue for the second part. Top Right: in red, input of the Shoulder Roll (SR) CPG; in blue, output of the Shoulder Roll (SR) CPG. Bottom Left: σ_S for the Shoulder Roll joint (red), the Shoulder Pitch joint (blue), the Elbow Yaw joint (green). Bottom Right: in red, input of the Shoulder Pitch (SP) CPG; in blue, output of the Shoulder Pitch (SP) CPG . . . 64
6.15 Top Left: phase portrait of the articular position, in green for the first part (before 15 s) and in blue for the second part. Top Right: in red, input of the Shoulder Roll (SR) CPG; in blue, output of the Shoulder Roll (SR) CPG. Bottom Left: σ_S for the Shoulder Roll joint (red), the Shoulder Pitch joint (blue), the Elbow Yaw joint (green). Bottom Right: in red, input of the Shoulder Pitch (SP) CPG; in blue, output of the Shoulder Pitch (SP) CPG . . . 65
6.16 Top Left: phase portrait of the articular position. Top Right: in red, input of the Shoulder Roll (SR) CPG; in blue, output of the Shoulder Roll (SR) CPG. Bottom Left: PLV for the Shoulder Roll joint (red), the Shoulder Pitch joint (blue), the Elbow Yaw joint (green). Bottom Right: in red, input of the Shoulder Pitch (SP) CPG; in blue, output of the Shoulder Pitch (SP) CPG . . . 66
6.17 General CPG Architecture used for the robot control. Each CPG receives an angular velocity as an input signal. The output of the CPG is also considered as a velocity. The arrows indicate the coupling between the CPGs . . . 66

6.18 Example of discrete movement: "Hip to the Left". Top: geometric method. Bottom: CPG method. Left: Angular position of the human and robot; Middle: angular speed of the human and robot. Right: error metrics for the geometric and CPG methods 68
6.19 Another example of discrete movement:"raise both arms laterally". Top: geometric method. Bottom: CPG method. Left: Angular position of the human and robot; Middle: angular speed of the human and robot. Right: error metrics for the geometric and CPG methods 68
6.20 Example of rhythmic movement. Top: geometric method, Bottom: CPG method. Left: angular position. Middle: angular velocity. Right: PLV 69

7.1 Overview of the timeline of an experiment. An example of condition order is also depicted 73
7.2 Setup for part 1 of the experiment. OpenVIBE manages the EEG acquisition and Captiv the motion sensors acquisition. OpenVIBE controls the videos of the human and VP and the waving of the robot through a Python script. It also sends 3.3 V triggers to the motion sensors receiver thanks to an Arduino Nano 74
7.3 Setup for part 2 of the experiment. The setup of part 1 is combined with a second computer which also processes the visual input with a pose estimation algorithm and feeds the hand position into the CPG controller to get the position orders. Robot commands are then transmitted to the first computer which controls the robot 75
7.4 Top: Experimental setup, the subject is seated in front of the partner (robot, VP or human). Bottom: The three interaction partners: VP, robot, human 76
7.5 Left: Location of the motion sensors (one in the back for reference, two on the right arm). Right: placement of the EEG electrodes on the participants' scalp. The electrodes crossed in red were not used. 77
7.6 Results of the post-processing questionnaire for the first part of the experiment. The answers ranged from 1 to 5 79
7.7 Engagement topography (obtained with the topoplot function) for non-adaptive conditions: human, VP, robot. A topography represents the human scalp and the positions of the EEG electrodes. The EEG data allow us to derive an engagement value for each electrode, hence the topography. The EEGLAB toolbox interpolates the values between the electrodes. 80
7.8 Results of the post-processing questionnaire for the first and second part of the experiment for the human partner 81
7.9 Results of the post-processing questionnaire for the first and second part of the experiment for the robot partner 81
7.10 Engagement topography for the non-adaptive human, adaptive human, non-adaptive robot and adaptive robot conditions 82

9.1 Illustration of the gaze extraction process: Face detection → landmarks detection → eye extraction 95
9.2 Coordination performance results. Left: boxplot representation of the coordination performance according to condition (AV, V, A) and child diagnosis (ASD, TD). Right: Interaction effect between the conditions 96
9.3 Coordination performance for each age group (See details in text) 97
9.4 Example of interaction where the robot imitates the child. In blue, the child's position OpenPose detected; In orange, the robot position. The signals are normalised 99

9.5 Series of movements performed by the robot (tilt hip to the right, tilt hip to the left, extend right arm, extend left arm, extend both arms, raise left arm, raise right arm) . . . 100
9.6 Example of interaction where the child imitates the robot. In blue, the child's position obtained with T-Sens sensors; In orange, the robot position. The signals are normalised . . . 101

A.1 Intrinsic frequency of the oscillator depending on σ_s for several values of τ_m, τ_s and the previously obtained expression $f = \frac{\omega}{2\pi} = \frac{1}{2\pi}\sqrt{\frac{1+\sigma_s-\sigma_f}{\tau_s\tau_m}}$ . . . 110
A.2 Evolution of σ_s with different initial values. . . . 112

B.1 Coupled oscillatory cells. $C_{\{E,F\}}$ indicates whether the neuron cell controls the extensor or the flexor . . . 113
B.2 Oscillatory cells integrated to the generalised Kasuga architecture. C_i, L_i, K_i, O_i are gains and $C_{i\{E,F\}}$ is the neuron cell for the joint i controlling the extensor or flexor and torque_i is the input signal . . . 115

C.1 Superposition of OpenPose inference for each body part. Left: confidence map of the body part locations. Middle: 2D vector field of part affinities heatmap. Right: Peaks of the body part heatmap . . . 117
C.2 2D pose estimation . . . 118
C.3 3D pose estimation . . . 118

Glossary

ABA Applied Behavioral Analysis. 85, 92

Afferent conducting or conducted inwards or towards something (for nerves, the central nervous system; for blood vessels, the organ supplied). In this thesis, afferent signal = input signal. The opposite of efferent. 36

ASD Autism Spectrum Disorders. 85, 87–89, 91, 93, 100

BOT2 Bruininks-Oseretsky Test of Motor Proficiency. 89

CPG Central Pattern Generator. xxv, 36, 37, 39, 41, 43, 44, 47, 48, 51, 61

DCD Developmental Coordination Disorder. 85, 87, 91

DMP Dynamics Movement Primitives. 20

DSM-V Fifth Edition of the Diagnosis and Statistical Manual of Mental Disorders, 2013. 85

DTW Dynamic Time Warping. 13, 98

EEG Electroencephalography. 5

Efferent conducted or conducting outwards or away from something (for nerves, the central nervous system; for blood vessels, the organ supplied). In this thesis, efferent signal = output signal. The opposite of afferent. 42, 44

FFT Fast Fourier Transform. 48

fMRI functional Magnetic Resonance Imaging. 5, 46, 88

HKB Haken Kelso Bunz model of bimanual coordination. 6

HRI Human-Robot Interaction. 14, 17, 18, 71, 82, 89, 105

IMU Inertial Motion Unit. 75

MN Motor Neuron. 42

MNS Motor Neuron System. 88

MRI Magnetic Resonance Imaging. 87

NARS Negative Attitude Towards Robots Scale. 72, 77, 78

PF Pattern Formation layer. 42

PLV Phase Locking Value. 10, 13, 25, 53, 58, 69, 78

praxis the ability to have an idea of what to do, plan and sequence the action, and execute the action. 87

SN Sensory Neuron. 42

TD Typical Development. 85, 89, 100

TEACCH Treatment and education of autistic and related communication handicapped children. 85, 92

VP Virtual Parner. 73

Introduction

1 Context

Human-Robot Interaction (HRI) is a multidisciplinary field of study at the intersection between robotics, computer science and social sciences. It is based on understanding, designing and evaluating robotic systems interacting with humans. Interaction implies communication per se, which may be verbal, gestural, emotional or sensory. This thesis will focus solely on the gestural aspect of the interaction, i.e. motor coordination. Synchrony is pervasive in biological systems, from bacteria to humans. For humans, physical and social interactions induce gestural communication based on rhythmic mechanisms and rhythmic movements [Paxton and Dale, 2017, Gueugnon et al., 2016, Nessler and Gilliland, 2009, Ellamil et al., 2016]. Synchrony thus finds itself at the genesis of interpersonal interactions and unconsciously affects people on the social level, as well as on the behavioural level [Delaherche et al., 2012]. Synchrony is inherent to human-human interactions and some studies find that adaptation is also expected from robots by humans, at the risk of experiencing a very awkward interaction. Indeed, HRI studies confirm that humans can hardly resist unintentional coordination with a robot moving at a constant frequency that is not too far from their own [Hasnain et al., 2013, Lorenz et al., 2013]. However, coordination may fail if the frequencies are too different. Humans enjoy the interaction more when the adaptation is bilateral. While robotics is a popular subject embellished by movies, literature and media outlet, expectations also tend to unreasonably rise. Truth be told, we are about as far from robots taking over the world as we are from robots behaving in a socially acceptable way.

Robotics historically likes to take inspiration from nature: from the desert ant to the hexapod, from the human to the humanoid robot... The human will naturally be the source of inspiration of this thesis as well. Motion generation in robotics has a strong biological inspiration and aims at being more human-like. Over the years, bio-inspired controllers have been developed, notably CPG (Central Pattern Generators) controllers [Ijspeert, 2008, Yu et al., 2014]. CPGs [Brown, 1912, Holst, 1935] are found in the spine of vertebrates [Grillner and Wallen, 1985] and in some invertebrates [Marder et al., 2005, Selverston, 2005], they are responsible for the generation of rhythmic patterns such as walking, chewing, breathing... CPGs are very versatile structures that are organised into networks. They can generate both rhythmic and discrete (non-rhythmic) movements. However, in robotics, while CPG controllers have predominantly been used for robot locomotion, they appear very scarcely for human-robot interaction and never for discrete movements. CPGs can be endowed with adaptive abilities so that the CPG behaviour evolves to act appropriately. Adaptive controllers should thus improve motor coordination in robots, which should, in turn, lead to more natural and bilateral interactions.

However, interactions will remain complicated and unilateral if the human has motor deficits. It has been established that auditory rhythmic cueing is an effective tool for gross motor rehabilitation in populations including stroke and Parkinson's disease. Indeed, persons with neurological disorders still retain intact synchronisation ability [LaGasse and Hardy, 2013].

Rhythmic cueing activates motor neurons via reticulospinal pathways, effectively priming the motor system and leads to rapid motor synchronisation to an external rhythmic cue [Thaut et al., 1999].

Coordination disorders affect 5 to 6% of children between 5 and 11 years old. This raises up to 79% for autistic children [Kopp et al., 2010, Peña de Moraes et al., 2017]. Autistic children are especially known for their communication deficits but although predominant, motor deficits remain a neglected aspect of autism, especially in robot-assisted therapy. Moreover, motor deficits are directly correlated with severity of autism [MacDonald et al., 2014, Dziuk et al., 2007] so this problematic could benefit from more attention. Besides, considering the high cost of therapy and the therapist shortage, a lot of autistic children cannot afford appropriate care. Robot-assisted therapy could help bridge the gap as autistic children respond favorably to robots [Diehl et al., 2012, Desideri, 2017, Costescu et al., 2014, Breazeal, 2011] and even better than to humans in the case of motor actions [Pierno et al., 2008]. Since autistic children have more limited social interactions, they have less opportunity for imitation which is a fundamental part of child development. Robots could help children improve social interactions, imitation and coordination. The goal of robot-assisted therapy, obviously, should not be to replace humans but to advocate a low-dose robotic approach where the robot can be used as a tool or as a mediator to help children develop better interaction skills with other humans [Robins et al., 2005a, Goodrich et al., 2011].

2 Problematic

The objective of this thesis is threefold in improving motor coordination in HRI. The first objective consists in observing and endeavouring to understand human synchronisation mechanisms. Second, the goal will be to endow robots with adaptive mechanisms, taking humans as an inspiration, to achieve motor coordination. To make these interactions as natural and enjoyable as possible, we shall use bio-inspired CPG controllers, more specifically the Rowat-Selverston model. Ultimately, the third objective resides in using robots with adaptive abilities to improve motor coordination in children with developmental coordination disorders, such as autistic children.

3 Contribution

The contribution of this thesis finds itself at the intersection between computer science, robotics and cognitive science (See Fig. 1).

In the first part, we evaluated and compared coordination and synchronisation measures. We also performed two observational studies to better understand human synchronisation in rhythmic interactions. The first one concerned involuntary synchronisation in children with the Pepper robot. We could notably observe that children synchronised with the robot while maintaining individual characteristics. The second one revealed that the sound the robot motors produce may disturb rhythmic interactions for humans due to their sensory dominance [Jouaiti and Henaff, 2019e].

In the second part, we endeavour to reproduce synchronisation mechanisms in robots. The Rowat-Selverston neuron was introduced in 1993 by [Rowat and Selverston, 1993]. However, this neuron model remains underused to this day. In this thesis, we extended this model with Hebbian and synaptic plasticity mechanisms to allow for more adaptation to an external stimulus [Jouaiti et al., 2018]. We also demonstrated that, in its discrete mode, the neuron behaves like a PID (Proportional Integral Derivative) controller [Jouaiti and Henaff, 2018a]. Additional

adaptive mechanisms were then integrated to take the discrete mode into account and to switch automatically from one mode to the other [Jouaiti and Henaff, 2019c].

We also performed a comparative study between the Rowat-Selverston, Matsuoka [Matsuoka, 1985] and Hopf [Hopf, 1942] oscillating neurons which highlighted the limits and advantages of each model [Jouaiti and Henaff, 2019a]. We illustrated the CPG coordination abilities in rhythmic interactions [Jouaiti and Henaff, 2018a, Jouaiti and Henaff, 2019b]. We compared our CPG control and direct geometric control in an imitation task. To this end, we required a vision-processing system so that the robot could perceive human movement and adapt to it in real time. We, therefore, used OpenPose which we adapted so that it could run on OSX with an AMD graphics card [2].

Finally, the controller was employed in a user study where participants interacted with different types of partners (robot, virtual agent, human) that could or could not adapt to them. We observed their influence on coordination performance, engagement and user perception.

In the third part, we wrote a systematic review on robot-assisted motor rehabilitation for autistic children [Jouaiti and Henaff, 2019d]. We realised two experiments with autistic children. The first study replicates the sensory dominance experiment from Part I but with neurotypical and autistic children. We show that, contrary to adults, the sound of robot motors reinforces the interaction for both types of children. The second experiment took place at the Strasbourg hospital and was a pilot study for motor rehabilitation based on child-robot motor imitation.

Independently from this thesis, we also worked on two other projects. First, on a cable robot project for insect tracking where we worked on the modelling and animation of an *Agrotis Ipsilon* moth for flight kinematics analysis. This lead to a publication that is currently under revisions in the Science Robotics journal. Second, we worked on the design of an hexapode prototype inspired by the RHex robot [3]. These contributions are not included in this thesis.

4 Organisation

This thesis is organised into three parts. The first and second parts contain three and four chapters respectively and the last part includes two chapters. The first chapter of each part will set up the context of the work and provide the bibliography. The other chapters will detail our contributions.

In the first part of this thesis, we will introduce synchrony in interpersonal interactions but in human-robot interactions, as well. Besides, we will give an overview of synchronisation and imitation accuracy measures. We will also observe and endeavour to understand human behaviour in two rhythmic human-robot interactions. The first one will focus on involuntary synchronisation and the second one on sensory dominance in rhythmic interactions.

The second part will present a bio-inspired controller for human-robot synchronisation in rhythmic interactions. The model we will employ is the Rowat-Selverston neuron. We will endow it with some new plasticity mechanisms, develop its non-rhythmic functioning mode and extend the model so that it can adapt to any rhythmic or non-rhythmic movement. We also analyse the results of a comparison study with other oscillating neurons and controllers to highlight the capabilities of this model. Moreover, we will validate the controller experimentally in a human-robot interaction study. This chapter will evaluate several aspects, such as coordination performance, engagement and user perception with different interaction partners that can or cannot adapt.

[2] https://github.com/mjouaiti/openPose-coreML
[3] https://github.com/mjouaiti/Hexplore

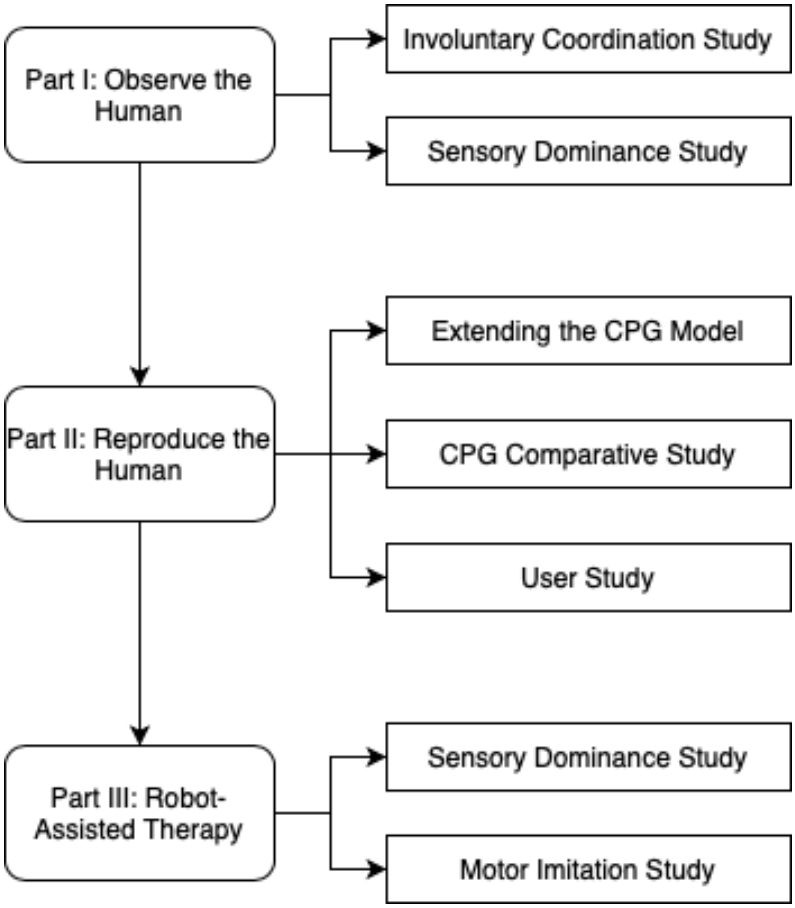


Figure 1: Thesis contributions

Finally, the third part will focus on the applications and perspectives of this thesis in robot-assisted therapy for children with motor deficits, notably with autistic children. First, we will review motor deficits in autism and the rehabilitation options with robot-based therapy. Then, we will present two experiments with autistic children. The first one studies the influence on sensory dominance in rhythmic interactions. The second one took place at the Strasbourg hospital and focuses on child-robot motor imitation.

Part I

Synchrony: From Interpersonal Interactions to Human-Robot Interactions

Chapter 1

Synchrony in Interpersonal Interactions

The term *synchronous* originates from the Greek and could be translated by "occurring at the same time". Synchronisation was studied for the first time in 1665 by Dutch researcher Christiaan Huygens who observed the movement of two pendulum clocks suspended on a wooden beam. Followed many other studies on synchronisation across the centuries in physics, electrical engineering, biology... Even biological clocks from humans to bacteria are synchronised with circadian and seasonal rhythms. Synchronisation can also be witnessed in populations which can be likened to groups of oscillators: flashing fireflies, applauding audience, walking troops...

1.1 Synchrony, Coordination, Synchronisation...

Though the terms *synchrony*, *synchronisation* and *coordination* are often interchangeably employed, their meanings actually differ. Synchrony denotes the state of two or more events occurring at the same time. In signal processing, *coordinated* describes events occurring with a constant phase difference (which can differ from zero). *Absolute coordination* takes place when coupled oscillators oscillate with the same period and a constant time difference. In contrast, *relative coordination* occurs if the coupled oscillators don't have the same period and keep adapting [Von Holst, 1973]. *Synchronised* indicates that the events are in phase (phase difference is zero) or in anti-phase (phase difference is π). Note that coordination and synchronisation are not states but dynamical processes.

1.1.1 Interpersonal Interactions

Human communication is not restricted to speech, far from it. Non-verbal behaviours such as posture, facial expressions, movements also contribute significantly to the interaction. Interpersonal synchrony can be observed in many different situations: head movements or posture in a conversation [Paxton and Dale, 2017, Gueugnon et al., 2016], crowd behaviour [Ellamil et al., 2016], walking [Nessler and Gilliland, 2009]...

For humans, physical and social interactions induce gestural communication based on rhythmic mechanisms and rhythmic movements. Rhythmic social interactions trigger behavioural changes at the motor level, as well as at the cognitive level. At the motor level, people experience two phenomena which can be observed in oscillators: the *magnet effect* which entrains both systems until they are coupled and synchronised; the *maintenance effect* which is the struggle of each system to conserve its own intrinsic frequency [Fernández and Cairns, 2017]. These two concepts were originally introduced by [Von Holst, 1973] who showed that individual biological

components possess intrinsic properties that persist despite coordination with other biological components. [Issartel et al., 2007] defined interpersonal coordination as "the outcome of a latent and never-ending struggle between maintenance tendency and magnet effects". Interpersonal coordination requires, first, incidental similarity. If the magnet effect is sufficiently strong, absolute coordination can be achieved (coordinated movement with a metronome for example). However, it may sometimes not be strong enough and only relative coordination can be achieved, in the case of a child and an adult coordinating their walking gait, for example, as both constantly adapt to overcome their individual intrinsic properties.

It is worth mentioning that most of the time synchrony is involuntary. In some studies, even when specifically instructed not to synchronise, participants could not help themselves from doing it anyway [Issartel et al., 2007]. At the cognitive level, humans learn from each interaction and create conscious or unconscious links between interaction partners [Delaherche et al., 2012]. Indeed, synchronised interactions improve cooperative abilities [Valdesolo et al., 2010], the likeability of the partner and facilitate cognitive tasks [Macrae et al., 2008].

These mechanisms could play a fundamental role in physical and social interpersonal interactions [Yonekura et al., 2012, Troje et al., 2006] and could be an emergent feature of these interactions where humans adapt to each other. Scientists also assume that emotional and social interactions involve a coupling between individuals which is achieved thanks to neural structures with similar properties as those implicated in the neural control of movements. Synchrony relies on low-level sensorimotor networks (vision, audition or touch), and leads to the synchronisation of inter-individual neural populations [Condon, 1976].

1.1.2 Imitation

Imitation is a paramount step in child development and is thought to contribute to the acquisition of social skills by developing self-awareness and/or other-awareness which could help interpreting the goals and others' intentions in social interactions [Legare and Nielsen, 2015, Meltzoff and Prinz, 2002, Tomasello, 1999, Whiten, 2017]. While contributing to social learning, it also plays a critical role in the development of Theory of Mind, social cognition and communication skills. Another fundamental step in child development occurs when children perform discriminative imitation [Gergely et al., 2002, Carpenter and Call, 2002], that is, they move from imitating everything to goal-directed imitation.

It was defined by Thorpe in 1956 as "copying of a novel or otherwise improbable act or utterance, or some act for which there is clearly no instinctive tendency" [Thorpe, 1956].

Deficits in imitation are usually associated with neurological disorders [Goldenberg and Hagmann, 1997, Rogers, 1999]. Imitation can be seen as reproducing a goal through a motor action with retention of certain characteristics of an observed motor act, it, however, does not imply exact reproduction of the observed motor action [Meltzoff, 1988]. On the other side, copying has no notion of intention but implies exact reproduction of a motor action. Last, mimicry (or chameleon effect [Chartrand and Bargh, 1999]) is the unintentional tendency to reproduce another's behaviour. The most obvious example occurs when a person's yawn triggers other peoples's yawning, but also mimicry of posture, facial expressions... Mimicry is often oblivious to all those involved in the interaction, nevertheless, it unconsciously leads to more enjoyable interactions and higher likeability.

Mirror neurons were discovered in the ventral premotor cortex of the macaque monkey [Gallese et al., 1996, Rizzolatti et al., 1996]. Mirror neurons fire both when monkeys perform a goal-directed action and when they perceive the same action performed by an experimenter [Gallese et al., 1996, Kohler et al., 2002, Rizzolatti et al., 1996, Umilta et al., 2001]. The human mirror

neuron system is located in the inferior frontal cortex and superior parietal lobe and is activated both when a goal-directed action is performed and when the same action is performed by another person [Rizzolatti and Craighero, 2004]. Mirror neurons may be important for understanding other people's actions and for learning new skills by imitation. The mirror neuron theory in humans may be quite popular amongst scientists but also has strong dissidents [Hickok, 2013, Lotto et al., 2009, Hickok, 2014]. Contradictory data, as well as uncertainty about the role and functioning of mirror neurons leave a lot of unanswered questions and some theories are disparaged by scientists as over-simplistic. Others do not believe that mirror neurons are a specific type of cell, but rather a behaviour exhibited by some cells in given situations [Hickok, 2009, Pascolo et al., 2009].

1.1.3 Coordination Dynamics

Coordination dynamics in the human brain is of great interest to scientists and has been studied with EEG headsets and fMRI. It has indeed been shown that brains become synchronised in interpersonal coordination tasks [Dumas et al., 2010].

Using EEG, [Tognoli, 2008] did an experiment where pairs of subjects performed repetitive finger movements at their preferred frequency and amplitude alone and in front of a partner. They identified a rhythm composed of two spectral components (above right centroparietal electrodes, at $10-12\ Hz$) that promoted intrinsic behavior (increased in uncoordinated interactions) and social behavior (increased in coordinated interactions). In an EEG experiment on interpersonal finger tapping, [Tognoli et al., 2007] demonstrated that the mirror neurons could be the specific neural medium responsible of the synchronisation dynamics. They discovered that mirror neuron activity increases during synchronised but not during non-synchronised joint actions. A dual EEG experiment where two partners could willingly engage in spontaneous imitation of hand movements showed no significant difference between imitative and non-imitative state [Dumas et al., 2010]. However, they observed that brain oscillatory couplings were present when the partners were synchronized and that statistical differences existed in interbrain phase synchronies for all analysed frequency bands (alpha-mu $[8-13\ Hz]$, beta$[13-30\ Hz]$ and gamma$[30-80\ Hz]$) except for the theta $[4-8\ Hz]$ band. The alpha-mu band is revealed to be the most robust to discriminate synchrony and non-synchrony since it is a neural correlate of the mirror neuron system. They also highlighted differences between imitating and being imitated and also between induced and spontaneous imitation [Dumas et al., 2012]. In a similar experiment, [Delaherche et al., 2015] compared spontaneous imitation and non-imitation. They showed statistical differences in the theta frequency band.

Coherence in the cortical motor regions was studied by [de Castelnau et al., 2008] for children with developmental coordination disorder while performing rhythmic finger flexion movements with an increasing frequency. They showed increased coherence between fronto-central regions compared to the control children (without developmental coordination disorder). A difference of brain activation when subjects performed synchronised finger tapping and when their movement was self-paced was also observed by [De Pretto et al., 2018].

Besides, [Perry et al., 2010] demonstrated that mu waves are weaker when watching a human movement than when watching a non-biological movement and [Fitzpatrick et al., 2019] observed that activation of alpha-mu waves is inversely proportional to intentional synchronisation in social synchrony.

All those studies demonstrate that synchronisation has a significant effect on the human brain. Moreover, motor coordination in interpersonal interactions leads to interbrain synchrony.

1.1.4 Theoretical Model of Motor Coordination

Haken, Kelso and Bunz developed a theoretical model (HKB) [Haken et al., 1985] of intra and later of inter-personal motor coordination based on experimental observations of bimanual coordination in a finger flexion/extension task [Kelso, 1984]. The HKB paradigm considers that, at low frequency, there are two stable attractors in rhythmic tasks: phase and anti-phase. Above a given threshold frequency, there is only one stable attractor: in phase. This phenomenon is depicted on figure 1.1. The equation of motion capturing this is defined as follows:

$$\dot{\Phi} = -a \sin \Phi - 2b \sin 2\Phi \qquad \text{with } a,\, b \geq 0 \tag{1.1}$$

Φ is the relative phase between the fingers, b/a is a ratio comprising coupling strengths a and b that situates the bifurcation between bi- and mono-stability. The period of movement is often implicitly set to 1 or 2π radians, since the 1985 equations do not break the symmetry and the movement frequency is not considered central to the qualitative changes observed in the system.

The model has been extended to take other phenomena into account (noise, different intrinsic frequencies...) by adding terms to the equation [Schöner et al., 1986, Kelso et al., 1990, Treffner and Turvey, 1996]. This was extensively observed in finger wiggling tasks, but also for leg swinging tasks [Schmidt et al., 1990], leg-arm coordination [Zanone and Kostrubiec, 2004] or walking [Jeka et al., 1993].

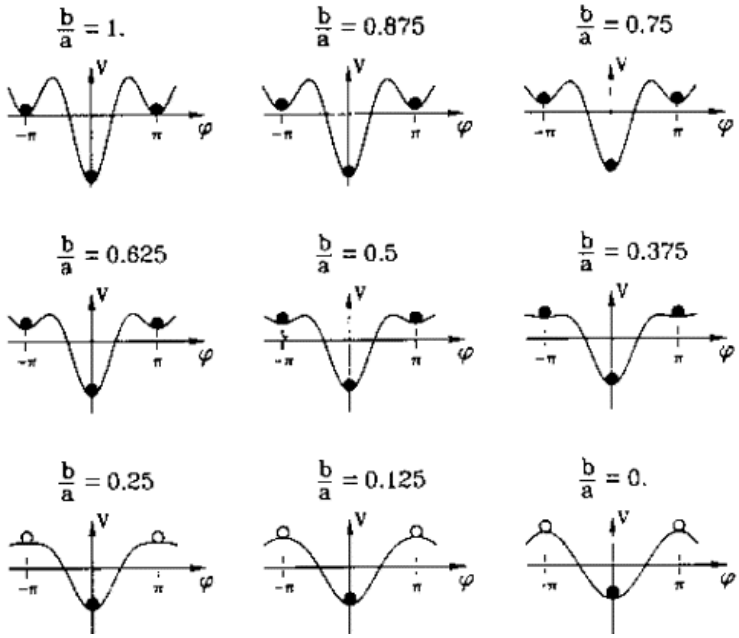


Figure 1.1: Illustration of HKB showing the potential field $V = -a \cos \Phi - b \cos 2\Phi$, i.e. the attractors of the system for varying values of b/a. The ratio b/a represents the effect of the oscillation frequency on the potential landscape. As the frequency increases (b/a decreases), the anti-phase mode becomes less stable. Below a given value for b/a, the potential becomes monostable. (Reproduced from [Monno et al., 2002])

1.2 Evaluation of the Interaction

A prerequisite for studying human-human or human-robot gestural interactions is a method to evaluate the coordination between the partners (See [Delaherche et al., 2012] for a review) and the similarity between the movements. Interactions can be captured by video analysis, motion tracking or psychophysiological and neurophysiological methods (See [Cornejo et al., 2017] for a review). In this section, we will present an overview of existing methods to evaluate coordination and similarity. A selection of these methods was tested in Python using the Scikit library or Matlab and evaluated on theoretical signals (See Fig. 1.2). When the method was not readily available, we implemented it.

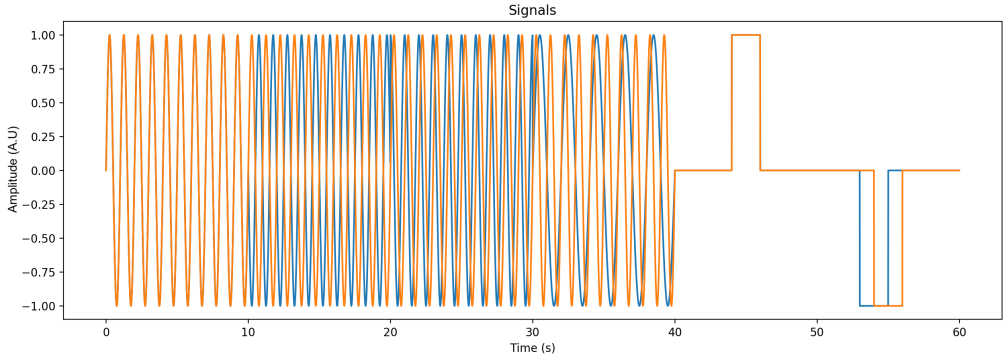


Figure 1.2: Artificial signals used to evaluate the coordination. They consist of 10s of sinusoidal signals in phase, 10s of sinusoidal signals in anti-phase, followed by 10s of sinusoidal signals with a phase difference of $\pi/2$ and 10s of sinusoidal signals with a factor of two between their frequencies, then steps occurring at the same time and finally delayed steps

1.2.1 Coordination

Three Correlation Methods

Correlation is probably the most popular method to evaluate synchrony in interactions. Different correlation or coherence indices are available. They provide only one averaging value to evaluate the whole interaction. These indices lead to a lot of information loss. Indeed, with a single value for the whole interaction, information such as synchronisation length, beginning of synchronisation or loss of synchronisation are not available.

Using a sliding window, instantaneous cross-correlation can be estimated between two time series. The cross-correlation between two signals is defined as follows:

$$S(x,y) = \frac{\sum_n (x_n - \overline{x})(y_n - \overline{y})}{\sqrt{\sum_n (x_n - \overline{x})^2}\sqrt{\sum (y_n - \overline{y})^2}} \tag{1.2}$$

with x and y two time series. A sliding window can be used to have a local estimate (See Fig. 1.3).

On the other hand, a two-dimensional map can represent the correlation across a given range of temporal delays (See Fig. 1.3). A sliding window is used to have a local estimate. This 2D correlation is defined as follows:

$$C_{xy}(k,d) = \frac{S_{xy}(k,d)}{\sqrt{S_{xx}(k,d) * S_{yy}(k,d)}} \tag{1.3}$$

where $S_{xy}(k,d) = S(x[k:k+w], y[k-d:k-d+w])$, $-d_{max} < d < d_{max}$ and w the width of the sliding window.

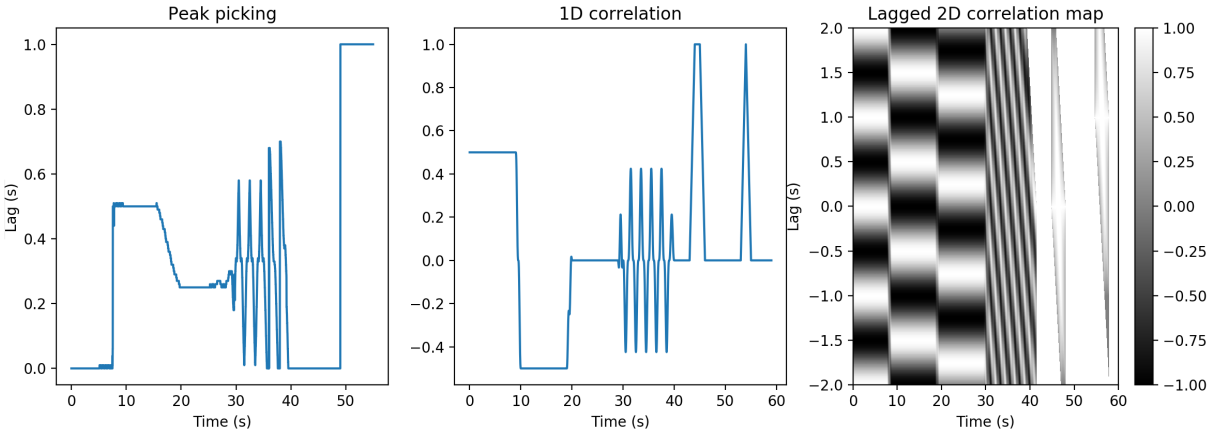


Figure 1.3: Three correlation measures applied to the artificial signals. Left: Peak picking P_{xy} ($w = 100$); Middle: 1D cross-correlation S_{xy} ($w = 100$); Right: 2D lagged cross-correlation C_{xy} ($w = 100$) (The correlation strength is represented with different shades)

Besides, a peak picking algorithm can estimate the time lag between two signals by finding the peak cross-correlation that is closest to zero. This is defined as follows:

$$P_{xy}(k) = min_x(peaks(S_{xy}(k,0))) \tag{1.4}$$

with $peaks(s)$ a list containing the peaks of the signal s and $min_x(l)$ the value of the list l with the smallest x coordinate, i.e. the closest peak to 0.

It can thus estimate the evolution of the time lag over time and reveal leader-follower relationships between the signals.

One can see on Figure 1.3 that the peak picking algorithm provides an information on the lag between the signals and it gives an indication on the phase difference between the signals so it does discriminate phase and anti-phase and also works for the step signals. It, however fails when the frequencies are not the same. The 1D correlation can also identify phase difference and we can see two peaks corresponding to the step signals. The 2D-correlation is indubitably the most complete representation, it allows to extract any information necessary.

Recurrence Methods

Meanwhile, cross-recurrence quantification analysis detects intricate recurrent structures between paired signals [Webber Jr and Zbilut, 1994, Shockley et al., 2002, Konvalinka et al., 2011]. It is a nonlinear method that allows quantification of dynamical systems and trajectories of non-stationary signals [Varni et al., 2008, Richardson and Dale, 2005, Varni et al., 2009]. Contrary to most methods, it does not perform any averaging which usually leads to data loss. In recurrence methods, the first time series is divided into time delayed vectors of dimension n which are compared with every vector of the second time series using a distance measure. This creates a

cross-recurrence matrix, on which a threshold is applied (See Fig. 1.4). The cross-recurrence matrix can be computed as follows:

$$R_{xy}(i,j) = \lfloor dist(x(i), y(j))/\epsilon \rfloor \tag{1.5}$$

$$R_{xy}(i,j) = \begin{cases} \text{thresh} & \text{if } R_{xy}(i,j) > thresh \\ R_{xy}(i,j) & \text{else} \end{cases} \tag{1.6}$$

with $dist(x, y)$ the Euclidean distance between x and y, ϵ a weight.

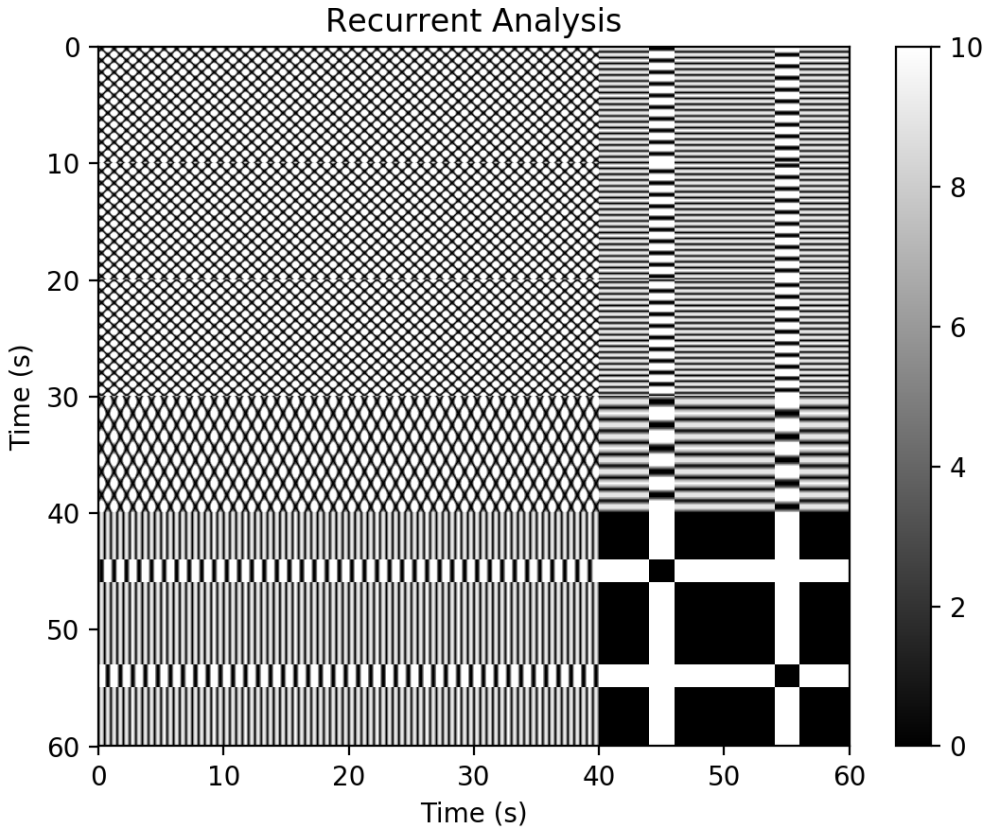


Figure 1.4: Cross-recurrence analysis applied to the theoretical signals in figure 1.2 ($\epsilon = 0.1$, $thresh = 10$)

This method can distinguish coordination from synchronisation and phase from anti-phase. It also gives a good indication when the signals have different frequencies. It is also able to discriminate the step signals (with and without time delay).

Spectral Methods

Several different methods first compute the instantaneous phase with the Hilbert transform or with the wavelet transform. Next, the phases are compared by computing the mean vector length of the angular dispersions of the phase difference in a complex space [Müller and Lindenberger, 2011]

or by simply comparing the instantaneous phase of two signals [Rosenblum et al., 1996, Kauppi et al., 2014] or by multiplying the wavelet transforms of both systems [Grinsted et al., 2004].

The *Continuous Wavelet Transform* (CWT), like the Fourier Transform is used to decompose a signal into analysing functions. While these functions are complex exponentials e^{jwt} for the Fourier transform, they are wavelets ψ for the CWT. The CWT compares the signal with scaled and time-delayed versions of the wavelet.

The CWT is defined by:

$$CWT(a, b, f, \psi) = \int_{-\infty}^{\infty} f(t) \frac{1}{a} \psi * \left(\frac{t-b}{a} \right) dt \tag{1.7}$$

with a and b the scale and position parameters respectively, the scale stretches or compresses the wavelet and the position parameter defines the time-shift applied to the wavelet, $*$ the complex conjugate symbol and f the function to evaluate. There are many choices for the wavelet depending on the type of signal (smooth, abrupt...). The cross-wavelet transform is defined as:

$$CCWT(a, b, f1, f2, \psi) = CWT(a, b, f1, \psi) * CWT(a, b, f2, \psi) \tag{1.8}$$

It allows to highlight similar parts in the signals and remove other parts. This method discriminates phase from anti-phase signals. It is also possible to identify the phase difference and find signals with different frequencies (See Fig. 1.5).

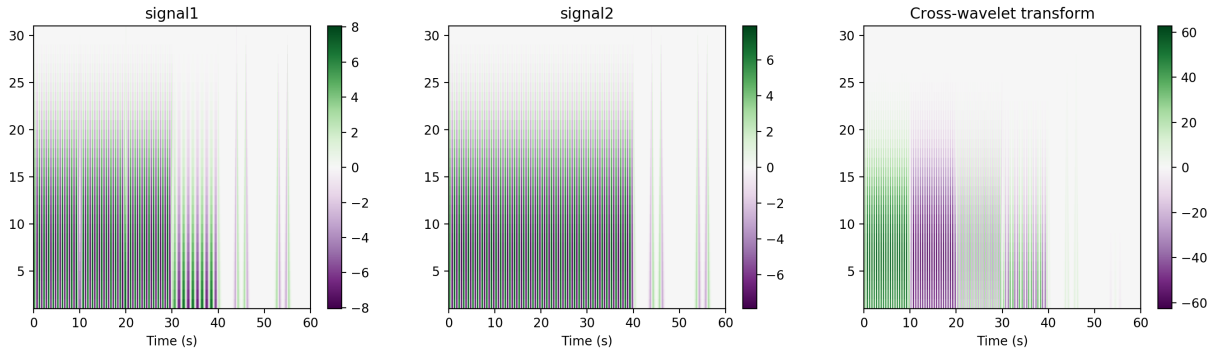


Figure 1.5: Wavelet transform of each signal and their cross-wavelet transform

The *Phase Locking Value* (PLV) has been introduced by [Lachaux et al., 1999] to measure coordination in brain signals. It relies on the assumption that both signals are locked with a constant phase difference but the PLV allows for deviations and evaluates this spread. It ranges from 0 (no coordination) to 1 (perfect coordination). First, the Hilbert transform is computed, providing the instantaneous phase ϕ for each signal, then the instantaneous PLV can be obtained:

$$PLV(t) = \frac{1}{N} \left| \sum_{i=0}^{N} e^{j(\phi_1(i) - \phi_2(i))} \right| \tag{1.9}$$

with N the sliding window size, $j = \sqrt{-1}$, ϕ_k the instantaneous phase of signal k. The application of the PLV to the artificial signals of figure 1.2 is shown in figure 1.6.

Since the PLV is a coordination measure, it is unable to give any information on phase difference.

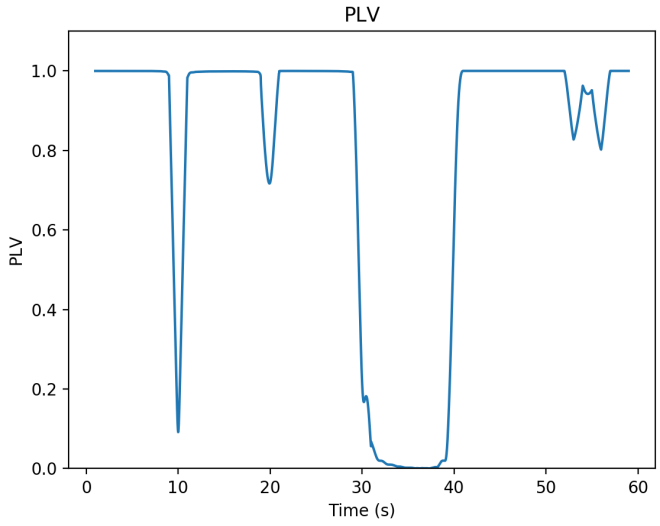


Figure 1.6: Phase Locking Value between the two theoretical signals

Synchrosqueezing introduced in the context of analysing auditory signals [Auger and Flandrin, 1995] aims to decompose signals into constituent components with time-varying oscillatory characteristics. It is assumed that signals have the following form:

$$f(t) = \sum_{k=1}^{K} f_k(t) + e(t) \tag{1.10}$$

with $f_k(t) = A_k(t)cos(2\pi\phi_k(t))$ a Fourier-like oscillatory mode and $e(t)$ noise.

First, the continuous Wavelet transform is computed:

$$W_s(a,b) = \int s(t)a^{-1/2}\overline{\psi\left(-\frac{t-b}{a}\right)}dt \tag{1.11}$$

with ψ an appropriate mother wavelet. A candidate instantaneous frequency $\omega_s(a,b)$ for the signal s can be derived:

$$\omega_s(a,b) = -i(W_s(a,b))^{-1}\frac{\delta W_s(a,b)}{\delta b} \tag{1.12}$$

The Wavelet Synchrosqueezing transform of f is defined as:

$$T_s(\omega_l,b) = (\Delta\omega)^{-1} \sum_{a:|\omega_s(a,b)-\omega_l|\leq\Delta\omega/2} W_s(a,b)a^{-3/2}\Delta a \tag{1.13}$$

with ω_l the center frequency bin where frequencies are closer to ω_l than to any other frequency.

Synchrosqueezing provides frequency information for one single signal but synchronisation concerns two signals, so based on the cross-wavelet transform defined in [Grinsted et al., 2004], we define Cross Synchrosqueezing as the product of Synchrosqueezing transform obtained for each signal. This operation is designed to highlight regions where the frequency is similar for both signals and to remove the other frequencies (See Fig. 1.7). Similar to the PLV, this is also a measure of coordination that cannot identify phase difference.

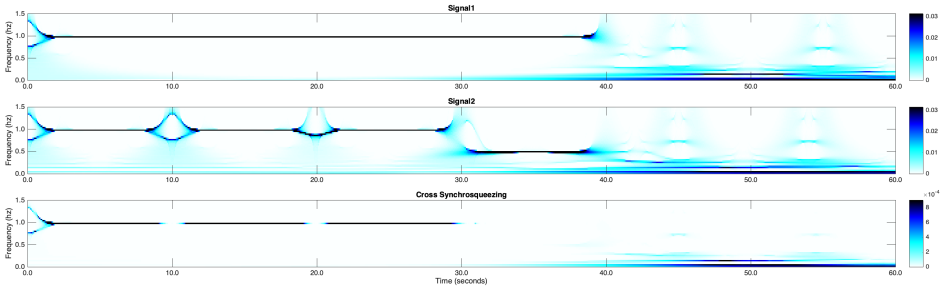


Figure 1.7: Synchrosqueezing of each theoretical signal and their cross-synchrosqueezing

1.2.2 Similarity Measures

The accurate evaluation of imitation, i.e. how good a partner reproduces the movements of another person appropriately, is a challenging task as imitation is not a purely geometrical concept. Intention also has to be taken into account.

For goal-oriented tasks, let us take the pick-and-place example. The first partner takes an object and moves it to a basket. The second one performs the same task and even though the goal is achieved and the intention was the same, geometric similarity methods may indicate large differences because the movements were not the same. In that case, similarity of imitation can be evaluated more appropriately in the cartesian space than in joint space. However, it does not take individual physical differences into account.

For non-goal-oriented actions, it is far from obvious what a *good imitation* should be. In our opinion, an amplitude difference between the movements should not lead to large discrepancies. If a partner raises his arm, the other one may raise his arm lower or higher but the fact that he also raised his arm should be the most important factor.

The cosine similarity measures the similarity of orientation (1 for the same direction, -1 for opposite directions), independently of the magnitude.

$$d(\vec{v_1}, \vec{v_2}) = \cos\theta = \frac{\vec{v_1} \cdot \vec{v_2}}{||\vec{v_1}||||\vec{v_2}||} \tag{1.14}$$

with $\vec{v}$ a vector, θ the angle between vectors $\vec{v_1}$ and $\vec{v_2}$.

The most trivial method consists in performing an Euclidian distance between corresponding angles over the whole trajectory and across all joints [Pomplun and Mataric, 2000]:

$$d(\alpha, \beta) = \sum_{t=0}^{T} \sum_{j=1}^{n} (\alpha_j(t) - \beta_j(t))^2 \tag{1.15}$$

with α_j and β_j two time series corresponding to the trajectory of joint j, T the length of the signals, n the number of joints.

One major drawback of this method is that a difference in speed or amplitude may lead to a large distance. The speed difference may be compensated by scaling the second trajectory over time to match the duration of the first. Likewise, the trajectories can be normalised. This needs to be done individually for each movement and can rapidly become tedious with series of movements. Movements can be segmented beforehand using a velocity histogram [Pomplun and Mataric, 2000].

The Dynamic Time Warping algorithm (DTW) [Berndt and Clifford, 1994] also gives a locally temporally invariant distance measure between time series. The DTW is an extended version

of the Euclidean distance where time-warping is applied to signals to align them optimally, beforehand so as to minimise the distance between them. The DTW can be recursively defined as:

$$DTW(i,j) = d(\alpha_i, \beta_j) + min\{DTW(i-1, j-1), DTW(i-1, j), DTW(i, j-1)\} \tag{1.16}$$

A DTW value is computed for each angle. The global DTW distance then yields:

$$D = \frac{\sum_{k=0}^{N} w_k DTW_k}{\sum_{k=0}^{N} w_k} \tag{1.17}$$

One can see on Figure 1.8 that the DTW is width- and offset-independent. It can however be influenced by amplitude. Signal normalisation could be performed beforehand to avoid this issue.

Moreover, when performing a specific task, not all joints are equally relevant and their contribution should be evaluated accordingly. Each joint is thus assigned a weight:

$$d(\alpha, \beta) = \sum_{t=0}^{T} \sum_{j=1}^{n} w_j (\alpha_j(t) - \beta_j(t))^2 \tag{1.18}$$

Similarity metrics can also take the angular speeds of each joint into account [Lee et al., 2002]. The metrics becomes:

$$\begin{aligned} d(\alpha, \beta) = \sum_{t=0}^{T} \Bigg(& w_p \sum_{j=1}^{n} w_j (\alpha_j(t-k...t+k) - \beta_j(t-k...t+k))^2 + \\ & w_s \sum_{j=1}^{n} w_j (\dot{\alpha}_j(t-k...t+k) - \dot{\beta}_j(t-k...t+k))^2 \Bigg) \end{aligned} \tag{1.19}$$

with $2 \cdot k$ the width of the sliding window, with $\dot{\alpha}_j$ and $\dot{\beta}_j$ the derivatives of two time series corresponding to the trajectory of joint j and w_p and w_s the weights.

Conclusion

Synchrony is an undissociable part of interpersonal interactions and gestural communication often triggers the emergence of unconscious motor coordination. Humans are known to attribute greater likeability to an adaptive partner, so it appears quite obvious that adaptive mechanisms in robots would be a step closer towards social acceptability.

Moreover, we give an overview of different evaluation methods for coordination/synchronisation in Table 1.1 (see below) and imitation. Throughout this thesis, we will use different coordination evaluation methods depending on our goal. Moreover, most of the time, we will be looking at motor coordination, independently of the phase difference, therefore simpler methods can be sufficient for our needs. For example, we will often be using the PLV which is a coordination measure and gives no information on phase difference. However, the PLV remains an interesting measure as it directly provides an instantaneous coordination score between 0 and 1 that is easily understandable. For similarity of imitation, we will employ either Eq. 1.19 on normalised movements or the DTW measure.

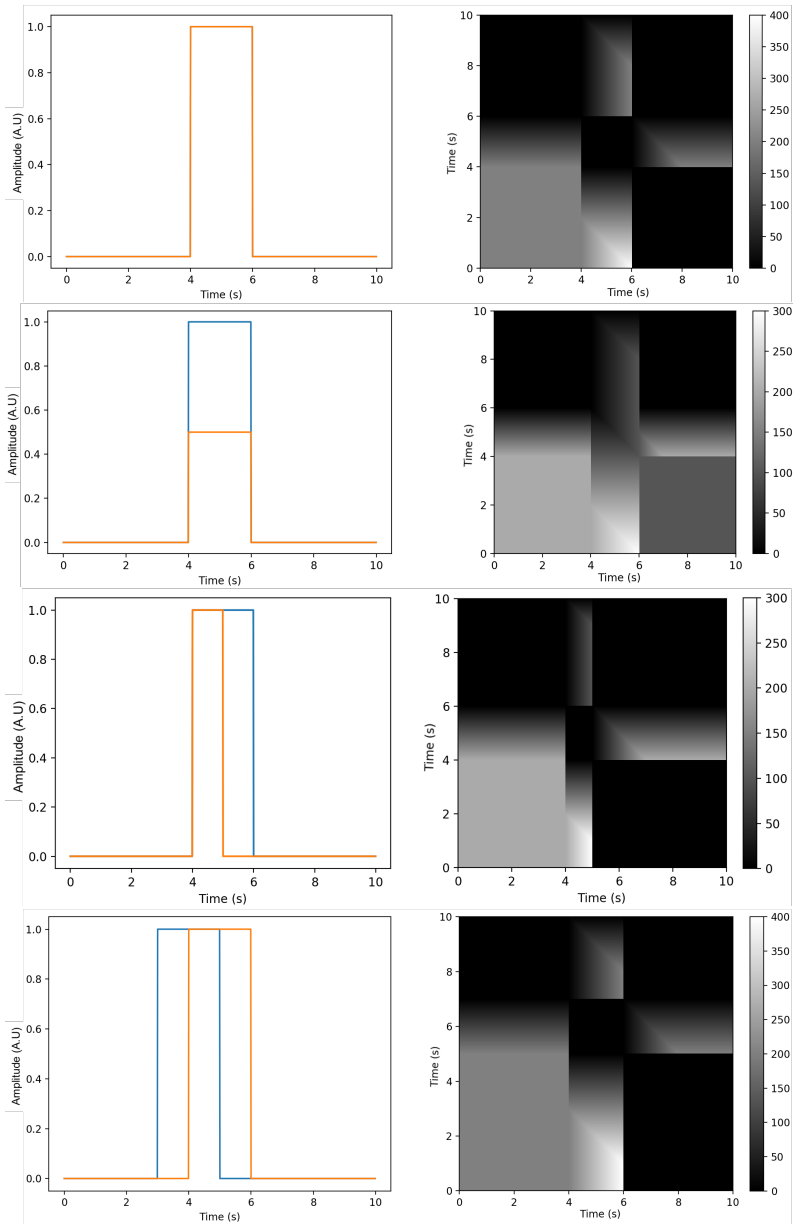


Figure 1.8: DTW on a series of examples. 1. DTW on similar step signals (DTW score = 0). 2. DTW on step signals with different amplitude (DTW score = 100). 3. DTW on step signals with different width (DWT score = 0). 4. DTW on step signals with different offsets (DWT score = 0)

In the next chapter, we will see previous works in HRI where robots were endowed with adaptive abilities to achieve motor coordination between a robot and a human. We will also give an overview of imitation in HRI.

Method	Synchronisation	Phase shift	Amplitude invariant	Robust to noise
Peak picking	✓	✓	✓	-
1D correlation	✓	✓	✓	+
2D correlation	✓	✓	✓	++
Cross-recurrence	✓	✓	✗	+
Phase Locking Value	✗	✗	✓	+
Cross-synchrosqueezing	✗	✗	✓	+
Cross-wavelet transform	✓	✓	✗	++

Table 1.1: Overview of the methods. The synchronisation column indicates whether the method can discriminate synchronisation and coordination. The second column "phase shift" documents whether the method can dissociate in phase and anti-phase, and more generally if it provides an accurate measure of the phase shift. The third column reveals whether the method is influenced by changes in amplitude. The last column indicates how the performance method may be affected by random noise

Chapter 2

Motor Coordination in Human Robot Interactions (HRI)

Synchronisation between a human and a robot is a relevant problematic any time a robot interacts with a human. While it is an interesting challenge in social robotics and a productivity and safety issue in collaborative robotics, it turns into a critical problem in robot-assisted therapy, with exoskeletons for example.

Moreover, biological movement increases acceptance of humanoid robots as human partners in motor interaction [Kupferberg et al., 2011].

2.1 Synchronisation in HRI

It is widely accepted that robots have to be adaptive in rhythmic tasks since humans expect them to be and humans may not adapt completely to a non-adaptive robot [Lorenz et al., 2013].

2.1.1 Adaptive Robots

Most of the research on motor coordination in HRI focuses on making the robot adaptive with a controller which usually relies on non-linear dynamical systems to take advantage of their attractor properties.

In [Pongas et al., 2005], a robotic arm was able to synchronise with an external signal and perform coordinated drum beating with a changing frequency. They employed the Dynamic Movement Primitives Framework presented in [Ijspeert et al., 2002]. In another drum beating study, [Degallier et al., 2006] presented an extended dynamical system which can perform both discrete and rhythmic movements by combining a Hopf oscillator and the VITE model (Vector-Integration-To-Endpoint, discrete pattern generator) [Bullock and Grossberg, 1988]. [Gams et al., 2009] use a set of oscillators endowed with learning mechanisms that are expected to adapt their frequencies to the frequency components of the input signal. They then extract the main frequency and phase to learn the waveform of the input signal. While that system is robust to perturbations, the convergence rate can be quite slow. It was validated on a drum beating task. [Petrič et al., 2011] developed the former system further and applied it to a yo-yo playing task. [Crick et al., 2006] also achieved synchronised drumming after sensory integration of visual and auditory information. Similarly, [Ansermin et al., 2016] also introduced a model designed to reproduce human rhythmic arm movements with the NAO robot. A reservoir of oscillators provides one with a close frequency and while the oscillator can be slightly entrained

during the interaction, the oscillators do not retain the frequency, going back to their original properties right afterwards. [Williamson, 1998a] proposed a neural network oscillator circuit for coordinated rhythmic arm motion. Human-robot rope turning [Maeda et al., 2001, Kim et al., 2009] and imitation of human rhythmic movements [Ubukata et al., 2009] have also been achieved using phase-locked loops [Hsieh and Hung, 1996] to estimate the movement frequency and phase. [Miyazaki et al., 2006] proposed a method for human-robot table tennis. It consists of input-output maps based on Locally Weighted Regression. The feed-forward control scheme is based on iterative learning control.

The Matsuoka neural oscillator [Matsuoka, 1985] has also been employed for synchronisation in HRI. [Kasuga and Hashimoto, 2005] introduced a framework for human-robot handshaking using neural oscillators. They were able to control how passive or active the robot handshake was and modulate the human perception of the response. Physical assistance for rhythmic knee movements using a robot suit has also been achieved using the Matsuoka model [Zhang and Hashimoto, 2009]. Both these experiments were also reproduced using online polynomial design method to model the attractor dynamics [Okada et al., 2002] of the interaction in order to achieve synchronisation [Sato et al., 2007]. [Ronsse et al., 2010] also controlled an exoskeleton with the Hopf oscillator.

Visual information can also be extracted for synchronisation of a dancing robot with children [Michalowski et al., 2007] or for the coordination of two robots [Blanchard and Canamero, 2005]. To synchronise upper limb movements with the Nao robot, [Hasnain et al., 2013] used a reservoir of oscillators composed of two mutually inhibiting neurons which can be slightly entrained due to natural properties of the oscillator. Frequency prediction allows them to select the oscillator closest to the detected frequency.

2.1.2 Of the Relevance of Synchronisation in HRI

HRI studies confirm that humans can hardly resist unintentional coordination with a robot moving at a constant frequency that is not too far from their own. However, coordination may fail if the frequencies are too different [Hasnain et al., 2013, Lorenz et al., 2013]. Coordination appears easier and more natural when the adaptation is bilateral. Mutual entrainment yields a common frequency that ranges half-way between the robot and human frequencies. Non-adaptive interactions may feel awkward for the participants.

[Marin et al., 2009] presented a framework of motor resonance, postulating that bidirectionality in implicit motor human-robot coordination could enhance the social competence of HRI. Motor resonance is defined as an activity of the motor system that would be similar when observing a task as when performing the same task. Motor resonance has been investigated when participants produce vertical or horizontal arm movements while watching another partner (human or industrial robotic arm) in front of them producing a spatially congruent (i.e. vertical when vertical, horizontal when horizontal) or a spatially incongruent arm movement [Kilner et al., 2003]. A significant interference effect was found when participants were facing another human, but not when they faced the robot. This experiment was reproduced with humanoid robots performing either congruent or incongruent movements [Oztop et al., 2005]. Contrary to the industrial robot, the humanoid robot caused a significant change in the variance of the movement depending on congruency. In another version of this experiment, the humanoid robot moved either with a biological motion or with an artificial motion [Chaminade et al., 2005]. There was a significant effect of congruency and type of movement on subjects' variance. The increased movement variance in incongruent conditions was only significant when the robot movements followed biological motion.

In the case of physical assistance with exoskeletons or robot suits, adaptive mechanisms based on oscillators lead to a muscular effort reduction on the patient's part. In [Ronsse et al., 2010], participants performed elbow flexion/extension with and without an exoskeleton. They could also observe that, while the oscillator adapted to the participants, the latter also adapted to the oscillator, still retaining full control of their movement.

2.2 Motor Imitation

Pose imitation by a robot essentially consists in three phases: observe the action, represent the action and reproduce it [Bakker and Kuniyoshi, 1996]. The other non-negligible issue is the correspondence problem, between the human and the robot, so that the robot can reproduce the gesture. We will not dwell on this and only consider humanoid robots where the correspondence is straightforward (See [Nehaniv et al., 2002, Nehaniv and Dautenhahn, 2001] for a systematic approach).

2.2.1 Action Observation

First, let us see how to observe the human action. The human can demonstrate the movement in several ways, each with their drawbacks (✗) and advantages (✓):

- recording of human movements based on vision [Ibrahim and Adiprawita, 2012], exoskeletons or sensors [Ott et al., 2008, Koenemann et al., 2014]:
  - ✓ the human can perform the movement freely and naturally
  - ✗ it requires an explicit mapping between the human and the robot, which can be quite cumbersome, depending on the robot
- kinesthetic teaching [Ehrenmann et al., 2001], i.e. the human manually operates the robot to get it through the task.
  - ✓ No correspondence issue
  - ✗ Not natural for the human as it often requires more effort and degrees of freedom to demonstrate a movement, e.g. raise the robot arm using two hands. Teaching movements which require the synchronisation of several limbs is therefore quite complex
- immersive teleoperation [Stanton et al., 2012], i.e. a human performs the task using the robot sensors and effectors by means of a joystick or a haptic device.
  - ✓ No correspondence issue
  - ✗ it requires training for the human to master the control interface, which can be quite complex
- natural language [Inamura et al., 2006]
  - ✓ High-level approach if sentences like "grab the bowl, pour the milk" are understood
  - ✗ it requires a mapping between speech and action

2.2.2 Action Representation

Learning by demonstration is often associated with reinforcement learning where the robot gets a reward when the goal is achieved [Guenter et al., 2007, Kober and Peters, 2009, Kormushev et al., 2010]. The robot can also autonomously determine the reward and optimal control policy using inverse reinforcement learning [Abbeel and Ng, 2004].

Different methods can be used to represent and learn the trajectories: Spline-based techniques [Aleotti and Caselli, 2006], Gaussian mixture regression [Gribovskaya et al., 2011] and Dynamics Movement Primitives (DMP) [Schaal et al., 2003] or Probabilistic Movement Primitives (ProMP) [Paraschos et al., 2013] which are probably the most famous. Movement primitives can be seen as parametrised control policies that can reproduce a learned movement. They are basically dynamical systems that can generate different complex motions according to a set of parameters. Gaussian Mixture Model and Dynamic Movement Primitives are the most commonly used.

Gaussian Mixture Model

The Gaussian probability density function is a statistical distribution defined by:

$$N(x;\mu,\sigma) = \frac{1}{\sigma\sqrt{2\pi}} e^{-\frac{(x-\mu)^2}{2\sigma^2}} \tag{2.1}$$

with μ the mean and σ^2 the variance.

A Gaussian mixture model is a combination of several Gaussian components. The probability density function of a Gaussian mixture model can be written as:

$$p(x) = \sum_{k=1}^{n} w_k N(x;\mu_k,\sigma_k) \tag{2.2}$$

with n the number of Gaussian components in the mixture. The parameter values (w_k, μ_k and σ_k) can be estimated using optimisation methods to learn a desired trajectory.

While this method is very effective [Chernova and Veloso, 2007, Bentivegna et al., 2004, Saunders et al., 2006], one drawback is that it cannot handle obstacle avoidance in real time.

Dynamics Movement Primitive (DMP)

The DMP framework [Schaal et al., 2003] relies on the assumption that complex movements are composed of basic primitive actions which are executed in sequence and/or in parallel. The system can learn a trajectory and reproduce it with arbitrary start and end positions. It relies on a non-linear dynamical system. This method is stable, robust to perturbations and can account for obstacles. The DMP can produce either discrete or rhythmic movements. The system for discrete movements takes an attractor point into account, whereas the rhythmic system considers a limit cycle. Let x_0 be the initial position and g the target position.

$$\begin{aligned} \tau\dot{v} &= K(g-x) - Dv + (g-x_0)f(s) \\ \tau\dot{x} &= v \end{aligned} \tag{2.3}$$

with τ a temporal scaling term, f a forcing term $f(s) = \frac{\sum_{i=1}^{N}\psi_i(s)w_i}{\sum_{i=1}^{N}\psi_i(s)}$ where $\psi_i(s) = e^{-h_i(s-c_i)^2}$. w_i is a weight for the Gaussian ψ_i of center c_i and variance h_i. In short, the forcing term is a set of Gaussians that activates as x reaches the target, i.e. a weighted summation of basis functions.

The system can be decomposed into three terms: a damping term $-Dv$, an attractor towards the target $K(g-x)$ and a forcing term $(g-x_0)f(s)$ with s a phase variable varying exponentially from 1 to 0 according to $\tau\dot{s} = -\alpha s$, α the desintegration ratio of s.

K and D depend on the system dynamics.

To imitate a trajectory, we need to calculate what the forcing term needs to be:

$$f_d = \dot{v}_d - \dot{v} = \frac{1}{K}(\tau\dot{v}_d - K(g-x) + Dv) \tag{2.4}$$

with $\dot{v}_d$, the desired trajectory acceleration. From there, the weights w_i need to be estimated with an optimisation technique so that the forcing term matches the trajectory. The target can be modified during the task execution and the controller will still adapt to reach it.

2.2.3 Imitation in HRI

Imitation in human-robot systems has been extensively studied but mostly with the goal of making the robot accurately imitate the human. The reverse, i.e. the human imitating the robot, to our knowledge, is only existent with special needs children or infants.

Mimicry of facial expressions has also been reproduced with various robots [Cid et al., 2014, Riek et al., 2010, Hofree et al., 2014]. [Nadel, 2005] displayed tongue protusion by a robot and a stranger in front of infants (2 months). They did not imitate the robot but did it with the stranger. Six-months-old however do not exhibit the same automatic imitation response. Automatic or over-imitation has disappeared and has been replaced by goal-oriented imitation.

On the one hand, many different approaches based on geometry or biology to imitate human movements have been developed over the years. Any method has to consider the robot capabilities by taking joint angle and speed limits into account. Once the correspondence is achieved, some relatively simple control policies can perform imitation in a straightforward manner: PD controllers [Pollard et al., 2002]; Cartesian impedance control from Kinect positions [Luo et al., 2013]; local coordinate system associated with each joint which defines a simplified kinematic model [Ibrahim and Adiprawita, 2012]. Imitation can also be considered as a non-linear optimisation problem to maximise the similarity between the demonstrated human movement and the imitation by the robot [Do et al., 2008]. The constraints are then set considering the physical limits of the robot. [Suleiman et al., 2008] then solved the optimisation problem recursively by using a dynamics algorithm, which computes the gradient function with respect to the control parameters analytically. On a more biological note, [Billard and Matarić, 2001] developed a model that consists of a hierarchy of artificial neural networks. The networks give an abstract and high-level representation of brain regions involved in visuo-motor control for primates. A robot can also learn by himself how to imitate while observing another robot [Hayes and Demiris, 1994] or human movements [Demiris and Hayes, 1996]. Finally, the Wizard-of-Oz approach where the robot is unknowingly teleoperated, can be employed [Tapus et al., 2012, Conti et al., 2015].

On the other hand, imitation can be used with autistic children to assess the imitation deficit by computing the imitation error when asked to imitate the robot [Srinivasan et al., 2013] or as therapy to improve joint attention or engagement [Zheng et al., 2016, Taheri et al., 2015, Kaur et al., 2013, Wainer et al., 2014, Feil-Seifer and Mataric, 2008, Nadel, 2005, Greczek et al., 2014, Bugnariu et al., 2013]. In some studies, the robot is imitated by the child but can also imitate him [Robins et al., 2005b, Conti et al., 2015, Boucenna et al., 2014, Fujimoto et al., 2011]. Moreover, visuomotor priming in imitation with robots for autistic children still does not have a clear answer. [Bird et al., 2007] observed imitative hand closing/opening between an autistic child and a human or a robot. They showed that the child imitated the human faster than the robot

and that this animacy bias [Kilner et al., 2003] was greater than for neurotypical children. This finding contradicts later results by [Pierno et al., 2008] who found visuomotor priming elicited by robotic movement.

Conclusion

Many studies have proposed a wide range of approaches to endow robots with adaptive or imitative mechanisms. However, the great majority of those methods do not take bio-inspiration into account. This seems to be an oversight as it has been evidenced that humans increase their acceptance of robots in motor interactions when they exhibit biological movement [Kupferberg et al., 2011]. Another aspect that has been neglected so far is the fact that robots produce actuator sound when they move. While interpersonal interactions are inherently multimodal with speech, gestures..., in the case of rhythmic interaction with the robot, the interaction partner receives two different pieces of information (visual and auditory) related to the same movement and this might be confusing. This is a fundamental difference between humans and robots and this may be an issue due to the way human sensory processing works. We therefore performed two experiments that will be introduced in the next chapter. The first one will allow us to verify whether the sound of actuators is a disturbance in the interaction [Jouaiti and Henaff, 2019e]. The second one will help us understand human behaviour better in rhythmic human-robot interactions, and especially the involuntary adaptation process.

Chapter 3

Observing Coordination in Human-Robot Interactions

Observing humans interacting rhythmically with a robot allows us to understand human behaviour and perception. In this chapter, we will present two experiments we performed to achieve that goal. The first one investigates whether the sound of robot actuators perturbs a rhythmic human-robot interaction [Jouaiti and Henaff, 2019e]. We will first recall previous findings related to the human perceptual system which justify our hypothesis that the sound the robot produces may be disturbing. The second one observes children interacting rhythmically with a Pepper robot, leader of the interaction.

3.1 The Sound of Actuators: Disturbance of Motor Coordination?

3.1.1 Human Sensory Perception

Humans are capable of adapting to various kinds of stimuli: auditory (metronome beats, music...), visual (flashing lights, human movement...), tactile. Human sensorimotor processing is much more precise and efficient for an auditory stimulus than for an equivalent visual stimulus (metronome beats vs light flashes) []. But what happens when a human is subjected simultaneously to a visual and an auditory signal?

Indeed, in our process to make a robot more adaptive and achieve motor coordination, there is an important difference between humans and robot that we have to take into account: robot actuators produce sound when the robot performs a movement. Research in neuroscience shows that this may very well be problematic since the human brain processes different sensory stimuli in different ways and sensory dominance can appear.

Vision may be dominant over audition in spatial localisation

[Posner et al., 1976] argued that visual information does not have the strong alerting capacity of auditory signals and therefore people are predisposed to direct their attention towards visual stimulation, thus causing visual dominance. Moreover, a modality-appropriateness hypothesis suggests that "the human perceptual system is cognizant of the fact that vision is a more trustworthy modality for spatial localisation than audition and proprioception and, for this reason,

it is more closely attended" [Welch, 1999]. In summary, vision may dominate audition in spatial judgments.

Audition may be dominant for temporal judgments

[Hidaka and Ide, 2015] showed that the auditory perception can severely alter or even remove the visual perception when the stimuli are spatially and temporally congruent, i.e. they occur at the same time and come from the same location. Indeed, white noise bursts heard through headphones degraded the ability to differentiate the orientation of different visual signals. However, for that suppression effect to take place, the sound and visual target stimuli had to be presented in an ipsilateral, spatially congruent manner. Besides, the auditory suppression effect mostly occurred when the sound and visual target stimuli took place in a temporally congruent manner.

Research has shown that short intervals (less than two seconds) are discriminated and reproduced with greater accuracy when the stimuli are auditory [Goldstone and Lhamon, 1974, Grondin et al., 1998, Lhamon and Goldstone, 1974]. Likewise, discrimination and reproduction of rhythmic patterns are superior in the auditory modality [Gault and Goodfellow, 1938].
[Repp and Penel, 2002] conducted an experiment on sensorimotor coordination. Participants were required to tap their finger in synchrony with an auditory or visual sequence. After each sequence, they had to report whether they had noticed a time-shifted event. In a second part, participants were subjected to both auditory and visual sequence and were instructed to ignore the auditory information. Results showed greater variability of movement, smaller involuntary phase correction response and poorer time-shifted event detection with a visual information than with an auditory information. In the second condition, variability was similar to the auditory sequences, and involuntary phase correction response depended more on auditory than on visual information, even though attention was always focused on the visual sequences. Moreover, people have greater difficulty synchronising finger taps with visual than with auditory sequences [Bartlett and Bartlett, 1959, Dunlap, 1910, Fraisse, 1948]. This suggests that there are different timing mechanisms in the two modalities. [Kolers and Brewster, 1985] and [Fraisse, 1948] have argued that the motor system is more responsive to auditory than to visual input. Moreover, simple reaction times are shorter with auditory than with visual stimuli, which suggests faster neural processing of auditory stimuli [Jaśkowski et al., 1990, Vroomen and Gelder, 2000]. However, deaf people synchronise better with a visual stimulus than people without hearing deficits, suggesting that auditory dominance can be influenced by experience [Iversen et al., 2015].

Sensory dominance is fragile

However, sensory dominance is fragile and can switch with intensity changes [Goldstone et al., 1959]. More intense tones and lights are judged as longer than less intense signals [Goldstone et al., 1978], so the stimulus with the longer subjective duration might be dominant [Walker and Scott, 1981]. Auditory dominance has also been found in the perception of sequence rate at fast rates (greater than 4 Hz). A variation in the rate of an auditory sequence causes the perceived rate of a constant visual sequence to change as well (auditory driving) [Gebhard and Mowbray, 1959, Myers et al., 1981, Shipley, 1964, Welch, 1999]. However, varying the rate of a visual sequence does not change the perceived rate of an auditory sequence.

On the other hand, in a Parkinson gait rehabilitation study, [Suteerawattananon et al., 2004] showed that auditory or visual perception and combined audiovisual perceptions all improve different aspects of gait. So, in some cases, the auditory and visual perception can reinforce each other.

The sound of actuators is an important aspect to consider for assistive robotics in motor therapy as the therapeutic effect of the interaction might be diminished due to the confusion created.

3.1.2 Experimental Protocol

Based on previous findings on human sensory processing and dominance, the goal of the experiment is to verify whether the sound the robot produces might be disturbing in human-robot rhythmic interactions.

Seventeen volunteers (including 8 women, mean age ± SD: 32.71 ± 12.08) participated in the experiment. They were equipped with T-Sens [tea, 2020] motion sensors on their right arm. The sensors allow us to record the movements of the participants. They are lightweight and should not hamper the participants' movements. They also wore a Tobii eye tracker at 100 Hz. Results from two participants were excluded because of technical issues and loss of data due to eye-glasses. Subjects were seated on a chair facing the Pepper robot (See Figure 3.1). Their right arm rested on a pillow so as to avoid muscle pain. The robot performed a waving-like gesture with its left elbow controlled by a sinusoidal signal. The participants were instructed to wave back at Pepper at the frequency which was comfortable for them. We were indeed interested in involuntary coordination and entrainment. We evaluated three conditions: eyes closed with only auditory perception, then with only visual perception using earplugs and finally with both auditory and visual perceptions for an overview of the conditions. The experimenter could observe the subject thanks to a webcam to ensure that the movement was properly performed and that their eyes remained closed when necessary. For each condition, the participants performed the motion nine times. Each individual has its own movement natural frequency but observation of human waving showed us that most people tend to naturally wave at 1.0 Hz. The frequency imposed by the robot was randomly chosen between 0.9 Hz, 1.0 Hz and 1.1 Hz so as to avoid frequency acclimatisation. Each waving motion lasted 10 seconds and was followed by 4 to 6 seconds rest. Waving and resting periods were indicated by an auditory signal generated by the computer. See the associated video [4] for an example of experiment in the Visual-Auditory condition. Overall the experiment lasted roughly thirty minutes.

3.1.3 Results

Coordination Results

Applying the PLV (See section 1.2.1) between the human and the robot movement, it can be observed that coordination performance is better in the visual condition (mean PLV: 0.70 ± 0.19) than in the auditory condition (mean: 0.68 ± 0.22) or the Visual-Auditory condition (mean: 0.61 ± 0.22). A 3x3 repeated measure ANOVA was conducted to examine the effect of condition and frequency on coordination performance (PLV). There was a statistically significant interaction between the effects of condition and frequency on coordination performance, p = 0.017.

Running a simple effect test on the data yields that for 0.9 Hz, there is a significant difference between the Auditory condition and the other two conditions ($p = 0.001$ and $p < 0.013$). For 1.0 Hz, there is a significant difference between the Visual-Auditory condition and the other two conditions ($p < 0.0001$ and $p = 0.002$). There is no significant difference between the conditions at 1.1 Hz.

[4] The associated video can be found at https://members.loria.fr/mjouaiti/files/EPIROB19_2.mp4.

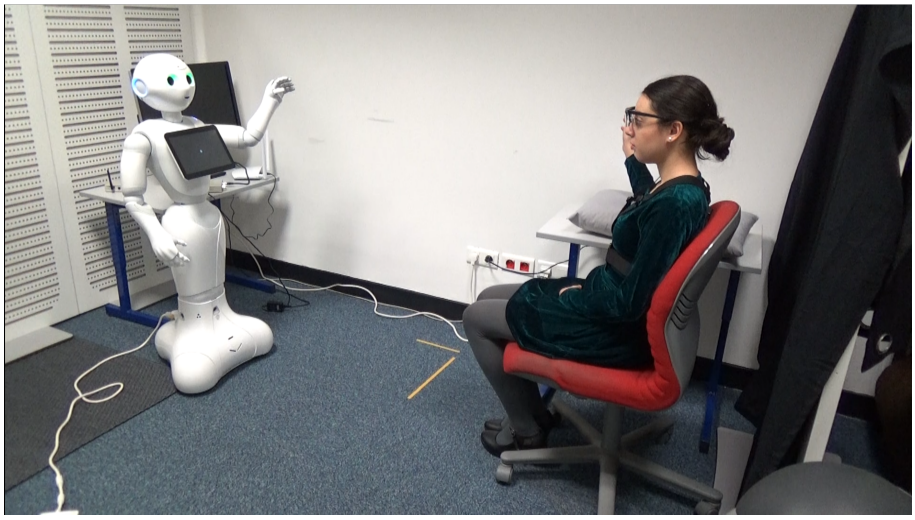


Figure 3.1: Experimental setup. The robot is placed in front of the human and waves. The human waves back with his/her arm supported by a pillow.

While the auditory and visual conditions yield similar results, the association of both signals seems to be perturbing for subjects at 0.9 Hz and 1.0 Hz.

Interestingly, there are also significant differences between the three imposed movement frequencies for the coordination performance. Participants coordinated better at 0.9 Hz (mean: 0.75±0.27) and 1.0 Hz (mean: 0.69 ± 0.29) than at 1.1 Hz (mean: 0.55 ± 0.31).

Comparing the frequencies for each condition yields that in the Visual-Auditory condition, there is a significant difference between 0.9 Hz and 1.0 Hz and between 0.9 Hz ($p \leq 0.05$) and 1.1 Hz ($p \leq 0.001$). For the Visual condition, there is a significant difference between 0.9 Hz and 1.1 Hz ($p \leq 0.01$) and between 1.0 Hz and 1.1 Hz ($p \leq 0.0001$). In the Auditory condition, all the frequencies are significantly different ($p \leq 0.01$ between 0.9 Hz and 1.0 Hz, $p \leq 0.0001$ between 0.9 Hz and 1.1 Hz and $p \leq 0.0001$ between 1.0 Hz and 1.1 Hz).

Finally, five participants coordinated better in the auditory condition, seven coordinated better in the visual condition and only three coordinated slightly better with both the auditory and visual perceptions.

Eye Tracker Results

The data from the eye tracker were meant to show us where the participants were really looking, especially in the visual-auditory condition. Indeed, in a preliminary experiment without the eye tracker, most subjects reported that they were bored during the task and started thinking about something else. They lost focus of attention on the robot and then remembered that they were supposed to look at the robot. They also said that this happened less in the visual condition since they had to focus more on the robot. In this preliminary experiment, we had no significant difference between the conditions. Consequently, our working hypothesis was that participants looked less at the robot in the visual-auditory condition and thus relied on their auditory perception. This would have explained the lack of difference. However, when reproducing the experiment with the eye tracker data, we were unable to find such a difference in gaze and participants really looked as much at the robot in both visual and auditory-visual conditions. Besides, with the eye tracker, the difference is significant between the conditions.

It can be assumed that the eye tracker made participants self-conscious about where they were looking and only one subject made the observation that he lost focus of attention on the robot. This suspected "eye-tracker awareness" is was observed [Risko and Kingstone, 2011] who showed that participants feel the eye-tracker as a social presence and modulate their looking behaviour accordingly.

3.2 Involuntary Coordination in Children

In the following experiment, we wanted to observe involuntary coordination with children and their perception in a human-robot rhythmic interaction where the robot is unable to adapt to them.

3.2.1 Experimental Protocol

In order to reach a large number of children, we installed the Pepper robot (Softbanks robotics) at a science fair. The people were informed that they were taking part in an experiment on rhythmic movements and that data were acquired. As groups came by our stand, a child was chosen in each group to interact with the robot. This child was seated against a black sheet and was instructed to just wave back at the robot with no constraints whatsoever, the aim being to observe a natural interaction. The interaction lasted 20 seconds. At the end, the robot thanked the participant and explained the experiment to the children. The children were told that the robot had adapted to their movement even though it was set to be the leader of the interaction. The waving frequency was randomly chosen between [0.8, 0.9, 1.0, 1.1, 1.2]Hz. The robot movement followed a sinusoid and commands were sent every 50 ms. The robot recorded a video at 20 Hz of each interaction, as well as the angular values of the left elbow joint which was used to wave.

Thirty-five children took part in the experiment. The experiment was anonymous and we requested no information from the children, except their first name (which was not saved) to personalise their experience with the robot. Ten children were eliminated because the robot camera was too high and did not capture the movement. One child was discarded because of technical difficulties with the robot. Five children did not adapt at all so they are not considered in the following study. Some children were not really focused on the experiment since some of them were very uncomfortable to be the center of attention and others were highly distracted by their friends. This may explain the lack of adaptation observed in a few children. Finally, nineteen children (11 girls, 8 boys from age 7 to 18) are included in the analysis.

The children can be divided into three age groups: elementary school (6-9 years old), middle school (10-12 years old) and high school (13-16 years old).

3.2.2 Results

One very interesting observation is that no matter the nature of the gesture, the children always ended up being synchronised with the robot. We recorded hand-only waving, rotational hand waving, elbow-based waving, very large and very small amplitudes. Some children even switched to an elbow-based waving after some time, to match the robot gesture. While most children directly performed the movement in phase with the robot, four of them started with an anti-phase movement and switched to phase after some delay (mean $\pm$ SD: 6.875 s $\pm$ 3.84). On the contrary, one child started in phase and switched to anti-phase afterwards (See Fig. 3.2, 3.3 and 3.4 for examples of interactions).

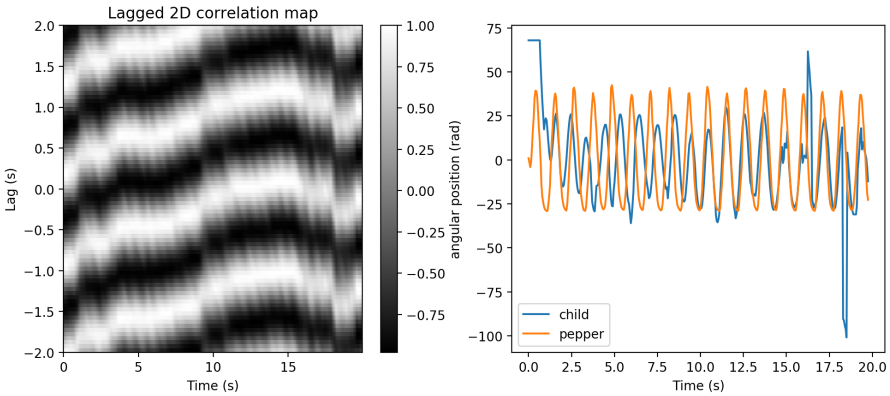


Figure 3.2: Example of interaction with switch between anti-phase and phase

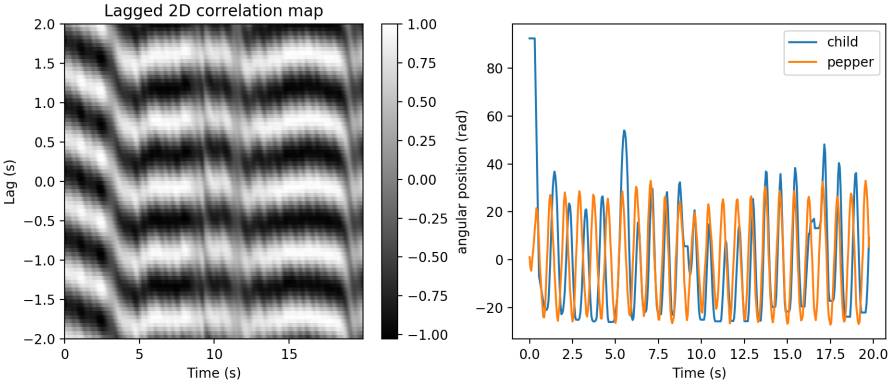


Figure 3.3: Example of interaction with short adaptation period

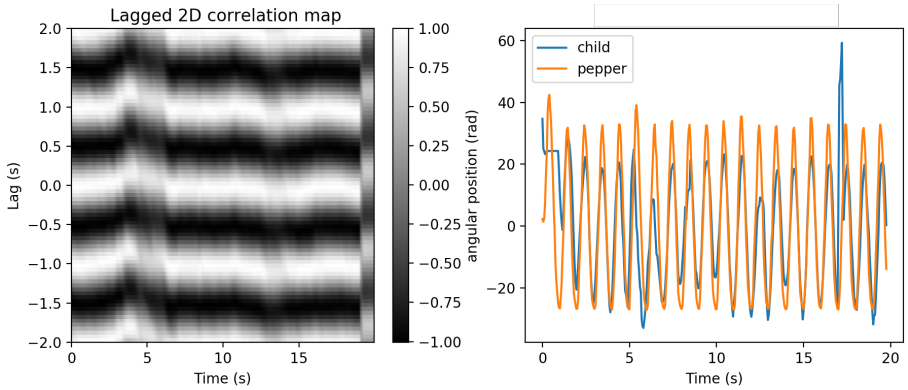


Figure 3.4: Example of interaction that would be best described as imitation, rather than intentional coordination

The interaction lasted 20 seconds, which seemed quite long to the children. Some of them stopped waving after a few seconds but were encouraged to continue. Some children also asked if it was over soon around the middle of the interaction. While this may seem quite long, some of them needed as much as 16 seconds to achieve motor coordination. Figure 3.5 shows a synchrosqueezing

analysis of these interactions.

When asked, most children were convinced that the robot adapted to their movement even though the robot had a set movement. This is an interesting observation on perception since the participants were subjected to unintentional motor coordination but they did not realise it. Is this due to a lack of awareness of what the body is really doing or an egocentric vision that everything adapts to oneself?

Besides, it appears that we witnessed both imitation (some of the children were immediately in phase with the robot, sometimes even reproducing a similar amplitude) and unintentional motor coordination, as some of them clearly had an adaptation phase. Imitation was more present in the youngest age group.

Conclusion

Considering previous findings on human sensory processing and dominance, we suspected that combined audiovisual perceptions might be detrimental for the interaction. The first study confirms that the auditory condition yields the best results for rhythmic interactions but the visual condition appears to be adequate too. However, the combination of both visual and auditory perceptions of a movement can be deemed perturbing while interacting with the robot. This was to be expected since both visual and auditory signals from the robot are congruent both temporally and spatially, so they would interfere with each other in the human perception system. This is also meant to be a cautionary tale: multi-sensory experience can be confusing in rhythmic human-robot interactions. This could be an important point to factor in, especially in therapeutic robotics. Even when the robot-therapy is effective, it might have been even better with the correct environmental settings. We unfortunately do not have a satisfactory solution to remove robot noise yet. One can easily see the technical limitations this could incur while attempting to maintain a natural interaction. Ideally, robots should be build with silent motors.

In the second study, we highlight that humans interacting rhythmically are subjected to involuntary coordination, but yet, retain individual movement characteristics (such as movement type, amplitude...) despite the adaptations. This is a direct evidence of the *maintenance effect*. A robot interacting with a human should also be able to exhibit such characteristics, as humans expect them to. One way to achieve this is to endow robot controllers with adaptive mechanisms to achieve more bio-realistic movements. We will attempt to do so in the following chapter.

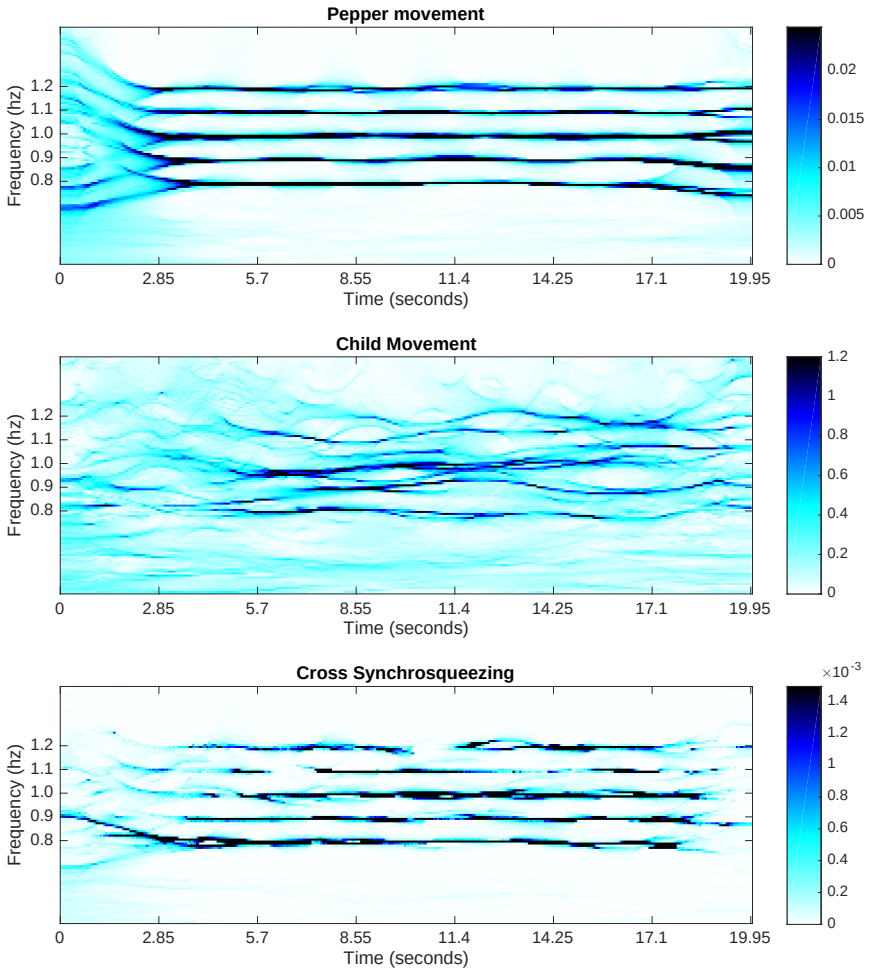


Figure 3.5: Superposed Synchrosqueezing for the 19 interactions. Top: Synchrosqueezing of the robot movement. Middle: Synchrosqueezing of the children's movements. Bottom: cross-synchrosqueezing between the robot and the children's movements.

Part II

The Bio-Inspired Controller

Chapter 4

Bio-inspired Control

Robot control usually relies on mechanics and strongly depends on an accurate robot model. On the other hand, some controllers also take bio-inspiration into account, considering sensory (proprioceptive and exteroceptive) feedback. In this chapter, we will try and understand human movement generation, from its genesis to its execution for voluntary movements and for rhythmic/stereotyped movements. We will also introduce the literature on bio-inspired controllers.

4.1 The Anatomy of Human Movement

4.1.1 Voluntary Movements

Generation of voluntary movements in humans is a complex process which involves many different brain regions [Cheney, 1985]. The motor cortex is the main actor in the planning, control and execution of voluntary movements. It can be divided into the primary motor cortex, the premotor cortex and the supplementary motor area. It is tightly connected to the Posterior Parietal Cortex for spatial sensorimotor transformation and primary somatosensory cortex for feedback (See Fig. 4.1). Outside the cortex, the cerebellum and basal ganglia are also involved. Although their contribution is still not completely understood, each brain region has a role in the movement generation, from sensory integration to motor execution (See Fig. 4.2 for a schematic representation).

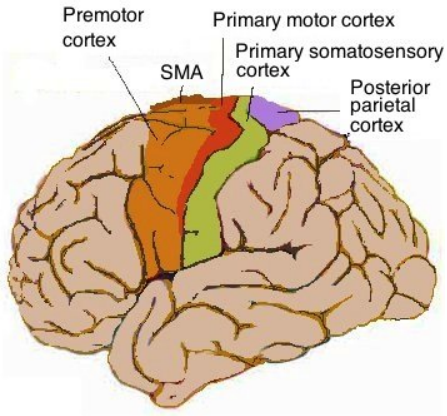


Figure 4.1: Motor cortex. *Reproduced from [Botrel, 2018]*

Visuomotor Processing

Visuomotor integration is the coordination of neuronal activity between visual-related and motor-related parts of the brain in order to plan motor actions, taking visual perception into account. The posterior parietal cortex assesses the environment and the context and transforms multisensory (vision, proprioceptive, exteroceptive) information into motor commands [Iacoboni, 2006].

Motor Planning

The posterior parietal areas then send this information to the premotor cortex and to the supplementary motor area. The premotor cortex is believed to be involved in the sensory guidance of movement, posture regulation and in the control of the more proximal muscles and trunk muscles of the body, i.e. it helps orient and balance the body [Passingham, 1985]. The supplementary motor area appears to be involved in the planning of complex movements and in coordinating the two sides of the body. The supplementary motor area and the premotor cortex both send information to the primary motor cortex as well as to brainstem motor regions.

Motor programs are generated in the basal ganglia. The basal ganglia organise motor programs for complex movements and regulate the activity of the premotor cortex [Turner and Desmurget, 2010]. Consequently, damage to this region may result in inappropriate movements [Gelb et al., 1999]. The likely role of the basal ganglia is to regulate the activity of the motor and premotor cortices and to select the appropriate actions and send output to other subcortical brain regions and to the motor cortex.

Motor Execution

The primary motor cortex (M1) is one of the principal brain areas involved in motor function. Its role is to generate neural activity that controls the execution of movement. Signals from one side of the hemisphere activate muscles on the opposite side of the body.

Motor neurons and interneurons can be found in the motor cortex, in the brainstem or in the gray matter on the inside of the spinal cord. Motor units are composed of a motor neuron, its axon and the muscle fibers it innervates. Motor units can innervate several muscle fibers, but each fiber is only innervated by one motor unit. Motor neurons can directly or indirectly control effector organs when they fire, as all the associated muscle fibers contract [Purves et al., 2001]. Force of muscle contraction is determined by the size of the motor units and the number of innervated fibers. The cerebellum seems to be involved in postural balance, muscle tone regulation and appropriate control of antagonist muscles. It also manages the timing and coordination of motor programs and is responsible for short-term adaptation and corrects errors between visual perception and motor output [Thach et al., 1992]. Moreover, it is involved when learning new motor programs, such as a new sport or a new music instrument.

4.1.2 Automatic Movements

While being voluntary, some movements are automatic and almost unconscious, such as breathing, swallowing, walking... In 1911, T. Graham Brown showed with a decerebrated cat that the spinal cord could generate a locomotor rhythm without input from the higher centers or afferent feedback. This paved the way for the discovery of Central Pattern Generators (CPGs). CPGs [Brown, 1912, Holst, 1935] are biological neural structures found in the central nervous system of vertebrates [Grillner and Wallen, 1985] or in some ganglia of invertebrates [Marder et al.,

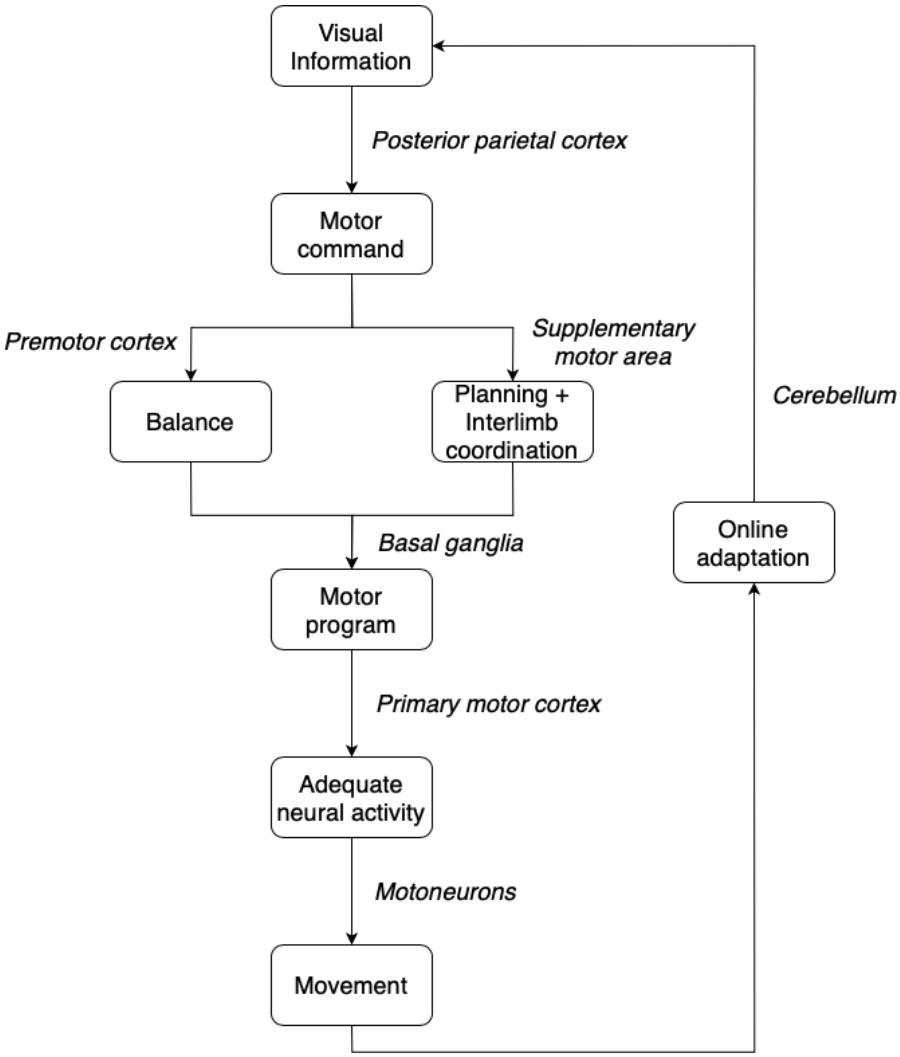


Figure 4.2: Overview of the motor generation process in the human brain for voluntary movements

2005, Selverston, 2005]. They are source of neural activity that controls rhythmic and stereotyped behaviours, such as locomotion, swimming, flying, breathing, swallowing, whisker movements...

CPGs can generate a rhythmic signal, even when no input signal is provided, modulated by afferent sensory feedbacks. For example, in the case of the walking gait, a baseline movement which does not depend on sensory inputs is automatically generated. This baseline movement can, however, be adjusted to specific situations: a slope, a faster treadmill, a pebble in a shoe... Note that in the last case, a sensory perturbation on one foot must affect the whole gait. This is possible since CPGs are organised in distributed networks.

CPGs are extremely versatile structures, not limited to a single function and capable of self-reorganisation. Besides, they are not restricted to the generation of rhythmic patterns, but can generate a wide range of behaviours, including discrete movements.

While their role in locomotion has been recognised and widely studied, their implication in upper limb movements is strongly suspected [Schaal, 2006, Zehr et al., 2004].

Mesoscopic CPGs are usually based on a pair of half-center neurons [Brown, 1914, Grillner and Wallen, 1985], controlling the extensor and flexor muscles. Half-center oscillators are composed of two neurons which would not have the ability to oscillate individually but their coupling leads to an oscillatory behaviour. With the half-center model, each limb is controlled by one CPG which contains two groups of neurons, each controlling the activity of the flexor or the extensor motor neurons. Moreover mutual inhibition ensures that only one group is active at a time since inhibition and activation of antagonist motor neurons are tightly coupled. When the excitability of a group decreases under a given threshold, the other is released from inhibition, thus triggering a phase switch.

4.2 CPG Controllers

CPGs have several interpretations which differ according to the level of bio-inspiration [Ijspeert, 2008, Yu et al., 2014]. Biologists usually present CPGs as complex structures which encompass sensory neurons, motor neurons and interneurons and receive sensory feedback [Rybak et al., 2006, Cattaert and Le Ray, 2001]. However, in computational neuroscience, some aspects tend to be neglected for simplicity's sake. While some studies endeavour to be biologically accurate [Nassour et al., 2019, Taga et al., 1991, Manoonpong et al., 2008], others present simplified interpretations [Mori et al., 2004, Wu and Ma, 2010].

The interest of using CPGs in robotics is nowadays widely recognised, so much so that a great variety of possibilities has been proposed (see [Yu et al., 2014, Ijspeert, 2008] for reviews). The term *CPG* refers to a network of coupled oscillators. Non-linear models of CPGs, composed of relaxation oscillators, can be entrained by an oscillatory input or with a coupled CPG if the coupling is strong enough or if the input frequency is close enough to the intrinsic frequency of the oscillator, thus ensuring coordination. Even though CPGs have mostly been used for robotic locomotion [Taga, 1995, Shan and Nagashima, 2002, Ayers, 2004, Kamimura et al., 2005, Arena et al., 2006, He et al., 2006, Pelc et al., 2008, Sprowitz et al., 2010, Liu et al., 2011, Pinto et al., 2012, Wang et al., 2013], see [Ijspeert, 2008] for a review, some studies explore how CPGs affect upper limb control as well [Williamson, 1998b, Yang et al., 2010]. The strength of CPGs resides in their self-synchronisation ability, their oscillating stability despite perturbation and the variety of behaviours they can generate. Moreover, plasticity mechanisms can be integrated, thus making the CPG even more robust and versatile. This is actually essential to have adaptive robot controllers.

A great variety of oscillators can be found in the literature at different modelling scales;

amongst the most popular, to name a few: microscopic [Hodgkin and Huxley, 1952] which models single neurons; mesoscopic [Rowat and Selverston, 1993, Matsuoka, 1985] which models populations of neurons, taking biological mechanisms into account and macroscopic [Hopf, 1942] which also models populations of neurons but with no bio-inspiration.

The non-linear Hopf oscillator [Hopf, 1942] is particularly popular in robotics. It has been widely applied to robot locomotion [Li et al., 2013, Matos and Santos, 2010, Ijspeert, 2004, Brambilla et al., 2006, Fuente et al., 2013, Buchli and Ijspeert, 2008, Righetti and Ijspeert, 2006, Righetti and Ijspeert, 2008] and robot swimming [Seo et al., 2010, Hu et al., 2011, Zhou and Low, 2012, Hu et al., 2014]; but also to robot hopping [Buchli et al., 2005, Buchli et al., 2006], drumming [Degallier et al., 2006], crawling, reaching [Degallier et al., 2008], the flight of a robotic bat [Chung and Dorothy, 2010]...

Introduced in 1985, the Matsuoka model [Matsuoka, 1985] is undoubtedly the most well-known and employed neural oscillator. In the original paper, a single neuron defined by two differential equations was studied, as well as its behaviour in networks of n coupled neurons. Since [Taga et al., 1991], it has become customary to couple two neurons in CPGs. While this model has mostly been used for robotic biped locomotion [Liu et al., 2006, Liu et al., 2007, Liu et al., 2008, Panwart and Kumar, 2012, Liu et al., 2012, Al-Busaidi et al., 2012], some original works applied it to achieve human-robot handshaking [Kasuga and Hashimoto, 2005], a chewing robot [Xu et al., 2009] or traffic light regulation [Fang et al., 2013].

Chapter 5

Extending the Rowat-Selverston CPG

The oscillating neuron employed in this thesis is the Rowat-Selverston neuron [Rowat and Selverston, 1993]. It is inspired by the CPG of the gastric mill of the lobster which controls its chewing movement. The cell model is a generalised Van der Pol oscillator and can exhibit several behaviours: endogenous oscillations, plateau potential, post-inhibitory rebound and post-burst hyperpolarisation [Marder and Bucher, 2001]. This neuron is better suited for our purpose as it is extremely versatile and leaves room for improvement thanks to plasticity mechanisms [Jouaiti and Henaff, 2019a].

5.1 The Rowat-Selverston CPG

5.1.1 The Rowat-Selverston Oscillator

Mathematical form

The free form of the Rowat-Selverston model of a cellular neuron is described by the equations (see [Rowat and Selverston, 1993] for details):

$$\begin{aligned} &\tau_m \dot{V} + V - A_f \tanh\left(\frac{\sigma_f}{A_f} V\right) + q = 0 \\ &\tau_s \dot{q} = -q + \sigma_s V \end{aligned} \tag{5.1}$$

with V the cellular membrane potential (or fast current), τ_m the time constant of the cellular membrane, $F(V) = V - A_f \tanh \frac{\sigma_f}{A_f} V$ is the voltage current I-V curve. F(V) is N-shaped, A_f determines the width of the N-Shape and σ_f the degree of the N-Shape. $F(V)$ needs to be sufficiently N-Shaped for the neuron to oscillate, this implies $\sigma_f > 1$ (See Fig. 5.1). q the slow current, τ_s is the time constant of slow current activation and $q_{\text{inf}} = \sigma_s V$ its I-V curve. σ_s and σ_f represent respectively the conductance of slow and fast currents, A_f influences the amplitude of V.

The oscillator can be rewritten as a Lienard system and forced with an external signal F. This form which will be employed in the rest of this thesis is given by (See Appendix A.1 for mathematical details):

$$\dot{V} = y + \epsilon F \tag{5.2}$$

$$\dot{y} = \frac{1}{\tau_m}\left(\sigma_f - \frac{\tau_m}{\tau_s} - 1 - \sigma_f \tanh^2\left(\frac{\sigma_f}{A_f} V\right)\right) y - \frac{1+\sigma_s}{\tau_s \tau_m} V + \frac{A_f}{\tau_s \tau_m} \tanh\left(\frac{\sigma_f}{A_f} V\right) \tag{5.3}$$

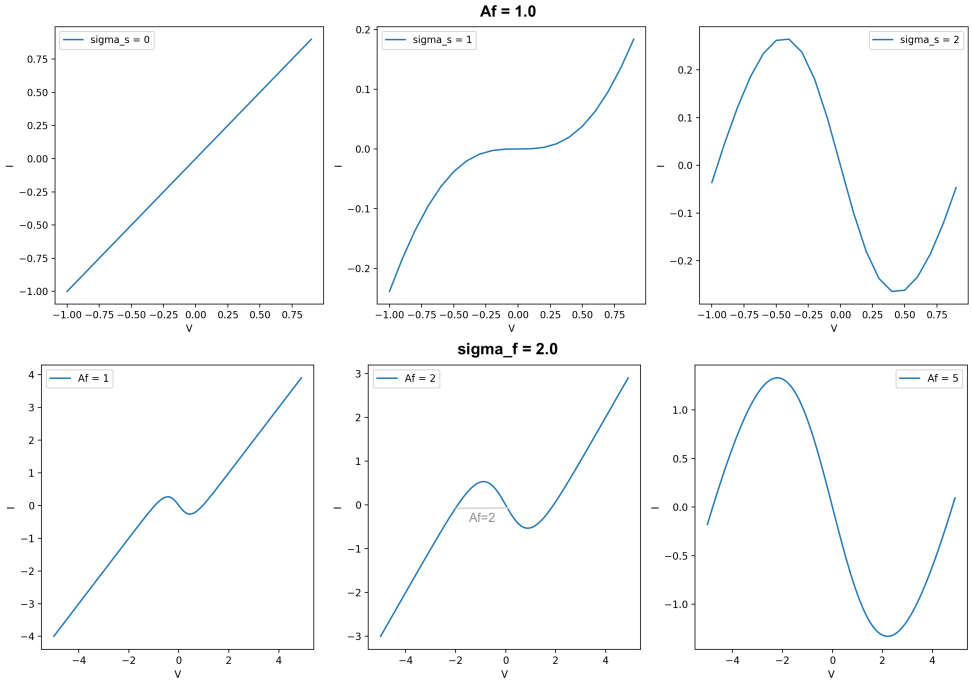


Figure 5.1: Current voltage I-V curves for the cellular membrane with various values of σ_f and A_f

As shown in [Rowat and Selverston, 1993], when unforced ($F = 0$), the intrinsic frequency of the neuron oscillations depends on τ_m, τ_s, σ_f and σ_s (See Fig. 5.2). Since the Rowat-Selverston oscillator can be written into a Van der Pol form (See Appendix A.1) and its parameters identified, the intrinsic frequency of the oscillator can thus be defined as:

$$f = \frac{1}{2\pi}\sqrt{\frac{\sigma_s}{\tau_m \cdot \tau_s}} \tag{5.4}$$

Intrinsic Modes

Biological systems such as stomatogastric neurons can exhibit several intrinsic modes, more commonly endogenous bursting (oscillations), post-inhibitory rebound and plateau potentials [Marder and Bucher, 2001]. The Rowat-Selverston oscillator also presents those behaviours, as shown in Figure 5.3.

Endogenous bursting can only be achieved if $\sigma_f > 1 + \frac{\tau_m}{\tau_s}$ $(\tau_m \ll \tau_s)$ and $\sigma_s > 1$. If $\sigma_f = 1$, $(\tau_m \ll \tau_s)$ and $\sigma_s > 1$, the oscillations will be damped. Otherwise, if $\sigma_f = 0$, there are no oscillations and the oscillator can exhibit plateau potentials-like behaviour. See table 5.1 for a summary of the oscillator behaviours depending on relevant parameters.

5.1.2 The CPG Architecture

Figure 5.4 shows a schematic representation of the CPG architecture. It is based on the model of half-center CPG proposed by McCrea and Rybak ([Rybak et al., 2006]). It takes inspiration from biological structures, such as the rhythmic layer, modulating layer, interneurons, sensory

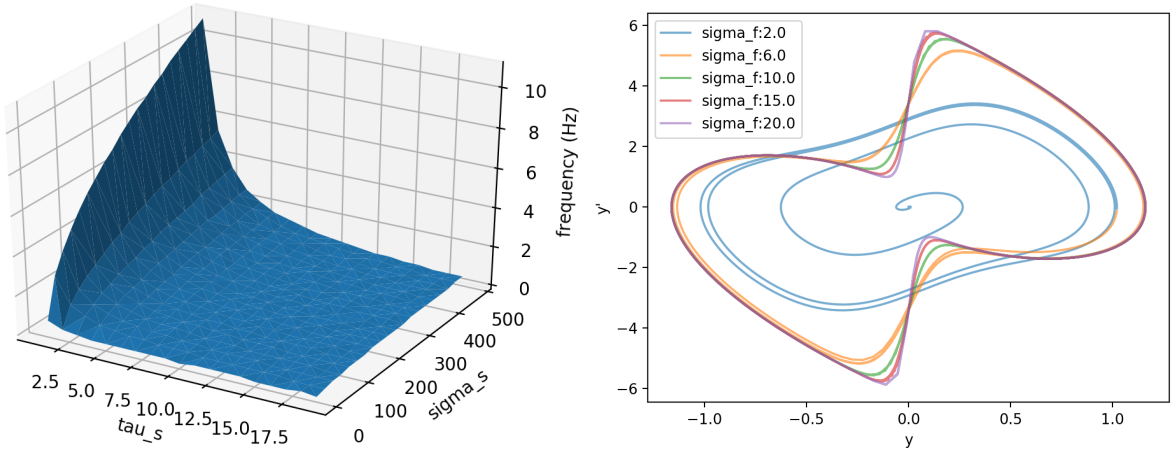


Figure 5.2: Left: Intrinsic frequency of the oscillator depending on the values of σ_s, τ_m ($\tau_s = 10\tau_m$). $\sigma_f = 2.0$. Right: Evolution of the limit cycle in the phase plane. The limit cycle begins as relatively circular and, with varying σ_f, becomes increasingly sharp

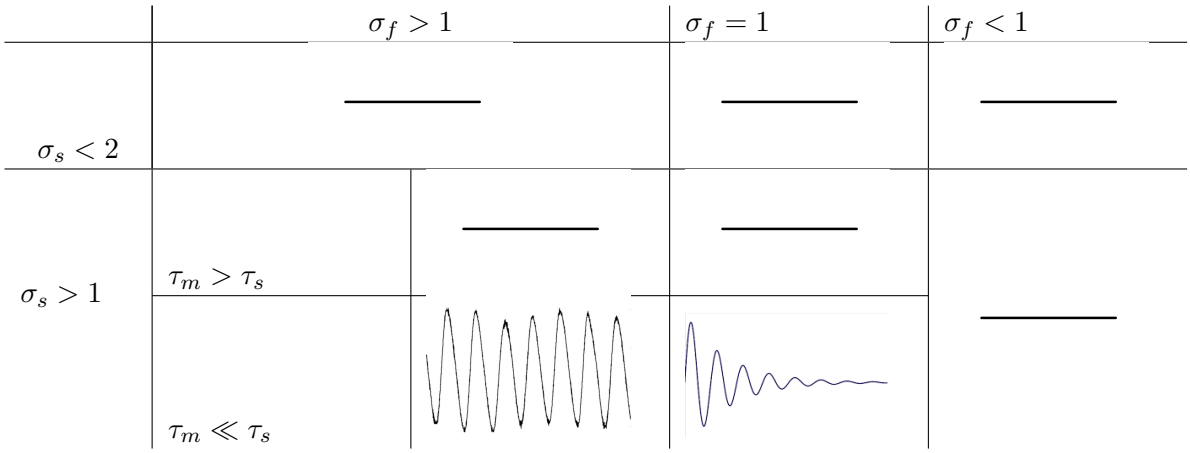


Table 5.1: Summary of the parameters leading to a rhythmic or non-rhythmic intrinsic mode

neurons, etc. Its architecture is divided into three layers: Rhythm Generator layer (composed of an inhibitory pair of oscillatory neurons), Pattern Formation layer (composed of interneurons) and Motor layer (composed of motor neurons).

The rhythm generator cells consist of Rowat-Selverston oscillators which can be coupled together as follows:

$$\dot{V}_{\{E,F\}} = y_{\{E,F\}} - W_{inhib}\frac{y_{\{E,F\}}}{1+e^{-4y_{\{F,E\}}}} + \epsilon_{\{E,F\}}F \tag{5.5}$$

$$\begin{aligned}\dot{y}_{\{E,F\}} = \frac{1}{\tau_m}\left(\sigma_f - \frac{\tau_m}{\tau_s} - 1 - \sigma_f \tanh^2\left(\frac{\sigma_f}{A_{f_{\{E,F\}}}}V_{\{E,F\}}\right)\right)y_{\{E,F\}} - \\ \frac{1+\sigma_{s_{\{E,F\}}}}{\tau_s\tau_m}V_{\{E,F\}} + \frac{A_{f_{\{E,F\}}}}{\tau_s\tau_m}\tanh\left(\frac{\sigma_f}{A_{f_{\{E,F\}}}}V_{\{E,F\}}\right)\end{aligned} \tag{5.6}$$

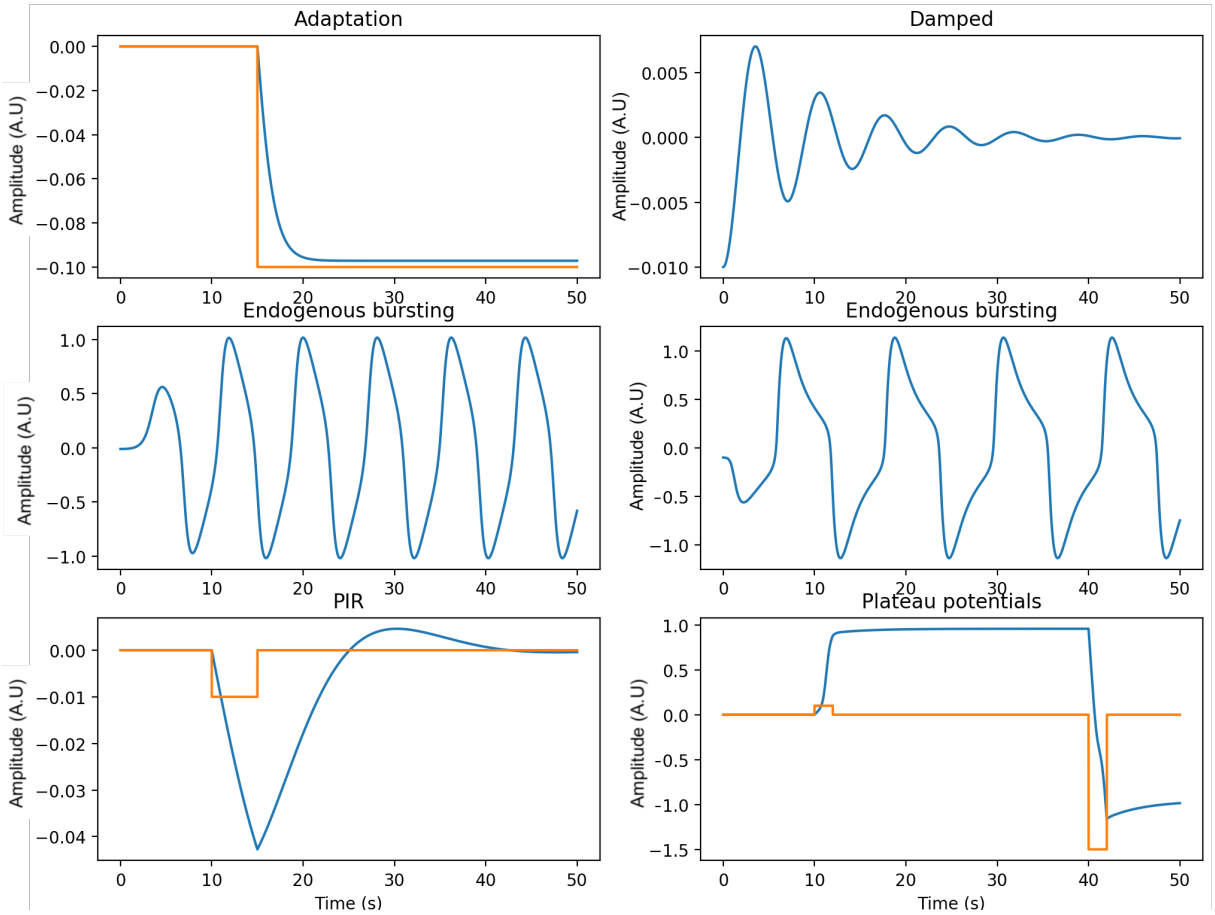


Figure 5.3: Intrinsic modes of the Rowat-Selverston neuron. In blue: the oscillator output. In orange: the input signal when applicable, otherwise there is no input signal. A: Discrete adaptation ($\sigma_s = 2$, $\sigma_f = 0$, $\tau_m = 0.5$, $\tau_s = 5$). B: Damped oscillations ($\sigma_s = 2$, $\sigma_f = 1$, $\tau_m = 0.5$, $\tau_s = 5$). C: Endogenous bursting ($\sigma_s = 2$, $\sigma_f = 2$, $\tau_m = 0.5$, $\tau_s = 5$). D: Endogenous bursting ($\sigma_s = 2$, $\sigma_f = 4$, $\tau_m = 0.5$, $\tau_s = 5$). E: Post-inhibitory rebound ($\sigma_s = 2$, $\sigma_f = 4$, $\tau_m = 10$, $\tau_s = 6$). F: Plateau potential ($\sigma_s = 0$, $\sigma_f = 2$, $\tau_m = 1$, $\tau_s = 0.2$)

with $\{E, F\}$ indicating whether the equation pertains to the extensor or the flexor cell and W_{inhib} the mutual inhibition.

Interneurons of pattern formation layer (neuron PF), sensory neurons (neuron SN) for proprioceptive feedback (e.g. measured values from robot sensors) and motor neurons (neurons MN) for efferent signals (e.g. position, velocity commands), are defined as a sigmoid function ([Nassour et al., 2014, Debnath et al., 2014]):

$$PF(V) = \frac{1}{1 + e^{\frac{-V}{2}}} \tag{5.7}$$

$$SN_s(v_{mes}) = \frac{1}{1 + e^{\alpha_s v_{mes}}} \tag{5.8}$$

$$MN(PF, SN_s) = \frac{1}{1 + e^{\alpha_m (PF - SN_s)}} \tag{5.9}$$

with $\alpha_s = -0.06$ and $\alpha_m = 3$. These coefficients were chosen to match the parameters of the

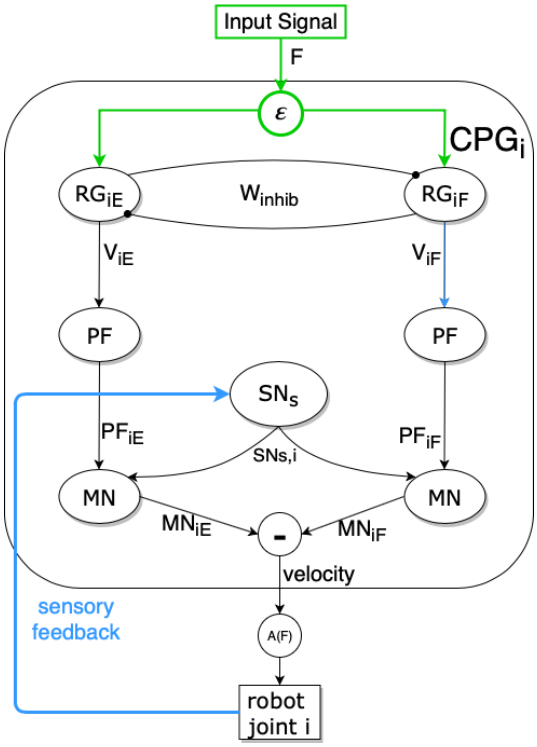


Figure 5.4: Generalised CPG architecture. When controlling a musculoskeletal model, the extensor and flexor muscles can be controlled independently with the CPG extensor and flexor outputs. This is, however, not the case for robots, so it has become common practice to subtract the outputs to obtain a single value

robot. For instance, the sigmoid slope of the sensory neuron is determined by the range of values of the speed. v_{mes} is a proprioceptive feedback from the robot (e.g. measured angular values: position, velocity, torque).

5.2 Integrating the CPG with Adaptive Mechanisms

5.2.1 Frequency Learning

A non-linear oscillator has the property of self-synchronisation with an oscillating external signal applied as its input, provided the frequency of this signal is close enough to the intrinsic frequency of the oscillator. Implementing a mechanism of frequency learning in a CPG is thus particularly interesting because it allows to synchronise the rhythmic activity of the CPG with the external signal even if the frequency of this signal is significantly different from the intrinsic one of the CPG ([Yazdani et al., 2017, Ijspeert, 2008]). [Righetti et al., 2006] proposed a model of frequency learning for a Van der Pol oscillator called Dynamic Hebbian learning (See Appendix A.2). They showed that this rule allows the oscillator to adapt its intrinsic frequency to synchronise with an external signal. The oscillator retains the learned frequency, even after the input signal is cut. It has also been applied to the Hopf oscillator and to the Fitzhugh-Nagumo oscillator in [Righetti et al., 2006]. In [Jouaiti et al., 2018], we applied the dynamic Hebbian learning rule proposed by

Righetti et al. to equation (5.2), which yields (See Appendix A.3 for details):

$$\boxed{\dot{\sigma_s} = 2\epsilon F\sqrt{\tau_m\tau_s}\sqrt{1+\sigma_s-\sigma_f}\frac{y}{\sqrt{V^2+y^2}}; \qquad \sigma_f < 1+\sigma_s} \tag{5.10}$$

5.2.2 Neuronal Plasticity for Amplitude Learning

Additionally, to improve the control realised by the CPG, we propose to learn the amplitude of neuronal oscillations by learning A_f depending on $F(t)$.

A_f contributes to the amplitude of the output of the CPG (efferent signals). When A_f is high, σ_s will oscillate globally before reaching stability. In equation 5.1, the expression $A_f \tanh(\frac{\sigma_f}{A_f}V)$ influences the amplitude of V and hence of the CPG output. If the amplitude is too large, the CPG becomes unstable due to the rapid switchings of the sigmoid function of interneurons located in the pattern formation layer, and if it is too small, the learning is slowed down (See Fig. 5.5). It is thus interesting to adapt the amplitude of the neuron oscillations in accordance with the applied signal $F(t)$. Therefore, one solution consists in using the error between the square of $F(t)$ and the square of the argument of $tanh()$ in equation (A.2) to match the amplitude of V with $F(t)$:

$$\boxed{\dot{A_f} = -\mu\left(\left(\nu\frac{\sigma_f V}{A_f}\right)^2 - F^2\right)} \tag{5.11}$$

where ν is a scale factor and μ a learning step.

The presence of A_f in the equation makes it a closed loop, guarantying the same end value for A_f no matter the initial value. Empirically, we found that 20 was the best value for ν.

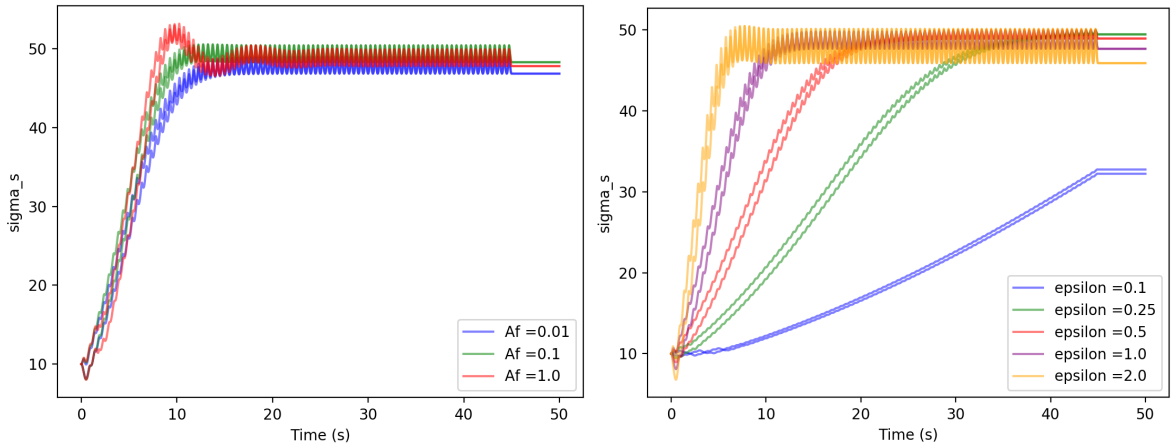


Figure 5.5: Evolution of σ_s according to various values of A_f (Left) and ϵ (Right)

5.2.3 Synaptic Plasticity for ϵ

We can also adapt ϵ in order to maintain an effective value of ϵ. This is particularly interesting when the input amplitude varies over time. The parameter ϵ in Eq. 5.2 acts like a learning step for σ_s (local oscillation) and determines how much σ_s will oscillate when a new input signal is applied before reaching stability. So, ϵ can be considered as a synaptic weight that could enable the CPG to better sense the external signal $F(t)$ by normalising it to magnitude 1. Besides, it

was empirically determined that if ϵF is too small (< 1), σ_s changes are too slow and may never reach a stable final value and when ϵF is too large (> 1), σ_s becomes unstable. Optimal results are obtained when the amplitude of product ϵF equals 1. From there, a learning equation of ϵ can be based also on a quadratic error pondered by a variable gain that limits extreme values of $F(t)$:

$$\boxed{\dot{\epsilon} = \lambda tanh(\xi F)\left(1 - (\epsilon F)^2\right)} \tag{5.12}$$

with ξ an empirically determined gain ensuring that the term inside the *tanh* is large enough (in our case, $\xi = 100$ yields good results). This term guarantees that learning occurs only when $F(t)$ is not equal to zero.

See Figure 5.6 for a comparison between the CPGs with and without plasticity mechanisms.

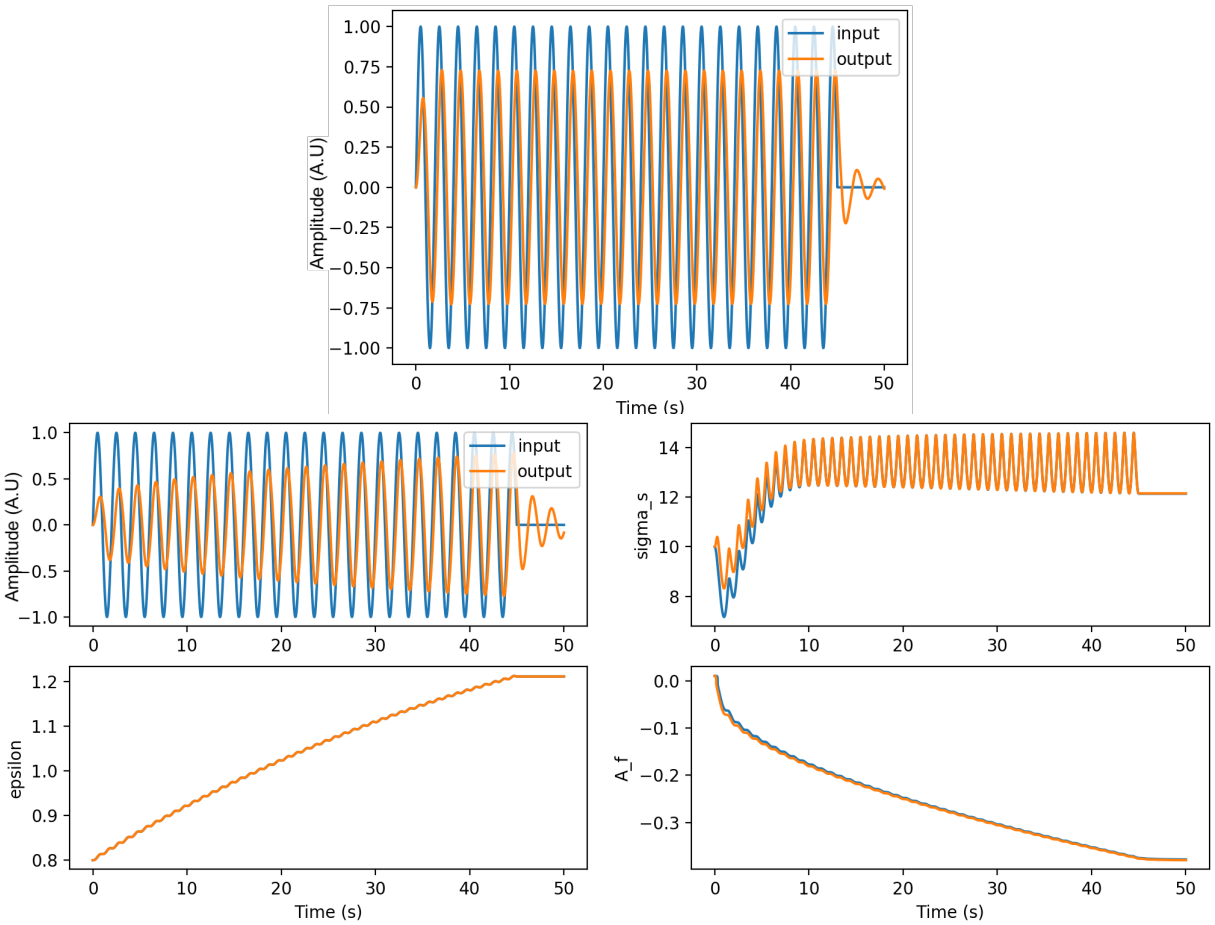


Figure 5.6: Top: Rowat-Selverston CPG as originally defined when subjected to a $1Hz$ signal. Bottom: CPG endowed with the three plasticity mechanisms previously defined and the evolution of σ_s, ϵ and A_f

5.3 Discrete Operating Mode

Discrete and rhythmic movements have been widely studied in motor neuroscience. Scientists have been wondering in which proportions movements are controlled by the central nervous

system or attributed to intrinsic limb mechanics, how the brain can create complex movements with a combination of discrete and rhythmic movements and how those transitions are made.

Discrete movements are defined as singularly occurring events preceded and followed by a period without motion; rhythmic movements are continuous and recurring periodically. It was proposed that rhythmic movements might be a concatenation of discrete movements [Baratto et al., 1986, Feldman, 1980] or on the contrary, discrete movements might be aborted rhythmic movements [Mottet and Bootsma, 1999, Guiard, 1993]. In an attempt to identify the neural structures involved, a fMRI study by [Schaal et al., 2004] revealed that rhythmic movements involve only a subset of the cortical activity observed in discrete movements.

Though those problems are not solved yet, it is obvious that complex tasks involve both discrete and rhythmic movements. If we want robots to be able to reproduce those tasks, their controllers need to be able to realise both and easily switch from one mode to the other. Several such structures have already been proposed, they are mainly a combination of rhythmic (Hopf, Matsuoka [Matsuoka, 1985]) and discrete (VITE model [Bullock and Grossberg, 1988]) pattern generators: Hopf - VITE [Degallier et al., 2011] or the Matsuoka - VITE [Sternad et al., 2000]. [de Rugy and Sternad, 2003, Sternad, 2008] proposed a model based solely on the Matsuoka oscillator but the discrete movement generated is merely the abortion of a rhythmic movement. As underlined by [Degallier and Ijspeert, 2010], the Matsuoka oscillator is intrinsically rhythmic and cannot generate real discrete movements.

5.3.1 CPG Behaves like a PID Controller

In [Rowat and Selverston, 1993], it was determined that the neuron cannot oscillate for $\sigma_f = 0$, since $\sigma_f > 1 + \frac{\tau_m}{\tau_s}$ is required for the neuron to oscillate. Let us apply $\sigma_f = 0$ to unforced 5.2:

$$\begin{aligned} \dot{V} &= y \\ \dot{y} &= -\left(\frac{1}{\tau_m} + \frac{1}{\tau_s}\right) y - \frac{1+\sigma_s}{\tau_s \tau_m} V = 0 \end{aligned} \tag{5.13}$$

Replacing y with $\dot{V}$ yields:

$$\ddot{V} + \frac{\tau_s + \tau_m}{\tau_s \tau_m}\dot{V} + \frac{1+\sigma_s}{\tau_s \tau_m} V = 0 \tag{5.14}$$

In a reaching task, the CPG input would be the distance between a given target position and the end effector. As such, the forcing term can be viewed as the error term $e(t)$, yielding:

$$\begin{aligned} \dot{V} &= y + e(t) \\ \ddot{V} + \frac{\tau_s + \tau_m}{\tau_s \tau_m}\dot{V} + \frac{1+\sigma_s}{\tau_s \tau_m} V &= 0 \end{aligned} \tag{5.15}$$

Injecting the expression of $\dot{V}$ into 5.15, we obtain:

$$\left(\dot{y} + \frac{de(t)}{dt}\right) + \frac{\tau_s + \tau_m}{\tau_s \tau_m}(y + e(t)) + \frac{1+\sigma_s}{\tau_s \tau_m}\int y + e(t)dt = 0 \tag{5.16}$$

Separating the terms:

$$\frac{\tau_s + \tau_m}{\tau_s \tau_m} y + \frac{1+\sigma_s}{\tau_s \tau_m}\int y dt + \dot{y} = -\left(\frac{\tau_s + \tau_m}{\tau_s \tau_m} e(t) + \frac{1+\sigma_s}{\tau_s \tau_m}\int e(t)dt + \frac{de(t)}{dt}\right) \tag{5.17}$$

Let us recall the equation of the PID controller:

$$u(t) = K_p e(t) + K_i \int e(t)dt + K_d \frac{de(t)}{dt} \tag{5.18}$$

Equation 5.3.1 is very similar to the PID equation 5.18, showing that the Rowat-Selverston neuron can behave like a PID controller under some conditions [Jouaiti and Henaff, 2018a]. This behaviour was also observed experimentally (see Figure 5.7).

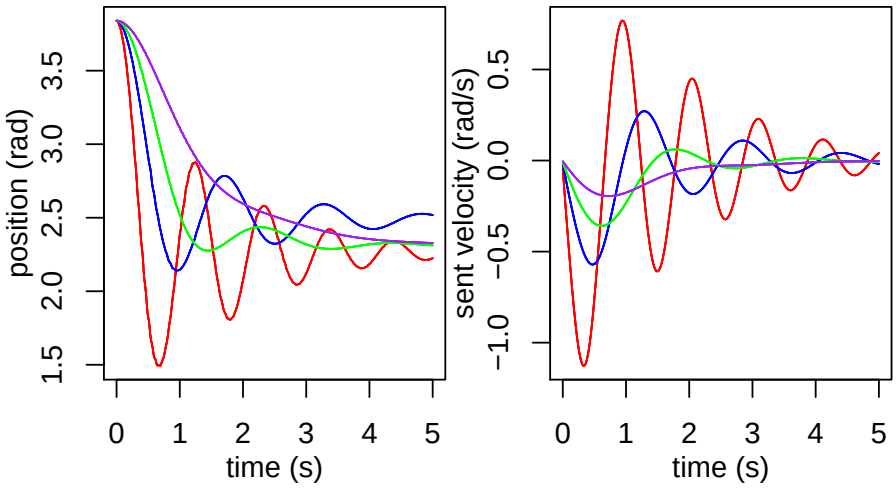


Figure 5.7: Evolution of the position (left) of a joint controlled by our CPG in discrete mode and the CPG output (right) for various values of ϵ. In red, $\epsilon = 5$; in blue, $\epsilon = 19$; in green, $\epsilon = 1$; in purple, $\epsilon = 0.5$.

5.3.2 Redefining Plasticity

The CPG can now seamlessly switch from one mode to the other by modifying the values of σ_f and σ_s. However, the plasticity rules we introduced previously were exclusively designed for the rhythmic mode and are not appropriate for discrete movements. It should be noted that the learning mechanisms can be freely modified to better suit one's purpose. Consequently, we modify the plasticity equations as follows [Jouaiti and Henaff, 2019c]:

To ensure that frequency learning is disabled in discrete mode, i.e. when $\sigma_f = 0.0$ and enabled when $\sigma_f = 1.0$, Equation 5.10 becomes:

$$\dot{\sigma}_s = \sigma_F \cdot 2\epsilon F \sqrt{\tau_m \tau_s (1 + \sigma_s - \sigma_f)} \cdot \frac{y}{\sqrt{V^2 + y^2}} \tag{5.19}$$

Moreover, considering ϵ, the amplitude of ϵF needs to remain 1.0 (optimal functioning mode) in the rhythmic mode, while the output amplitude needs to match the input amplitude in the discrete mode. Therefore, Equation 5.12 becomes:

$$\dot{\epsilon} = \tanh^2(\xi F) \cdot [(1 - \sigma_f) \cdot \lambda(F^2 - output^2) + \sigma_f \cdot \lambda(1.0 - (\epsilon \cdot F)^2)] \tag{5.20}$$

To demonstrate the effectiveness of the newly designed rules, we tested the model with systematic data: a step, a ramp and a sinusoid. We can observe in Figure 5.8 that although the CPG without learning effectively reproduces the signal, it does not match the amplitude of the signal. However, with the new learning rule for ϵ, the CPG also adapts to the input amplitude.

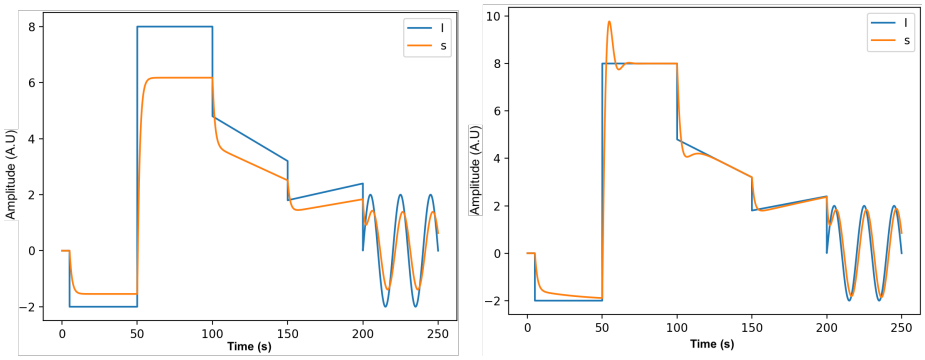


Figure 5.8: In blue: input signal of the CPG; in orange: CPG output. Left: CPG without any learning rule. Right: CPG with the new learning rule

5.4 Movement Classification

Since movements are rarely purely rhythmic or discrete but a combination/concatenation of both, the CPG should be able to switch automatically from the rhythmic mode to the discrete mode. To classify the signal as rhythmic or discrete, we use the Fast Fourier Transform (FFT) over n rectangular sliding windows of size $\{1, ..., n\}$ seconds [Jouaiti and Henaff, 2019c]. If the difference between the maximum of the FFT and its mean value (integral of the FFT) is large, then we assume that there is a frequency peak. We also consider the spread of the peak. Combining several window sizes also allows to take a wider range of frequency into account. This yields the following equation for $C(x,t)$ the classification result at time t with x the input signal:

$$C(x,t) = \sum_{N=1}^{n} P(\{x_{t-N}...x_t\}) + \alpha \cdot S(\{x_{t-N}...x_t\}) \tag{5.21}$$

where

$$P(x) = max(FFT(x)) - \overline{FFT(x)} - stdDev(FFT(x)) \tag{5.22}$$

$$S(x) = len\left(FFT(x) > \overline{FFT(x)}\right) \tag{5.23}$$

with n the number of windows, α an empirically determined weight, N the window width n seconds, $FFT(x)$ the FFT of x, $stdDev(x)$ the standard deviation of x and $len(FFT > \overline{FFT})$ the number of values greater than the average FFT. The classification results C are positive for rhythmic movements and negative for discrete movements.

This allows us to introduce a new synaptic rule for σ_f related to the rhythmic / discrete movement detection:

$$\dot{\sigma_f} = \gamma \cdot \left(\frac{\tanh\left(100.0 \cdot C(x,t)\right) + 1.0}{2.0} - \sigma_f \right) \tag{5.24}$$

with γ a learning step.

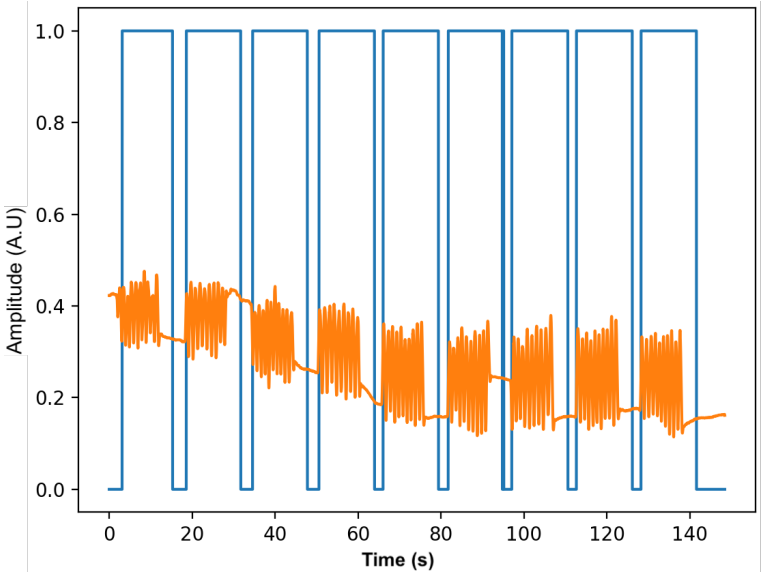


Figure 5.9: Example of classification result. In orange, the movement data, in blue, the classification result (1 for rhythmic and 0 for discrete)

The classification is thus amplified with a gain, smoothed and normalised using a sigmoid. According to this rule, σ_f converges towards 1 when the classification result is positive and towards 0 when it is negative.

The classification algorithm runs on average in 2 ms on an Intel Core i9 CPU for each time step, allowing real time classification. The classification algorithm has been tested on human motion data acquired with the T-Sens Motion Sensors [tea, 2020]. The participants were performing series of nine ten-seconds waving followed each time by four to six seconds rest. Sampling frequency was 64 Hz. 4457.53 seconds of data were manually labelled as rhythmic or discrete and the classification was evaluated on these data.

Let us define precision, recall and F1-score as follows:

$$precision = \frac{TP}{TP + FP} \tag{5.25}$$

$$recall = \frac{TP}{TP + FN} \tag{5.26}$$

$$F1 - score = 2 \cdot \frac{precision \cdot recall}{precision + recall} \tag{5.27}$$

with TP the number of true positives, FP the number of false positives and FN the number of false negatives.

Overall, we obtained 65% ($\pm$5%) of precision, 100% ($\pm 6.2E-6\%$) of recall and a F1 score of 0.79 ($\pm$0.04). Figure 5.9 shows an example of classification.

Failures of classification mostly come from data which look more like noise and fail to be classified as rhythmic but also from delay in recognising discrete movements that is due to the windows width. Moreover, although the classification immediately detects a switch from discrete to rhythmic, there is a delay for the transition between rhythmic and discrete.

Conclusion: Overview of the Extended CPG

In this chapter, we first introduced the CPG controller and the neuroscience background. We integrated Hebbian plasticity mechanisms for frequency learning according to [Righetti et al., 2006]. Then we also endowed the CPG with synaptic plasticity mechanisms for amplitude and synaptic weight learning. These adaptation mechanisms are meant to increase the versatility of the CPG. However, parameter tuning can be quite cumbersome and may require some getting used to.

These rules were adapted to take the discrete mode into account since we demonstrated that the CPG behaves like a PID controller in its discrete mode. Afterwards, since movements are rarely solely rhythmic or discrete, we wrote a classification algorithm and designed one last plasticity mechanisms so that the CPG could automatically switch from one mode to the other.

The final system of differential equations defining the CPG can be written as follows:

$$\dot{V} = y + \epsilon F \tag{5.28}$$

$$\dot{y} = \frac{1}{\tau_m}\left(\sigma_f - \frac{\tau_m}{\tau_s} - 1 - \sigma_f \tanh^2\left(\frac{\sigma_f}{A_f}V\right)\right) y - \frac{1+\sigma_s}{\tau_s\tau_m}V + \frac{A_f}{\tau_s\tau_m}\tanh\left(\frac{\sigma_f}{A_f}V\right) \tag{5.29}$$

$$\dot{\sigma_s} = \sigma_F \cdot 2\epsilon F\sqrt{\tau_m\tau_s(1+\sigma_s-\sigma_f)} \cdot \frac{y}{\sqrt{V^2+y^2}} \tag{5.30}$$

$$\dot{\epsilon} = \tanh^2(\xi F) \cdot [(1-\sigma_f)\cdot\lambda(F^2 - output^2) + \sigma_f \cdot \lambda(1.0 - (\epsilon\cdot F)^2)] \tag{5.31}$$

$$\dot{A_f} = -\mu\left(\left(\nu\frac{\sigma_f V}{A_f}\right)^2 - F^2\right) \tag{5.32}$$

$$\dot{\sigma_f} = \gamma \cdot \left(\frac{\tanh(100.0\cdot C(x,t)) + 1.0}{2.0} - \sigma_f\right) \tag{5.33}$$

The CPG is now endowed with various plasticity mechanisms and able to determine the type of input it is receiving and then to switch its parameters accordingly. We demonstrate this with human motion in figure 5.10.

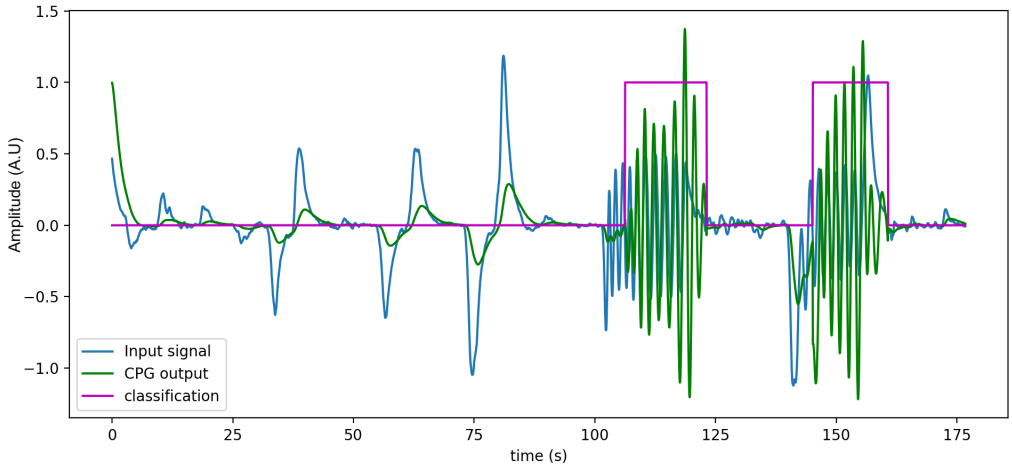


Figure 5.10: Example of classification result. In blue, the CPG input, in magenta, the classification result (1 for rhythmic and 0 for discrete), in green the CPG output

Chapter 6

Evaluation of the CPG-Controller

In this chapter, we will theoretically and experimentally evaluate the entrainment and synchronisation capabilities, as well as the power consumption of the Rowat-Selverston neuron by comparing it with two other oscillator models. We will also study the abilities of the CPG controller for rhythmic motor coordination. Finally, the CPG controller will be assessed on motor imitation and compared with a direct geometric control.

6.1 Comparative Study of Several Oscillators

To understand the strengths and weaknesses of our model, we will compare it with two other oscillating models: the Matsuoka neuron and the Hopf oscillator [Jouaiti and Henaff, 2019a]. The oscillators will be assessed with and without adaptive mechanisms on their entrainment range, synchronisation ability and power consumption.

6.1.1 Oscillating Neuron Models

The three neurons are placed in the same generalised control architecture [Kasuga and Hashimoto, 2005]. See Appendix B for implementation details.

Matsuoka neuron

A Matsuoka neuron is a mesoscopic model defined by the following equations:

$$\dot{x} = \frac{1}{T}(-x - bv + c + \epsilon F) \tag{6.1a}$$

$$\dot{v} = \frac{1}{\tau}(-v + y) \tag{6.1b}$$

$$y = \max(x, 0) \tag{6.1c}$$

where F represents the input signal, T and τ are time constants and b the self-inhibition (or neuron fatigue), y is the cell output and c the excitatory tonic input.

For adaptive mechanisms in the Matsuoka model, one could modulate the global output as done in [Taga et al., 1991] or change the time constants [de Rugy et al., 2003]. We will present the latter option. Note, however, that such plasticity mechanisms are not biologically plausible. This method consists in comparing the oscillator period P_r and the target period P_t and if this difference exceeds a given threshold δ, the following adaptation equation is enabled:

$$\tau = c_1 \cdot P_t \tag{6.2}$$
$$T = c_2 \cdot P_t \tag{6.3}$$

with c_1 and c_2 two empirically determined constants and P_t the target period, i.e. the input period.

Hopf oscillator

The Hopf oscillator can be considered as a macroscopic model of neural oscillator structures, so it does not have the half center structure usually present in neural oscillators. The equations for a Hopf cell are defined as follows:

$$\dot{x} = (\mu - (x^2 + y^2))x - \theta y + \epsilon F \tag{6.4a}$$
$$\dot{y} = (\mu - (x^2 + y^2))y + \theta x \tag{6.4b}$$

with F the input signal and y the neuron output. For $\mu < 0.5$, oscillations are damped. μ determines the output amplitude which can be influenced by ϵ the input gain. θ determines the intrinsic frequency of the oscillator ($\omega \approx 0.155 \cdot \theta$).

[Righetti et al., 2006] presented a frequency adaptation rule for the Hopf oscillator. This rule allows the oscillator to learn the input frequency and truly adapt to the input signal. Besides, when the interaction stops, the system retains the learning and remains at the learned frequency:

$$\dot{\theta} = -\eta \frac{y}{\sqrt{x^2 + y^2}} F \tag{6.5}$$

with η the learning step.

6.1.2 An Overview of Parameter Tuning

The intrinsic properties of each oscillator model can be modulated thanks to the various parameters. Properties of interest are the intrinsic frequency and amplitude of the oscillations.

For the Matsuoka model, the amplitude is determined by c, though this is merely an offset so the amplitude really does not change. For Hopf and Rowat-Selverston, μ and A_f determine the amplitude respectively but it can be further influenced by the input amplitude ϵF. Note though that setting the amplitude of Hopf is rather troublesome and some output amplitudes are just impossible to set, Rowat-Selverston is more straightforward because the amplitude is proportional to A_f.

In the Matsuoka model, four parameters determine the intrinsic frequency $\left(\omega = \frac{1}{\tau}\sqrt{\frac{(T+\tau)b}{T \cdot W} - 1}\right)$ and two conditions have to be met in order to obtain oscillations ($W > 1 + T/\tau$ and $b > W + 1$) (see [Matsuoka, 2011] for details). Note also that Matsuoka synchronises better with an input signal when it is unable to oscillate by itself. For Hopf, if $\mu < 0.5$, the oscillations are damped; the intrinsic frequency depends solely on θ. Finally, the Rowat-Selverston model produces oscillations if $\sigma_f > 1 + \tau_m/\tau_s$. The intrinsic frequency is dependent on τ_m, τ_s, σ_s, σ_f. While the Rowat-Selverston model seems as difficult to control as the Matsuoka model, at first sight, it actually is not so. Setting a particular intrinsic frequency is, in both cases, a complicated endeavour but putting the oscillator in conditions such that it can adapt to a wide range of frequencies is

actually fairly easy with Rowat-Selverston. Indeed, by choosing wisely τ_m and τ_s, the oscillator can cover the desired frequency range quite easily, even if it is quite wide. Then the value of σ_s hardly matters, thanks to the learning rule. On the contrary, in order to change the frequency range of the Matsuoka model, the time constants have to be changed since they are only able to cover a small range. In biological systems, the membrane time constants are set and cannot be modulated so this kind of plasticity is not biologically sound.

6.1.3 The Kasuga Control Architecture

[Kasuga and Hashimoto, 2005] introduced a control architecture for human-robot handshaking using Matsuoka neurons. This framework was validated in simulation and experimentally. This architecture controls two robot joints which are coupled together (see Figure 6.1). The input of each neural oscillator is the weighted sum of the force exerted on the joint, absolute value of the force and output of the other joint controller. The force inputs determine the oscillation amplitude and whether the handshake is passive or active. Coupling the two joints together prevents the amplitude from decreasing, which has been observed with the Matsuoka oscillator by [Kasuga and Hashimoto, 2005]. The output is considered as an angular velocity command. See Appendix B for implementation details.

Unless stated otherwise, the various gains are: $O_i = 0.2$, $K_i = 0.5$, $L_{i2} = 0.4$, $L_{i1} = 0.5$ for Rowat-Selverston and Hopf oscillators. For the Matsuoka oscillator, the input gains differ: $L_{i2} = 0.02$, $L_{i1} = 0.035$.

6.1.4 Entrainment Range

In order to determine their entrainment range, each oscillator model is subjected to various input frequencies for 100 s. At the beginning, the input frequency is low at 0.1 Hz and increases by $0.1Hz$ every 100 s. At each frequency change, the average PLV is computed between the input and output values of the oscillator, taking only the last 100 s into account. If this value is below 0.95, the input frequency is considered outside the bandwidth of the oscillator.

The process is repeated for several intrinsic frequencies of the oscillators. Since the intrinsic frequency depends on the parameters, they are tuned in order to get matching frequencies: σ_s, θ and b for Rowat-Selverston, Hopf and Matsuoka respectively.

Table 6.1 shows the entrainment range of each model for various intrinsic frequencies. We can clearly observe that the Matsuoka model is very limited and is not able to synchronise if the input frequency differs too much from its own. Besides, Rowat-Selverston cannot synchronise if the input frequency is too low, contrary to Hopf, but its frequency range is considerably larger. Plasticity slightly extends the entrainment range, especially for Matsuoka which now has an entrainment range similar to Hopf.

We can note that the entrainment capacity $\Delta\omega$ of Hopf is highly dependent on the value of ϵ. The stronger the coupling, i.e the higher ϵ, the better the oscillator synchronises. On the contrary, ϵ has to be small for Matsuoka and neither too small, nor too large for Rowat-Selverston. Due to those discrepancies, we did not employ the same ϵ value for the oscillators but rather chose to put them all in the best possible synchronisation conditions which were determined by running simulations with an extensive range of values of ϵ, we then selected the value of ϵ which yielded the higher PLV score.

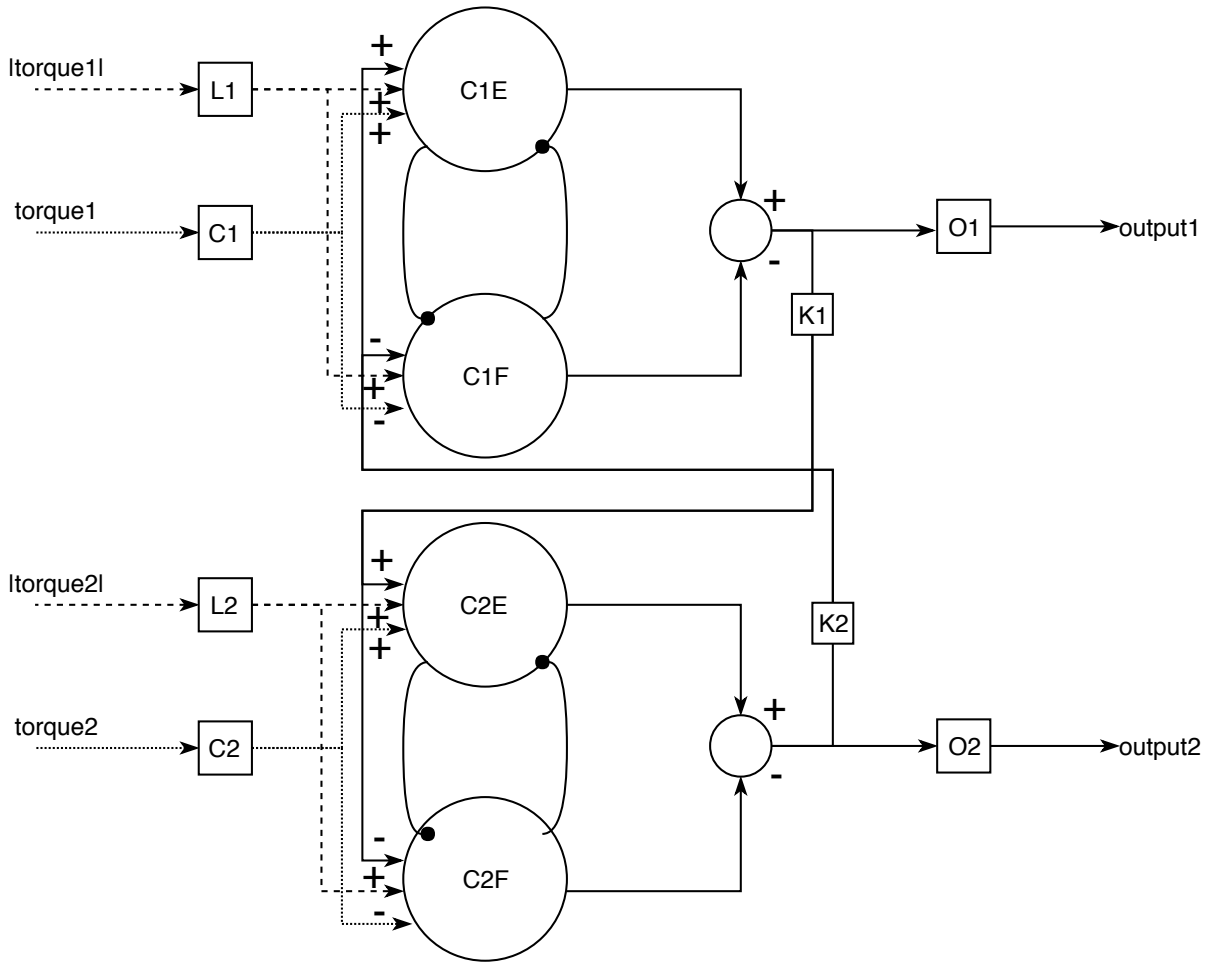


Figure 6.1: Oscillatory cells integrated to the generalised Kasuga architecture. C_i, L_i, K_i, O_i are gains and $C_{i\{E,F\}}$ is the neuron cell for the joint i controlling the extensor or flexor and torque_i is the input. Note that one cell receives torque - |torque| as an input and the other -torque - |torque|; for a sinusoidal signal, this means that one cell is receiving the positive components of the signal and the other the negative ones.

6.1.5 Simulated Handshaking

In order to evaluate the three oscillators, they are placed into the version of the Kasuga architecture introduced previously in section 6.1.3, which has been generalised such that any oscillator can be integrated.

The simulations have been conducted with the Kinova Mico robot in the V-REP simulator. Since grasping cannot accurately be simulated, we realise an oversimplified handshake with a static collidable ball instead of the human hand. The ball is animated with an up and down motion of amplitude 0.16 m and frequency 2 Hz, unless stated otherwise. The 2 Hz frequency was found appropriate for handshaking [Tagne et al., 2016]. In this system, the torque is applied by the ball to the gripper, which in turns entrains the robot joints and thus provides the CPG inputs (see Figure 6.2). Because of the mechanical coupling, they form a closed loop with the human partner.

The Mico arm has six degrees of freedom, but in the current setup, inspired by [Kasuga and

Model		ω_{intr} [Hz]	ω_{min} [Hz]	ω_{max} [Hz]	$\Delta\omega_1$	$\Delta\omega_2$
	σ_s					
Rowat-Selverston Frequency Learning	13	0.5	0.1	14.1	14	13.7
	50	1.0	0.1	18.6	18.5	18.2
	120	1.5	0.1	24.1	24	23.5
	200	2.0	0.1	29.2	29.1	28.7
	340	2.5	0.1	37.5	37.4	36.6
	490	3.0	0.1	46.6	46.5	45.2
	θ					
Hopf Frequency Learning	3.5	0.5	0.1	13.6	13.5	9.4
	7	1.0	0.1	14.0	13.9	9.7
	10	1.5	0.1	14.2	14.1	9.9
	14	2.0	0.1	14.7	14.6	10.2
	16	2.5	0.1	14.9	14.8	10.4
	20	3.0	0.1	15.5	15.4	10.7
	b					
Matsuoka T, τ Adaptation	3.5	0.5	0.1	10.1	10.0	0.3
	8	1.0	0.2	14.9	13.7	0.3
	13	1.5	0.3	13.6	13.3	0.3

Table 6.1: Synchrony frequency range where $PLV \geq 0.95$ for each oscillator with plasticity. $\Delta\omega_1$ and $\Delta\omega_2$ define the frequency entrainment with plasticity and without plasticity

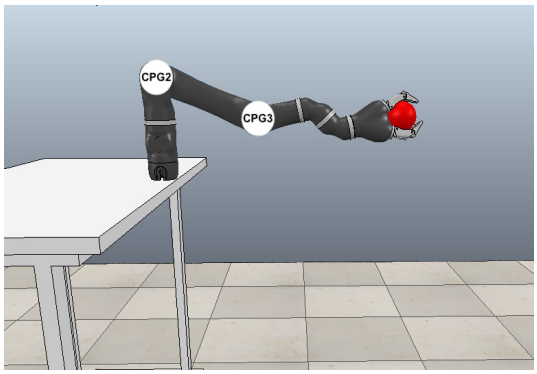


Figure 6.2: Simulated robotic arm with the static ball inside its gripper. We control the ball kinematics. We consider a rigid mechanical link because we want to impose a force on the robot which cannot be influenced. We set the ball position repeatedly according to a sinusoidal signal. The time step is small enough so that the motion appears smooth

Hashimoto, 2005], two joints, only the shoulder and elbow (joints 2 and 3 of the Mico robot) are controlled, the four other joints are locked. At the beginning of the simulation, the robot is not subjected to any external force (other than gravity). Then, the ball moves in the vertical plane, applying a perturbation to the robotic arm. Finally, the interaction stops and the ball is released.

In order to evaluate how the oscillators react when subjected to various frequency changes, the input signal applied to the ball varies across time: from $t = 0$ s to $t = 20$ s, 0.5 Hz; from $t = 20$ s to $t = 40$ s, 1.0 Hz; from $t = 40$ s to $t = 60$ s, 1.5 Hz; from $t = 60$ s to $t = 80$ s, 2.0 Hz;

from $t = 80\ s$ to $t = 100\ s$, $1.5\ Hz$; at $t = 100\ s$, the ball is released and until $t = 110\ s$, no force is applied. Oscillator parameters were obtained empirically. One important criterion was that the ball should stay inside the gripper. Indeed, some parameters created instability and unpredictable behaviour of the robot. Then, the parameters were fine-tuned to try and get the best possible performance.

6.1.6 Results Without any Plasticity Mechanisms

At the beginning of the interaction, the intrinsic frequency of each oscillator is $1\ Hz$. See Table 6.2 for the parameters used in the simulations.

Model	Parameters
Matsuoka	$\tau = 0.5$, $T = 0.25$, $c = 0.1$, $W = 4.0$, $b = 10.0$
Rowat-Selverston	$\tau_m = 0.2$, $\tau_s = 2.0$, $\sigma_f = 1.0$, $W = 0.05$, $A_{f_2} = 0.5$, $A_{f_3} = 0.9$, $\sigma_s = 20$
Hopf	$\mu = 0.5$, $\theta = 7.0$

Table 6.2: Oscillator parameters.

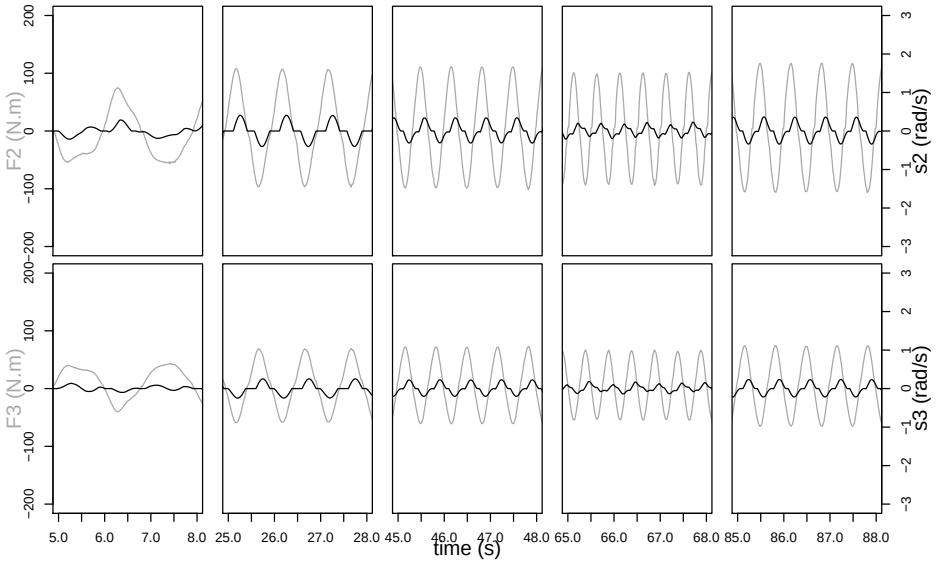


Figure 6.3: Response of the Matsuoka oscillator. In gray: CPG input, in black: CPG output for both joints

Figures 6.3, 6.4 and 6.5 represent the CPG input and output over 3 s for each frequency range. Matsuoka appears unable to synchronise at 0.5 Hz and the motion is irregular during the whole simulation (Figure 6.3). [Kasuga and Hashimoto, 2005]'s results had a smooth and regular motion because the oscillator was put in a non-oscillating mode where the Matsuoka oscillator synchronised better. Hopf and Rowat-Selverston, however, have satisfactory frequency entrainment and the motion is regular, except for 0.5 Hz where Hopf struggles to synchronise (Figure 6.4). For the three oscillators, we can also observe that the input signal slightly precedes the output signal.

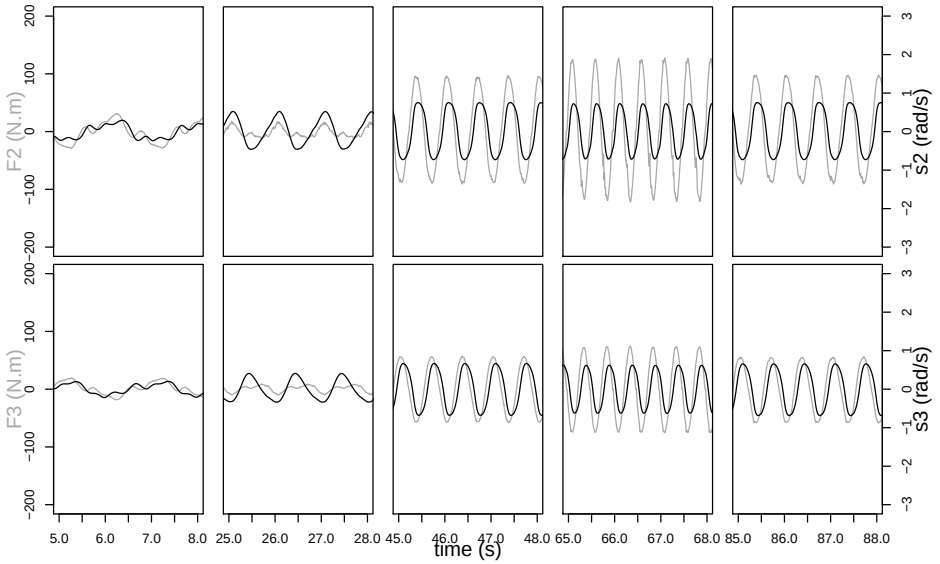


Figure 6.4: Response of the Hopf oscillator. In gray: CPG input, in black: CPG output for both joints

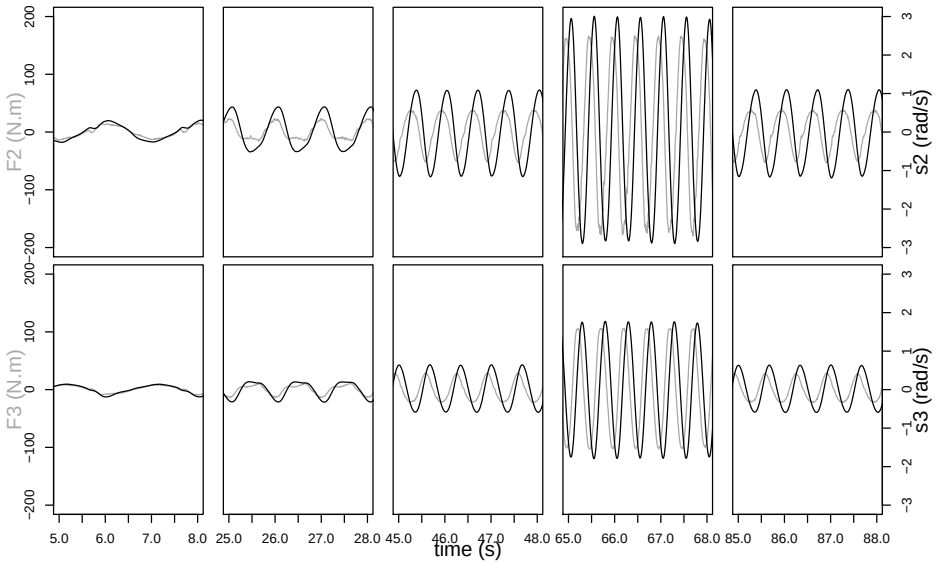


Figure 6.5: Response of the Rowat-Selverston oscillator. In gray: CPG input, in black: CPG output for both joints

The PLV, represented on Figure 6.6 is used to evaluate the coordination between the force exerted on the joints and each neural oscillator model. This confirms what we previously observed: while the Matsuoka PLV (mean PLV: 0.91, 0.86) appears satisfactory, it actually never reaches 1.0 and is highly irregular for 0.5 Hz. This can be explained by the fact that the PLV quality and accuracy decrease when the signals are not perfectly sinusoidal. The PLV of Rowat-Selverston (0.93, 0.93) is more regular than Hopf (0.91, 0.9) for 0.5 Hz, their performances are similar for

the rest of the simulation, though the transitions are more noticeable for Rowat-Selverston.

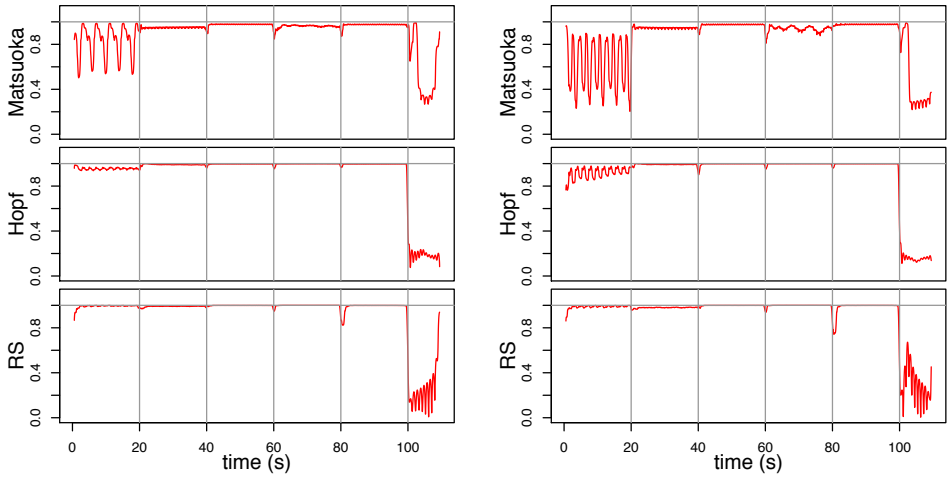


Figure 6.6: PLV for joint 2 (left), joint 3 (right). The vertical grey lines delimit each frequency range. The horizontal line indicates the reference for perfect coordination at 1.0 (See details in text)

6.1.7 Results with Plasticity Mechanisms

In this section, Hebbian plasticity mechanisms are integrated to Hopf and Rowat-Selverston in order to have more adaptable and versatile systems. For Matsuoka, a time constant adaptation mechanism is implemented. Then, the oscillators are once more evaluated.

Simulations were run with the same parameters as previously. Additionally, for Rowat-Selverston, $\lambda = 0.005$, $\mu = 5e^{-6}$; $\epsilon_2 = 0.2$, $\epsilon_3 = 0.3$ and for Hopf, $\eta_2 = 0.2$, $\eta_3 = 0.25$. Besides, plasticity could not be applied with the previous Kasuga parameters, L_{i1} had to be set to zero. For Matsuoka, $C_i = 0.08$ and $K_i = 0.1$.

Figures 6.7, 6.8, 6.9 and 6.10 represent the CPG input and output over 3 s for each frequency range. Plasticity has little effect on the PLV (see Figure 6.11). The Matsuoka PLV (mean PLV: 0.86, 0.84) still never reaches 1.0 and is highly irregular for 0.5 Hz and 1 Hz. Rowat-Selverston with frequency learning (0.93, 0.92) and all plasticities (0.92, 0.89) is similar to Hopf (0.90, 0.89) overall. The PLV appears to decrease for joint 3 with Rowat-Selverston with plasticities, however, this can be explained by the fact that the force decreases so much, it becomes mostly noise, which the PLV does not handle well since the PLV requires a narrowly-defined frequency content and noise has a broad spectrum.

Comparing with the simulations without plasticity, we see that the force applied on the joints for the three oscillators without plasticity never decreased. This shows that while the oscillator seems to adapt, it merely moves along, entrained by the ball, hence the delay between the input and output. This is further illustrated by the fact that once the interaction is over, the oscillator does not retain the ball frequency but returns to its own. On the other hand, for the oscillators endowed with plasticity, once they adapt (new frequency learned), the delay disappears and a decrease in force can be observed, even more so for the Rowat-Selverston oscillator with all plasticity mechanisms.

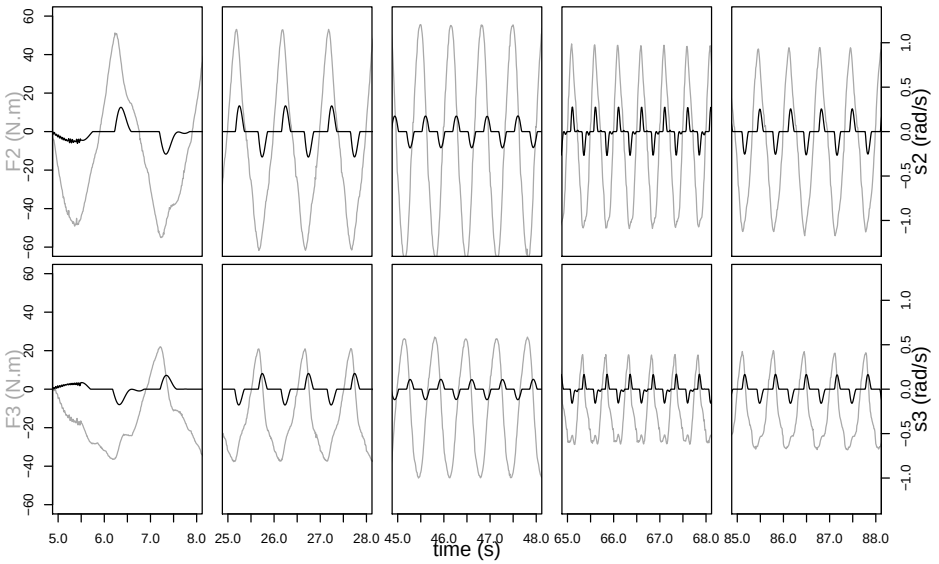


Figure 6.7: Response of the Matsuoka oscillator with time constant adaptation. In gray: CPG input, in black: CPG output for both joints

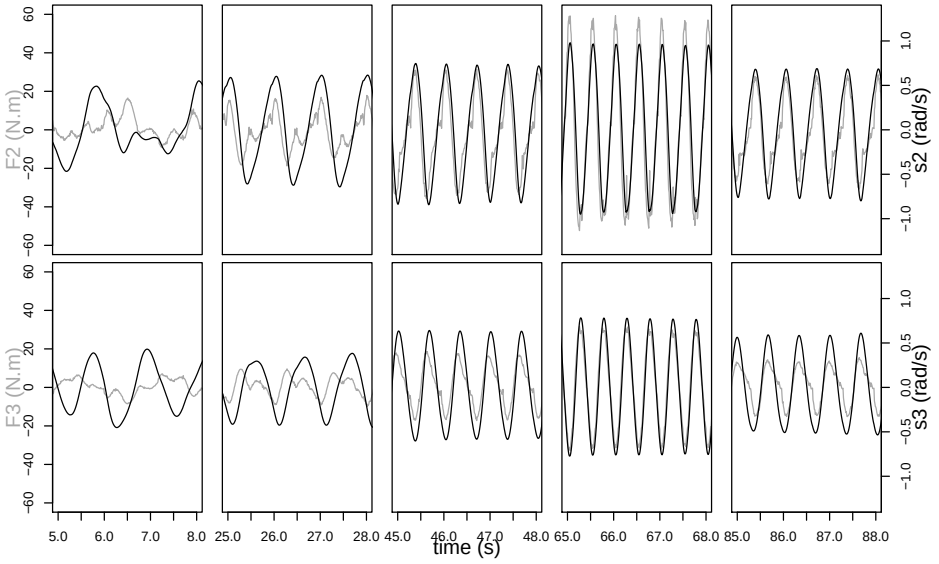


Figure 6.8: Response of the Hopf oscillator with Frequency Learning. In gray: CPG input, in black: CPG output for both joints

6.1.8 Power Consumption

Plasticity mechanisms also particularly improve the energetic impact of the oscillator. Indeed, if the intrinsic properties (amplitude, intrinsic frequency) of the oscillator are able to adapt to a varying input by learning more suitable parameters, the CPG will be able to *anticipate* the input signal and will not exert so much force on the robotic arm and hence the amplitude of the force applied would be less important. This anticipation is evidenced by the fact that the delay

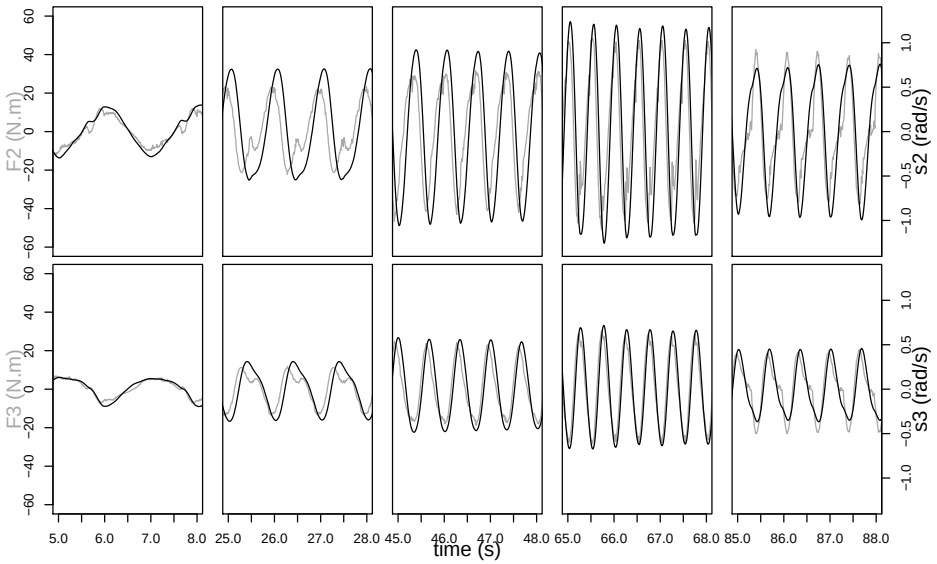


Figure 6.9: Response of the Rowat-Selverston oscillator with Frequency Learning. In gray: CPG input, in black: CPG output for both joints

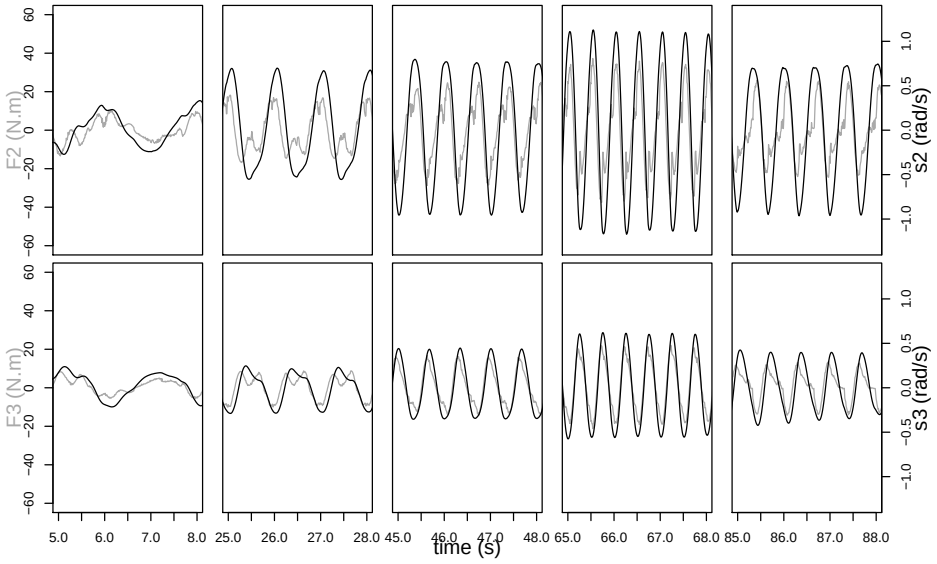


Figure 6.10: Response of the Rowat-Selverston oscillator with all the plasticity mechanisms. In gray: CPG input, in black: CPG output for both joints

between the input and output has now disappeared for Hopf and Rowat-Selverston. It is however still present for Matsuoka. Table 6.3 shows that frequency learning already leads to a significant decrease of the average power consumed by the robot for all three oscillators. Furthermore, A_f and ϵ learning for Rowat-Selverston decrease this consumption further.

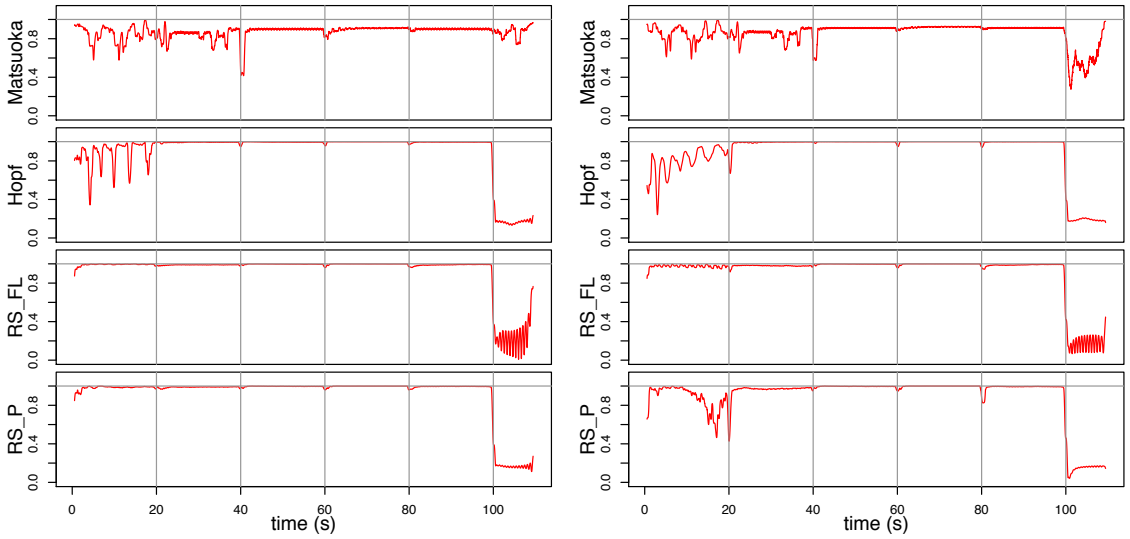


Figure 6.11: PLV for joint 2 (left), joint 3 (right). The vertical grey lines delimit each frequency range. The horizontal line indicates the reference for perfect coordination at 1.0

Model	Joint 2	Joint 3
Rowat-Selverston	2.15	1.41
Rowat-Selverston - σ_s Learning	0.33	0.20
Rowat-Selverston - σ_s, A_f, ϵ Learning	0.23	0.10
Hopf	1.12	1.07
Hopf - θ Learning	0.34	0.24
Matsuoka	1.16	0.27
Matsuoka - Time constants adaptation	0.54	0.1

Table 6.3: Average power $\frac{1}{T_{max}} \sum_{t,i} |F_i(t) \cdot vel_i(t)|$ (Watt) applied to both joints using the various neural oscillators, with vel_i the measured velocity of joint i

6.2 Motor Coordination with the CPG Controller

This study [Jouaiti and Henaff, 2019b] focuses on complex rhythmic motor coordination tasks with a CPG architecture inspired by human vision. In human vision, starburst cells are important in the computation of direction-selectivity [Fried and Masland, 2007]. Those are interneurons which respond to a visual stimulus moving in a specific direction. In this work, we replicate this behaviour with the CPGs, making them direction-specific. We demonstrate the CPG capabilities through four different interactions, each highlighting a different aspect: frequency adaptation, movement adaptation, amplitude adaptation, coordinated complex movements.

6.2.1 Experimental Protocol

Experiments were carried out with the SoftBank Robotics robot Pepper. The code was implemented in Python and run with NaoQi. Pepper front camera provides a visual signal at 10 fps. Using this video stream, the human hand position, obtained with a background subtraction algorithm, is extracted. All the image processing steps were performed with OpenCV 3.4. In order to avoid noise (due to lighting) in the detection, Pepper was placed facing a black background.

Besides, to ensure a quality signal, some basic image processing steps were additionally performed. First, if needed, the image was enhanced with Contrast Limited Adaptive Histogram Equalisation. Then, the hand of Pepper moving in front of the camera could also be wrongly detected as the moving human hand, so an additional thresholding step was added to remove the white parts from the picture, followed by a Gaussian blur and morphological opening and closing [5]. Finally, so that the human arm or clothes would not be mistaken for the hand and so that the best possible signal would be obtained, the human partner was also wearing black sleeves (Note that any other color works but the signal obtained is not as clean). Furthermore, passing the signal through a low-pass filter with 5 Hz cut-off frequency, helps remove detection aberrations.

6.2.2 CPG Architecture

In the present experiments, three joints of the left arm, the shoulder roll, the shoulder pitch and the elbow yaw joints, are controlled by CPGs. The shoulder pitch receives the vertical component of the hand position as an input and the shoulder roll receives the horizontal component. The shoulder pitch and shoulder roll joints are controlled by CPG_1 and CPG_2 respectively (Fig. 6.12), that is, the shoulder pitch joint will be dedicated to the vertical component of motion and its output is the input of the CPG controlling the elbow yaw joint (CPG_3); the shoulder roll joint is responsible for the horizontal part of motion.

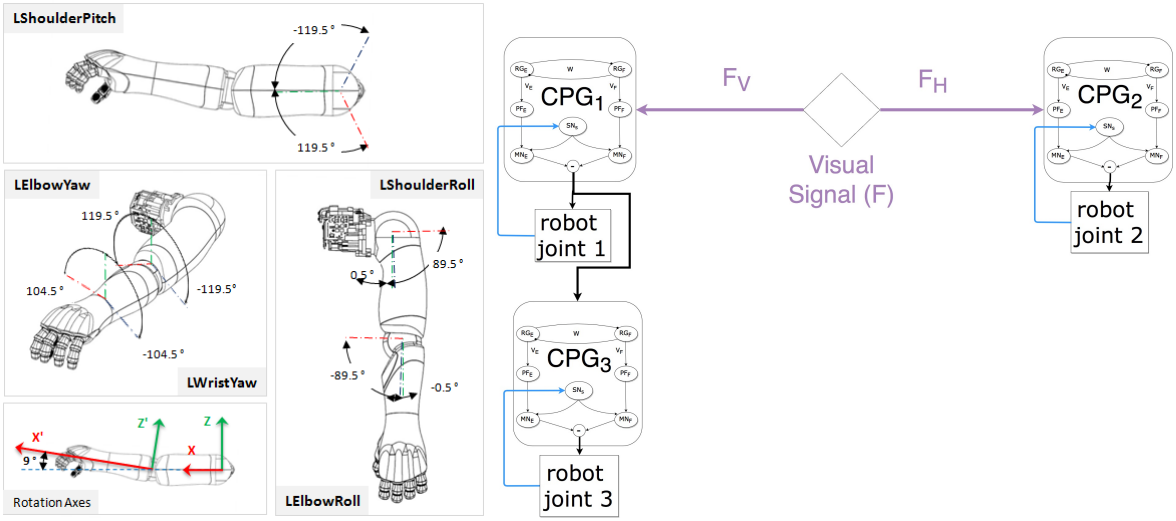


Figure 6.12: Left: arm joints for the Pepper robot (reproduced from Aldebaran). Right: CPG architecture. The shoulder pitch joint receives the vertical visual signal F_V as an input and its output is the input of the CPG controlling the elbow yaw joint; the shoulder roll joint receives the horizontal visual signal F_H as an input

Moreover, the right CPGs need to be used in order to achieve a given movement. For example, while a circular motion requires two degrees of freedom, only the shoulder roll joint or the elbow yaw joint would be sufficient for waving. To achieve this, the required joints need to be weighted more than the other ones. Input amplitude can be used to assess the importance of each joint. First, the input signal is normalised so that it is always between -1 and 1. The amplitude of the input signal is constantly computed over a moving window of 1 second, this allows rapid reconfiguration during the interaction. Then, the output of each CPG is weighted by its input

[5] 6

signal. This scales the movement and "removes" one dimension when the amplitude is too small. The equation of the output thus becomes:

$$output(t) = (\max_{t-1 \leq k \leq t}(F(k)) - \min_{t-1 \leq k \leq t}(F(k))) \cdot (MN_F - MN_E) \tag{6.6}$$

6.2.3 Experimental Results

Before the interaction starts, Pepper is at its resting position. If the robot detects a person agitating the arm, it activates the CPGs and responds. Each interaction lasts 30 seconds and the human partner was careful to maintain the same movement frequency as much as possible (see the associated video [7]).

The parameters used for the experiments are as follows: $\tau_M = 0.35$, $\tau_S = 3.5$, $W = 0.005$, $\sigma_F = 1.0$, $\lambda = 0.02$, $\mu = 5 \cdot 10^{-6}$. They were determined empirically.

Frequency Adaptation

The first interaction aims at demonstrating the frequency adaptation abilities of the CPG controller. To that effect, the human will perform one motion slowly for fifteen seconds and then increase the frequency for the remaining time. This can be observed on Figure 6.13.

The intrinsic frequency of the CPG controller depends on the parameter σ_S. On Figure 6.13, σ_S decreases in the first part of the interaction to adapt to the slow human movement and stabilises around ten. In the second part of the interaction, it increases to accommodate the fast movement but does not stabilise since the human movement is not perfectly homogeneous and the frequency keeps increasing. Bear in mind that adaptation time until stabilisation may appear quite long since the CPGs are purposely placed in unfavourable initial conditions to illustrate the adaptation abilities.

Amplitude Adaptation

In the second interaction, we will show the amplitude adaptation capacities of the controller. This time, the human will perform a circular gesture and reduce the movement amplitude after fifteen seconds.

The phase portrait of Figure 6.14 roughly represents the movement performed by the robot. First, the robot is indeed able to achieve a circular motion and two distinct ellipses with different amplitudes can be seen. The amplitude adaptation can also be observed in the CPG outputs. The amplitude of the command sent to the robot effectively decreases when the human motion amplitude decreases.

Note that the robot is *not* copying the human movement because the amplitude of the robot movement does not match the amplitude of the human movement. However as shown previously, if the human reduces the amplitude, the robot will as well.

Movement Adaptation

We tested the robot on rhythmic motions of three levels of difficulty: easy with waving motion (horizontal/vertical/diagonal), intermediate with a circular motion and difficult with an infinity symbol motion. In this third interaction, we will highlight the movement adaptation capacities of the controller. This time, the human will switch to another movement after fifteen seconds.

[7] The associated video can be found at https://members.loria.fr/mjouaiti/files/EPIROB19_1.mp4

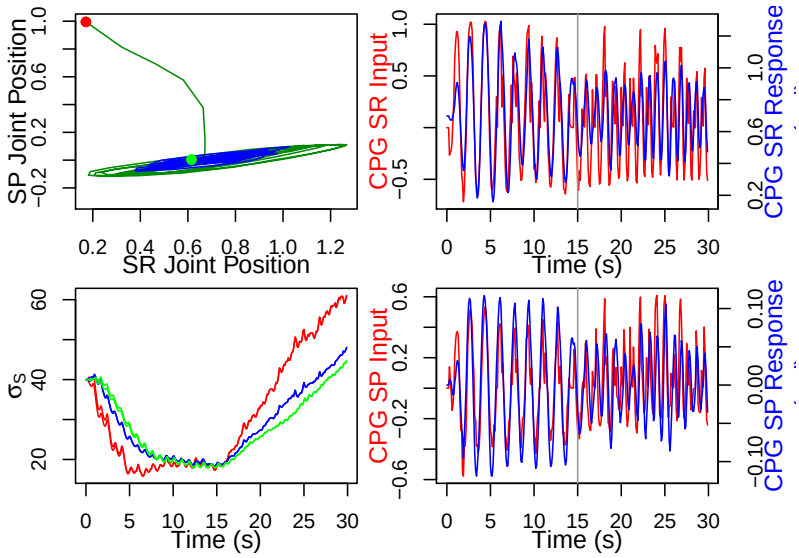


Figure 6.13: Top Left: phase portrait of the articular position, in green for the first part (before 15 s) and in blue for the second part. Top Right: in red, input of the Shoulder Roll (SR) CPG; in blue, output of the Shoulder Roll (SR) CPG. Bottom Left: σ_S for the Shoulder Roll joint (red), the Shoulder Pitch joint (blue), the Elbow Yaw joint (green). Bottom Right: in red, input of the Shoulder Pitch (SP) CPG; in blue, output of the Shoulder Pitch (SP) CPG

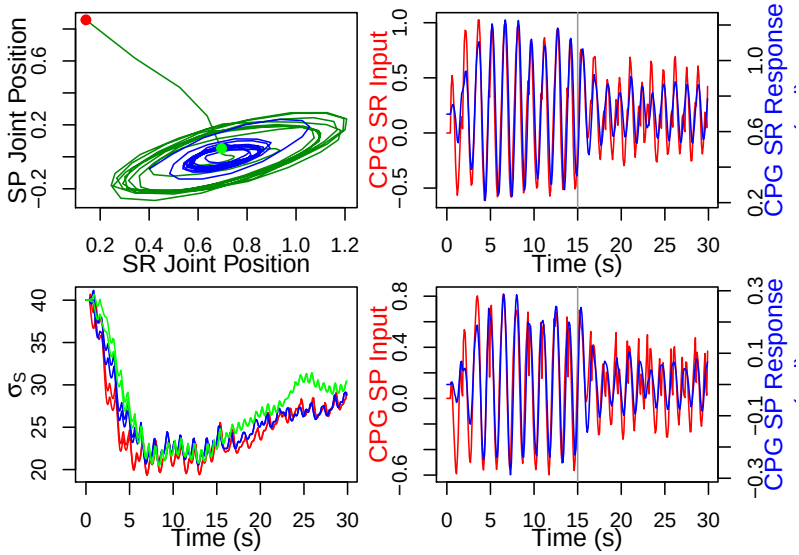


Figure 6.14: Top Left: phase portrait of the articular position, in green for the first part (before 15 s) and in blue for the second part. Top Right: in red, input of the Shoulder Roll (SR) CPG; in blue, output of the Shoulder Roll (SR) CPG. Bottom Left: σ_S for the Shoulder Roll joint (red), the Shoulder Pitch joint (blue), the Elbow Yaw joint (green). Bottom Right: in red, input of the Shoulder Pitch (SP) CPG; in blue, output of the Shoulder Pitch (SP) CPG

We will not show all the possible movements but we will illustrate the concept. In the first fifteen seconds, the human performs a horizontal waving gesture and then switches to a circular motion. The two different movements can be observed on the phase portrait of Figure 6.15. So

the controller is able to adapt to different human movements without any reconfiguration of the CPG architecture.

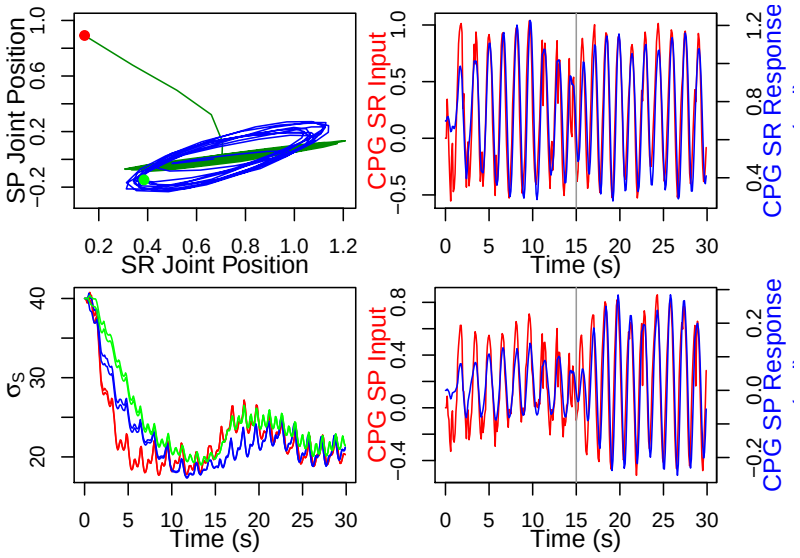


Figure 6.15: Top Left: phase portrait of the articular position, in green for the first part (before 15 s) and in blue for the second part. Top Right: in red, input of the Shoulder Roll (SR) CPG; in blue, output of the Shoulder Roll (SR) CPG. Bottom Left: σ_S for the Shoulder Roll joint (red), the Shoulder Pitch joint (blue), the Elbow Yaw joint (green). Bottom Right: in red, input of the Shoulder Pitch (SP) CPG; in blue, output of the Shoulder Pitch (SP) CPG

Coordinated Complex Movements

In this last part, we show that the controller is able to reproduce more complex movements (infinity-like gesture). Moreover, we can observe that the motion performed by the robot is not perfectly symmetrical. This is due to the human motion not being symmetrical either. The CPG maintains human characteristics.

6.3 Comparison Between the CPG-Controller and Geometric Direct Control

In this section, we compare two control methods: CPG control and direct geometric control in a motor imitation task. The robot has to imitate human movements and the controller is thus coupled with a vision system (See Appendix C). From the robot camera, we obtain the angular position and speed of each joint.

6.3.1 Direct Geometric Angular Control

We are using a SoftBank Robotics Pepper robot which is a humanoid robot so the correspondence from the human to the robot is relatively straightforward. However, the angles obtained from OpenPose are directly used to control the appropriate robot joints. They, however, need to be mapped to the robot joints to take the angular limitations into account. Pepper can only be

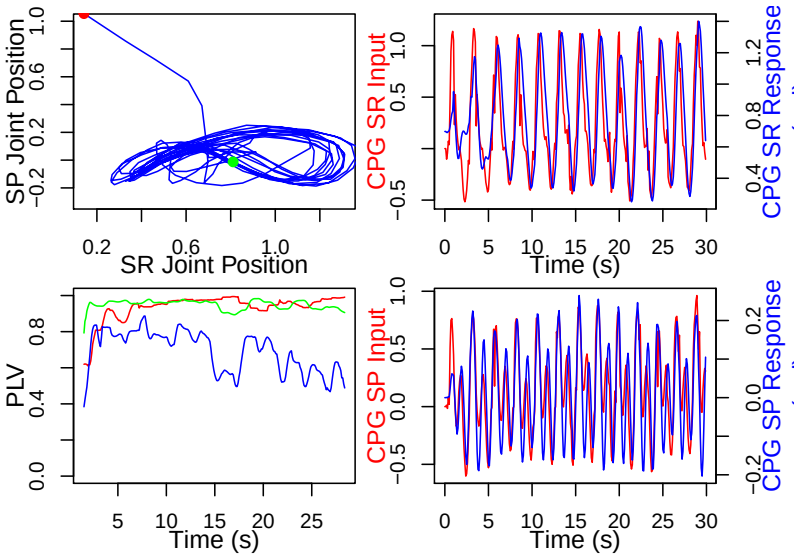


Figure 6.16: Top Left: phase portrait of the articular position. Top Right: in red, input of the Shoulder Roll (SR) CPG; in blue, output of the Shoulder Roll (SR) CPG. Bottom Left: PLV for the Shoulder Roll joint (red), the Shoulder Pitch joint (blue), the Elbow Yaw joint (green). Bottom Right: in red, input of the Shoulder Pitch (SP) CPG; in blue, output of the Shoulder Pitch (SP) CPG

controlled with angular positions, so each angle command is sent to the robot through its API at each timestep.

6.3.2 CPG Architecture

The general architecture for the CPG is represented on Figure 6.17. Each degree of freedom is controlled by a CPG. The CPGs are coupled with each other, thus forming a CPG network. Each CPG is endowed with plasticity mechanisms allowing it to adapt to varying amplitude, frequency and types of movement.

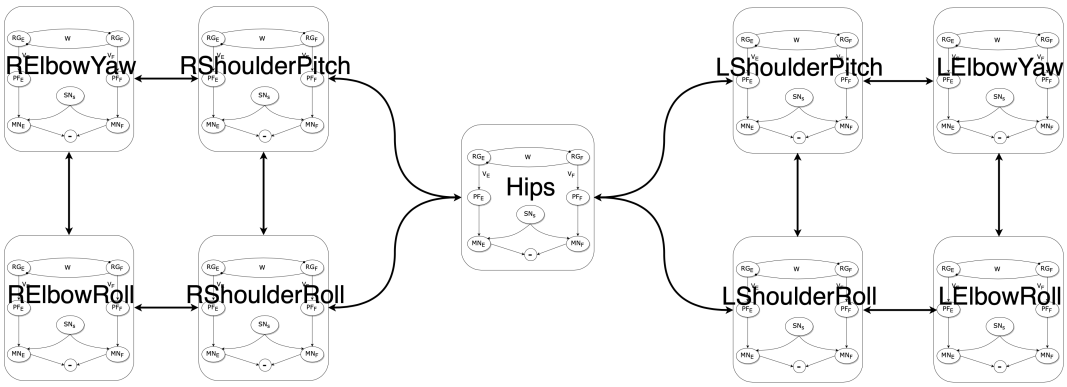


Figure 6.17: General CPG Architecture used for the robot control. Each CPG receives an angular velocity as an input signal. The output of the CPG is also considered as a velocity. The arrows indicate the coupling between the CPGs

Movement	Error Metrics geometric (rad)	Error Metrics CPG (rad)
Hip to the left	0.98 ± 1.32	0.97 ± 1.35
Hip to the right	0.60 ± 0.92	0.57 ± 0.91
Raise both arms laterally	1.59 ± 2.28	1.08 ± 1.66
Raise left arm and forearm	0.90 ± 1.33	1.00 ± 1.56
raise left arm laterally	0.60 ± 0.77	0.74 ± 1.06
raise left arm to the front	0.98 ± 1.38	1.15 ± 1.64
raise left forearm	0.72 ± 1.07	0.72 ± 1.05
raise left forearm laterally	0.73 ± 1.09	0.83 ± 1.30
raise right arm and forearm	0.88 ± 1.59	0.84 ± 1.53
raise right arm laterally	0.83 ± 1.26	1.02 ± 1.41
raise right arm to the front	0.92 ± 1.36	0.98 ± 1.44
raise right forearm	0.63 ± 0.92	0.62 ± 0.92
raise right forearm laterally	0.69 ± 1.23	0.85 ± 1.55

Table 6.4: Results of the error metrics for the geometric and CPG control methods

Human perception of movement varies depending on the type of movement. For rotational movements, the human brain processes angular speed [Barraza and Grzywacz, 2002, Freeman and Harris, 1992]. Since a human limb can be likened to a pendulum, angular speed will therefore be the input of the CPG controllers. Since the Pepper robot is used, it can only be controlled in position. However, the CPG output is still considered as an angular velocity and is applied to the current real joint value. As the CPG is capable of performing both discrete and rhythmic movements by setting σ_f to 0.0 and 1.0, each mode will be evaluated independently.

6.3.3 Results

We validate our model with videos in order to compare both control methods on the same data. It was also evaluated in real human-robot interactions (See associated video [8]).

Discrete Mode

The CPG parameters used for this study are as follows: $\tau_M = 0.35$, $\tau_S = 3.5$, $W = 0.005$, $\sigma_F = 0.0$, $\lambda = 0.1$, $\mu = 5 \cdot 10^{-6}$. They were determined empirically.

We evaluated both control methods on a wide variety of movements (See Table 6.4). Since there is an obvious constant delay between the pose estimation and the reaction of the robot, we applied the metrics after matching the signals to avoid loss of accuracy due to delay. The direct geometric and CPG methods have similar accuracy for most of the movements. One also has to note that the input signal is very noisy, sometimes due to pose estimation failures. We can see on Figures 6.18 and 6.19 that the CPG strongly filters the signal since it behaves like a PID controller in discrete mode, which leads to more delay. However, both controllers still manage to reproduce the gesture appropriately.

[8] The associated video can be found at https://members.loria.fr/mjouaiti/files/imitation.mp4.

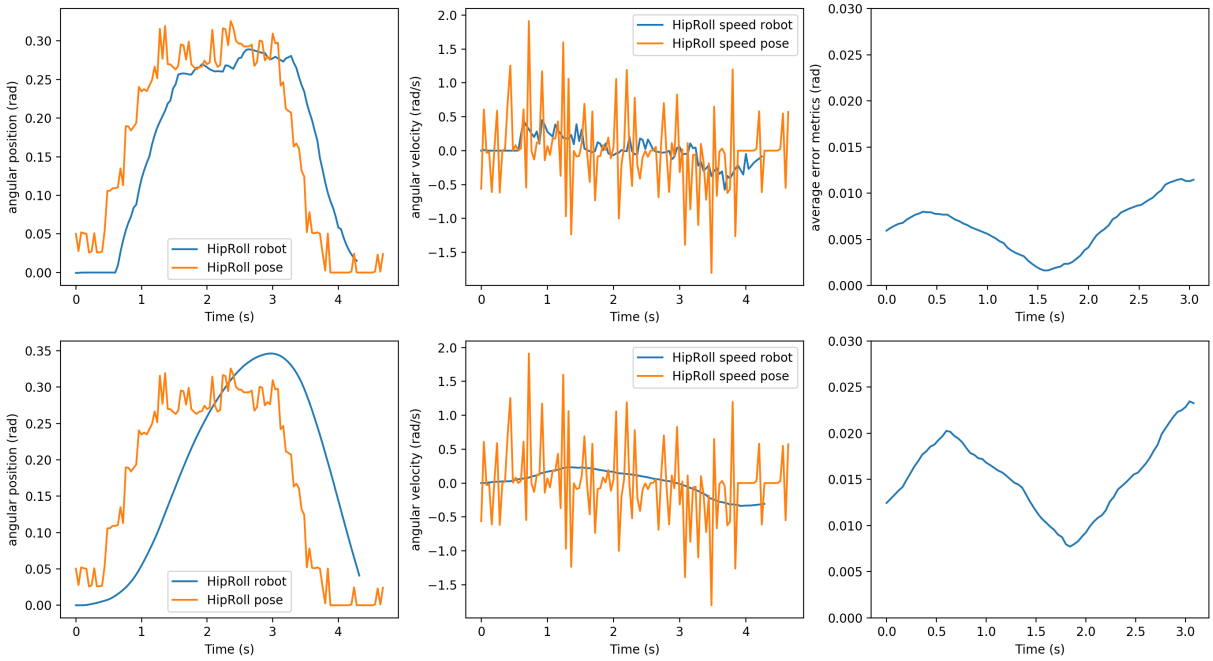


Figure 6.18: Example of discrete movement: "Hip to the Left". Top: geometric method. Bottom: CPG method. Left: Angular position of the human and robot; Middle: angular speed of the human and robot. Right: error metrics for the geometric and CPG methods

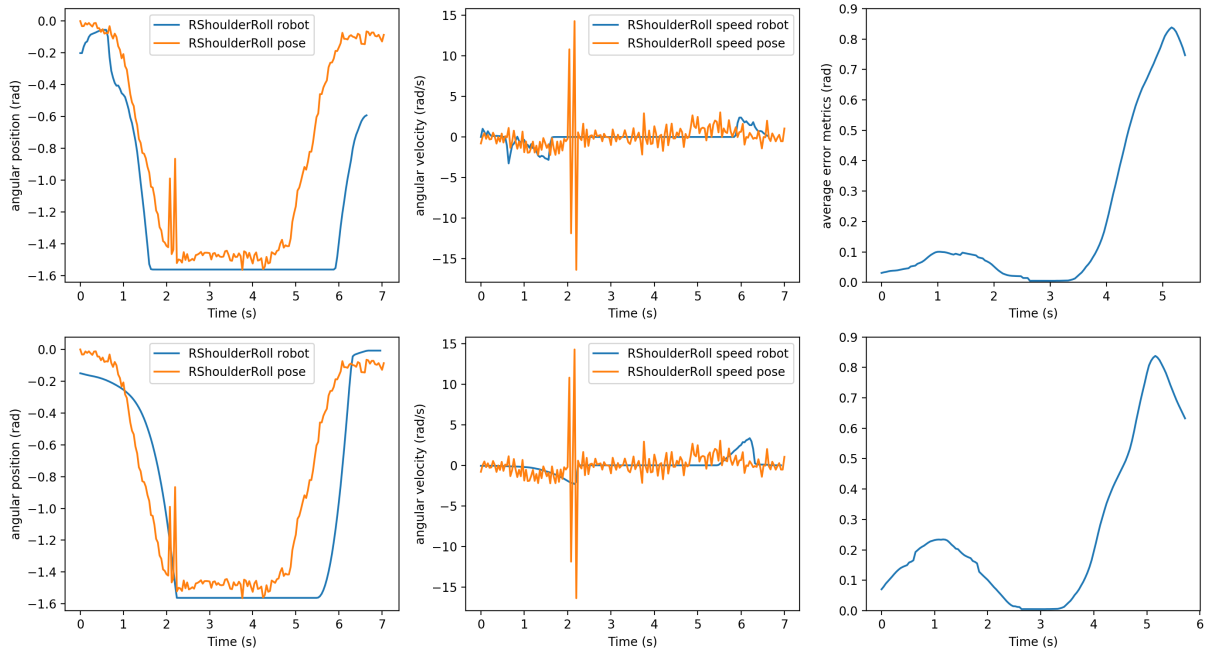


Figure 6.19: Another example of discrete movement:"raise both arms laterally". Top: geometric method. Bottom: CPG method. Left: Angular position of the human and robot; Middle: angular speed of the human and robot. Right: error metrics for the geometric and CPG methods

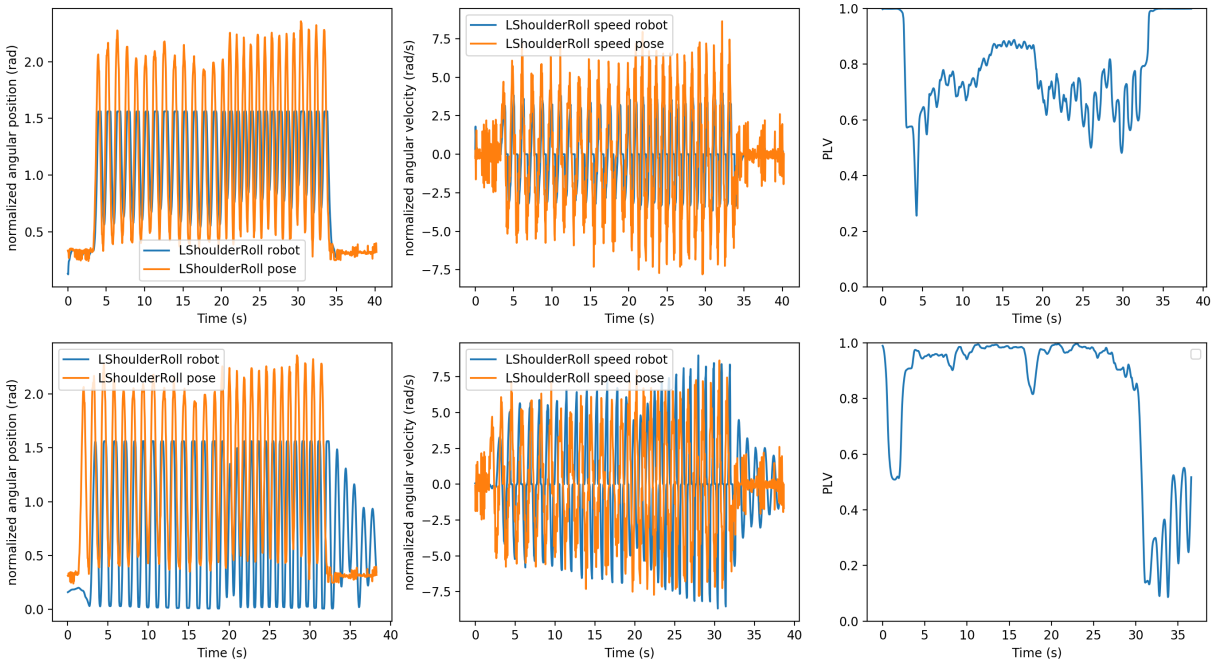


Figure 6.20: Example of rhythmic movement. Top: geometric method, Bottom: CPG method. Left: angular position. Middle: angular velocity. Right: PLV

Rhythmic Mode

The CPG parameters used for this study are as follows: $\tau_M = 0.35$, $\tau_S = 3.5$, $W = 0.005$, $\sigma_F = 1.0$, $\lambda = 0.02$, $\mu = 5 \cdot 10^{-6}$. They were determined empirically.

To evaluate the rhythmic mode of the CPG, we performed rhythmic shoulder and elbow movements. Only the needed joints were set to rhythmic mode, the others remained in discrete mode. The coordination performance of each movement was evaluated with the PLV. Overall, the geometric method had an average PLV of 0.63 ± 0.47 and the CPG method of 0.85 ± 0.21. The CPG method fared much better in the rhythmic mode (see Fig. 6.20). Indeed, by learning the parameters of the interaction, the CPG is able to adapt and "anticipate" the movement, thus being perfectly coordinated. The direct geometric method is however still struggling to catch up with the input signal. We can also notice that the CPG continues to oscillate even after the movement has finished, this illustrates its ability to learn and retain the frequency of the movement. Indeed, the oscillating frequency can be inferred from the final value of σ_s and this single value is enough to put the CPG in the same oscillating conditions again.

Conclusion

In this chapter, we evaluated the bio-inspired controller theoretically and experimentally. First we compared the Rowat-Selverston neuron with the Matsuoka neuron and the Hopf oscillator. The three oscillators were evaluated according to their entrainment range and their synchronisation capacity during a handshaking simulation. Plasticity mechanisms were integrated into each model and the impact on the energetic cost is observed. Integrating plasticity mechanisms into the three oscillators has no real impact on coordination performance but can lead to a significant

power consumption decrease and to an extended entrainment range. Though more complex, the Rowat-Selverston neuron leaves more space for adaptation and versatility.

The Matsuoka oscillator has a cumbersome parameter tuning process and a limited entrainment range. On the one hand, Hopf synchronises as well as (sometimes better than) Rowat-Selverston and is easier to control, but less adaptive. On the other hand, Rowat-Selverston is obviously more complex with more parameters to handle but it makes it possible to design plasticity mechanisms allowing the system to truly adapt and not only to offer a wide entrainment range but also a significantly lower power consumption. Rowat-Selverston is also the only oscillator that has a discrete mode.

Furthermore, we showed that a robot can achieve motor coordination with a human partner through a visual signal of a hand performing rhythmic movements. The robot is able to adapt its frequency, amplitude and motion generation according to the human motion. However, we do not achieve copying of the motion but rather, the robot adapts to the frequency and movement while retaining its own identity. This is similar to what we observed in part I in our study on involuntary coordination where individuals perform the same movement at the same frequency but maintain their own characteristics.

Finally, we compared the CPG control with a direct geometric control. While both methods present a similar performance for discrete movements, the CPG fares much better for rhythmic movements as it is able to adapt and "anticipate" the movement. This study presents several limitations. First, the geometric control is quite basic. Maybe controllers that take the robot dynamics into account would be more effective. Second, we were limited by the transformation from the 2D to the 3D pose which did not handle every case appropriately. Indeed, the neural network by [Martinez et al., 2017] was trained on similar postures and does not generalise very well. For example, arms stretched to the front or even arms raised above the head systematically led to inaccurate poses. The training dataset should be complemented with a wider variety of movements. We are very willing to grant that the quality of the pose estimation is lower than with motion capture, or even Kinect, but we also believe that this kind of interaction, though imperfect at times, is more natural as it does not involve any specific environment nor extra or invasive equipment. The accuracy of the 2D estimation can actually be further increased but at a much higher computational cost and the interaction would not be real time anymore. In the future, we will work on increasing the robustness of the detection and reducing the noise while maintaining a reasonable computation cost. The present system allows us to effectively control the robot in real time at 30 fps, 30 fps being the limitation set by the robot camera.

In the next chapter, we will evaluate the controller in real human-robot physical interactions, with all the variability this entails. On the one hand, this will confirm the versatility of the controller and that it is suitable for real-life interactions. On the other hand, we will also evaluate the subjective judgment of social coordination to examine the relevance of such a bio-inspired control.

Chapter 7

User Study: Influence of Adaptive Mechanisms on Engagement and Coordination

This chapter aims at evaluating the CPG controller in user studies and studying human subjective judgment of social coordination. We will evaluate the impact of different interaction partners (human/robot/virtual agent; adaptive/non-adaptive) on engagement and coordination performance.

Engagement has many different definitions, notably depending on the field of study. Engagement is a process to keep attention in a task. It includes concentration and task motivation which can be interpreted as a commitment to the task. Collaborative engagement can be defined as "the process by which two (or more) participants establish, maintain and end their perceived connection during interactions they jointly undertake" [Sidner et al., 2005]. [Dmochowski et al., 2012] also defined "emotionally laden attention" as a potential marker of engagement. In HRI, engagement is often defined as the value participants are willing to attribute to being with their interaction partner and to continuing the interaction [Poggi, 2007].

Monitoring and evaluating levels of task engagement in a social context to identify which situations lead to a loss of engagement is very helpful for the identification of more accurate and efficient methods for robots to interact with humans. To understand the difference between level of engagement and coordination performance in rhythmic interactions with different partners, we designed the experiment presented in this paper.

In our experiment, participants interact rhythmically by performing a waving-like gesture with different interaction partners: first, a human, a robot and a virtual agent, all unable to adapt and lead the interaction and second, a human and a robot able to adapt their movement to the participant. We chose the waving gesture because it is an unequivocally social gesture and it is a very simple task which we can use as a benchmark to understand rhythmic interactions better. Participants were equipped with motion sensors to record movements and analyse coordination and an EEG cap to assess engagement. Leadership, in this experiment, means that the partner could not be influenced by the subject. The partner always initiated the interaction on a predefined cue. This was necessary for the synchronisation of the systems and since EEG required a highly controlled interaction.

This experimental design can be used as a benchmark to test our hypothesis about motor coordination and engagement in human-robot interactions. Our working hypothesis was that engagement may be correlated with coordination performance. We also expected that people

would engage more and hence coordinate better with another human, then a robot and finally the virtual partner in the non-adaptive mode. Adaptive mechanisms were finally foreseen to improve the engagement.

7.1 Methods

7.1.1 Study Overview

Participants were asked to wave back at either a human, a robot or a virtual partner (See Fig. 7.4). Depending on the condition, the partners could adapt their movement (human, robot) or not (videotaped human, robot, VP) to the participant's movements. Each participant performed all the conditions. Overall, the experiment lasted between 1.5 and 2 hours and was divided into two parts: the non-adaptive and the adaptive.

7.1.2 Experiment Design

At first, the task and the different conditions were explained to the subject but not the true goal of the study. They signed an informed consent and filled in the NARS questionnaire (see Sec. 7.1.5). Then, they were equipped with the EEG cap and motion sensors (see Fig. 7.5 for the sensor placement). The waving task was explained to them in detail and they were comfortably seated on a chair isolated from the experimenter. They also wore active noise cancelling earbuds (Bose QuietComfort 20i) to remove the sound of robot actuators [Jouaiti and Henaff, 2019e]. This is necessary to be in homogeneous conditions for all the partners since the robot produces noise when it moves and subjects could be influenced by it. We also had to use such earbuds since earplugs and noise cancelling headphones were not sufficient and headphones would have applied unwanted pressure on the EEG cap.

Subjects performed a test of the task and additional information was provided if the experimenters noticed confusion.

The participants were instructed to wave back at the different partners using their right forearm and their right arm rested on a pillow in order to avoid muscular fatigue, pain and unnecessary muscular artefacts in the EEG signal.

The experiment was divided into two parts, the first one with three conditions which correspond to the three non-adaptive partners (videotaped human, robot, VP) and the second one with two conditions which correspond to the two adaptive partners (human, robot). After each part, the participants received the post-recording questionnaire to evaluate their perception of the interactions (see Fig. 7.1 for an overview of the timeline).

The order of conditions was randomised so that each condition would take place thrice, would not happen twice in a row and so that each permutation of conditions was experienced. Overall, each condition was performed twenty-seven times by each participant. Each condition started with a 15-second baseline and involved nine waving interactions of 10 seconds each, separated by a 4-second rest.

The experiment was divided into two parts:

Part 1

In the first part of the experiment, we wished to evaluate whether the different types of partners could influence engagement or coordination, and whether engagement was correlated with coordination performance. In this part, the interaction partners (videotaped human, robot, VP)

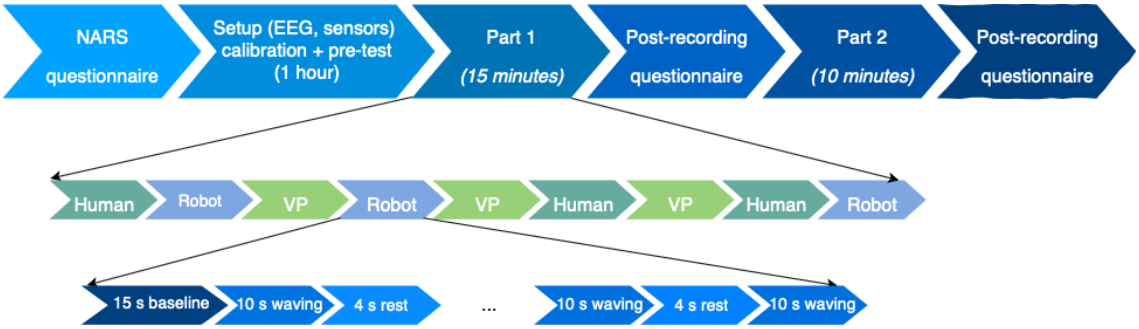


Figure 7.1: Overview of the timeline of an experiment. An example of condition order is also depicted

were leaders of the interaction and imposed the waving frequency on the subject. The partners initiated and stopped the interaction. The waving frequency of each interaction was randomly chosen between 0.9, 1.0 and 1.1 Hz to avoid subjects getting used to the frequency from one interaction to the other. While these frequencies may seem numerically close, they are actually very different in the human perception.

Part 2

The goal of the second part was to evaluate the influence of endowing the interaction partner (human, robot) with adaptive mechanisms on coordination and engagement. Therefore, the interaction partners were able to adapt to the participant's movement in this part. The human partner initiated and stopped the interaction. The robot eyes turned green at the beginning of the interaction but it did not move until the subject moved. The robot stopped the interaction.

7.1.3 Technical Setup

The EEG data acquisition is handled by OpenVIBE [Renard et al., 2010]. OpenViBE is a software platform for real-time neuroscience dedicated to designing, testing and using brain-computer interfaces. It is possible to create and run custom applications. The motion sensor data are recorded with T-REC receivers and handled by the proprietary software Captiv [tea, 2020]. See Figure 7.2 for an overview of the experimental setup.

All the systems were synchronised together thanks to a Python script managed by OpenVIBE. One script was created for each condition, it performed the following tasks:

- Control the interaction: control the robot movements when necessary and change its eyes color; launch the videos (VP, human) and update them at each time step; trigger an auditory signal to indicate the beginning and end of the interaction in the adaptive human condition for the experimenter.

- Receive triggers from OpenVIBE and in return, control an Arduino Nano to send triggers at the beginning of each interaction to the motion sensors receiver (T-Rec).

- Save the data: Robot real angular values for the arm yaw joint, VP and human randomised imposed frequency order for the non-adaptive mode

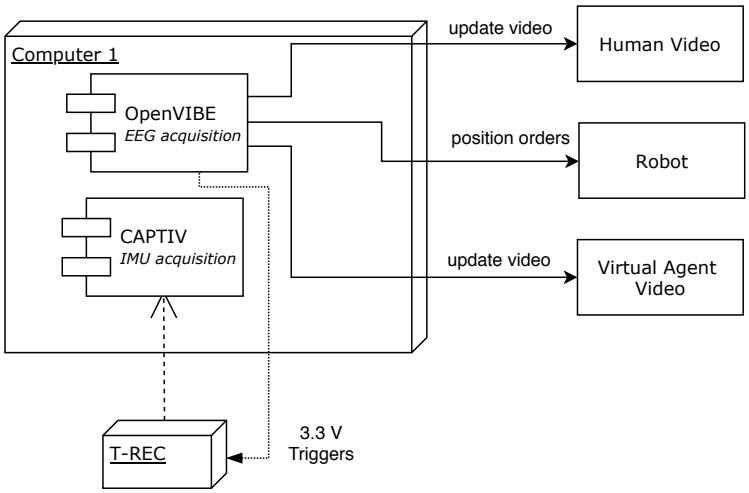


Figure 7.2: Setup for part 1 of the experiment. OpenVIBE manages the EEG acquisition and Captiv the motion sensors acquisition. OpenVIBE controls the videos of the human and VP and the waving of the robot through a Python script. It also sends 3.3 V triggers to the motion sensors receiver thanks to an Arduino Nano

This ensured that we could reliably analyse and synchronise the data acquired by different systems.

In the second part of the experiment (See Fig. 7.3), we added an extra computer due to operating system requirements for OpenPose. So, one computer which could not communicate with the robot acquired the image of a webcam positioned towards the participants. It then performed pose estimation, updated the CPG controller and sent the resulting angular command to the OpenVIBE script which controlled the robot.

7.1.4 Participants

Thirteen right-handed subjects aged 21-31 participated to our experiment. One subject was excluded due to a false contact in the motion sensor acquisition system. After exclusion, we had 12 subjects (5 women, average age: 25.67 $\pm$2.4). The experiment was approved by the Inria ethical committee. The subjects were provided an information notice beforehand and were required to sign an informed consent. The information notice and informed consent were available both in French and English. Each participant was assigned a numerical identifier to anonymise the data.

7.1.5 Materials

Interaction partners

All the interaction partners performed the same waving movement using the left arm so that it mirrored the subject's movement (See Figure 7.4). They were placed about 2 meters away from the subject and at eye-level.

Robot: We used a Pepper robot [Pandey and Gelin, 2018] (Softbanks Robotics) programmed to wave according to a sinusoidal signal in the non-adaptive mode. In the adaptive mode, its movement was controlled with a CPG (Central Pattern Generator) controller able to adapt to the subject's movement [Jouaiti and Henaff, 2019b] which was estimated using pose estimation

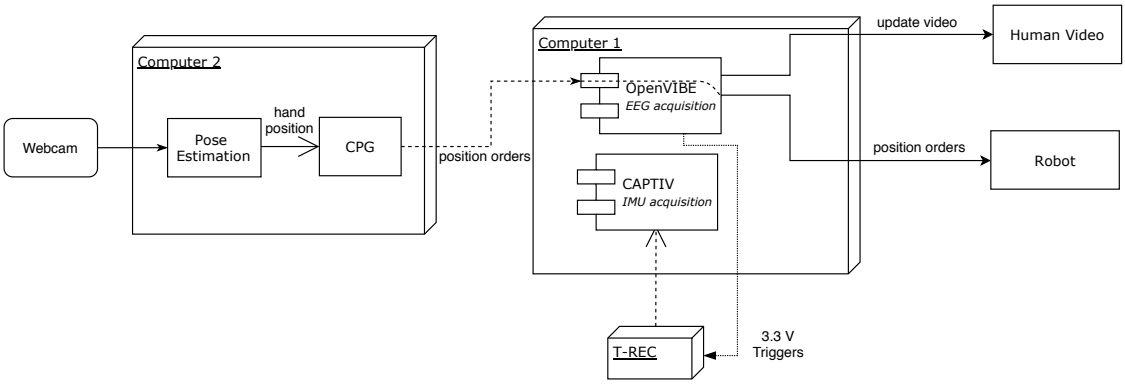


Figure 7.3: Setup for part 2 of the experiment. The setup of part 1 is combined with a second computer which also processes the visual input with a pose estimation algorithm and feeds the hand position into the CPG controller to get the position orders. Robot commands are then transmitted to the first computer which controls the robot

[Cao et al., 2017, tf-, 2017]. The robot woke up from its rest state at the beginning of each series of interactions. Waving periods were indicated by the robot eyes becoming green, they were unlit otherwise. At the end of each series, the robot returned to its rest state.

VP: We used videos of a virtual agent [9] modelled with MakeHuman [mak, 2018] and animated with Blender [ble, 2018]. The VP started waving at the beginning of each interaction and stopped at the end. Subjects were instructed to wave back when the VP was waving. There was no adaptive mode for the VP.

Human: The human partner was one of the experimenters, a 22 year-old woman. In the non-adaptive mode, we used pre-recorded videos of the human partner to ensure that the latter was leader of the interaction and could not adapt to the subject. The use of a video [10] appeared necessary as we made several trials with real humans who had to follow a frequency imposed by a metronome or a flashing light while placed in front of another human. In either case, the human was unable to respect the imposed frequency and was strongly influenced by the subject in front of him. This is hardly surprising since humans are inherently adaptive creatures and motor resonance is particularly strong for biological movements. Moreover, humans have an adaptation period until the emergence of synchronisation with a rhythmic signal. This delay can be counted in seconds and would bias the interaction. The use of a video ensures that none of the problems mentioned above can occur. This videotaped human will be referred to as "non-adaptive human" in the rest of the paper. In the adaptive mode, the human partner was sitting in front of the subject and was also equipped with inertial units. An auditory signal indicated the beginning and the end of the interaction for the experiment. The participants were instructed to wave when the human partner was waving.

Acquired Data & Questionnaires

The subjects were equipped with a Waveguard EEG cap by ANT with 32 electrodes placed according to the International 10-20 system. A TMSI Refa 32 amplifier [tms, 2017] collected brain activity at 512 Hz. They also wore TEA T-Sens Motion (IMU) sensors [tea, 2020] on the right arm to gather motion data at 64 Hz.

[9] https://members.loria.fr/mjouaiti/files/vp10.mp4
[10] https://members.loria.fr/mjouaiti/files/h10.mp4



Figure 7.4: Top: Experimental setup, the subject is seated in front of the partner (robot, VP or human). Bottom: The three interaction partners: VP, robot, human

EEG analysis

Data processing was performed using MATLAB. We mostly used EEGLAB [Delorme and Makeig, 2004] functions for EEG data preprocessing and visualisation. During visual data inspection, we noticed very noisy channels on peripherical electrodes (A1, A2, T7, T8, O1, O2, Oz) due to a large cap size for some subjects. Thus these electrodes were removed for all subjects. First, each dataset was bandpass-filtered using a FIR-filter with low cutoff at 4 Hz and high cutoff at 30 Hz. Then, we cleaned the data using EEGLAB function to remove flatline channels, low-frequency drifts, noisy channels and short-time bursts. Finally, we cut out the data (periods without movement) in between interactions as they didn't contain any relevant information and might have negative influence on the results. These steps were performed with the Artifact Subspace Reconstruction method [cle, 2019] using the *pop_ eegfiltnew* (parameters: low cutoff frequency=4; high cutoff frequency=30; filter order=2000; invert filter=false) and *clean_ rawdata* (parameters: flatline criterion = 5; Transition band for the high-pass filter= [0.25, 0.75]; Minimum channel correlation=0.85; Line Noise Criterion=4; Burst Criterion = 3; Window Criterion=0.05) functions. After all these steps, at least 90% of the original data remained in each condition (294 interactions of 10 seconds for the non-adaptive human; 299 for the non-adaptive robot; 295 for the non-adaptive VP; 301 for the adaptive human; 307 for the adaptive robot).

Cleaned data were filtered into theta, alpha and beta frequency bands and we computed the spectral power of each band using the Fast Fourier Transform. The engagement index [Pope et al., 1995] we employed is thus defined as follows:

$$engagement = \frac{SP(\beta)}{SP(\alpha) + SP(\theta)} \tag{7.1}$$

with $SP(f)$ the spectral power of the frequency band f.

This index was computed for each electrode over the ten seconds of each interaction. We

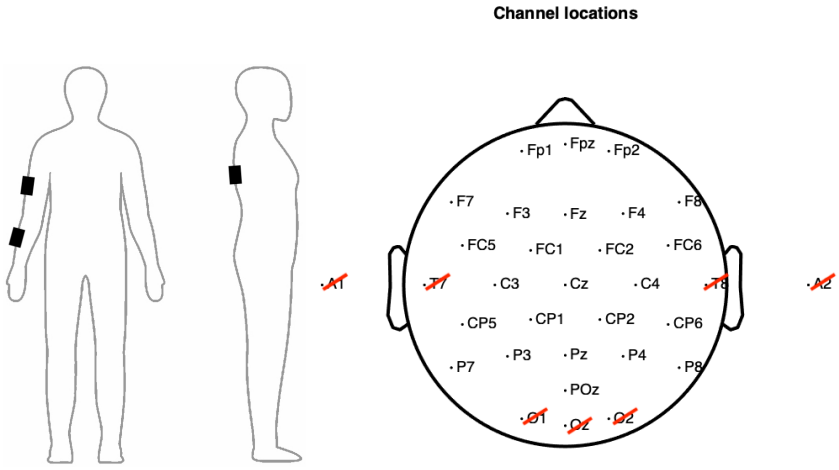


Figure 7.5: Left: Location of the motion sensors (one in the back for reference, two on the right arm). Right: placement of the EEG electrodes on the participants' scalp. The electrodes crossed in red were not used.

consider the average across all electrodes for each interaction. In the results section, we show the average for all subjects in each condition.

Questionnaire

Prior to the experiment, the subjects were asked to fill in the NARS (Negative Attitudes towards Robots Scale) questionnaire [Nomura et al., 2004] (See Appendix D.1) which evaluates negative attitude towards communicating with robots. It is divided into three subscales:

- **S1**: Negative Attitude toward Situations of Interaction with Robots;
- **S2**: Negative Attitude toward Social Influence of Robots;
- **S3**: Negative Attitude toward Emotions in Interaction with Robots.

This questionnaire was also adapted to evaluate negative bias toward virtual partners. The NARS results were not used as an exclusion criterion.

Afterward, the participants filled in a post-recording questionnaire at the end of each part. For each partner, they rated the following items between 1 and 5:

"During my interaction with the **X** partner, I globally had the feeling that:

- **Q1** it adapted its movement;
- **Q2** it influenced my movement;
- **Q3** we were synchronised;
- **Q4** this interaction was easy to perform for me;
- **Q5** I found this interaction enjoyable;
- **Q6** performing the gesture necessitated learning on my part;
- **Q7** I think that this interaction is easy to perform for most people."

7.2 Results

A result is considered significant if $p < 0.05$. However, since we perform multiple tests on the same dataset, we apply a Bonferroni correction. The level of significance thus becomes 0.0167 for the engagement and coordination results. It remains $p < 0.05$ for the evaluation of the NARS and post-recording questionnaires that undergo only one test.

7.2.1 NARS Results

The NARS questionnaire revealed that the participants had a stronger negative bias towards virtual agents than towards robots across all scales (See Table 7.1).

	S1	S2	S3
Robot	10.33 ± 3.06	12.75 ± 3.52	13.25 ± 5.12
VP	11.83 ± 4.97	13.83 ± 3.71	14.67 ± 5.55

Table 7.1: Results of the NARS Questionnaire for each subscale (defined in section 7.1.5. The higher the score, the higher the negative bias towards the partner. The values provided are averaged across participants for the relevant questions of the subscale 7.2.1)

7.2.2 Do Different Types of Partners influence Coordination?

To evaluate the motor coordination for each interaction, we computed the PLV between the participant's arm movement and the videotaped human's arm movement, the angular position of Pepper's arm (obtained from the robot sensors) and the sinusoid which generated the arm movement of the VP. For each interaction, we computed the average PLV (See Table 7.2.2).

Subject	PLV Human	PLV VP	PLV Robot
1	0.58	0.50	0.72
2	0.28	0.74	0.61
3	0.60	0.55	0.70
4	0.51	0.77	0.73
5	0.29	0.90	0.94
6	0.60	0.34	0.60
7	0.52	0.90	0.87
8	0.20	0.89	0.72
9	0.35	0.59	0.70
10	0.63	0.64	0.61
11	0.59	0.83	0.62
12	0.16	0.91	0.97
Average	0.44 ± 0.17	0.73 ± 0.13	0.71 ± 0.19

Table 7.2: Results for Coordination Performance

The coordination data (324 interactions for each condition) were evaluated with a repeated measure one-way ANOVA. It revealed a significant difference between all the conditions [$F(2, 324)=87.732$, $p \leq 0.0001$] with subjects being notably more coordinated in the robot (0.71 ± 0.19) and virtual agent conditions (0.73 ± 0.13) than in the human condition (0.44 ± 0.17). A Post-

hoc test (Tukey) confirms the significant difference between the Robot-Human and VP-Human conditions but shows no significant difference between the Robot and VP conditions.

Interestingly, we can see from the post-recording questionnaire (See Fig. 7.6) that even though the partner was master of the interaction, at least half of the participants had the feeling that the partner adapted to them in each condition. Also, they had the feeling that the robot (4.2 ± 0.6) influenced their movement more than the human (3.2 ± 1.2) or the virtual agent (3.83 ± 0.94). Besides, participants felt more synchronised with the robot (3.83 ± 1.03) than with the VP (3.58 ± 1.51) or the human (3.0 ± 1.3). They also reported that the interaction with the robot (4.1 ± 0.54) was easier than with the human (3.83 ± 0.58) or VP (3.5 ± 1.0). The interaction with the robot was enjoyed the most (4.08 ± 0.67) and the one with the VP the least (2.5 ± 0.9) (human: 3.67 ± 0.78). For all conditions, subjects felt that it necessitated similar learning on their part (human: 2.42 ± 1.0; robot: 2.58 ± 1.0; VP: 2.67 ± 1.07). Finally, participants answered that the human interaction (4.5 ± 0.67) might be the easiest to perform compared with the robot (3.92 ± 1.0) or VP (3.2 ± 1.11) one.

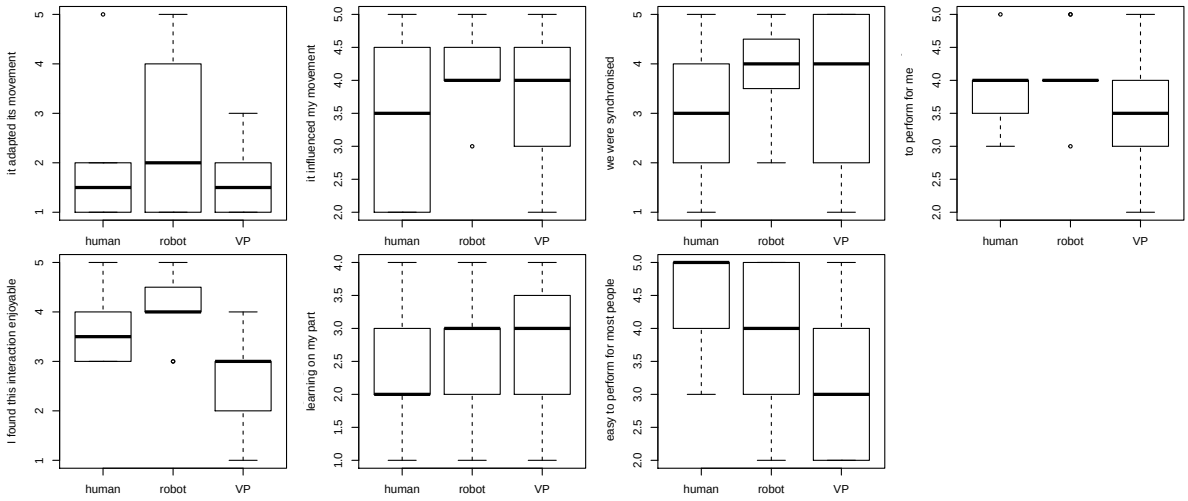


Figure 7.6: Results of the post-processing questionnaire for the first part of the experiment. The answers ranged from 1 to 5

We also ran a Pearson correlation on the NARS answers and the coordination performance which revealed no significant correlation.

7.2.3 Do Different Types of Partners influence Engagement?

Despite the fact that participants were much less coordinated with the human partner, they were more engaged (0.200 ± 0.01) than with the robot (0.192 ± 0.006) or with the VP (0.178 ± 0.003) (See Figure 7.7 for an overview of the engagement results). Moreover, on the engagement topography, we can see more activation in the temporal lobe.

A one-way ANOVA showed a significant difference in engagement between all three conditions [$F(2) = 5.68$, $p < 0.01$]. A Post-hoc test (Tukey) confirms the significant difference between the VP and human conditions but shows no significant difference between the Robot-VP and the Robot-Human conditions.

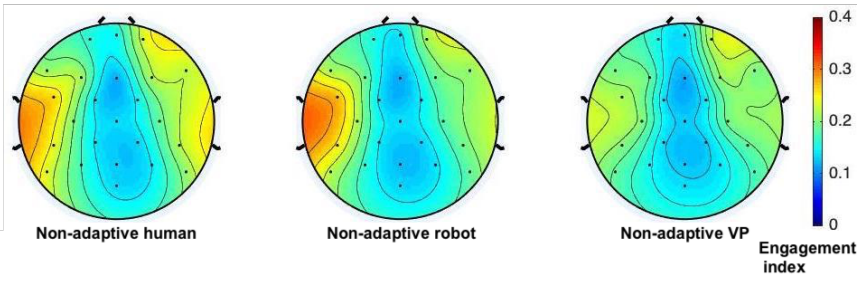


Figure 7.7: Engagement topography (obtained with the topoplot function) for non-adaptive conditions: human, VP, robot. A topography represents the human scalp and the positions of the EEG electrodes. The EEG data allow us to derive an engagement value for each electrode, hence the topography. The EEGLAB toolbox interpolates the values between the electrodes.

7.2.4 Does Engagement correlate with Coordination?

A Pearson correlation analysis between the engagement index (average across all electrodes) and the coordination performance for each interaction also revealed a significant correlation between the engagement and the coordination performance in the human [$t = 3.39$, $p < 0.001$] and VP [$t = -4.12$, $p < 0.0001$] conditions but not in the robot condition [$t = 0.60$, $p = 0.547$].

7.2.5 Do Adaptive Abilities Improve Engagement or Coordination?

A paired Wilcoxon signed-rank test on the post-recording questionnaire for the human partner (See Fig. 7.8) (adaptive and videotaped human) showed that there was a statistically significant difference in the perception of adaptation from the human partner [$Z = -2.840$, $p \leq 0.01$], perception of being influenced ($Z = -2.565$, $p \leq 0.01$), perception of being synchronised [$Z = -2.719$, $p \leq 0.01$] and enjoyment [$Z = -2.333$, $p < 0.05$]. On average, the participants were better coordinated with the adaptive human (0.87 ± 0.09) than with the non-adaptive human (0.44 ± 0.17). However, the interaction was not perceived as easier to perform or more enjoyable .

A paired Wilcoxon signed-rank test on the post-recording questionnaire for each question for the robot partner (See Fig. 7.9) (adaptive and non-adaptive robot) showed that there was only a statistically significant change in the perception of being influenced by the robot [$Z = -2.232$, $p \leq 0.05$]. Overall, people reportedly enjoyed less the interaction with the adaptive robot. This can be explained by the fact that this condition was more constrained due to the arm detection and when the detection failed, the robot would stop moving. Indeed, the human detection failed for some subjects with very colourful clothes or when the arm was not properly positioned (not visible enough). For the results analysis, we removed problematic segments from the experiment, in average 15% ± 14% of the interaction for each subject. Note that most subjects had between 0 and 11% removed. After removal, 276 interactions remained for the analysis.

A paired Wilcoxon signed-rank test also reveals a significant difference in coordination performance between the adaptive human condition (0.87 ± 0.09) and the non-adaptive human condition (0.44 ± 0.17) [$V = 0$, $p \leq 0.001$]. There was however, no significant difference between the adaptive robot condition (0.56 ± 0.03) and the non-adaptive robot condition (0.71 ± 0.2) [$V = 64$, $p = 0.052$]. A paired Wilcoxon signed-rank test also showed a significant difference for engagement between the adaptive human condition (0.225 ± 0.01) and the non-adaptive human condition (0.200 ± 0.01) [$V = 13594$, $p \leq 0.0001$], there is however no significant difference

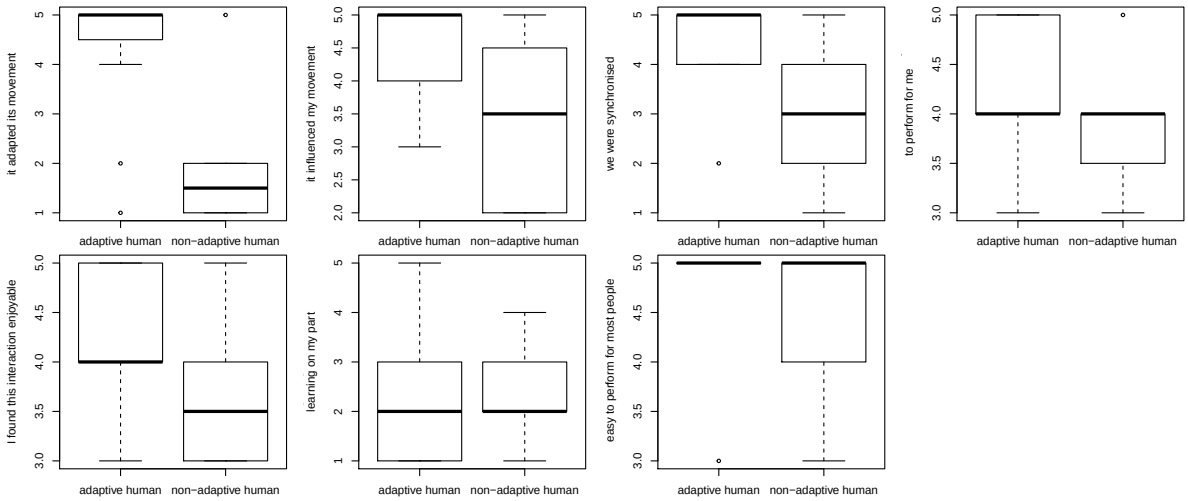


Figure 7.8: Results of the post-processing questionnaire for the first and second part of the experiment for the human partner

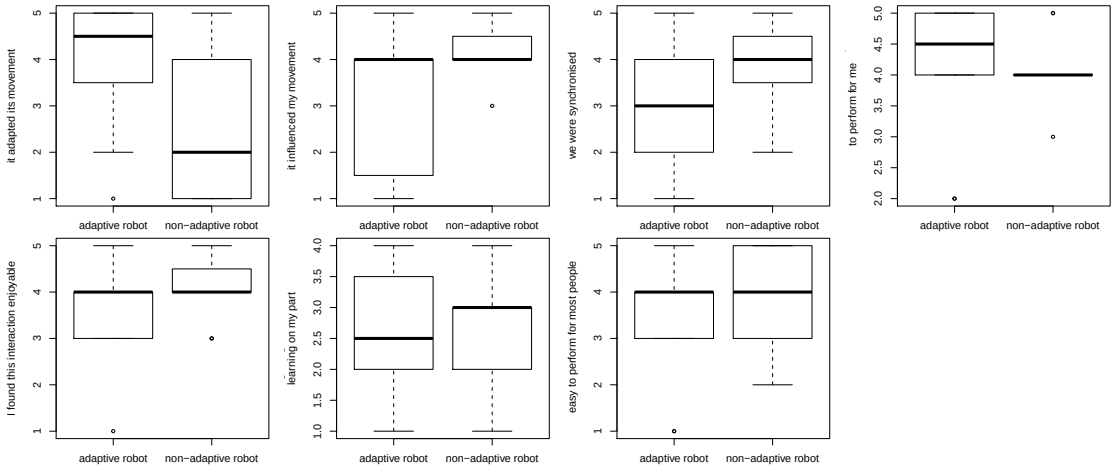


Figure 7.9: Results of the post-processing questionnaire for the first and second part of the experiment for the robot partner

between the non-adaptive robot condition (0.192 ± 0.006) and the adaptive robot condition (0.199 ± 0.006) [V=20004, p = 0.106] (See Figure 7.10).

Conclusion

Preliminary results support that the type of interaction partner has an influence on engagement and coordination. In the non-adaptive part, participants were more engaged with the videotaped human than with the robot or VP. They appeared, however, much better coordinated with the robot and with the VP than with the human.

This seems to go against our hypothesis that engagement is correlated with motor coordination. Moreover, participants were better coordinated and engaged with the adaptive human than with the non-adaptive one. There was, however, no significant difference between the non-adaptive

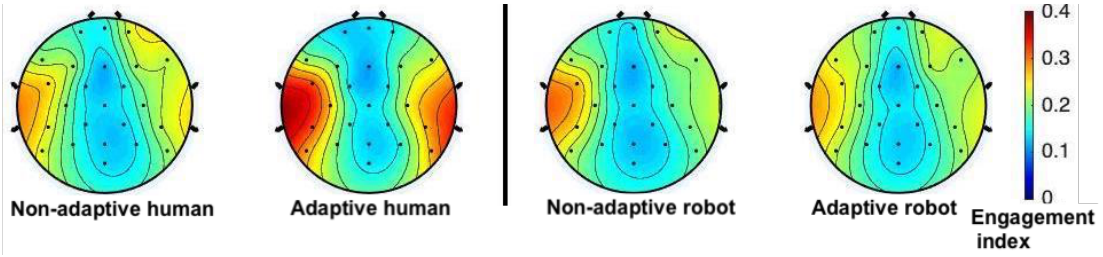


Figure 7.10: Engagement topography for the non-adaptive human, adaptive human, non-adaptive robot and adaptive robot conditions

robot and the adaptive one.

As one might expect, subjects were more coordinated and engaged in the human adaptive condition than in the non-adaptive condition. Indeed, unilateral adaptation in HRI already comes across as awkward [Lorenz et al., 2013], but humans have even higher expectations for other humans. This confirms previous results [Lorenz et al., 2013, Hasnain et al., 2013] that a non-adaptive human partner feels very unnatural. Besides, there was no significant difference between the adaptive and non-adaptive conditions for the robot. There were some technical difficulties in the adaptive robot condition where the pose estimation was sometimes failing and the robot was not adapting. While some participants got annoyed at the condition when it was not working, others seemed to thoroughly enjoy it, as they were trying to test the limits of the robot and playing with it. Even though the engagement results are not as high as we expected, possibly due to those technical difficulties, we are confident that adaptive capabilities improve the quality of the interpersonal interactions as we could clearly see it in the behaviour of the subjects who were bored or even drowsy in the non-adaptive conditions. This hypothesis should be confirmed with a more robust pose estimation algorithm and more subjects.

Now that we have validated the CPG controller theoretically and experimentally, we will direct this work towards motor rehabilitation for autistic children in the next part of this thesis. First, we will give an overview of robot-assisted motor rehabilitation for autistic children. Second, we will present two pilot studies with autistic children.

Part III

Towards Robot-Assisted Motor Therapy for Autism

Chapter 8

Motor Coordination in Autism Spectrum Disorders (ASD)

In this chapter, we realised a systematic review of robot-assisted motor rehabilitation for autistic children [Jouaiti and Henaff, 2019d].

8.1 Autism spectrum disorder

Autism spectrum disorder (ASD) is a heterogeneous neuro-developmental disorder of multifactorial origin, usually characterised by deficits in social interaction, communication and motor coordination skills. The first description of Autism Spectrum Disorder (ASD) was realised by Kanner in 1943. ASD is an umbrella term with different manifestations of autism at various levels of severity (formerly Kanner's autism, Asperger syndrome, high functioning autism).

As of 2018, the prevalence of ASD is estimated at 1.7 % of the population (2.7 % of boys and 0.67% of girls). Diagnosis of ASD has been increasing for decades, but there is no consensus whether this is a result of increased awareness, improved detection, expanding definitions, increase in incidence or a combination of all these factors. Diagnosis now relies on the DSM-V (Fifth Edition of the Diagnosis and Statistical Manual of Mental Disorders, 2013). It highlights two areas of impairment: social communication and behavioural domain which can be rated by level of severity. ASD is usually associated to a wide range of comorbidities such as developmental coordination disorder (DCD), attention deficit hyperactivity disorder (ADHD), obsessive compulsive disorder (OCD), gastrointestinal symptoms...

ASD cannot be "cured" but abilities can be enhanced thanks to different types of therapy. Early intervention is thus paramount. Some popular therapies are ABA, TEACCH (Treatment and education of autistic and related communication handicapped children [Watson, 1989]).
ASD requires sustained therapy to stimulate the children as much as possible and improve their interaction capacity. As such, human-based therapy is extremely expensive. ASD children usually love interacting with animals and this has proved to be effective in enhancing social skills [Redefer and Goodman, 1989, Martin and Farnum, 2002, Bass et al., 2009, Silva et al., 2018]. Unfortunately, animal therapy is also highly constrained because the animals have to be trained and taken care of. On the other side, robots are low-maintenance and create less constraints. There is also evidence that some individuals with ASD prefer robots to non-robotic toys or humans [Diehl et al., 2012, Desideri, 2017, Costescu et al., 2014]. This, however, raises ethical concerns and some researchers advocate a "low-dose" robot therapy (20% is advised)

where humans should be fully included [Robins et al., 2005a, Goodrich et al., 2011]. Indeed, the goal of robot therapy is not for the children to interact solely with the robot, but to open up to humans. Thus, robot therapy has to be carefully designed to avoid children withdrawing socially and interacting only with robots.

Studies also reported that severity of motor skills impairment was directly correlated with severity of social and communication impairments [MacDonald et al., 2014, Dziuk et al., 2007]. These impairments are usually divided into three categories: social interaction, social communication and imagination [dsm, 1993].

8.1.1 Social Interaction

Every child is different and presents his own difficulties. While some are completely oblivious towards people, others desperately seek to make friends without being able to do so since they are not aware of social norms, do not understand social cues and other people's feelings or behaviour. Ability to make eye contact, understand feelings, interpret the tone of voice and decipher facial expressions are also impaired or non-existent. Those difficulties make social interactions extremely challenging and often lead the individual to avoid such situations. ASD children often engage in their own repetitive activities alone. This withdrawal prevents children from acquiring fundamental skills and hinders their developmental progress.

8.1.2 Social Communication

Social communication deficits enclose both verbal and non-verbal communication. Speech can be completely absent and language delay is quite common (except in Asperger's). When speech is present, it is often idiosyncratic. Tone and pitch of voice are often impaired (high pitch, monotonous intonation) and associated to a lack of understanding of it. Speech may be irrelevant to the conversation or the context but focused on the individual's interests. ASD individuals often present the inability to initiate or meaningfully contribute to a conversation. They are also blind to facial expressions, body language and social cues which are an essential part of interpersonal interactions. Though non-verbal communication is not innate and has to be learned, ASD individuals struggle to master it.

8.1.3 Imagination

Deficits in imaginative and conceptual skills can lead to the inability to generalise learned skills or to think in abstract terms. This is usually associated with a rigid way of thinking and doing things, repetitive activity and narrow interests. This also hinders adaptability and unplanned changes or perturbations are often met with anxiety and distress [Baron-Cohen and Wheelwright, 1999]. Lack of imagination can also be found in the repetitive patterns when ASD children play or don't play at all.

8.2 Motor Deficits in ASD

Impaired motor functioning has been consistently observed by parents and clinicians (see [Peña de Moraes et al., 2017] for a review of impaired motor learning in ASD). It involves mostly general clumsiness in gait [Biffi et al., 2018, Dufek et al., 2017, Rinehart et al., 2006a, Rinehart et al., 2006b, Vernazza-Martin et al., 2005], balance [Molloy et al., 2003], manual dexterity [Kushki et al., 2011, Alaniz et al., 2015], praxis [Abu-Dahab et al., 2013, Rodgers et al., 2019, Sacrey et al.,

2014, Glazebrook et al., 2006, Nazarali et al., 2009] and coordination [Curioni et al., 2017, Xavier et al., 2018, David et al., 2009, Romero et al., 2016].

Studies also reported that severity of motor skills impairment was directly correlated with severity of social and communication impairments [MacDonald et al., 2014, Dziuk et al., 2007, Manwaring et al., 2017, Dadgar et al., 2017, Higashionna et al., 2017, Jasmin et al., 2009, Purpura et al., 2016, Hilton et al., 2012, Goldman et al., 2009] since motor skills are a paramount part of social communication and can impact the understanding of others' actions [Gallese et al., 2013]. [Cummins et al., 2005] showed that autistic children with motor deficits had less empathy and greater social difficulties.

34 to 79 % of the autistic population (opposed to 5% of the typical population) is affected by Developmental Coordination Disorders (DCD) [Kopp et al., 2010]. This involves nervous tics, laterality disorders, tip-toeing, synkinesis, catatony, oculomotor disorders, diadochokinesis, dysgraphy, inappropriate manual force, low digital speed and slowness of dexterity. Overall 80% - 90% of children with ASD show some degree of motor abnormality [David et al., 2009, Dziuk et al., 2007, Ghaziuddin and Butler, 1998, Hilton et al., 2012, Ming et al., 2007, Provost et al., 2007].

Motor control is classically divided into motor planning in the higher levels and execution in the lower levels. Besides, movement execution involves connections between multiple brain regions. First, the prefrontal cortex communicates with the basal ganglia and decides the motor strategy based on sensory information (auditory, visual, somatic, proprioceptive). Then the primary motor cortex, supplementary motor area and the cerebellum compute the muscles activation sequence to perform the task. It is believed that the angular and supramarginal gyri are the site of storage of learned time-space movement representations which help to program the premotor cortex. Finally, the premotor cortex is involved in translating movement representations into motor programs, which then activates the motor cortex for execution. The motoneurons and spinal interneurons generate the movement and adjust it, if needed.

A crucial step in motor learning is the ability to form internal models [Krakauer and Shadmehr, 2007], i.e. predict the consequences of motor commands and learn from errors to adapt. The cerebellum is a site for acquisition of internal models and it has been observed in post-mortem exams that the cerebellum is indeed abnormal in individuals with ASD [Williams et al., 1980, Ritvo et al., 1986, Bauman and Kemper, 2005, Bailey et al., 1998, Fatemi et al., 2002]. However, [Larson et al., 2008] showed that ASD children had no problem acquiring new internal models, thus hypothesising that the dysfunction stems from another region (basal ganglia, frontal or parietal) or from connectivity abnormalities between regions [Balsters et al., 2018]. Indeed, low activation of the cerebellum and of motor execution networks also occurs in motor coordination tasks [Mostofsky et al., 2009]. Autism is characterised by hypo-functioning of the connections in the higher level of the brain (connection between the frontal lobe and the rest of the cortex) and hyper-functioning at the lower level. It has thus been hypothesised that the decreasing cerebellum activity could evidence a difficulty to transmit motor execution from the cortical regions to the areas associated with "automated" motor execution [Stoit et al., 2013, Oldehinkel et al., 2018, Schipul et al., 2011]. Over-connectivity between the thalamus and cortical sensory processing areas [Traynor et al., 2018, Mizuno et al., 2006], as well as between basal ganglia and somatosensory and motor cortices has also been reported [Traynor et al., 2018, Di Martino et al., 2011, Turner et al., 2006, Cerliani et al., 2015]. MRI studies have shown a microstructural compromise in motor, sensory and cerebellar pathways [Nair et al., 2013, Carper et al., 2015, Sivaswamy et al., 2010, Hanaie et al., 2013, Nair et al., 2015]. Recently, altered white matter has been discovered in the left somatosensory area and its descending pathways connecting to the cerebellum [Lin et al., 2019].

Besides, fMRI studies have reported reduced volume in the fastigial nuclei and cerebellar vermis lobules VI-VII. This region is responsible for ocular motor function, verbal working memory and speech coordination.

However, in ASD, implicit motor learning ability remains intact [Nemeth et al., 2010, Izadi-Najafabadi et al., 2015, Gordon and Stark, 2007]. Implicit motor learning is defined as the acquisition of motor skill without conscious access to what was learned or even to the fact that learning occurred. Explicit motor learning occurs when the goal and the execution are plainly explained to the children. So children can exhibit a clumsy gait when consciously walking and walking becomes smooth when they focus on another task.

Moreover, imitation is an essential part of child development. It can be defined as the replication with retention of certain characteristics of an observed motor act by an individual. Imitation follows the observed act. While contributing to social learning, it also plays a critical role in the development of Theory of Mind, social cognition and communication skills. A popular belief is that ASD individuals lack Theory of Mind. Theory of Mind is the ability to attribute mental states to oneself and to others as well as understand that others have different mental states from one's own. It also involves inferring that those states can cause action [Baron-Cohen et al., 2001, Heyes, 2001]. [Jones et al., 2018] showed that there is an association between lack of Theory of Mind and restricted repetitive behaviours (motor stereotypies).

In the case of ASD, there is a controversy concerning imitation deficits [Xavier et al., 2015, Rogers et al., 2010, Vivanti et al., 2011, Salowitz et al., 2013, Vanvuchelen et al., 2011, Vivanti et al., 2014, Sowden et al., 2016] and the broken mirror theory which postulates that a deficient motor neuron system (MNS) contributes to imitation deficits [Southgate and Hamilton, 2008]. The MNS encompasses regions in the inferior frontal gyrus and the inferior parietal lobule. It is involved in both the movement production and action observation [Rizzolatti and Craighero, 2004, Guillot et al., 2009]. While some researchers reported autism-specific impairments in imitation [Meltzoff, 1993, Rogers and Pennington, 1991] and a dysfunctional MNS [Iacoboni et al., 2005, Oberman and Ramachandran, 2007], others showed intact ability to engage in imitation [Hammes and Langdell, 1981, Press et al., 2010, Bird et al., 2007], preserved action representation and thus a functional MNS [Chen et al., 2018, Carmo et al., 2013, Hamilton et al., 2007]. However, neuroimaging studies evidenced that neural activity and connectivity in regions for imitation may be abnormal in ASD [Bernier et al., 2007, Dapretto et al., 2006]. [Nishitani et al., 2004] examined oral-facial imitation in TD (Typical Development) and ASD using magnetoencephalography (MEG). They observed neural activity that temporally progressed from the primary visual cortex (V1) to the superior temporal sulcus (STS) to the inferior parietal lobule (IPL) to the inferior frontal gyrus (IFG) and finally to the primary motor cortex. Similar activation was observed in both TD and ASD participants, but activation was weaker and delayed in IFG for the ASD group. [Villalobos et al., 2005] also found decreased functional connectivity between V1 and IFG bilaterally in a fMRI study where they investigated interregional synchronisation with visual areas.

[Vanvuchelen et al., 2011] postulated that imitation deficits can be explained by either an impairment in the selection mechanism due to a poor preferential attention to biological motion and in recognising intentional actions or by an impaired correspondence mechanism due to a poor viewpoint transformation and visuomotor mapping.

Furthermore, some individuals with ASD are hyposensitive. Their touch can be inappropriate since they do not have correct sensory feedback and they can unwillingly hurt other persons [Foss-Feig et al., 2012]. On the other hand, others present hypersensitivity and can be overwhelmed by touch [Blakemore et al., 2006, Riquelme et al., 2016]. Tactile interaction could be a useful communication tool to complete inadequate verbal skills. [Caldwell, 1996] even suggests that

touch can replace defective means of communication.

8.3 Robot-Assisted Therapy for Motor Rehabilitation in ASD

HRI is a challenging research field at the intersection of psychology, cognitive science, social sciences, artificial intelligence, computer science, robotics and human-system interaction. HRI can occur in very different contexts such as assistive interactions, social encounters, work cooperation but also in a therapeutic context. The term "therapy" can be considered as a synonym of "treatment" and implies some form of correction to restore normal function to a human being.

Motor skills can be tackled from different points of view as they encompass a wide range of skills: fine motor skills, gross motor skills, motor coordination, motor imitation, sensorimotor skills. Research studies usually focus on one specific skill. Let us review those studies.

8.3.1 Coordination

[Moorthy and Pugazhenthi, 2016] used a custom-made LEGO snatcher robot to enhance psychomotor skills in ASD children. They had 20-30 minutes weekly sessions for an undetermined period. Five ASD children participated in the study and imitated the robot in four different activities which basically consisted in turning and picking up a basket. This imitation task was meant to improve non verbal imitation, hand-eye coordination, balanced body movements and backward walking. The children's progress was assessed thanks to success rate and therapists' testimony. It was reported that the children had been able to generalise the concept of pick and place and had improved eye-hand coordination.

[So et al., 2018] used the Nao robot to tell social stories while gesturing. Fifteen ASD children participated in the intervention condition in four 30-minutes sessions. They were instructed to imitate the robot gestures (fourteen intransitive gestures). They had control groups of fifteen ASD children and fifteen TD children. Results showed improvement of accurate or appropriate intransitive gestures for the intervention group and also that gestural production accuracy became similar to the TD group. The intervention group also produced more verbal markers while gesturing. Moreover, they found that gestural recognition skills were correlated to the learning ability of gestural production accuracy. Before the study, language and communication abilities and motor skills were assessed by the Psychoeducational Profile, Third Edition [Schopler, 2005] and the BOT2 (Bruininks-Oseretsky Test of Motor Proficiency [Bruininks, 1978]) test. Delayed BOT2 post-test showed that progress was maintained.

[Srinivasan et al., 2015] compared rhythm and robot intervention (Nao and Rovio) with thirty-six ASD children. The children were divided into three groups: robot, rhythm intervention and control group. Each group engaged in joint action-based gross motor and/or fine motor activities that promoted social skills (eye contact, turn taking, greeting and imitation) as well as communication skills. The rhythm and robot groups promoted balance, coordination, interpersonal synchrony, imitation and manual dexterity. The control group focused on fine motor skills. Training lasted eight weeks and four sessions were provided each week. Motor skill deficits were assessed with the MABC-2 test (Movement Assessment Battery for Children [Henderson and Sugden, 1992]) and evolution was followed with the BOT2. They observed more negative behaviours in the robot and rhythm groups but the frequency decreased over the weeks for the rhythm group. Negative behaviours can be explained by the fact that the activities in those groups were highly unconstrained, which generated a lot of stress for the children. However, there was no improvement for the robot group. The authors attributed this to poor robot performance.

According to this paper, rhythm therapy should be favoured as long as robots are so technically

restricted, especially on the movement generation side. Indeed, in long-term interventions, children tend to grow bored of such limited robots.

8.3.2 Imitation

Robots have been extensively used in ASD children-robot interactions to observe imitation abilities [Boucenna et al., 2014, Bugnariu et al., 2013, Conti et al., 2015]. While [Pierno et al., 2008] observed that seeing a robot movement elicits a faster movement to grasp a ball than seeing a human movement in ASD children, [Bird et al., 2007] showed that ASD adults imitate the hand of a robot more often than the hand of a human.
[Greczek et al., 2014] studied the influence of graded cueing feedback to improve imitation with twelve ASD children during five sessions over the course of 2.5 weeks. Six children received maximum feedback while the others received adaptive feedback depending on their performance. They computed imitation accuracy using a Kinect sensor and showed that graded cueing led to non-decreasing trend in imitation accuracy compared to the non-adaptive condition. Moreover, [Zheng et al., 2016] also used the Nao robot with eight ASD and eight TD children. They were asked to imitate a robot or a human raising one hand, raising two hands, waving and opening their arms. They evaluated accuracy of imitation using a Kinect. They observed more engagement when the child interacted with the robot and better imitation improvement in the robot session for the ASD children than in the human condition. The typical children, however, showed no significant improvement. [Ali et al., 2019] designed a study to improve joint attention and imitation, which they tested with twelve ASD children across eight sessions over six months. The children observed two robots imitating each other and then had to imitate one of the robots performing arm gestures. Success rates from the Kinect and EEG data were assessed. The paper focuses mainly on joint attention, for which it shows improvement, there was however no improvement in imitation skills. [Beer et al., 2016] combined music therapy with the Nao robot to improve imitation with four ASD children over the course of six weeks. The robot was integrated to the regular music therapy sessions of the children. The robot performed dance moves in accordance with the therapy music. They observed an increase in frequency of imitating the robot dance and a decrease in the therapist's prompts.

8.3.3 Fine Motor Skills

[Srinivasan et al., 2015] used the robot Nao and the mobile robot Rovio in a motor rehabilitation study. They had thirty-six ASD children divided into three groups: control, rhythmic and robot groups. The control group did table top activities to develop fine motor skills. The rhythm group performed whole-body discrete imitation and interpersonal synchrony-based rhythmic games with music. The robot group performed dual and multilimb imitation and synchrony-based games. The aim for the latter groups was to improve balance, bilateral coordination, imitation, interpersonal synchrony and manual dexterity.
[So et al., 2019] endeavoured to improve fine motor skills in a study where a robot or a human (control group) engaged in daily life conversations and demonstrated fourteen intransitive gestures to twenty-three ASD children. The intervention lasted nine weeks. It started with a pre-test (BOT2) and post-tests were performed immediately after the training and two weeks after to assess the generalisation effect. Results showed that the robot acting as a teacher was as effective as the human. However, children in the robot group were more likely to engage eye-contact with the teachers. Gestural production improved for both groups.
[Palsbo and Hood-Szivek, 2012] used a haptic robot

to improve fine motor skills of eighteen children with motor impairments (AHDH, attention deficit disorder, cerebral palsy and ASD) including five children with ASD. They underwent 15-20 daily sessions of 25-30 minutes each over 4-8 weeks. The children performed different writing tasks designed according to their writing difficulties (slowness, reversed letters...). They also performed robot-assisted glyph formation. Progress was assessed with the BEERY-VMI (Beery-Buktenica Developmental Test of Visual-Motor Integration) test. For the ASD children, progress was observed in writing speed and letter reversal. The therapy was however ineffective for children under age 9.
[Moorthy et al., 2016] developed a shoe-like robot to teach ASD children to recognise left and right shoe and improve fine motor skills when closing a velcro band. When properly closed, positive visual feedback was provided. They tested the system with eight ASD children over four consecutive daily sessions. They performed pre-tests and post-tests which consisted in identifying real shoes, recognising the left and right one and closing the velcro band. They observed improvements in this everyday task.

8.3.4 Sensorimotor Skills

[Robins and Dautenhahn, 2014] used the Kaspar robot to teach appropriate tactile behaviour. The children could explore touch and interaction and were able to perform inappropriate behaviour. The robot reacted to touch and indicated inappropriate behaviour or hurtful contact. The authors observed that the children became more aware of their force and started paying attention to their actions.
[Costa et al., 2015] also used a robot to teach eight ASD children, across seven sessions of ten minutes, how to use the appropriate force when physically interacting with a partner and to acquire the awareness of their body parts. The robot successfully acted as mediator and they observed increased triadic interaction. Inappropriate force also decreased compared to the first session.
[Lee et al., 2014] designed a study to improve control of hand force using a sphere which could change colour. Eight children had to apply the required force and maintain it until the end of the test. They performed the experiment with and without feedback from the robot. The experimenters observed success rate as well as target keeping. Authors reported that children performed better with robot feedback.

Conclusion

We remark that most therapeutic studies are focused on improving emotion or social skills. While those are obviously an issue and should be extensively studied, motor skills should not be neglected since they are directly correlated with severity of communication skills and hence of ASD and DCD is indeed a prominent comorbidity of ASD. However, so far, there are very few sound studies proposing a therapy to improve motor skills.

Here is a list of the shortcomings that could be observed:

- The studies are studies on small groups of children (average: 9.27 ± 5.52)
- Vast heterogeneity in the process and the results making it extremely difficult to compare or evaluate
- Dubious choice of evaluation methods when clinical motor assessment tests exist. These tests should be performed before the intervention, at regular intervals during the intervention

and at the end of it

- No use of control group or evaluation on typical children. One group should interact with the robot and another one undergo another form of therapy to sensibly demonstrate that robot-therapy for motor rehabilitation is more effective than usual methods
- It is rarely taken into account whether the children already have another treatment and how it might affect the motor therapy
- There is seldom a follow-up to check if the skills have been retained

Moreover, while many studies observe children's behaviour and assess deficits, few propose a therapy. There exists several possibilities for motor rehabilitation, such as exercise therapy, rhythm therapy, occupational therapy, technology-based therapy (augmented reality, virtual reality...). However few seem to be exploited to their full extent. Indeed, while there is a significant amount of research in motor rehabilitation for stroke, spinal cord injuries, Parkinson or cerebral palsy, those studies rarely extend to ASD. Despite compelling arguments [Janzen and Thaut, 2018, Tryfon et al., 2017, LaGasse and Hardy, 2013, Jamey et al., 2019], rhythm rehabilitation still is dauntingly underdeveloped for ASD. It has indeed been observed that despite cerebellar abnormalities, individuals are still capable of motor entrainment and synchronisation. Moreover, engaging in short rhythmic motor activities leads to brain plasticity and involves structural and functional changes in the brain [Luft et al., 2004]. In spite of a regain of interest in the last few years, motor rehabilitation for ASD is also still particularly neglected in the robotics field and would benefit from more rigorous methodology and from scientists willing to involve themselves in that problematic. Even when the research aims to help and improve skills, it seldom has a clearly identified goal and it is rarely methodologically sound. Indeed, most experiments have very few subjects, no control groups and no follow-up test to evaluate improvement. A lot of studies also rely only on parent questionnaires and have no objective assessment despite the existence of recognised tests such as the BOT2. Finally, it is very hard to quantify efficiency since other interventions underwent by the children at the same time are not always taken into account and there is rarely long-term control. While most studies inspire themselves from ABA or TEACCH, few combine exercise therapy, rhythm therapy or even occupational therapy with robots. We understand that exercise or occupational therapies might be complicated due to robot limitations but we feel that combining the efficacy of rhythm rehabilitation and the engagement ASD children have with robots may be a very promising perspective.

Finally, most research employing robots is robot-centered and focuses on what design, which features to endow the robot with. This perspective was not reviewed. We do not think that the design of the robot is the most paramount aspect of the problem since children react similarly to a theatrical robot or to an actual robot. However, [Srinivasan et al., 2015] suggested that children could get bored due to robot technical limitations. Robot-oriented research is also an important aspect but a lot is already being done in this field. Instead of focusing on making an engineering contribution, it is high time research was oriented towards a more human goal.

Chapter 9

ASD Child-Robot Interactions: Pilot Studies

This chapter will introduce a study on sensory dominance in human-robot rhythmic interactions with ASD and neurotypical children and a pilot study on motor imitation for motor rehabilitation with ASD children.

9.1 Sensory Dominance in ASD

We showed in part I section 3.1 that the sound of robot actuators disturbs the motor coordination of neurotypical adult subjects in a rhythmic task. The sensory processing of ASD children is however different and this sound may affect them in other ways. Besides, this is a relevant question since robot actuators always produce a sound and this may be perturbing in a therapeutic setting.

The development of sensory systems in children appears to be related to their developmental process [Renshaw, 1930, Zaporozhets, 1961, Birch, 1962]. In young children, proximal receptors (touch, taste, smell) are more developed than distal receptors which gradually supersede the former with age.

ASD is usually associated with abnormal sensory processing where a stimulus can either trigger no reaction or a disproportionate/exaggerated response [Ornitz and Ritvo, 1968b, Goldfarb, 1963, Bergman and Escalona, 1947]. Contrary to neurotypical children, autistic children are known to prefer the use of proximal receptors (touch, taste) rather than distal receptors (vision, audition) [Goldfarb, 1956, Schopler, 1965, Schopler, 1966, Masterton and Biederman, 1983]. However, both neurotypical and autistic children respond more to a visual stimulus than to an auditory stimulus [O'Connor and Hermelin, 1965, O'Connor, 1971, Hermelin and O'connor, 1970]. In a multi-sensory experiment, [Hermelin and O'Connor, 1964] subjected children to multi-sensory stimuli. When combining visual and auditory stimuli, TD and ASD children reacted predominantly to vision. However, for the combination of touch and sound, TD children responded more to sound while ASD children responded more to touch.

Atypical functional asymmetry in the autistic brain has also been observed for nonverbal sounds, this would indicate general auditory disturbances [Bruneau et al., 1992, Ogawa et al., 1982]. [Boddaert et al., 2004] also reported an abnormal cortical activation for auditory stimuli in autistic children.

Autistic children may exhibit an unpredictable or inconsistent motor response to sensory stimuli, that is either an inhibited or facilitated motor response [Ornitz and Ritvo, 1968a, Ornitz and Ritvo, 1968b]. Moreover, [Hermelin and O'connor, 1970] showed that a visual stimulus is

more likely to elicit a movement stimulation than an auditory stimulus.

9.1.1 Experimental Protocol

The goal of this experiment is to study the sensory dominance of ASD and TD children during a human-robot rhythmic interaction. This will allow us to better understand sensory processing in such interactions and thus to better design motor therapies involving a robot.

Study Overview

This study replicates the sensory dominance study introduced in section I.3.1. Participants were asked to wave back at the Pepper robot depending on three conditions that subjected the participants to various sensory stimuli. The experiment session lasted about one hour.

Experiment Design

The parents were asked to fill in the Bogdashina sensory profile questionnaire [Bogdashina, 2016] for their child, beforehand. This questionnaire allows us to assess the sensory characteristics of each child.

During the experiment session, the child and his parent were first asked to answer robot acceptability questionnaires about the Pepper robot. The robot was visible but turned off during this time. Afterwards, the robot was switched on and the child was free to interact with it in its built-in interaction mode. This part could last between ten and twenty minutes depending on the interest the child exhibited.

Then, the child was equipped with TEA Motion sensors on the right arm. The child was seated in front of the robot, his arm resting on a pillow. The child was instructed to wave back at the robot under various conditions:

- a baseline condition where the child could hear and see the robot (AV)
- a condition where the child could not see the robot thanks to a removable panel (A)
- a condition with white noise through headphones (V)

The child was videotaped during the interaction.

Finally, the child and his parent were asked again to answer the acceptability questionnaires.

Participants

Twenty children participated in the experiment. Five children were autistic (only boys, 9.6 $\pm$ 2.07 years old). The other fifteen were neurotypical (including 7 girls, 9.1 $\pm$ 2.0 years old). Two neurotypical children were excluded from the study results due to a motion sensor malfunction. Moreover, due to the COVID-19 outbreak, we had to cancel additional experiments and recruitment was interrupted. This experiment was approved by Inria ethical committee. The accompanying parent of each child gave a written informed consent.

Materials

The Robot We used a Pepper robot [Pandey and Gelin, 2018] (Softbanks Robotics) programmed to wave according to a sinusoidal signal. The signal frequency varied from one interaction to the other ($0.9Hz$, $1.0Hz$ or $1.1Hz$) to avoid frequency acclimatisation. The robot woke up from its

rest state at the beginning of each series of interactions. Waving periods were indicated by an auditory stimulus and by the robot eyes becoming green, they were unlit otherwise. At the end of each series, the robot returned to its rest state. Each condition consisted of a series of nine waving interactions.

Acceptability Questionnaires

At the beginning and at the end of the session, the robot acceptability was evaluated for the child with a picture-sorting task and a social acceptance questionnaire [Kory-Westlund and Breazeal, 2019] and for the parent with a combination of four questionnaires (See details in Appendix D):

- Technology Anxiety questionnaire from [Meuter et al., 2005] (adapted from [Raub, 1981])
- Questionnaire to assess acceptance of assistive social agent [Heerink et al., 2010]
- Questionnaire to evaluate technological familiarity [Thompson, 2011]
- Attrakdiff [Lallemand and Gronier, 2015]

Acceptability results will not be reported in this thesis as this analysis had to be delayed to the COVID-19 outbreak.

Gaze analysis

Using the video of the child, we can extract gaze direction (See Fig. 9.1). The program [11] first detects the face in the picture, then identifies face landmarks to extract the eyes. Applying a threshold on the image allows to extract the pupil coordinates.

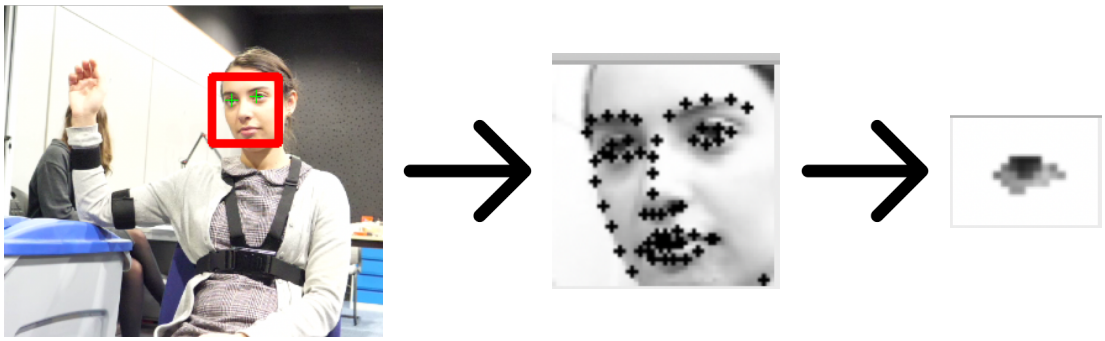


Figure 9.1: Illustration of the gaze extraction process: Face detection → landmarks detection → eye extraction

9.1.2 Results

Coordination performance

To ascertain that the child was actually looking at the robot when required, we extracted the gaze direction from the video. Interactions where the child's gaze direction varied too much were excluded from the data analysis. It is worth mentioning that children's gaze was more focused on the robot in the V condition (ASD:48.2%, TD:52.8%) than in the AV condition (ASD: 22.2%, TD: 26.9%).

[11] https://github.com/antoinelame/GazeTracking

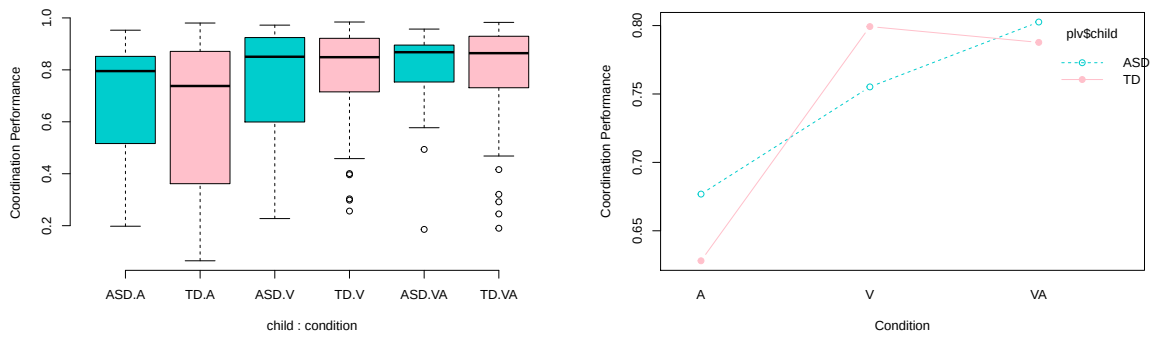


Figure 9.2: Coordination performance results. Left: boxplot representation of the coordination performance according to condition (AV, V, A) and child diagnosis (ASD, TD). Right: Interaction effect between the conditions

Preliminary results show that autistic children were more coordinated in the AV condition while neurotypical children were similarly coordinated in the AV and A conditions. See Table 9.1 and Figure 9.2 for an overview of the results.

condition	AV	A	V
TD	0.79 ± 0.20	0.63 ± 0.27	0.80 ± 0.17
ASD	0.80 ± 0.17	0.76 ± 0.23	0.68 ± 0.23

Table 9.1: Coordination performance

A two-way ANOVA reveals a significant difference between the conditions ($p < 0.001$) but not between the different children diagnosis ($p = 0.28$). A post-hoc Tukey test on the conditions showed a significant difference between the VA and A conditions ($p < 0.001$) and between the V and A conditions ($p < 0.001$), but not between the VA and V conditions ($p = 0.99$).

A two-way ANOVA also reveals a significant difference between age groups ($p < 0.001$). A post-hoc Tukey test on the age groups showed a significant difference between six year-olds and every other age group ($p < 0.001$).

Sensory Profile

The sensory profile revealed that most ASD children appear to be more sensitive to visual stimuli (See Table 9.2).

VA	V	A	PSV	PSA
0.69	**0.80**	0.70	**8**	4
0.66	**0.83**	0.66	11	**12**
0.92	**0.93**	0.86	**13**	**13**
0.82	0.63	0.64	**8**	5
0.68	0.48	0.53	**9**	7

Table 9.2: Summary table with Coordination performance scores and sensory profile scores (PSV: visual sensory profile; PSA: auditory sensory profile) for the 5 ASD children in the study

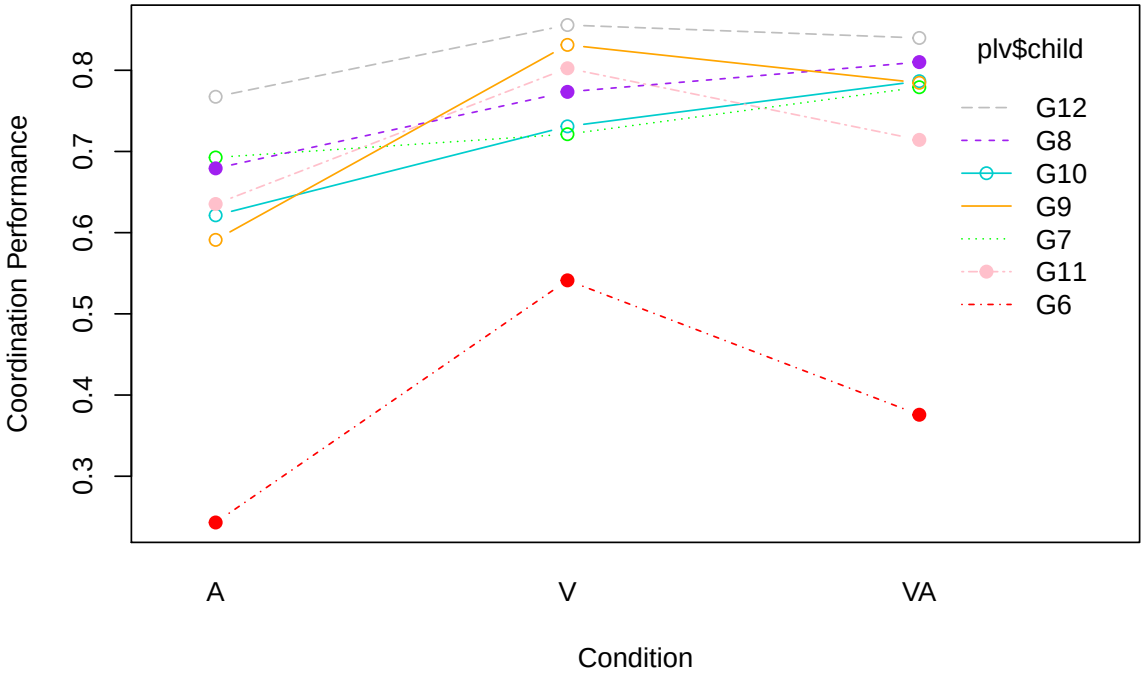


Figure 9.3: Coordination performance for each age group (See details in text)

For the neurotypical children, only two appear to be more sensitive to visual stimuli and five to auditory stimuli. A statistical analysis reveals no correlation between sensory profile results and coordination performance

9.2 Imitation with CPG Controllers in ASD

Child-robot imitation is a widespread approach in robot-assisted therapy, notably with autistic children. Although imitation deficits in ASD are still controversial, it has been observed that autistic children may present developmental coordination disorders with motor imitation deficits.

In this experiment, we propose a novel method for motor imitation using Central Pattern Generators (CPGs) and employ it in a pilot study involving autistic children and the Pepper robot.

9.2.1 Experimental Protocol

Experiment Design

Experiments were carried out across ten days with the Pepper robot in the Department of child psychiatry of the Strasbourg hospital. During the first three days, the children had the opportunity to discover the robot in its interactive mode and talk to it.

Then, if they were willing and if their parent had given written informed consent, they could perform the imitation experiment which was integrated into their timetable. In the experiment

session, the child was equipped with five T-Sens inertial units [tea, 2020] (one in the back and two on each arm). First, the child could move freely and the robot attempted to imitate him. Second, the child was instructed to imitate the robot.

Method

To achieve pose imitation with the robot, we employed the imitation method explained in section 6.3.2. Angular values were estimated from the robot camera using the algorithms described in Appendix C. The result of the pose estimation is passed through a low-pass filter with 1.5 Hz cut-off frequency, to remove detection aberrations. Angular speed is then used as the CPG input for each controlled joint (Hip pitch, Shoulder pitch and roll for both arms, elbow roll and yaw for both arms). The CPG output is considered as a speed command.

The code was implemented in Python and run with NaoQi.

Participants

The hospital takes care of 23 autistic children. Due to unforeseen circumstances, only 7 of them (between 7 and 11 years old, all boys) were able to take part in the experiment. This experiment has been approved by Inria ethical committee. Parents were informed of the presence of the Pepper robot and were given an information notice about the experiment. They gave written informed consent.

9.2.2 Robot Imitation

When the robot imitated the child, the latter was instructed to perform simple movements and was shown the various movements that the robot could imitate suitably. Indeed, due to technical limitations (joint limits) and OpenPose limitations, the robot cannot imitate just any movement. Most children attempted complicated gestures anyway. Some children opted to be imitated by the robot several times.

Table 9.3 reveals quite heterogeneous imitation scores. For example, child 7 did not respect the instructions in the first interaction so the robot struggled to imitate him. However, in the second interaction, he took the limitations into account which leads to a much better score. Overall, the CPG architecture was successful in imitating most gestures (See Fig. 9.4).

child	r_1	r_2	r_3	h
1	1.08	NA	NA	0.96
2	2.18	2.98	2.52	1.16
3	0.97	0.95	NA	1.65
4	0.56	NA	NA	1.23
5	0.65	NA	NA	1.48
6	0.92	1.10	NA	1.53
7	2.59	0.84	NA	1.53

Table 9.3: DTW scores for each child/interaction. The lower the score, the higher the imitation similarity. Columns r_i correspond to the interactions where the robot imitated the child. Column h correspond to the interaction where the child imitated the robot

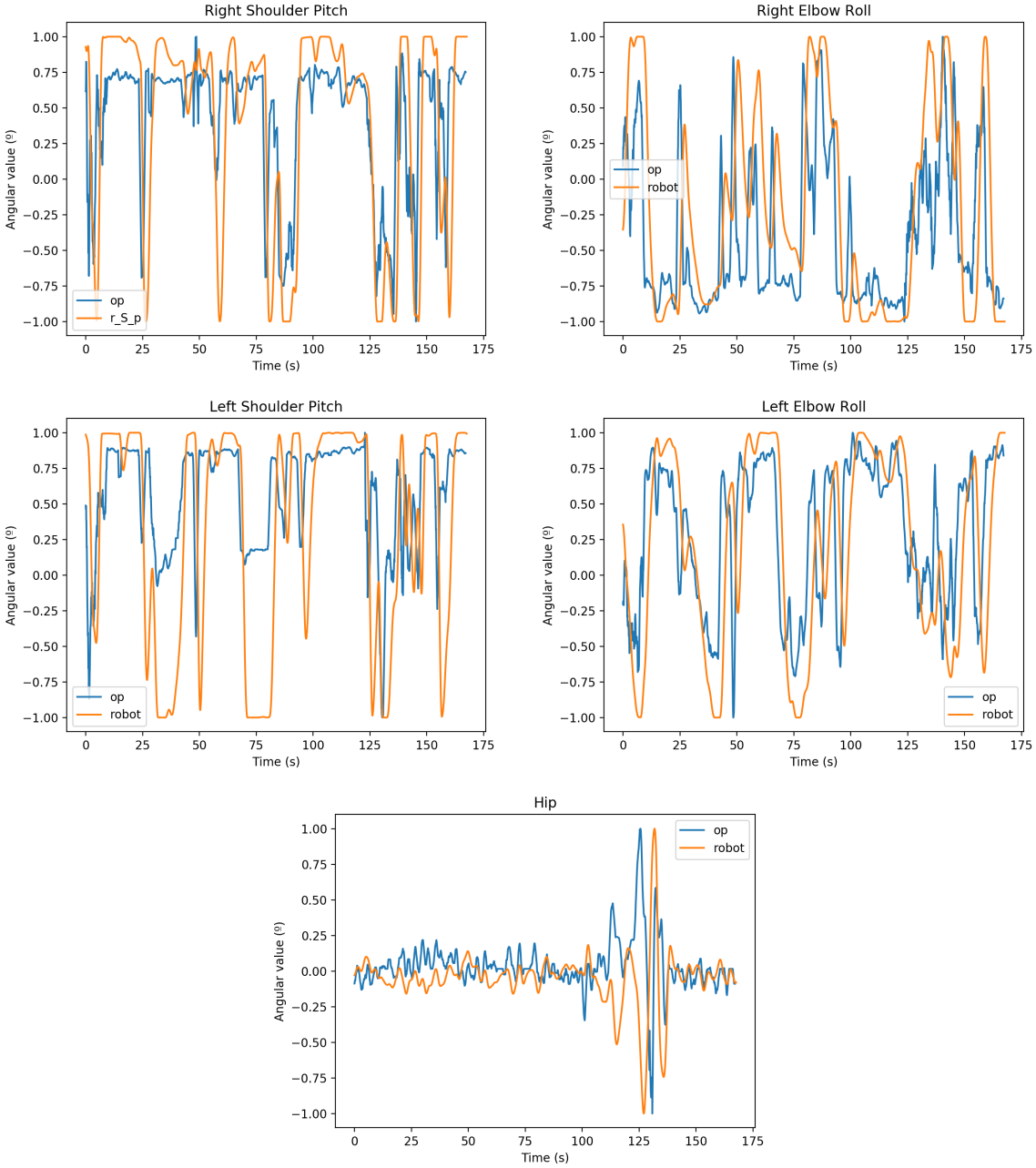


Figure 9.4: Example of interaction where the robot imitates the child. In blue, the child's position OpenPose detected; In orange, the robot position. The signals are normalised

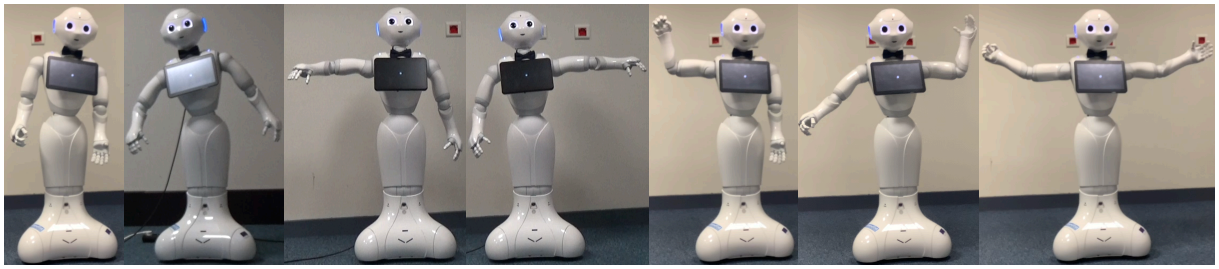


Figure 9.5: Series of movements performed by the robot (tilt hip to the right, tilt hip to the left, extend right arm, extend left arm, extend both arms, raise left arm, raise right arm)

9.2.3 Child Imitation

In the second part of the experiment, the children were asked to imitate the robot which performed a series of movements (See Fig. 9.5).

Most of the children imitated the robot gestures very well (See Fig. 9.6). We noticed that some of them seemed to have a lack of body awareness as they were convinced of being in the right position when this was not the case. Moreover, child 3 could not seem to understand that he was supposed to imitate the robot. He repeatedly asked "Why isn't the robot doing the same?".

9.3 Conclusion

In this chapter, we presented two experiments: a study on sensory dominance in a rhythmic interaction with TD and ASD children and a pilot study for motor rehabilitation using the Pepper robot with ASD children.

In the first study, preliminary results show that both ASD and TD children coordinate better with a visual signal or with a visual-auditory combination than with an auditory signal alone. This predominance of vision over audition is in concordance with previous studies [Hermelin and O'connor, 1970, Hermelin and O'Connor, 1964, O'Connor, 1971, O'Connor and Hermelin, 1965]. Besides, the children tend to look less at the robot when they can also hear the sound of the robot motors than when they cannot. While this should obviously be confirmed with a higher number of children, the children results appear to differ from the ones from the adults. While adults were perturbed in their coordination when subjected to both visual and auditory stimuli, this combination may reinforce the children's interaction and lead to better coordination.

The second study was a pilot for a potential clinical trial concerning motor rehabilitation using the Pepper robot. In this experiment, the CPG control method was effectively employed in a pilot study with autistic children. The main goal was to evaluate feasibility by first validating the controller in real life conditions but also by seeing the children's reaction with the robot. This first trial proved to be rather successful and allowed us to identify other specific needs where the robot could help. The Pepper robot was very popular with children but also with the medical staff. During the interactive phase, they noticed that some children with speech impairments were providing extra efforts to be understood by the robot. Moreover, children who usually have issues with the sense of personal space were not intrusive with the robot and waited patiently for their turn to speak. This pilot study validated the imitation method, although there are still some issues with the pose estimation for some postures. The children were very eager to be imitated by the robot, but also to imitate it. They were very forgiving with the robot limitations "It has not learned that yet". This pilot study should be turned into a long-term study to evaluate

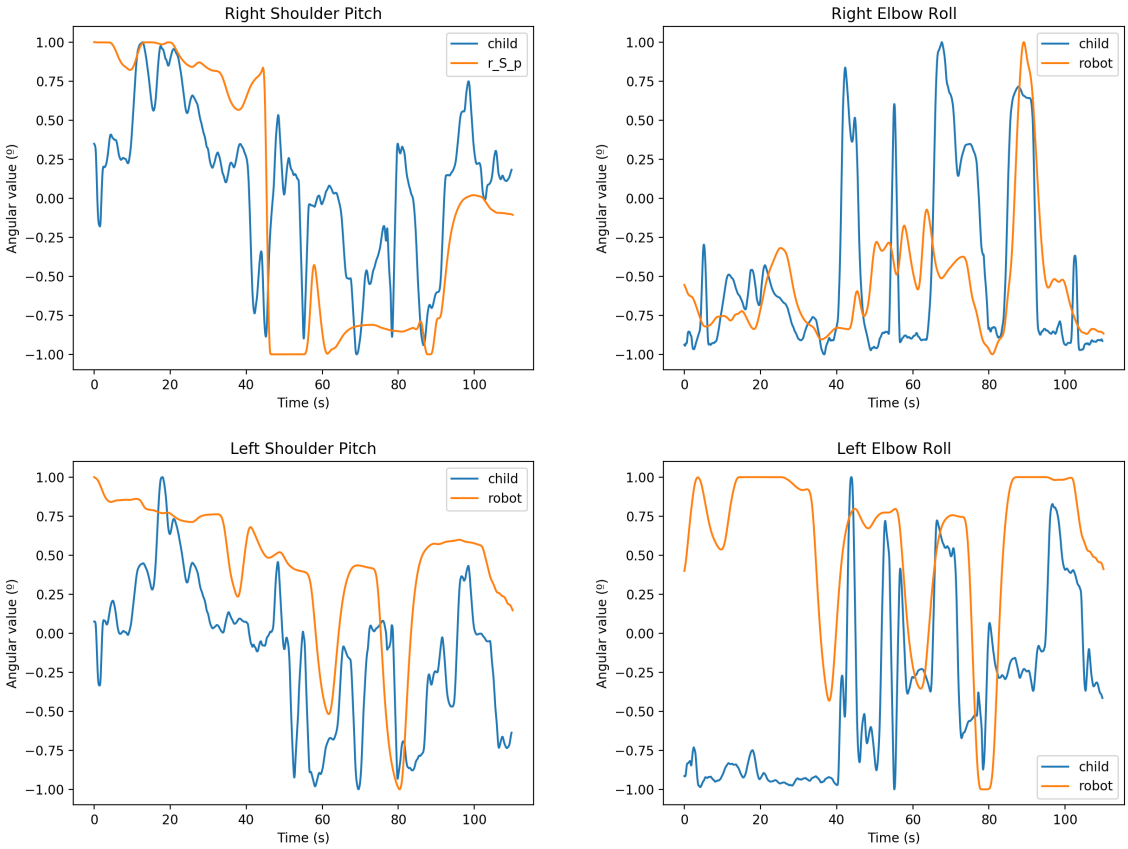


Figure 9.6: Example of interaction where the child imitates the robot. In blue, the child's position obtained with T-Sens sensors; In orange, the robot position. The signals are normalised

the impact of the robot on motor skills. The robot might also be used to improve speech or turn-taking.

Discussion

This thesis focused on motor coordination in HRI by first, observing humans, second reproducing human behaviour with robots using adaptive bio-inspired CPG controllers and third, using those robots towards motor rehabilitation for ASD children. Overall, the contribution of this thesis lies at the interface between computer science, robotics and cognitive science.

Summary & Contributions

Part I

In the first part, we recalled the background of synchrony which is an undissociable part of interpersonal interactions. Since humans are known to attribute greater likeability to partner who can adapt to them, it appeared relevant to endow robots with adaptive mechanisms to enhance social acceptability. Moreover, we gave an overview of different evaluation methods for coordination/synchronisation and imitation accuracy. Throughout this thesis, we used various coordination evaluation methods depending on our needs.

In robotics, most methods for adaptation or imitation do not take bio-inspiration into account. This seems to be an oversight as it has been evidenced that humans increase their robot acceptance in motor interactions when they exhibit biological movements [Kupferberg et al., 2011]. Another interesting aspect is the fact that robots produce actuator sound when they move. In the case of rhythmic interactions with a robot, humans thus receive two congruent pieces of information (visual and auditory) related to the same movement. Adults have an auditory sensory dominance over vision but audition can also severely alter the visual perception if the stimuli are spatially and temporally congruent. Considering the way human sensory processing works, we designed an experiment to test whether stimulus interference might be perturbing in HRI [Jouaiti and Henaff, 2019e].

This study confirmed that the auditory condition yielded the best results for rhythmic interactions but the visual condition appeared to be adequate too. However, the combination of both visual and auditory perceptions of a movement was deemed disturbing while interacting with the robot. This result was to be expected since both visual and auditory signals from the robot are congruent both temporally and spatially, so they would interfere with each other in the human perception system. This may be an important point to factor in, especially in therapeutic robotics. We unfortunately have not found an effective solution to remove robot noise yet.

Then, we also performed an observational study on involuntary coordination between children and a robot. We witnessed that while the children were indeed subjected to involuntary coordination, they still retained individual movement characteristics such as type of movement and amplitude. This is direct evidence of the *maintenance effect* [Holst, 1935]. From this, we reached the conclusion that a robot interacting with a human should also be able to adapt while exhibiting its own characteristics. We thus attempted to do so by employing a bio-inspired

controller endowed with plasticity mechanisms.

Part II

In the second part, we endeavoured to reproduce synchronisation mechanisms in robots. The Rowat-Selverston neuron was introduced in 1993 by [Rowat and Selverston, 1993]. However, this neuron model remains underused to this day. We integrated Hebbian plasticity mechanisms for frequency learning [Jouaiti et al., 2018] according to [Righetti et al., 2006]. We also endowed the CPG with synaptic plasticity mechanisms for amplitude and synaptic weight learning [Jouaiti et al., 2018]. These rules were then adapted to take the discrete mode into account since we demonstrated that the CPG behaved like a PID controller in its discrete mode [Jouaiti and Henaff, 2018a]. Afterwards, since movements are rarely solely rhythmic or discrete, we wrote a classification algorithm and designed one last plasticity mechanism so that the CPG could automatically switch from one mode to the other [Jouaiti and Henaff, 2019c]. These adaptation mechanisms are meant to increase the versatility of the CPG.

Moreover, we evaluated the bio-inspired controller theoretically and experimentally. First we compared the Rowat-Selverston neuron with the Matsuoka neuron and the Hopf oscillator [Jouaiti and Henaff, 2019a]. The three oscillators were tested according to their entrainment range and their synchronisation capacity during a handshaking simulation. Plasticity mechanisms were integrated into each model and the impact on the energetic cost is estimated. Integrating plasticity mechanisms into the three oscillators had no real impact on coordination performance but led to a significant power consumption decrease and to an extended entrainment range. The Matsuoka oscillator revealed a cumbersome parameter tuning process and a limited entrainment range. Hopf synchronised as well as (sometimes better than) Rowat-Selverston and proved easier to control, but is less adaptive. While Rowat-Selverston appeared more complex with more parameters to handle, we can easily design plasticity mechanisms allowing the system to truly adapt. It also offers a wide entrainment range but also a significantly lower power consumption. Rowat-Selverston is also the only oscillator that has a discrete mode.

Furthermore, we showed experimentally that a robot could achieve motor coordination with a human partner through a visual signal of a hand performing rhythmic movements [Jouaiti and Henaff, 2018b, Jouaiti and Henaff, 2019b]. The robot can adapt its frequency, amplitude and motion generation according to the human motion. However, the robot did not *copy* the motion but rather, the robot adapted to the frequency and to the movement while retaining its own identity. This is consistent to the maintenance effect we observed in part I in our study on involuntary coordination.

Afterwards, we decided to perform more complex multi-joint gestures, so we required a state of the art vision-processing system to perceive human movement. We, therefore, used OpenPose which we adapted with coreML so that it could run with OSX on an AMD graphics card (Radeon pro Vega 20 4GB) [12]. We also handled multi-person detection. Inference time is around 30 ms, which allows real time processing. The 2D pose estimation is also coupled with another neural network that transforms the 2D pose into a 3D pose. However, the neural network by [Martinez et al., 2017] was trained on similar postures and did not generalise very well. For example, arms stretched to the front or even arms raised above the head systematically led to inaccurate poses.

Using this system, we compared the CPG control with a direct geometric control. While both methods revealed a similar performance for discrete movements, the CPG fared much better for rhythmic movements due to its ability to adapt and "anticipate" the movement. It would be

[12] https://github.com/mjouaiti/openPose-coreML

interesting to compare the CPG with other controllers that take the robot dynamics into account and that would maybe be more effective.

We validated all of this research in a user study to evaluate the influence of the type of partner (human, robot, VP | adaptive or not) on coordination, engagement and user perception. Preliminary results supported that the type of interaction partner had an influence on engagement and coordination. As one might expect, subjects were more coordinated and engaged in the human adaptive condition than in the non-adaptive condition. Indeed, unilateral adaptation in HRI already comes across as awkward [Lorenz et al., 2013], but humans have even higher expectations for other humans. This confirms previous results [Lorenz et al., 2013, Hasnain et al., 2013] that a non-adaptive human partner feels very unnatural. Engagement was not as high as we expected with the adaptive robot due to technical difficulties that led to frustration for some subjects. The others, however, thoroughly enjoyed the interaction and engaged with the robot. Questionnaire results also revealed that most subjects thought the partners were adapting to them in the non-adaptive condition. This illustrates perfectly involuntary coordination as subjects are not aware of adapting themselves.

After having experimentally validated the CPG controller and knowing that rhythm therapy is one of the most effective forms of therapy since persons with neurological disorders retain intact motor synchronisation ability, we decided to direct this work towards motor rehabilitation for autistic children.

Part III

In the third part, we wrote a systematic review on robot-assisted motor rehabilitation for autistic children. We noticed that most therapeutic studies involving robots were focused on improving emotional or social skills. While those are obviously an issue, motor skills should not be neglected since DCD is indeed a prominent comorbidity and motor deficits are directly correlated with severity of communication skills. However, so far, there are very few sound therapies to improve motor skills in ASD. Indeed, while there is a significant amount of research in motor rehabilitation for other pathologies such as stroke, spinal cord injuries, Parkinson or cerebral palsy, those studies rarely extend to ASD. Despite compelling arguments [Janzen and Thaut, 2018, Tryfon et al., 2017, LaGasse and Hardy, 2013, Jamey et al., 2019], rhythm rehabilitation still is dauntingly underdeveloped for ASD. It has indeed been observed that despite cerebellar abnormalities, individuals are still capable of motor entrainment and synchronisation. Moreover, engaging in short rhythmic motor activities leads to brain plasticity and involves structural and functional changes in the brain [Luft et al., 2004]. We thus feel that combining the efficacy of rhythm rehabilitation and the engagement ASD children usualy have with robots may be a very promising perspective.

We therefore realised two observational experiments with autistic children. The first study replicates the sensory dominance experiment from Part I but with neurotypical and autistic children. Due to the COVID-19 outbreak, we were only able to present preliminary results which showed that both ASD and TD children coordinate better with a visual signal or with a visual-auditory combination than with an auditory signal alone. This predominance of vision over audition is in concordance with previous studies [Hermelin and O'connor, 1970, Hermelin and O'Connor, 1964, O'Connor, 1971, O'Connor and Hermelin, 1965]. While this should obviously be confirmed with a higher number of children, the children's results appear to differ from the adults' ones. While adults were perturbed in their coordination when subjected to both visual and auditory stimuli, this combination may reinforce the children's interaction and lead to better coordination.

The second experiment was a pilot study for a potential clinical trial concerning motor rehabilitation using the Pepper robot. In this experiment, the CPG control method was effectively employed in a pilot study with autistic children. The main goal was to evaluate feasibility by first validating the controller in real life conditions but also by seeing the children's reactions with the robot. This first trial proved to be rather successful and allowed us to identify other specific needs where the robot could help. Besides, the Pepper robot was very popular with children but also with the medical staff. During the interactive phase, the latter noticed that some children with speech impairments were providing extra efforts to be understood by the robot. Moreover, children who usually have issues with the sense of personal space were not intrusive with the robot and waited patiently for their turn to speak. This pilot study validated the imitation method, although there are still some issues with the pose estimation for some postures. The children were very eager to be imitated by the robot, but also to imitate it. They were very forgiving with the robot limitations: "It has not learned that yet".

Perspectives

Human-like motion generation is a relevant aspect of interactions since several studies claim that humans display greater acceptance for a biological movement than for an artificial movement [Perry et al., 2010, Kupferberg et al., 2011, Chaminade et al., 2005]. Since, our model of CPG controller is bio-inspired, it would be very interesting to study the human perception of CPG control compared to an artificial control and to biological movement.

Besides, gestural interactions are either with or without contact. In the case of interactions with contact, mechanical locking takes place and the robot is physically forced to adapt with the human, contrary to interactions without contact where adaptation relies solely on the controller. In this thesis, we only presented interactions without contact.

Moreover, the pilot study in Strasbourg received very positive feedback from the children and the medical staff. This pilot study should be turned into a long-term study to accurately evaluate the impact of the robot on motor skills. [Yoo and Kim, 2018] presented a rhythm rehabilitation study for ASD that involved dyadic drumming between an experimenter and a child. The experiment was divided into three phases: first, the experimenter adapted to the child; second, the child adapted to the experimenter; third, the child adapted to the experimenter and the coordination was randomly disrupted. Disruption of coordination leads to better self-awareness [Mundy and Jarrold, 2010]. This protocol led to improved coordination and imitation for ASD children. It would be extremely interesting to replicate this experiment with a robot and compare the outcome of traditional rhythm therapy and robot-assisted rhythm therapy. We earnestly hope that, in the long run, this work may be useful for motor rehabilitation with children affected by DCD.

Besides, as we could notice during our pilot study, the robot might also be used to improve other skills, such as speech or turn-taking. This immersion at the hospital allowed us to better understand the various needs and expectations of those children. This opened new perspectives on how to help those children in concrete terms.

My Contributions

Peer-Reviewed Journal articles

- Melanie Jouaiti, Lancelot Caron, Patrick Hénaff, Hebbian Plasticity in CPG Controllers Facilitates Self-Synchronization for Human-Robot Handshaking - **Frontiers in Neurorobotics**, Frontiers, 2018, 12, pp.1-15. - DOI : 10.3389/fnbot.2018.00029

- Melanie Jouaiti, Patrick Hénaff, Comparative Study of Forced Oscillators for the Adaptive Generation of Rhythmic Movements in Robot Controllers - **Biological Cybernetics**, Springer Berlin Heidelberg, 113: 547 - September 2019 - DOI: 10.1007/s00422-019-00807-8

- Melanie Jouaiti, Patrick Hénaff, Robot-Based Motor Rehabilitation in Autism: a Systematic Review - **International Journal of Social Robotics**, Springer Netherlands, 11, 753–764 - October 2019 - DOI: 10.1007/s12369-019-00598-9

- Rémi Pannequin, Melanie Jouaiti, Mohamed Boutayeb, Philippe Lucas, Dominique Martinez, Lab-on-cables: Automatic tracking of free-flying insects, **Science Robotics** - Under Revisions

Peer-Reviewed Conference papers

- Melanie Jouaiti, Patrick Hénaff, CPG-based Controllers can Trigger the Emergence of Social Synchrony in Human-Robot Interactions - ARSO 2018 – **IEEE International Workshop on Advanced Robotics and its Social Impacts**, Sep 2018, Genoa, Italy

- Melanie Jouaiti, Patrick Hénaff, CPG-based Controllers can Generate Both Discrete and Rhythmic Movements - IROS 2018 – **IEEE/RSJ International Conference on Intelligent Robots and Systems**, Oct 2018, Madrid, Spain

- Melanie Jouaiti, Patrick Hénaff, Motor Coordination Learning for Rhythmic Movements - EPIROB 2019 - **Development and Learning and Epigenetic Robotics (ICDL-Epirob)**, 2019 Joint IEEE International Conferences on, Oslo, Norway - August 2019

- Melanie Jouaiti, Patrick Hénaff, The Sound of Actuators: Disturbance in Human-Robot Rhythmic Interactions? - **EPIROB 2019 - Development and Learning and Epigenetic Robotics (ICDL-Epirob)**, 2019 Joint IEEE International Conferences on, Oslo, Norway - August 2019

- Maria Rodalyn V. Sanchez, Satoru Mishima, Masayuki Fujiwara, Guangyi Ai, Melanie Jouaiti, Yuliia Kobryn, Sébastien Rimbert, Laurent Bougrain, Patrick Hénaff, Hiroaki Wagatsuma, Methodological Design for Integration of Human EEG Data with Behavioral Analyses into Human-Human/Robot Interactions in a Real-World Context, **14th International Conference on Innovative Computing, Information and Control (ICICIC2019)**, Seoul, Korea - 2020

- Melanie Jouaiti, Improving Motor Coordination in HRI with Bio-Inspired Controllers, **HRI Pioneers 2020**, Cambridge - March 2020

3.1 Other Papers

- Melanie Jouaiti, Patrick Hénaff, Real Time Movement Classification in Versatile CPG Control - **Workshop on Robust Artificial Intelligence for Neurorobotics** - Edinburgh, August 2019

3.2 Poster Presentations

- **GDR Robotique GT8 / ACAI** - Paris - Poster: Motor Coordination Learning for Rhythmic Movements
- **Workshop Women in Robotics (@RSS Conference)** - Freiburg - Poster: Rhythmic - Discrete Movements Classification Using CPGs

3.3 Other Presentations

- **Journées Nationales de la Robotique Humanoïde (JNRH)** – Nancy – Presentation: Plastic CPG-based Robot Controllers for Human-Robot Rhythmic Interactions
- **Plate-Forme Intelligence Artificielle (PFIA) – Journée Robotique et IA** – Nancy – Presentation: Contrôleurs plastiques bio-inspirés pour l'interaction rythmique Humain-Robot
- **GDR Robotique GT8** – Nancy – Presentation: Adaptive CPG-based Controllers Increase Compliance in Rhythmic Physical Human-Robot Interactions
- **Tohoku/University of Lorraine Seminar** - Nancy - Presentation: Versatile CPG Control for Human Robot Interactions

Repositories

- Code associated with the Frontiers paper https://github.com/mjouaiti/Code_Frontiers
- Code forReal-time data visualisation in OpenGL https://github.com/mjouaiti/Grapher
- Wrapper for the Kinova SDK https://github.com/mjouaiti/KinovaSDKWrapper
- OpenPose for AMD graphics card (OSX) https://github.com/mjouaiti/openPose-coreML
- CAD files for Hexplore robot https://github.com/mjouaiti/Hexplore

Dissemination

- Science Fair - October 2018
- RoboTech Girls Week - April 2019
- Science Fair - October 2019
- TV report on using the Pepper robot to help ASD children at the Strasbourg hospital - France 3 Alsace - February 2020

Appendix A

Mathematical Details for the Rowat-Selverston Neuron

A.1 Van der Pol Form of Rowat-Selverston Neuron

The free form (i.e. without any input signal applied) of the Van der Pol oscillator can be written as :

$$\begin{aligned} \dot{x} &= y \\ \dot{y} &= -\alpha\left(x^2 - p\right) y - \omega^2 x \end{aligned} \tag{A.1}$$

where y is the output of the oscillator, p amplitude of y, α controls the degree of nonlinearity of the system and ω mainly influences the frequency of the oscillator.

The free form of the Rowat-Selverston model of a cellular neuron is described by:

$$\tau_m \dot{V} + V - A_f \tanh\left(\frac{\sigma_f}{A_f} V\right) + q = 0 \tag{A.2a}$$

$$\tau_s \dot{q} = -q + \sigma_s V \tag{A.2b}$$

with V being the cellular membrane potential, q the slow current, τ_m the time constant of the cellular membrane, τ_s is the time constant of slow current activation ($\tau_m \ll \tau_s$), σ_s and σ_f represent respectively the conductance of slow and fast currents, A_f influences the amplitude of V.

Because Rowat-Selverston is a generalised Van der Pol oscillator, its equations can be rewritten in a Van der Pol form equation (A.1). To do that, equation (A.2a) can be differentiated, yielding:

$$\tau_m \ddot{V} + \dot{V} - \sigma_f \left(1 - \tanh^2\left(\frac{\sigma_f}{A_f} V\right)\right) \dot{V} + \dot{q} = 0 \tag{A.3}$$

and $\dot{q}$ replaced by the expression given in equation (A.2b):

$$\tau_m \ddot{V} + \dot{V} - \sigma_f \left(1 - \tanh^2\left(\frac{\sigma_f}{A_f} V\right)\right) \dot{V} + \frac{1}{\tau_s}(\sigma_s V - q) = 0 \tag{A.4}$$

Then we replace q by its expression from equation (A.2a):

$$\tau_m \ddot{V} + \dot{V} - \sigma_f \left(1 - \tanh^2\left(\frac{\sigma_f}{A_f} V\right)\right) \dot{V} + \frac{\sigma_s}{\tau_s} V + \frac{1}{\tau_s} V + \frac{\tau_m}{\tau_s} \dot{V} - \frac{A_f}{\tau_s} \tanh\left(\frac{\sigma_f}{A_f} V\right) = 0 \tag{A.5}$$

and group the terms:

$$\tau_m \ddot{V} + \left(\frac{\tau_m}{\tau_s} + 1 - \sigma_f + \sigma_f \tanh^2 \left(\frac{\sigma_f}{A_f} V \right) \right) \dot{V} + \frac{1+\sigma_s}{\tau_s} V - \frac{A_f}{\tau_s} \tanh \left(\frac{\sigma_f}{A_f} V \right) = 0 \tag{A.6}$$

We can approximate the tanh function to a linear one, $\tanh(x) \approx x$, thus yielding:

$$\tau_m \ddot{V} + \left(\frac{\tau_m}{\tau_s} + 1 - \sigma_f + \frac{\sigma_f^3}{A_f^2} V^2 \right) \dot{V} + \frac{1+\sigma_s}{\tau_s} V - \frac{\sigma_f}{\tau_s} V = 0 \tag{A.7}$$

By setting, $\dot{V} = y$, we can transform the model into the following unforced Van der Pol form:

$$\begin{aligned} \dot{V} &= y \\ \dot{y} &= \frac{-\sigma_f^3}{\tau_m A_f^2} \left(V^2 - \frac{A_f^2(\sigma_f \tau_s - \tau_m - \tau_s)}{\tau_s \sigma_f^3} \right) y - \frac{1+\sigma_s-\sigma_f}{\tau_s \tau_m} V \end{aligned} \tag{A.8}$$

By comparing this equation to equation (A.1), we can finally identify the Van der Pol parameters ω, α and p of the unforced Rowat-Selverston oscillating neuron:

$$\boxed{\omega = \sqrt{\frac{1+\sigma_s-\sigma_f}{\tau_s \tau_m}}; \qquad \alpha = \frac{\sigma_f^3}{\tau_m A_f^2}; \qquad p = \frac{A_f^2(\tau_s(\sigma_f - 1) - \tau_m)}{\tau_s \sigma_f^3}; \qquad \text{with } \sigma_f < 1 + \sigma_s} \tag{A.9}$$

We can see on figure A.1 that despite the approximations, $f = \frac{\omega}{2\pi}$ gives an accurate expression of the intrinsic frequency.

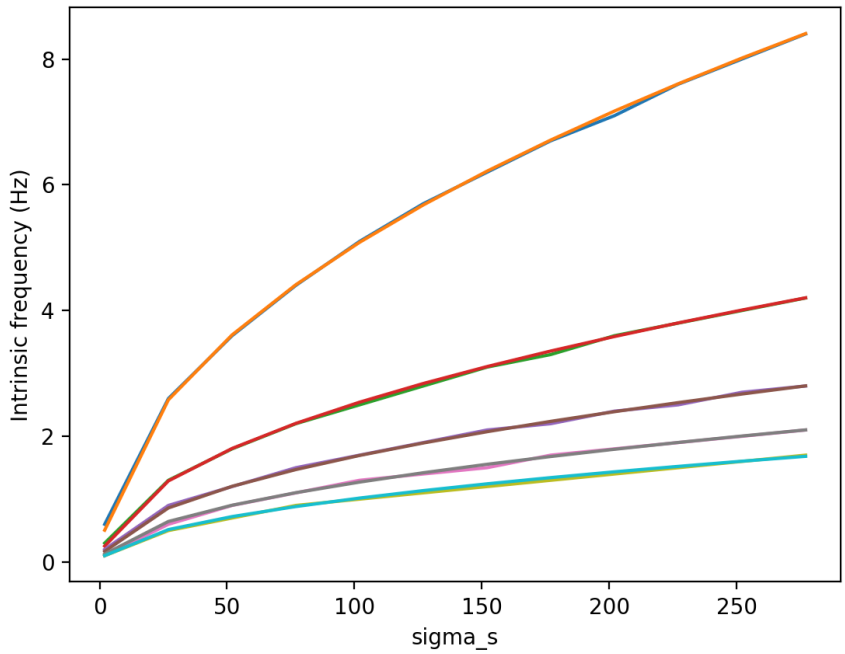


Figure A.1: Intrinsic frequency of the oscillator depending on σ_s for several values of τ_m, τ_s and the previously obtained expression $f = \frac{\omega}{2\pi} = \frac{1}{2\pi}\sqrt{\frac{1+\sigma_s-\sigma_f}{\tau_s \tau_m}}$

A.2 Recall of Righetti's Model for Dynamic Hebbian Learning into Van der Pol Oscillators

The free form (i.e. without any input signal applied) of the Van der Pol oscillator can be written as :

$$\begin{aligned} \dot{x} &= y \\ \dot{y} &= -\alpha \left(x^2 - p\right) y - \omega^2 x \end{aligned} \tag{A.10}$$

where y is the output of the oscillator, p amplitude of y, α controls the degree of nonlinearity of the system and ω mainly influences the frequency of the oscillator.
When the Van der Pol oscillator is forced by an oscillating input signal $F(t)$, the model can be written as:

$$\begin{aligned} \dot{x} &= y + \epsilon F \\ \dot{y} &= -\alpha \left(x^2 - p\right) y - \omega^2 x \end{aligned} \tag{A.11}$$

where ϵ can be seen as a gain or a weight.

In order to synchronise the oscillator with the input $F(t)$, [Righetti et al., 2006] proposed to learn the frequency of the oscillator following a Hebbian learning rule :

$$\dot{\omega} = \epsilon F \frac{y}{\sqrt{x^2 + y^2}} \tag{A.12}$$

They showed that this rule allows the oscillator to change its intrinsic frequency to synchronise with the oscillating signal $F(t)$. The oscillator preserves the learned frequency, even after the input signal is cut. It has been applied to the Hopf oscillator and the Fitzhugh-Nagumo oscillator.

A.3 Applying Dynamic Hebbian Learning to the Rowat-Selverston Neuron

In order to identify a Righetti learning rule in the Rowat-Selverston neuron model, we use the Van der Pol form identified in section 1.

Following the idea of [Righetti et al., 2006], we propose to learn σ_s depending on the external signal $F(t)$ applied to the neuron and weighted by ϵ. Thus, neural plasticity for frequency learning can be obtained by deriving the expression of ω^2 from A.9 :

$$\dot{\sigma}_s = 2\dot{\omega}\omega\tau_m\tau_s = 2\dot{\omega}\sqrt{\tau_m\tau_s}\sqrt{1 + \sigma_s - \sigma_f} \tag{A.13}$$

By applying the dynamic Hebbian learning rule proposed by [Righetti et al., 2006] to equation (A.12), we obtain :

$$\boxed{\dot{\sigma_s} = 2\epsilon F\sqrt{\tau_m\tau_s}\sqrt{1 + \sigma_s - \sigma_f}\frac{y}{\sqrt{V^2 + y^2}}; \qquad \sigma_f < 1 + \sigma_s} \tag{A.14}$$

We can see that this learning rule depends on the CPG time constants. The presence of σ_s on the right side of the equation, makes it a closed loop ensuring that the end value of σ_s does not depend on its initial value (See Fig. A.2).

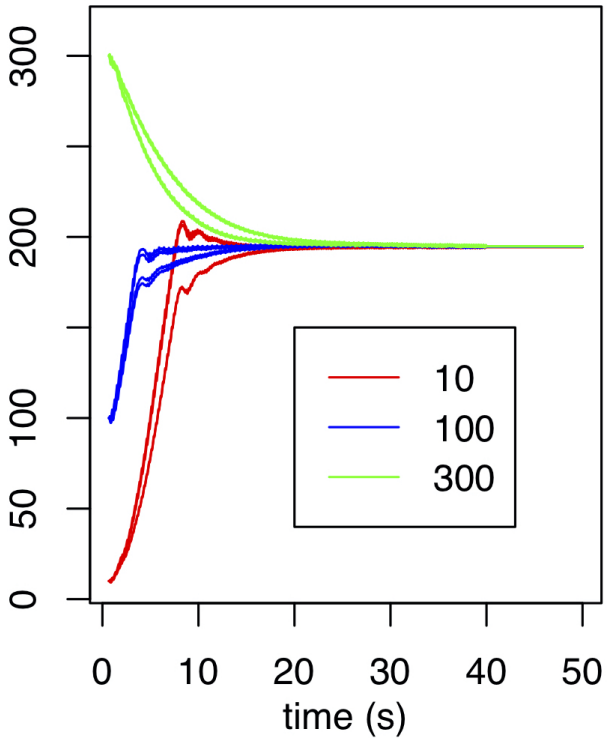


Figure A.2: Evolution of σ_s with different initial values.

Appendix B

Details on Comparing the Oscillator Models

B.1 Coupling the Oscillatory Neurons

We consider two coupled oscillators controlling the flexor and the extensor muscles in reference to the half center structure introduced by [Rybak et al., 2006]. However, in robotics, this is hardly applicable as such since robots have a single joint in place for the flexor and extensor parts. It is then common practice to subtract both commands to obtain the output (see Figure B.1).

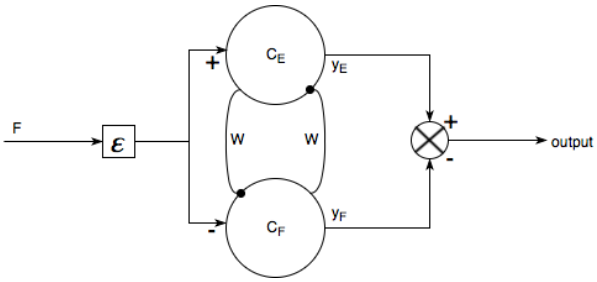


Figure B.1: Coupled oscillatory cells. $C_{\{E,F\}}$ indicates whether the neuron cell controls the extensor or the flexor

In all equations, the term in W models the mutual inhibition between the extensor and the flexor cells. The equations are thus rewritten as follows (with $F_F = -F_E$):

B.1.1 Matsuoka Model

$$\dot{x}_{\{E,F\}} = \frac{1}{T}(-x_{\{E,F\}} - W \cdot y_{\{F,E\}} - b \cdot v_{\{E,F\}} + c + \epsilon F_{\{E,F\}}) \tag{B.1a}$$

$$\dot{v}_{\{E,F\}} = \frac{1}{\tau}(-v_{\{E,F\}} + y_{\{E,F\}}) \tag{B.1b}$$

$$y_{\{E,F\}} = \max(x_{\{E,F\}}, 0) \tag{B.1c}$$

B.1.2 Hopf Model

$$\begin{aligned}\dot{x}_{\{E,F\}} =&(\mu - (x^2_{\{E,F\}} + y^2_{\{E,F\}}))x_{\{E,F\}} - \\ & W\tanh(x_{\{F,E\}}) - \theta y_{\{E,F\}} + \epsilon F_{\{E,F\}} \end{aligned} \tag{B.2a}$$

$$\begin{aligned}\dot{y}_{\{E,F\}} =&(\mu - (x^2_{\{E,F\}} + y^2_{\{E,F\}}))y_{\{E,F\}} + \\ & \theta x_{\{E,F\}} \end{aligned} \tag{B.2b}$$

Note that the term $W\tanh(x_j)$ has been added to the original model in order to couple the two Hopf cells and thus obtain a half center model. In the rest of the paper, we consider $W = 1$ for Hopf.

B.1.3 Rowat-Selverston Model

$$\begin{aligned}\dot{V}_{\{E,F\}} =&y_{\{E,F\}} - W\frac{y_{\{E,F\}}}{1 + e^{-4y_{\{F,E\}}}} \\ & + \epsilon F_{\{E,F\}} \end{aligned} \tag{B.3a}$$

$$\begin{aligned}\dot{y}_{\{E,F\}} =&\frac{1}{\tau_m}\left(\sigma_f - \frac{\tau_m}{\tau_s} - 1 - \right. \\ & \left.\sigma_f \tanh^2\left(\frac{\sigma_f}{A_f}V_{\{E,F\}}\right)\right) y_{\{E,F\}} - \\ & \frac{1 + \sigma_s}{\tau_s\tau_m}V_{\{E,F\}} + \\ & \frac{A_f}{\tau_s\tau_m}\tanh\left(\frac{\sigma_f}{A_f}V_{\{E,F\}}\right) \end{aligned} \tag{B.3b}$$

B.2 The Kasuga Control Architecture

In order to integrate the oscillators into the Kasuga architecture for joints i and j, the cells equations become:

B.2.1 Matsuoka Model

$$\begin{aligned}\dot{x}_{i_{\{E,F\}}} =& \frac{1}{T}(-x_{i_{\{E,F\}}} - W \cdot y_{i_{\{F,E\}}} - b \cdot v_{i_{\{E,F\}}} + c) \\ & + L_{i2}F_{i_{\{E,F\}}} + L_{i1}|F_{i_{\{E,F\}}}| + \\ & K_{i_{\{E,F\}}}(y_{j_E} - y_{j_F}) \end{aligned} \tag{B.4a}$$

$$\dot{v}_{i_{\{E,F\}}} = \frac{1}{\tau}(-v_{i_{\{E,F\}}} + y_{i_{\{E,F\}}}) \tag{B.4b}$$

$$y_{i_{\{E,F\}}} = \max(x_{i_{\{E,F\}}}, 0) \tag{B.4c}$$

With $F_{i_E} = -F_{i_F}$, $K_{i_E} = -K_{i_F}$ and j the other joint.

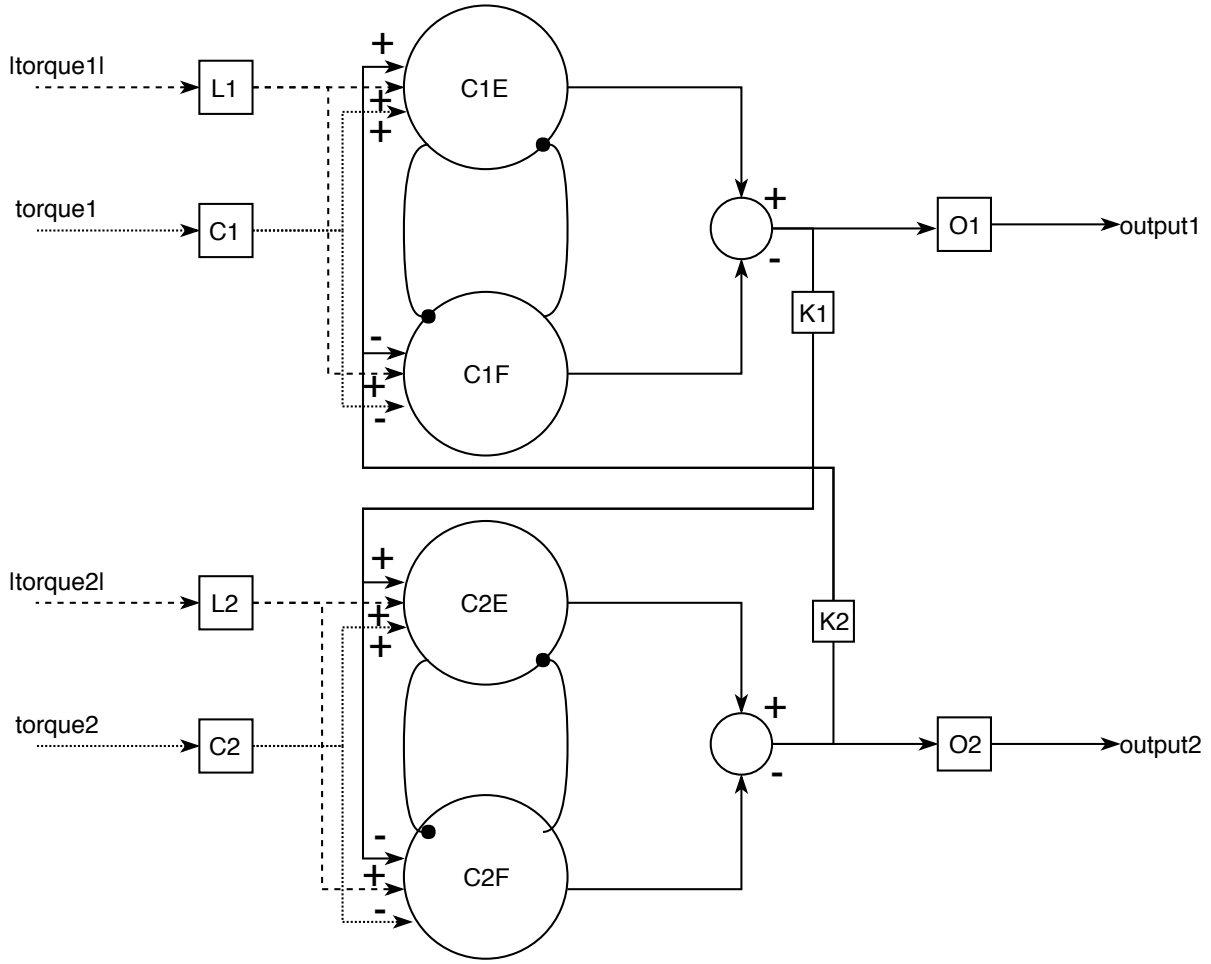


Figure B.2: Oscillatory cells integrated to the generalised Kasuga architecture. C_i, L_i, K_i, O_i are gains and $C_{i\{E,F\}}$ is the neuron cell for the joint i controlling the extensor or flexor and torque$_i$ is the input signal

B.2.2 Hopf Model

$$\begin{aligned}\dot{x}_{i_{\{E,F\}}} = &(\mu - (x^2_{i_{\{E,F\}}} + y^2_{i_{\{E,F\}}}))x_{i_{\{E,F\}}} \\ &- tanh(x_{i_{\{F,E\}}}) - \theta_i y_{i_{\{E,F\}}} + \\ &L_{i2}F_{i_{\{E,F\}}} + L_{i1}|F_{i_{\{E,F\}}}| + \\ &K_{i_{\{E,F\}}}(x_{j_E} - x_{j_F})\end{aligned} \tag{B.5a}$$

$$\begin{aligned}\dot{y}_{i_{\{E,F\}}} = &(\mu - (x^2_{i_{\{E,F\}}} + y^2_{i_{\{E,F\}}}))y_{i_{\{E,F\}}} + \\ &\theta_i x_{i_{\{E,F\}}}\end{aligned} \tag{B.5b}$$

B.2.3 Rowat-Selverston Model

$$\begin{aligned}\dot{V}_{i_{\{E,F\}}} =& y_{i_{\{E,F\}}} - W\frac{y_{i_{\{E,F\}}}}{1+e^{-4y_{i_{\{F,E\}}}}}+ \\ & \cdot L_{i2}F_{i_{\{E,F\}}} + L_{i1}|F_{i_{\{E,F\}}}|+ \\ & K_{i_{\{E,F\}}}(V_{j_E} - V_{j_F})\end{aligned} \tag{B.6a}$$

$$\begin{aligned}\dot{y}_{i_{\{E,F\}}} =& \frac{1}{\tau_m}\left(\sigma_f - \frac{\tau_m}{\tau_s} - 1 - \right. \\ & \left.\sigma_f \tanh^2\left(\frac{\sigma_f}{A_{f_i}}V_{i_{\{E,F\}}}\right)\right) y_{i_{\{E,F\}}} - \\ & \frac{1+\sigma_s}{\tau_s\tau_m}V_{i_{\{E,F\}}}+ \\ & \frac{A_{f_{i_{\{E,F\}}}}}{\tau_s\tau_m}\tanh\left(\frac{\sigma_f}{A_{f_{i_{\{E,F\}}}}}V_{i_{\{E,F\}}}\right)\end{aligned} \tag{B.6b}$$

Appendix C

The Vision Processing System

C.1 2D Pose Estimation Inference

For the 2D pose estimation inference, we employ a re-implementation [13] of [Cao et al., 2018, tf-, 2017] which runs on an AMD Radeon Pro Vega 20 graphics card on a Mac computer. The pose estimation inference is performed by coreML with the MobileNet model on 320x320 images. Multiple person detection is handled thanks to part affinity fields. First, a feed-forward model predicts a confidence map of the body part locations and a 2D vector field of part affinities. These maps are then parsed by greedy inference to obtain the body part keypoints. [Cao et al., 2017].

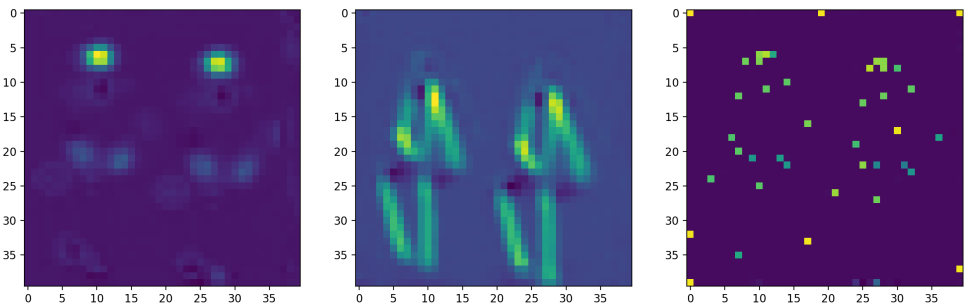


Figure C.1: Superposition of OpenPose inference for each body part. Left: confidence map of the body part locations. Middle: 2D vector field of part affinities heatmap. Right: Peaks of the body part heatmap

C.2 3D Pose Estimation Inference

From the previous 2D pose, we can infer a 3D pose with the neural network trained in [Martinez et al., 2017]. The result of the 3D pose estimation is then passed through a low-pass filter with 1.5 Hz cut-off frequency to remove detection aberrations.

Consistent errors were observed in the 3D pose, tilted torso, offset for the arm angles. We corrected them in our program.

[13] https://github.com/mjouaiti/openPose-coreML.git

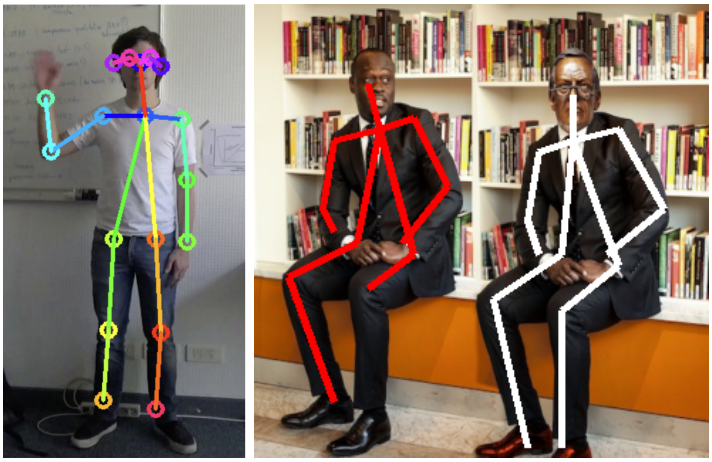


Figure C.2: 2D pose estimation

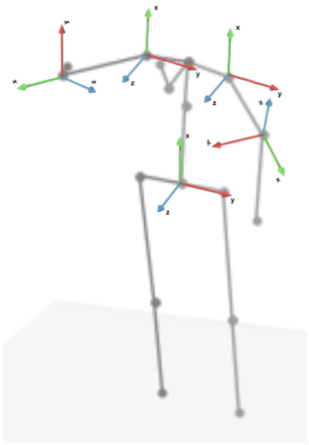


Figure C.3: 3D pose estimation

C.3 Angular Values Computation

A local coordinate system is assigned to each joint of the 3D pose (See Figure C.3). The x axis of each coordinate system is colinear with the previous joint segment in the kinematic chain. That is, the hips are represented in the absolute coordinate system. The shoulders are associated with the hip coordinate system and the elbows with their respective shoulder coordinate system. This allows us to compute the angular positions of the human joints.

Appendix D

Questionnaires

D.1 NARS Questionnaire

Please rate each questionnaire item according to the following scale:
1: I strongly disagree
2: I disagree
3: Undecided
4: I agree
5: I strongly agree

Subscale	**Questionnaire item**
S2	I would feel uneasy if robots really had emotions
S2	Something bad might happen if robots developed into living beings
S3	I would feel relaxed talking with robots*
S1	I would feel uneasy if I was given a job where I had to use robots
S3	If robots had emotions, I would be able to make friends with them*
S3	I feel comforted being with robots that have emotions*
S1	The word "robot" means nothing to me
S1	I would feel nervous operating a robot in front of other people
S1	I would hate the idea that robots or artificial intelligences were making judgments about things
S1	I would feel very nervous just standing in front of a robot
S2	I feel that if I depend on robots too much, something bad might happen
S1	I would feel paranoid talking with a robot
S2	I am concerned that robots would be a had influence on children
S2	I feel that in the future society will be dominated by robots

* indicates a reverse item.

- **S1**: Negative Attitude toward Situations of Interaction with Robots;
- **S2**: Negative Attitude toward Social Influence of Robots;
- **S3**: Negative Attitude toward Emotions in Interaction with Robots.

D.2 Technology Anxiety

Questionnaire from [Meuter et al., 2005] (adapted from [Raub, 1981]) evaluated on a 5 point Likert-type scale ranging from 1 to 5 (totally disagree – disagree – don't know – agree – totally agree)

- I feel apprehensive about using technology
- Technical terms sound like confusing jargon to me
- I have avoided technology because it is unfamiliar to me
- I hesitate to use most forms of technology for fear of making mistakes I cannot correct

D.3 Acceptance of Assistive Social Agent

Questionnaire to assess acceptance of assistive social agent [Heerink et al., 2010] evaluated on a 5 point Likert-type scale ranging from 1 to 5 (totally disagree – disagree – don't know – agree – totally agree)

- If I should use the robot, I would be afraid to make mistakes with it
- If I should use the robot, I would be afraid to break something
- I find the robot scary
- I find the robot intimidating
- I think it's a good idea to use the robot
- The robot would make life more interesting
- It's good to make use of the robot
- I have everything I need to use the robot
- I know enough of the robot to make good use of it
- I think I'll use the robot during the next few days
- I'm certain to use the robot during the next few days
- I plan to use the robot during the next few days
- I think the robot can be adaptive to what I need
- I think the robot will only do what I need at that particular moment
- I think the robot will help me when I consider it to be necessary
- I enjoy the robot talking to me
- I enjoy doing things with the robot
- I find the robot enjoyable

- I find the robot fascinating
- I find the robot boring
- I think I will know quickly how to use the robot
- I find the robot easy to use
- I think I can use the robot without any help
- I think I can use the robot when there is someone around to help me
- I think I can use the robot when I have a good manual
- I consider the robot a pleasant conversational partner
- I find the robot pleasant to interact with I feel the robot understands me
- I think the robot is nice
- I think the robot is useful to me
- It would be convenient for me to have the robot
- I think the robot can help me with many things
- I think the staff would like me using the robot
- I think it would give a good impression if I should use the robot
- When interacting with the robot I felt like I'm talking to a real person
- It sometimes felt as if the robot was really looking at me
- I can imagine the robot to be a living creature
- I often think the robot is not a real person
- Sometimes the robot seems to have real feelings
- I would trust the robot if it gave me advice
- I would follow the advice the robot gives me

D.4 Attrakdiff

Pragmatic Quality		
Technical	○ ○ ○ ○ ○ ○ ○	Human
Complicated	○ ○ ○ ○ ○ ○ ○	Simple
Impractical	○ ○ ○ ○ ○ ○ ○	Practical
Cumbersome	○ ○ ○ ○ ○ ○ ○	Straightforward
Unpredictable	○ ○ ○ ○ ○ ○ ○	Predictable
Confusing	○ ○ ○ ○ ○ ○ ○	Clearly structured
Unruly	○ ○ ○ ○ ○ ○ ○	Manageable
Hedonistic Identification Quality		
Isolating	○ ○ ○ ○ ○ ○ ○	Connective
Unprofessional	○ ○ ○ ○ ○ ○ ○	Professional
Tacky	○ ○ ○ ○ ○ ○ ○	Stylish
Cheap	○ ○ ○ ○ ○ ○ ○	Premium
Alienating	○ ○ ○ ○ ○ ○ ○	Integrating
Separates me	○ ○ ○ ○ ○ ○ ○	Brings me closer
Unpresentable	○ ○ ○ ○ ○ ○ ○	Presentable
Hedonistic Stimulation Quality		
Conventional	○ ○ ○ ○ ○ ○ ○	Inventive
Uninmaginative	○ ○ ○ ○ ○ ○ ○	Creative
Cautious	○ ○ ○ ○ ○ ○ ○	Bold
Conservative	○ ○ ○ ○ ○ ○ ○	Innovative
Dull	○ ○ ○ ○ ○ ○ ○	Captivating
Undemanding	○ ○ ○ ○ ○ ○ ○	Challenging
Ordinary	○ ○ ○ ○ ○ ○ ○	Novel
Attractiveness		
Unpleasant	○ ○ ○ ○ ○ ○ ○	Pleasant
Ugly	○ ○ ○ ○ ○ ○ ○	Attractive
Disagreeable	○ ○ ○ ○ ○ ○ ○	Likeable
Rejecting	○ ○ ○ ○ ○ ○ ○	Inviting
Bad	○ ○ ○ ○ ○ ○ ○	Good
Repelling	○ ○ ○ ○ ○ ○ ○	Appealing
Discouraging	○ ○ ○ ○ ○ ○ ○	Motivating

Table D.1: Attrakdiff Questionnaire. Items are rated between -3 and 3

D.5 Technological familiarity

You consider that you have a good level of knowledge about these technologies	○ ○ ○ ○ ○ ○ ○	You consider that you have a very poor level of knowledge about these technologies
You consider yourself very well-informed about these technologies	○ ○ ○ ○ ○ ○ ○	You consider yourself very uninformed about these technologies
You consider yourself familiar with these technologies	○ ○ ○ ○ ○ ○ ○	You consider yourself very unfamiliar with these technologies

Table D.2: Technological Familiarity Questionnaire. Items are rated between -3 and 3

Bibliography

[dsm, 1993] (1993). American psychiatric association. task force on dsm-iv. In Amer Psychiatric Pub, A., editor, *DSM-IV draft criteria*.

[tf-, 2017] (2017). tf-openpose https://github.com/ildoonet/tf-pose-estimation.

[tms, 2017] (2017). Tmsi https://www.tmsi.com/products/refa/.

[ble, 2018] (2018). Blender: Open source 3d creation https://www.blender.org.

[mak, 2018] (2018). Makehuman: Open source tool for making 3d characters http://www.makehumancommunity.org.

[cle, 2019] (2019). cleandata function https://github.com/sccn/clean_rawdata.

[tea, 2020] (2020). Captiv tea, france http://teaergo.com/.

[Abbeel and Ng, 2004] Abbeel, P. and Ng, A. Y. (2004). Apprenticeship learning via inverse reinforcement learning. In *Proceedings of the twenty-first international conference on Machine learning*, page 1. ACM.

[Abu-Dahab et al., 2013] Abu-Dahab, S. M., Skidmore, E. R., Holm, M. B., Rogers, J. C., and Minshew, N. J. (2013). Motor and tactile-perceptual skill differences between individuals with high-functioning autism and typically developing individuals ages 5–21. *Journal of autism and developmental disorders*, 43(10):2241–2248.

[Al-Busaidi et al., 2012] Al-Busaidi, A. M., Zaier, R., and Al-Yahmadi, A. S. (2012). Control of biped robot joints' angles using coordinated matsuoka oscillators. In *International Conference on Artificial Neural Networks*, pages 304–312. Springer.

[Alaniz et al., 2015] Alaniz, M. L., Galit, E., Necesito, C. I., and Rosario, E. R. (2015). Hand strength, handwriting, and functional skills in children with autism. *The American journal of occupational therapy : official publication of the American Occupational Therapy Association*, 69 4:6904220030p1–9.

[Aleotti and Caselli, 2006] Aleotti, J. and Caselli, S. (2006). Robust trajectory learning and approximation for robot programming by demonstration. *Robotics and Autonomous Systems*, 54(5):409–413.

[Ali et al., 2019] Ali, S., Mehmood, F., Dancey, D., Ayaz, Y., Khan, M. J., Naseer, N., de Cassia Amadeu, R., Sadia, H., and Nawaz, R. (2019). An adaptive multi-robot therapy for improving joint attention and imitation of asd children. *IEEE Access*.

[Ansermin et al., 2016] Ansermin, E., Mostafaoui, G., Beaussé, N., and Gaussier, P. (2016). Learning to synchronously imitate gestures using entrainment effect. In *International conference on simulation of adaptive behavior*, pages 219–231. Springer.

[Arena et al., 2006] Arena, P., Fortuna, L., Frasca, M., Patane, L., and Pollino, M. (2006). An autonomous mini-hexapod robot controlled through a cnn-based cpg vlsi chip. In *Cellular Neural Networks and Their Applications, 2006. CNNA'06. 10th International Workshop on*, pages 1–6. IEEE.

[Auger and Flandrin, 1995] Auger, F. and Flandrin, P. (1995). Improving the readability of time-frequency and time-scale representations by the reassignment method. *IEEE Transactions on signal processing*, 43(5):1068–1089.

[Ayers, 2004] Ayers, J. (2004). Underwater walking. *Arthropod structure & development*, 33(3):347–360.

[Bailey et al., 1998] Bailey, A., Luthert, P., Dean, A., Harding, B., Janota, I., Montgomery, M., Rutter, M., and Lantos, P. (1998). A clinicopathological study of autism. *Brain: a journal of neurology*, 121(5):889–905.

[Bakker and Kuniyoshi, 1996] Bakker, P. and Kuniyoshi, Y. (1996). Robot see, robot do: An overview of robot imitation. In *AISB96 Workshop on Learning in Robots and Animals*, pages 3–11.

[Balsters et al., 2018] Balsters, J. H., Mantini, D., and Wenderoth, N. (2018). Connectivity-based parcellation reveals distinct cortico-striatal connectivity fingerprints in autism spectrum disorder. *NeuroImage*, 170:412 – 423. Segmenting the Brain.

[Baratto et al., 1986] Baratto, L., Morasso, P., and Zaccaria, R. (1986). Complex motor patterns: Walking. In *Advances in Psychology*, volume 33, pages 60–81. Elsevier.

[Baron-Cohen and Wheelwright, 1999] Baron-Cohen, S. and Wheelwright, S. (1999). Obsessions' in children with autism or asperger syndrome: Content analysis in terms of core domains of cognition. *The British Journal of Psychiatry*, 175(5):484–490.

[Baron-Cohen et al., 2001] Baron-Cohen, S., Wheelwright, S., Hill, J., Raste, Y., and Plumb, I. (2001). The "reading the mind in the eyes" test revised version: A study with normal adults, and adults with asperger syndrome or high-functioning autism. *Journal of child psychology and psychiatry*, 42(2):241–251.

[Barraza and Grzywacz, 2002] Barraza, J. F. and Grzywacz, N. M. (2002). Measurement of angular velocity in the perception of rotation. *Vision research*, 42(21):2457–2462.

[Bartlett and Bartlett, 1959] Bartlett, N. R. and Bartlett, S. C. (1959). Synchronization of a motor response with an anticipated sensory event. *Psychological review*, 66(4):203.

[Bass et al., 2009] Bass, M. M., Duchowny, C. A., and Llabre, M. M. (2009). The effect of therapeutic horseback riding on social functioning in children with autism. *Journal of autism and developmental disorders*, 39(9):1261–1267.

[Bauman and Kemper, 2005] Bauman, M. L. and Kemper, T. L. (2005). Neuroanatomic observations of the brain in autism: a review and future directions. *International journal of developmental neuroscience*, 23(2-3):183–187.

[Beer et al., 2016] Beer, J. M., Boren, M., and Liles, K. R. (2016). Robot assisted music therapy: A case study with children diagnosed with autism. In *The Eleventh ACM/IEEE International Conference on Human Robot Interaction*, pages 419–420. IEEE Press.

[Bentivegna et al., 2004] Bentivegna, D. C., Atkeson, C. G., and Cheng, G. (2004). Learning from observation and practice using primitives. In *AAAI 2004 Fall Symposium on Real-life Reinforcement Learning*. Citeseer.

[Bergman and Escalona, 1947] Bergman, P. and Escalona, S. K. (1947). Unusual sensitivities in very young children. *The psychoanalytic study of the child*, 3(1):333–352.

[Berndt and Clifford, 1994] Berndt, D. J. and Clifford, J. (1994). Using dynamic time warping to find patterns in time series. In *KDD workshop*, volume 10, pages 359–370. Seattle, WA.

[Bernier et al., 2007] Bernier, R., Dawson, G., Webb, S., and Murias, M. (2007). Eeg mu rhythm and imitation impairments in individuals with autism spectrum disorder. *Brain and cognition*, 64(3):228–237.

[Biffi et al., 2018] Biffi, E., Costantini, C., Ceccarelli, S. B., Cesareo, A., Marzocchi, G. M., Nobile, M., Molteni, M., and Crippa, A. (2018). Gait pattern and motor performance during discrete gait perturbation in children with autism spectrum disorders. *Frontiers in Psychology*, 9:2530.

[Billard and Matarić, 2001] Billard, A. and Matarić, M. J. (2001). Learning human arm movements by imitation:: Evaluation of a biologically inspired connectionist architecture. *Robotics and Autonomous Systems*, 37(2-3):145–160.

[Birch, 1962] Birch, H. G. (1962). Dyslexia and the maturation of visual function. *Reading disability: Progress and research needs in dyslexia*, pages 161–169.

[Bird et al., 2007] Bird, G., Leighton, J., Press, C., and Heyes, C. (2007). Intact automatic imitation of human and robot actions in autism spectrum disorders. *Proceedings of the Royal Society of London B: Biological Sciences*, 274(1628):3027–3031.

[Blakemore et al., 2006] Blakemore, S.-J., Tavassoli, T., Calò, S., Thomas, R. M., Catmur, C., Frith, U., and Haggard, P. (2006). Tactile sensitivity in asperger syndrome. *Brain and cognition*, 61(1):5–13.

[Blanchard and Canamero, 2005] Blanchard, A. and Canamero, L. (2005). Using visual velocity detection to achieve synchronization in imitation. In *Procs 3rd Int Symposium on Imitation in Animals and Artifacts*. SSAISB.

[Boddaert et al., 2004] Boddaert, N., Chabane, N., Belin, P., Bourgeois, M., Royer, V., Barthelemy, C., Mouren-Simeoni, M.-C., Philippe, A., Brunelle, F., Samson, Y., et al. (2004). Perception of complex sounds in autism: abnormal auditory cortical processing in children. *American Journal of Psychiatry*, 161(11):2117–2120.

[Bogdashina, 2016] Bogdashina, O. (2016). *Sensory perceptual issues in autism and asperger syndrome: different sensory experiences-different perceptual worlds*. Jessica Kingsley Publishers.

[Botrel, 2018] Botrel, L. (2018). Brain-computer interfaces (bcis) based on sensorimotor rhythms-evaluating practical interventions to improve their performance and reduce bci inefficiency.

[Boucenna et al., 2014] Boucenna, S., Anzalone, S., Tilmont, E., Cohen, D., and Chetouani, M. (2014). Learning of social signatures through imitation game between a robot and a human partner. *IEEE Transactions on Autonomous Mental Development*, 6(3):213–225.

[Brambilla et al., 2006] Brambilla, G., Buchli, J., and Ijspeert, A. J. (2006). Adaptive four legged locomotion control based on nonlinear dynamical systems. In *International Conference on Simulation of Adaptive Behavior*, pages 138–149. Springer.

[Breazeal, 2011] Breazeal, C. (2011). Social robots for health applications. In *2011 Annual international conference of the IEEE engineering in medicine and biology society*, pages 5368–5371. IEEE.

[Brown, 1912] Brown, T. G. (1912). The factors in rhythmic activity of the nervous system. *Proceedings of the Royal Society of London. Series B, Containing Papers of a Biological Character*, 85(579):278–289.

[Brown, 1914] Brown, T. G. (1914). On the nature of the fundamental activity of the nervous centres; together with an analysis of the conditioning of rhythmic activity in progression, and a theory of the evolution of function in the nervous system. *The Journal of physiology*, 48(1):18–46.

[Bruneau et al., 1992] Bruneau, N., Dourneau, M.-C., Garreau, B., Pourcelot, L., and Lelord, G. (1992). Blood flow response to auditory stimulations in normal, mentally retarded, and autistic children: a preliminary transcranial doppler ultrasonographic study of the middle cerebral arteries. *Biological psychiatry*, 32(8):691–699.

[Bruninks, 1978] Bruninks, R. (1978). Bruninks oseretsky test of motor proficiency: Examiners manual. *Minnesota: American Guidance Service*.

[Buchli et al., 2006] Buchli, J., Iida, F., and Ijspeert, A. J. (2006). Finding resonance: Adaptive frequency oscillators for dynamic legged locomotion. In *Intelligent robots and systems, 2006 ieee/rsj international conference on*, pages 3903–3909. IEEE.

[Buchli and Ijspeert, 2008] Buchli, J. and Ijspeert, A. J. (2008). Self-organized adaptive legged locomotion in a compliant quadruped robot. *Autonomous Robots*, 25(4):331.

[Buchli et al., 2005] Buchli, J., Righetti, L., and Ijspeert, A. J. (2005). A dynamical systems approach to learning: a frequency-adaptive hopper robot. In *European Conference on Artificial Life*, pages 210–220. Springer.

[Bugnariu et al., 2013] Bugnariu, N., Young, C., Rockenbach, K., Patterson, R. M., Garver, C., Ranatunga, I., Beltran, M., Torres-Arenas, N., and Popa, D. (2013). Human-robot interaction as a tool to evaluate and quantify motor imitation behavior in children with autism spectrum disorders. In *2013 International Conference on Virtual Rehabilitation (ICVR)*, pages 57–62. IEEE.

[Bullock and Grossberg, 1988] Bullock, D. and Grossberg, S. (1988). The vite model: a neural command circuit for generating arm and articulator trajectories. *Dynamic patterns in complex systems*, pages 305–326.

[Caldwell, 1996] Caldwell, P. (1996). *Getting in touch: Ways of working with people with severe learning disabilities and extensive support needs*. Pavilion.

[Cao et al., 2018] Cao, Z., Hidalgo, G., Simon, T., Wei, S.-E., and Sheikh, Y. (2018). Openpose: realtime multi-person 2d pose estimation using part affinity fields. *arXiv preprint arXiv:1812.08008*.

[Cao et al., 2017] Cao, Z., Simon, T., Wei, S.-E., and Sheikh, Y. (2017). Realtime multi-person 2d pose estimation using part affinity fields. In *Proceedings of the IEEE Conference on Computer Vision and Pattern Recognition*, pages 7291–7299.

[Carmo et al., 2013] Carmo, J. C., Rumiati, R. I., Siugzdaite, R., and Brambilla, P. (2013). Preserved imitation of known gestures in children with high-functioning autism. *ISRN neurology*, 2013.

[Carpenter and Call, 2002] Carpenter, M. and Call, J. (2002). The chemistry of social learning. *Developmental Science*, 5(1):22–24.

[Carper et al., 2015] Carper, R. A., Solders, S. K., Treiber, J., Fishman, I., and Müller, R. A. (2015). Corticospinal tract anatomy and functional connectivity of primary motor cortex in autism. *Journal of the American Academy of Child and Adolescent Psychiatry*, 54 10:859–67.

[Cattaert and Le Ray, 2001] Cattaert, D. and Le Ray, D. (2001). Adaptive motor control in crayfish. *Progress in neurobiology*, 63(2):199–240.

[Cerliani et al., 2015] Cerliani, L., Mennes, M., Thomas, R. M., Di Martino, A., Thioux, M., and Keysers, C. (2015). Increased functional connectivity between subcortical and cortical resting-state networks in autism spectrum disorder. *JAMA psychiatry*, 72(8):767–777.

[Chaminade et al., 2005] Chaminade, T., Franklin, D. W., Oztop, E., and Cheng, G. (2005). Motor interference between humans and humanoid robots: Effect of biological and artificial motion. In *Proceedings. The 4th International Conference on Development and Learning, 2005*, pages 96–101. IEEE.

[Chartrand and Bargh, 1999] Chartrand, T. L. and Bargh, J. A. (1999). The chameleon effect: the perception–behavior link and social interaction. *Journal of personality and social psychology*, 76(6):893.

[Chen et al., 2018] Chen, Y.-T., Tsou, K.-S., Chen, H.-L., Wong, C.-C., Fan, Y.-T., and Wu, C.-T. (2018). Functional but inefficient kinesthetic motor imagery in adolescents with autism spectrum disorder. *Journal of autism and developmental disorders*, 48(3):784–795.

[Cheney, 1985] Cheney, P. D. (1985). Role of cerebral cortex in voluntary movements: A review. *Physical therapy*, 65(5):624–635.

[Chernova and Veloso, 2007] Chernova, S. and Veloso, M. (2007). Confidence-based policy learning from demonstration using gaussian mixture models. In *Proceedings of the 6th international joint conference on Autonomous agents and multiagent systems*, page 233. ACM.

[Chung and Dorothy, 2010] Chung, S.-J. and Dorothy, M. (2010). Neurobiologically inspired control of engineered flapping flight. *Journal of guidance, control, and dynamics*, 33(2):440–453.

[Cid et al., 2014] Cid, F., Moreno, J., Bustos, P., and Núnez, P. (2014). Muecas: a multi-sensor robotic head for affective human robot interaction and imitation. *Sensors*, 14(5):7711–7737.

[Condon, 1976] Condon, W. S. (1976). An analysis of behavioral organization. *Sign Language Studies*, (13):285–318.

[Conti et al., 2015] Conti, D., Di Nuovo, S., Buono, S., Trubia, G., and Di Nuovo, A. (2015). Use of robotics to stimulate imitation in children with autism spectrum disorder: A pilot study in a clinical setting. In *Robot and Human Interactive Communication (RO-MAN), 2015 24th IEEE International Symposium on*, pages 1–6. IEEE.

[Cornejo et al., 2017] Cornejo, C., Cuadros, Z., Morales, R., and Paredes, J. (2017). Interpersonal coordination: Methods, achievements, and challenges. *Frontiers in psychology*, 8:1685.

[Costa et al., 2015] Costa, S., Lehmann, H., Dautenhahn, K., Robins, B., and Soares, F. (2015). Using a humanoid robot to elicit body awareness and appropriate physical interaction in children with autism. *International journal of social robotics*, 7(2):265–278.

[Costescu et al., 2014] Costescu, C. A., Vanderborght, B., and David, D. O. (2014). The effects of robot-enhanced psychotherapy: A meta-analysis. *Review of General Psychology*, 18(2):127.

[Crick et al., 2006] Crick, C., Munz, M., Nad, T., and Scassellati, B. (2006). Robotic drumming: Synchronization in social tasks. In *IEEE ROMAN*, pages 97–102.

[Cummins et al., 2005] Cummins, A., Piek, J. P., and Dyck, M. J. (2005). Motor coordination, empathy, and social behaviour in school-aged children. *Developmental medicine and child neurology*, 47 7:437–42.

[Curioni et al., 2017] Curioni, A., Minio-Paluello, I., Sacheli, L. M., Candidi, M., and Aglioti, S. M. (2017). Autistic traits affect interpersonal motor coordination by modulating strategic use of role-based behavior. *Molecular Autism*, 8(1):23.

[Dadgar et al., 2017] Dadgar, h., Alaghband Rad, J., Soleymani, Z., Khorammi, A., and Maroufizadeh, S. (2017). Relationship between motor, imitation and, early social communication skills in children with autism. *Iranian Journal of Psychiatry*, 12(4):233–237.

[Dapretto et al., 2006] Dapretto, M., Davies, M. S., Pfeifer, J. H., Scott, A. A., Sigman, M., Bookheimer, S. Y., and Iacoboni, M. (2006). Understanding emotions in others: mirror neuron dysfunction in children with autism spectrum disorders. *Nature neuroscience*, 9(1):28.

[David et al., 2009] David, F. J., Baranek, G. T., Giuliani, C. A., Mercer, V. S., Poe, M. D., and Thorpe, D. E. (2009). A pilot study: Coordination of precision grip in children and adolescents with high functioning autism. *Pediatric Physical Therapy*, 21(2):205–211.

[de Castelnau et al., 2008] de Castelnau, P., Albaret, J.-M., Chaix, Y., and Zanone, P.-G. (2008). A study of eeg coherence in dcd children during motor synchronization task. *Human Movement Science*, 27(2):230–241.

[De Pretto et al., 2018] De Pretto, M., Deiber, M.-P., and James, C. E. (2018). Steady-state evoked potentials distinguish brain mechanisms of self-paced versus synchronization finger tapping. *Human movement science*, 61:151–166.

[de Rugy and Sternad, 2003] de Rugy, A. and Sternad, D. (2003). Interaction between discrete and rhythmic movements: reaction time and phase of discrete movement initiation during oscillatory movements. *Brain Research*, 994(2):160–174.

[de Rugy et al., 2003] de Rugy, A., Wei, K., Müller, H., and Sternad, D. (2003). Actively tracking 'passive'stability in a ball bouncing task. *Brain research*, 982(1):64–78.

[Debnath et al., 2014] Debnath, S., Nassour, J., and Cheng, G. (2014). Learning diverse motor patterns with a single multi-layered multi-pattern cpg for a humanoid robot. In *Humanoid Robots (Humanoids), 2014 14th IEEE-RAS International Conference on*, pages 1016–1021. IEEE.

[Degallier and Ijspeert, 2010] Degallier, S. and Ijspeert, A. (2010). Modeling discrete and rhythmic movements through motor primitives: a review. *Biological cybernetics*, 103(4):319–338.

[Degallier et al., 2011] Degallier, S., Righetti, L., Gay, S., and Ijspeert, A. (2011). Toward simple control for complex, autonomous robotic applications: combining discrete and rhythmic motor primitives. *Autonomous Robots*, 31(2-3):155–181.

[Degallier et al., 2008] Degallier, S., Righetti, L., Natale, L., Nori, F., Metta, G., and Ijspeert, A. (2008). A modular bio-inspired architecture for movement generation for the infant-like robot icub. In *Biomedical Robotics and Biomechatronics, 2008. BioRob 2008. 2nd IEEE RAS & EMBS International Conference on*, pages 795–800. IEEE.

[Degallier et al., 2006] Degallier, S., Santos, C. P., Righetti, L., and Ijspeert, A. (2006). Movement generation using dynamical systems: a humanoid robot performing a drumming task. In *Humanoid Robots, 2006 6th IEEE-RAS International Conference on*, pages 512–517. IEEE.

[Delaherche et al., 2012] Delaherche, E., Chetouani, M., Mahdhaoui, A., Saint-Georges, C., Viaux, S., and Cohen, D. (2012). Interpersonal synchrony: A survey of evaluation methods across disciplines. *IEEE Transactions on Affective Computing*, 3(3):349–365.

[Delaherche et al., 2015] Delaherche, E., Dumas, G., Nadel, J., and Chetouani, M. (2015). Automatic measure of imitation during social interaction: a behavioral and hyperscanning-eeg benchmark. *Pattern Recognition Letters*, 66:118–126.

[Delorme and Makeig, 2004] Delorme, A. and Makeig, S. (2004). Eeglab: an open source toolbox for analysis of single-trial eeg dynamics including independent component analysis. *Journal of neuroscience methods*, 134(1):9–21.

[Demiris and Hayes, 1996] Demiris, J. and Hayes, G. (1996). *Imitative learning mechanisms in robots and humans*. University of Edinburgh, Department of Artificial Intelligence.

[Desideri, 2017] Desideri, L. (2017). Exploring the use of a humanoid robot to engage children with autism spectrum disorder (asd).

[Di Martino et al., 2011] Di Martino, A., Kelly, C., Grzadzinski, R., Zuo, X.-N., Mennes, M., Mairena, M. A., Lord, C., Castellanos, F. X., and Milham, M. P. (2011). Aberrant striatal functional connectivity in children with autism. *Biological psychiatry*, 69(9):847–856.

[Diehl et al., 2012] Diehl, J. J., Schmitt, L. M., Villano, M., and Crowell, C. R. (2012). The clinical use of robots for individuals with autism spectrum disorders: A critical review. *Research in autism spectrum disorders*, 6(1):249–262.

[Dmochowski et al., 2012] Dmochowski, J. P., Sajda, P., Dias, J., and Parra, L. C. (2012). Correlated components of ongoing eeg point to emotionally laden attention–a possible marker of engagement? *Frontiers in human neuroscience*, 6:112.

[Do et al., 2008] Do, M., Azad, P., Asfour, T., and Dillmann, R. (2008). Imitation of human motion on a humanoid robot using non-linear optimization. In *Humanoids 2008-8th IEEE-RAS International Conference on Humanoid Robots*, pages 545–552. IEEE.

[Dufek et al., 2017] Dufek, J. S., Eggleston, J. D., Harry, J. R., and Hickman, R. A. (2017). A comparative evaluation of gait between children with autism and typically developing matched controls. *Medical Sciences*, 5(1).

[Dumas et al., 2012] Dumas, G., Martinerie, J., Soussignan, R., and Nadel, J. (2012). Does the brain know who is at the origin of what in an imitative interaction? *Frontiers in human neuroscience*, 6:128.

[Dumas et al., 2010] Dumas, G., Nadel, J., Soussignan, R., Martinerie, J., and Garnero, L. (2010). Inter-brain synchronization during social interaction. *PloS one*, 5(8):e12166.

[Dunlap, 1910] Dunlap, K. (1910). Reaction to rhythmic stimuli with attempt to synchronize. *Psychological Review*, 17(6):399.

[Dziuk et al., 2007] Dziuk, M., Larson, J. G., Apostu, A., Mahone, E., Denckla, M., and Mostofsky, S. (2007). Dyspraxia in autism: association with motor, social, and communicative deficits. *Developmental Medicine and Child Neurology*, 49(10):734–739.

[Ehrenmann et al., 2001] Ehrenmann, M., Rogalla, O., Zöllner, R., and Dillmann, R. (2001). Teaching service robots complex tasks: Programming by demonstration for workshop and household environments. In *Proceedings of the 2001 International Conference on Field and Service Robots (FSR)*, volume 1, pages 397–402.

[Ellamil et al., 2016] Ellamil, M., Berson, J., and Margulies, D. S. (2016). Influences on and measures of unintentional group synchrony. *Frontiers in psychology*, 7:1744.

[Fang et al., 2013] Fang, F., Xu, W. L., Lin, K., Alam, F., and Potgieter, J. (2013). Matsuoka neuronal oscillator for traffic signal control using agent-based simulation. *Procedia Computer Science*, 19:389–395.

[Fatemi et al., 2002] Fatemi, S. H., Halt, A. R., Realmuto, G., Earle, J., Kist, D. A., Thuras, P., and Merz, A. (2002). Purkinje cell size is reduced in cerebellum of patients with autism. *Cellular and molecular neurobiology*, 22(2):171–175.

[Feil-Seifer and Mataric, 2008] Feil-Seifer, D. and Mataric, M. (2008). Robot-assisted therapy for children with autism spectrum disorders. In *Proceedings of the 7th international conference on Interaction design and children*, pages 49–52. ACM.

[Feldman, 1980] Feldman, A. (1980). Superposition of motor programs—i. rhythmic forearm movements in man. *Neuroscience*, 5(1):81–90.

[Fernández and Cairns, 2017] Fernández, E. M. and Cairns, H. S. (2017). *The Handbook of Psycholinguistics*. John Wiley & Sons.

[Fitzpatrick et al., 2019] Fitzpatrick, P., Mitchell, T., Schmidt, R., Kennedy, D., and Frazier, J. A. (2019). Alpha band signatures of social synchrony. *Neuroscience letters*, 699:24–30.

[Foss-Feig et al., 2012] Foss-Feig, J. H., Heacock, J. L., and Cascio, C. J. (2012). Tactile responsiveness patterns and their association with core features in autism spectrum disorders. *Research in autism spectrum disorders*, 6(1):337–344.

[Fraisse, 1948] Fraisse, P. (1948). Auditory rhythms and visual rhythms. *ANNEE PSYCHOLOGIQUE*, 49:21–42.

[Freeman and Harris, 1992] Freeman, T. C. and Harris, M. G. (1992). Human sensitivity to expanding and rotating motion: effects of complementary masking and directional structure. *Vision research*, 32(1):81–87.

[Fried and Masland, 2007] Fried, S. I. and Masland, R. H. (2007). Image processing: how the retina detects the direction of image motion. *Current Biology*, 17(2):R63–R66.

[Fuente et al., 2013] Fuente, L. A., Lones, M. A., Turner, A. P., Caves, L. S., Stepney, S., and Tyrrell, A. M. (2013). Adaptive robotic gait control using coupled artificial signalling networks, hopf oscillators and inverse kinematics. In *Evolutionary Computation (CEC), 2013 IEEE Congress on*, pages 1435–1442. IEEE.

[Fujimoto et al., 2011] Fujimoto, I., Matsumoto, T., De Silva, P. R. S., Kobayashi, M., and Higashi, M. (2011). Mimicking and evaluating human motion to improve the imitation skill of children with autism through a robot. *International Journal of Social Robotics*, 3(4):349–357.

[Gallese et al., 1996] Gallese, V., Fadiga, L., Fogassi, L., and Rizzolatti, G. (1996). Action recognition in the premotor cortex. *Brain*, 119(2):593–609.

[Gallese et al., 2013] Gallese, V., Rochat, M. J., and Berchio, C. (2013). The mirror mechanism and its potential role in autism spectrum disorder. *Developmental Medicine & Child Neurology*, 55(1):15–22.

[Gams et al., 2009] Gams, A., Ijspeert, A. J., Schaal, S., and Lenarčič, J. (2009). On-line learning and modulation of periodic movements with nonlinear dynamical systems. *Autonomous robots*, 27(1):3–23.

[Gault and Goodfellow, 1938] Gault, R. H. and Goodfellow, L. D. (1938). An empirical comparison of audition, vision, and touch in the discrimination of temporal patterns and ability to reproduce them. *The Journal of General Psychology*, 18(1):41–47.

[Gebhard and Mowbray, 1959] Gebhard, J. and Mowbray, G. (1959). On discriminating the rate of visual flicker and auditory flutter. *The American journal of psychology*, 72(4):521–529.

[Gelb et al., 1999] Gelb, D. J., Oliver, E., and Gilman, S. (1999). Diagnostic criteria for parkinson disease. *Archives of neurology*, 56(1):33–39.

[Gergely et al., 2002] Gergely, G., Bekkering, H., and Király, I. (2002). Developmental psychology: Rational imitation in preverbal infants. *Nature*, 415(6873):755.

[Ghaziuddin and Butler, 1998] Ghaziuddin, M. and Butler, E. (1998). Clumsiness in autism and asperger syndrome: a further report. *Journal of Intellectual Disability Research*, 42(1):43–48.

[Glazebrook et al., 2006] Glazebrook, C. M., Elliott, D., and Lyons, J. (2006). A kinematic analysis of how young adults with and without autism plan and control goal-directed movements. *Motor control*, 10(3):244–264.

[Goldenberg and Hagmann, 1997] Goldenberg, G. and Hagmann, S. (1997). The meaning of meaningless gestures: A study of visuo-imitative apraxia. *Neuropsychologia*, 35(3):333–341.

[Goldfarb, 1956] Goldfarb, W. (1956). Receptor preferences in schizophrenic children. *AMA Archives of Neurology & Psychiatry*, 76(6):643–652.

[Goldfarb, 1963] Goldfarb, W. (1963). Self-awareness in schizophrenic children. *Archives of General Psychiatry*, 8(1):47–60.

[Goldman et al., 2009] Goldman, S., Wang, C., Salgado, M. W., Greene, P. E., Kim, M., and Rapin, I. (2009). Motor stereotypies in children with autism and other developmental disorders. *Developmental Medicine and Child Neurology*, 51(1):30–38.

[Goldstone et al., 1959] Goldstone, S., Boardman, W. K., and Lhamon, W. T. (1959). Intersensory comparisons of temporal judgments. *Journal of Experimental Psychology*, 57(4):243.

[Goldstone and Lhamon, 1974] Goldstone, S. and Lhamon, W. T. (1974). Studies of auditory-visual differences in human time judgment: 1. sounds are judged longer than lights. *Perceptual and motor skills*, 39(1):63–82.

[Goldstone et al., 1978] Goldstone, S., Lhamon, W. T., and Sechzer, J. (1978). Light intensity and judged duration. *Bulletin of the Psychonomic Society*, 12(1):83–84.

[Goodrich et al., 2011] Goodrich, M. A., Colton, M. A., Brinton, B., and Fujiki, M. (2011). A case for low-dose robotics in autism therapy. In *Proceedings of the 6th international conference on Human-robot interaction*, pages 143–144. ACM.

[Gordon and Stark, 2007] Gordon, B. and Stark, S. (2007). Procedural learning of a visual sequence in individuals with autism. *Focus on Autism and Other Developmental Disabilities*, 22(1):14–22.

[Greczek et al., 2014] Greczek, J., Kaszubski, E., Atrash, A., and Matarić, M. (2014). Graded cueing feedback in robot-mediated imitation practice for children with autism spectrum disorders. In *Robot and Human Interactive Communication, 2014 RO-MAN: The 23rd IEEE International Symposium on*, pages 561–566. IEEE.

[Gribovskaya et al., 2011] Gribovskaya, E., Khansari-Zadeh, S. M., and Billard, A. (2011). Learning non-linear multivariate dynamics of motion in robotic manipulators. *The international journal of robotics research*, 30(1):80–117.

[Grillner and Wallen, 1985] Grillner, S. and Wallen, P. (1985). Central pattern generators for locomotion, with special reference to vertebrates. *Annual review of neuroscience*, 8(1):233–261.

[Grinsted et al., 2004] Grinsted, A., Moore, J. C., and Jevrejeva, S. (2004). Application of the cross wavelet transform and wavelet coherence to geophysical time series. *Nonlinear processes in geophysics*, 11(5/6):561–566.

[Grondin et al., 1998] Grondin, S., Meilleur-Wells, G., Ouellette, C., and Macar, F. (1998). Sensory effects on judgments of short time-intervals. *Psychological Research*, 61(4):261–268.

[Guenter et al., 2007] Guenter, F., Hersch, M., Calinon, S., and Billard, A. (2007). Reinforcement learning for imitating constrained reaching movements. *Advanced Robotics*, 21(13):1521–1544.

[Gueugnon et al., 2016] Gueugnon, M., Salesse, R. N., Coste, A., Zhao, Z., Bardy, B. G., and Marin, L. (2016). Postural coordination during socio-motor improvisation. *Frontiers in psychology*, 7:1168.

[Guiard, 1993] Guiard, Y. (1993). On fitts's and hooke's laws: Simple harmonic movement in upper-limb cyclical aiming. *Acta psychologica*, 82(1-3):139–159.

[Guillot et al., 2009] Guillot, A., Collet, C., Nguyen, V. A., Malouin, F., Richards, C., and Doyon, J. (2009). Brain activity during visual versus kinesthetic imagery: an fmri study. *Human brain mapping*, 30(7):2157–2172.

[Haken et al., 1985] Haken, H., Kelso, J. S., and Bunz, H. (1985). A theoretical model of phase transitions in human hand movements. *Biological cybernetics*, 51(5):347–356.

[Hamilton et al., 2007] Hamilton, A. F. d. C., Brindley, R. M., and Frith, U. (2007). Imitation and action understanding in autistic spectrum disorders: how valid is the hypothesis of a deficit in the mirror neuron system? *Neuropsychologia*, 45(8):1859–1868.

[Hammes and Langdell, 1981] Hammes, J. and Langdell, T. (1981). Precursors of symbol formation and childhood autism. *Journal of Autism and Developmental Disorders*, 11(3):331–346.

[Hanaie et al., 2013] Hanaie, R., Mohri, I., Kagitani-Shimono, K., Tachibana, M., Azuma, J., Matsuzaki, J., Watanabe, Y., Fujita, N., and Taniike, M. (2013). Altered microstructural connectivity of the superior cerebellar peduncle is related to motor dysfunction in children with autistic spectrum disorders. *The Cerebellum*, 12(5):645–656.

[Hasnain et al., 2013] Hasnain, S. K., Mostafaoui, G., Salesse, R., Marin, L., and Gaussier, P. (2013). Intuitive human robot interaction based on unintentional synchrony: a psycho-experimental study. In *2013 IEEE Third Joint International Conference on Development and Learning and Epigenetic Robotics (ICDL)*, pages 1–7. IEEE.

[Hayes and Demiris, 1994] Hayes, G. M. and Demiris, J. (1994). *A robot controller using learning by imitation*. University of Edinburgh, Department of Artificial Intelligence.

[He et al., 2006] He, J., Lu, C., and Yin, S. (2006). The design of cpg control module of the bionic mechanical crab. In *Robotics and Biomimetics, 2006. ROBIO'06. IEEE International Conference on*, pages 280–285. IEEE.

[Heerink et al., 2010] Heerink, M., Kröse, B., Evers, V., and Wielinga, B. (2010). Assessing acceptance of assistive social agent technology by older adults: the almere model. *International journal of social robotics*, 2(4):361–375.

[Henderson and Sugden, 1992] Henderson, S. and Sugden, D. (1992). Movement assessment battery for children. *London, The Psychological Corperation Ltd*, 62.

[Hermelin and O'Connor, 1964] Hermelin, B. and O'Connor, N. (1964). Effects of sensory input and sensory dominance on severely disturbed, autistic children and on subnormal controls. *British Journal of Psychology*, 55(2):201–206.

[Hermelin and O'connor, 1970] Hermelin, B. and O'connor, N. (1970). Psychological experiments with autistic children.

[Heyes, 2001] Heyes, C. (2001). Causes and consequences of imitation. *Trends in cognitive sciences*, 5(6):253–261.

[Hickok, 2009] Hickok, G. (2009). Eight problems for the mirror neuron theory of action understanding in monkeys and humans. *Journal of cognitive neuroscience*, 21(7):1229–1243.

[Hickok, 2013] Hickok, G. (2013). Do mirror neurons subserve action understanding? *Neuroscience letters*, 540:56–58.

[Hickok, 2014] Hickok, G. (2014). *The myth of mirror neurons: The real neuroscience of communication and cognition*. WW Norton & Company.

[Hidaka and Ide, 2015] Hidaka, S. and Ide, M. (2015). Sound can suppress visual perception. Technical report, Sci. Rep. 5, 10483.

[Higashionna et al., 2017] Higashionna, T., Iwanaga, R., Tokunaga, A., Nakai, A., Tanaka, K., Nakane, H., and Tanaka, G. (2017). Relationship between motor coordination, cognitive abilities, and academic achievement in japanese children with neurodevelopmental disorders. In *Hong Kong journal of occupational therapy : HKJOT*.

[Hilton et al., 2012] Hilton, C. L., Zhang, Y., Whilte, M. R., Klohr, C. L., and Constantino, J. (2012). Motor impairment in sibling pairs concordant and discordant for autism spectrum disorders. *Autism*, 16(4):430–441. PMID: 22013131.

[Hodgkin and Huxley, 1952] Hodgkin, A. L. and Huxley, A. F. (1952). A quantitative description of membrane current and its application to conduction and excitation in nerve. *The Journal of physiology*, 117(4):500–544.

[Hofree et al., 2014] Hofree, G., Ruvolo, P., Bartlett, M. S., and Winkielman, P. (2014). Bridging the mechanical and the human mind: spontaneous mimicry of a physically present android. *PloS one*, 9(7):e99934.

[Holst, 1935] Holst, E. v. (1935). Die koordination der bewegung bei den arthropoden in abhängigkeit von zentralen und peripheren bedingungen. *Biological Reviews*, 10(2):234–261.

[Hopf, 1942] Hopf, E. (1942). Abzweigung einer periodischen lösung von einer stationären lösung eines differentialsystems. *Ber. Math.-Phys. Kl Sächs. Akad. Wiss. Leipzig*, 94:1–22.

[Hsieh and Hung, 1996] Hsieh, G.-C. and Hung, J. C. (1996). Phase-locked loop techniques. a survey. *IEEE Transactions on industrial electronics*, 43(6):609–615.

[Hu et al., 2014] Hu, Y., Liang, J., and Wang, T. (2014). Parameter synthesis of coupled nonlinear oscillators for cpg-based robotic locomotion. *IEEE Transactions on Industrial Electronics*, 61(11):6183–6191.

[Hu et al., 2011] Hu, Y., Tian, W., Liang, J., and Wang, T. (2011). Learning fish-like swimming with a cpg-based locomotion controller. In *Intelligent Robots and Systems (IROS), 2011 IEEE/RSJ International Conference on*, pages 1863–1868. IEEE.

[Iacoboni, 2006] Iacoboni, M. (2006). Visuo-motor integration and control in the human posterior parietal cortex: evidence from tms and fmri. *Neuropsychologia*, 44(13):2691–2699.

[Iacoboni et al., 2005] Iacoboni, M., Molnar-Szakacs, I., Gallese, V., Buccino, G., Mazziotta, J. C., and Rizzolatti, G. (2005). Grasping the intentions of others with one's own mirror neuron system. *PLoS biology*, 3(3):e79.

[Ibrahim and Adiprawita, 2012] Ibrahim, A. R. and Adiprawita, W. (2012). Analytical upper body human motion transfer to naohumanoid robot. *International Journal on Electrical Engineering and Informatics*, 4(4):563.

[Ijspeert, 2008] Ijspeert, A. J. (2008). Central pattern generators for locomotion control in animals and robots: A review. *Neural networks*, 21(4):642–653.

[Ijspeert et al., 2002] Ijspeert, A. J., Nakanishi, J., and Schaal, S. (2002). Learning rhythmic movements by demonstration using nonlinear oscillators. In *Proceedings of the ieee/rsj int. conference on intelligent robots and systems (iros2002)*, number BIOROB-CONF-2002-003, pages 958–963.

[Ijspeert, 2004] Ijspeert, J. (2004). A simple adaptive locomotion toy-system. In *From Animals to Animats 8: Proceedings of the Seventh [ie Eighth] International Conference on Simulation of Adaptive Behavior*, volume 8, page 153. MIT Press.

[Inamura et al., 2006] Inamura, T., Kojo, N., and Inaba, M. (2006). Situation recognition and behavior induction based on geometric symbol representation of multimodal sensorimotor patterns. In *2006 IEEE/RSJ International Conference on Intelligent Robots and Systems*, pages 5147–5152. IEEE.

[Issartel et al., 2007] Issartel, J., Marin, L., and Cadopi, M. (2007). Unintended interpersonal co-ordination:"can we march to the beat of our own drum?". *Neuroscience letters*, 411(3):174–179.

[Iversen et al., 2015] Iversen, J. R., Patel, A. D., Nicodemus, B., and Emmorey, K. (2015). Synchronization to auditory and visual rhythms in hearing and deaf individuals. *Cognition*, 134:232–244.

[Izadi-Najafabadi et al., 2015] Izadi-Najafabadi, S., Mirzakhani-Araghi, N., Miri-Lavasani, N., Nejati, V., and Pashazadeh-Azari, Z. (2015). Implicit and explicit motor learning: Application to children with autism spectrum disorder (asd). *Research in developmental disabilities*, 47:284–296.

[Jamey et al., 2019] Jamey, K., Foster, N. E., Sharda, M., Tuerk, C., Nadig, A., and Hyde, K. L. (2019). Evidence for intact melodic and rhythmic perception in children with autism spectrum disorder. *Research in Autism Spectrum Disorders*, 64:1 – 12.

[Janzen and Thaut, 2018] Janzen, T. B. and Thaut, M. H. (2018). Rethinking the role of music in the neurodevelopment of autism spectrum disorder. *Music & Science*, 1:2059204318769639.

[Jaśkowski et al., 1990] Jaśkowski, P., Jaroszyk, F., and Hojan-Jezierska, D. (1990). Temporal-order judgments and reaction time for stimuli of different modalities. *Psychological Research*, 52(1):35–38.

[Jasmin et al., 2009] Jasmin, E., Couture, M., Mckinley, P. K., Reid, G., Fombonne, E. J., and Gisel, E. (2009). Sensori-motor and daily living skills of preschool children with autism spectrum disorders. *Journal of autism and developmental disorders*, 39 2:231–41.

[Jeka et al., 1993] Jeka, J. J., Kelso, J., and Kiemel, T. (1993). Spontaneous transitions and symmetry: Pattern dynamics in human four-limb coordination. *Human Movement Science*, 12(6):627–651.

[Jones et al., 2018] Jones, C. R., Simonoff, E., Baird, G., Pickles, A., Marsden, A. J., Tregay, J., Happé, F., and Charman, T. (2018). The association between theory of mind, executive function, and the symptoms of autism spectrum disorder. *Autism Research*, 11(1):95–109.

[Jouaiti et al., 2018] Jouaiti, M., Caron, L., and Hénaff, P. (2018). Hebbian plasticity in cpg controllers facilitates self-synchronization for human-robot handshaking. *Frontiers in Neurorobotics*, 12:29.

[Jouaiti and Henaff, 2018a] Jouaiti, M. and Henaff, P. (2018a). Cpg-based controllers can generate both discrete and rhythmic movements. In *2018 IEEE/RSJ International Conference on Intelligent Robots and Systems (IROS)*.

[Jouaiti and Henaff, 2018b] Jouaiti, M. and Henaff, P. (2018b). Cpg-based controllers can trigger the emergence of social synchrony in human-robot interactions. In *2018 IEEE Workshop on Advanced Robotics and its Social Impacts (ARSO)*.

[Jouaiti and Henaff, 2019a] Jouaiti, M. and Henaff, P. (2019a). Comparative study of forced oscillators for the adaptive generation of rhythmic movements in robot controllers. *Biological Cybernetics*, 113(5-6):547–560.

[Jouaiti and Henaff, 2019b] Jouaiti, M. and Henaff, P. (2019b). Motor coordination learning for rhythmic movements. In *2019 Joint IEEE 9th International Conference on Development and Learning and Epigenetic Robotics (ICDL-EpiRob)*, pages 290–295. IEEE.

[Jouaiti and Henaff, 2019c] Jouaiti, M. and Henaff, P. (2019c). Real time movement classification in versatile cpg control. In *Workshop on Robust Artificial Intelligence for Neurorobotics*.

[Jouaiti and Henaff, 2019d] Jouaiti, M. and Henaff, P. (2019d). Robot-based motor rehabilitation in autism: A systematic review. *International Journal of Social Robotics*, 11(5):753–764.

[Jouaiti and Henaff, 2019e] Jouaiti, M. and Henaff, P. (2019e). The sound of actuators: Disturbance in human-robot interactions? *Joint IEEE International Conference on Development and Learning and Epigenetic Robotics (ICDL-EpiRob)*.

[Kamimura et al., 2005] Kamimura, A., Kurokawa, H., Yoshida, E., Murata, S., Tomita, K., and Kokaji, S. (2005). Automatic locomotion design and experiments for a modular robotic system. *IEEE/ASME Transactions on mechatronics*, 10(3):314–325.

[Kasuga and Hashimoto, 2005] Kasuga, T. and Hashimoto, M. (2005). Human-robot handshaking using neural oscillators. In *Robotics and Automation, 2005. ICRA 2005. Proceedings of the 2005 IEEE International Conference on*, pages 3802–3807. IEEE.

[Kauppi et al., 2014] Kauppi, J.-P., Pajula, J., and Tohka, J. (2014). A versatile software package for inter-subject correlation based analyses of fmri. *Frontiers in Neuroinformatics*, 8:2.

[Kaur et al., 2013] Kaur, M., Gifford, T., Marsh, K. L., and Bhat, A. (2013). Effect of robot–child interactions on bilateral coordination skills of typically developing children and a child with autism spectrum disorder: A preliminary study. *Journal of Motor Learning and Development*, 1(2):31–37.

[Kelso, 1984] Kelso, J. (1984). Phase transitions and critical behavior in human bimanual coordination. *American Journal of Physiology-Regulatory, Integrative and Comparative Physiology*, 246(6):R1000–R1004.

[Kelso et al., 1990] Kelso, J., Del Colle, J., and Schöner, G. (1990). Action-perception as a pattern formation process.

[Kilner et al., 2003] Kilner, J. M., Paulignan, Y., and Blakemore, S.-J. (2003). An interference effect of observed biological movement on action. *Current biology*, 13(6):522–525.

[Kim et al., 2009] Kim, C. H., Yonekura, K., Tsujino, H., and Sugano, S. (2009). Physical control of the rotation center of an unsupported object rope turning by a humanoid robot. In *2009 9th IEEE-RAS International Conference on Humanoid Robots*, pages 148–153. IEEE.

[Kober and Peters, 2009] Kober, J. and Peters, J. R. (2009). Policy search for motor primitives in robotics. In *Advances in neural information processing systems*, pages 849–856.

[Koenemann et al., 2014] Koenemann, J., Burget, F., and Bennewitz, M. (2014). Real-time imitation of human whole-body motions by humanoids. In *2014 IEEE International Conference on Robotics and Automation (ICRA)*, pages 2806–2812. IEEE.

[Kohler et al., 2002] Kohler, E., Keysers, C., Umilta, M. A., Fogassi, L., Gallese, V., and Rizzolatti, G. (2002). Hearing sounds, understanding actions: action representation in mirror neurons. *Science*, 297(5582):846–848.

[Kolers and Brewster, 1985] Kolers, P. A. and Brewster, J. M. (1985). Rhythms and responses. *Journal of Experimental Psychology: Human Perception and Performance*, 11(2):150.

[Konvalinka et al., 2011] Konvalinka, I., Xygalatas, D., Bulbulia, J., Schjødt, U., Jegindø, E.-M., Wallot, S., Van Orden, G., and Roepstorff, A. (2011). Synchronized arousal between performers and related spectators in a fire-walking ritual. *Proceedings of the National Academy of Sciences*, 108(20):8514–8519.

[Kopp et al., 2010] Kopp, S., Beckung, E., and Gillberg, C. (2010). Developmental coordination disorder and other motor control problems in girls with autism spectrum disorder and/or attention-deficit/hyperactivity disorder. *Research in developmental disabilities*, 31(2):350–361.

[Kormushev et al., 2010] Kormushev, P., Calinon, S., and Caldwell, D. G. (2010). Robot motor skill coordination with em-based reinforcement learning. In *2010 IEEE/RSJ international conference on intelligent robots and systems*, pages 3232–3237. IEEE.

[Kory-Westlund and Breazeal, 2019] Kory-Westlund, J. M. and Breazeal, C. (2019). Assessing children's perceptions and acceptance of a social robot. In *Proceedings of the 18th ACM International Conference on Interaction Design and Children*, pages 38–50.

[Krakauer and Shadmehr, 2007] Krakauer, J. W. and Shadmehr, R. (2007). Towards a computational neuropsychology of action. *Progress in brain research*, 165:383–394.

[Kupferberg et al., 2011] Kupferberg, A., Glasauer, S., Huber, M., Rickert, M., Knoll, A., and Brandt, T. (2011). Biological movement increases acceptance of humanoid robots as human partners in motor interaction. *AI & society*, 26(4):339–345.

[Kushki et al., 2011] Kushki, A., Chau, T., and Anagnostou, E. (2011). Handwriting difficulties in children with autism spectrum disorders: A scoping review. *Journal of autism and developmental disorders*, 41(12):1706–1716.

[Lachaux et al., 1999] Lachaux, J.-P., Rodriguez, E., Martinerie, J., Varela, F. J., et al. (1999). Measuring phase synchrony in brain signals. *Human brain mapping*, 8(4):194–208.

[LaGasse and Hardy, 2013] LaGasse, A. B. and Hardy, M. W. (2013). Rhythm, movement, and autism: using rhythmic rehabilitation research as a model for autism. *Frontiers in integrative neuroscience*, 7:19.

[Lallemand and Gronier, 2015] Lallemand, C. and Gronier, G. (2015). *Méthodes de design UX: 30 méthodes fondamentales pour concevoir et évaluer les systèmes interactifs*. Editions Eyrolles.

[Larson et al., 2008] Larson, J. C. G., Bastian, A. J., Donchin, O., Shadmehr, R., and Mostofsky, S. H. (2008). Acquisition of internal models of motor tasks in children with autism. *Brain : a journal of neurology*, 131 Pt 11:2894–903.

[Lee et al., 2002] Lee, J., Chai, J., Reitsma, P. S., Hodgins, J. K., and Pollard, N. S. (2002). Interactive control of avatars animated with human motion data. In *ACM Transactions on Graphics (ToG)*, volume 21, pages 491–500. ACM.

[Lee et al., 2014] Lee, J., Obinata, G., and Aoki, H. (2014). A pilot study of using touch sensing and robotic feedback for children with autism. In *Proceedings of the 2014 ACM/IEEE international conference on Human-robot interaction*, pages 222–223. ACM.

[Legare and Nielsen, 2015] Legare, C. H. and Nielsen, M. (2015). Imitation and innovation: The dual engines of cultural learning. *Trends in cognitive sciences*, 19(11):688–699.

[Lhamon and Goldstone, 1974] Lhamon, W. T. and Goldstone, S. (1974). Studies of auditory-visual differences in human time judgment: 2. more transmitted information with sounds than lights. *Perceptual and Motor skills*, 39(1):295–307.

[Li et al., 2013] Li, C., Lowe, R., and Ziemke, T. (2013). Humanoids learning to walk: a natural cpg-actor-critic architecture. *Frontiers in neurorobotics*, 7:5.

[Lin et al., 2019] Lin, C.-W., Lin, H.-Y., Lo, Y.-C., Chen, Y.-J., Hsu, Y.-C., Chen, Y.-L., Tseng, W.-Y. I., and Gau, S. S.-F. (2019). Alterations in white matter microstructure and regional volume are related to motor functions in boys with autism spectrum disorder. *Progress in Neuro-Psychopharmacology and Biological Psychiatry*, 90:76 – 83.

[Liu et al., 2011] Liu, C., Chen, Q., and Wang, D. (2011). Cpg-inspired workspace trajectory generation and adaptive locomotion control for quadruped robots. *IEEE Transactions on Systems, Man, and Cybernetics, Part B (Cybernetics)*, 41(3):867–880.

[Liu et al., 2012] Liu, C., Fan, Z., Seo, K., Tan, X., and Goodman, E. (2012). Synthesis of matsuoka-based neuron oscillator models in locomotion control of robots. In *Intelligent Systems (GCIS), 2012 Third Global Congress on*, pages 342–347. IEEE.

[Liu et al., 2007] Liu, G. L., Habib, M. K., Watanabe, K., and Izumi, K. (2007). The design of central pattern generators based on the matsuoka oscillator to generate rhythmic human-like movement for biped robots. *Journal of Advanced Computational Intelligence and Intelligent Informatics*, 11(8).

[Liu et al., 2008] Liu, G. L., Habib, M. K., Watanabe, K., and Izumi, K. (2008). Central pattern generators based on matsuoka oscillators for the locomotion of biped robots. *Artificial Life and Robotics*, 12(1-2):264–269.

[Liu et al., 2006] Liu, G. L., Watanabe, K., and Izumi, K. (2006). The parameter design of central pattern generators composed of some matsuoka oscillators for the leg movements of human-like robots. In *SCIS & ISIS SCIS & ISIS 2006*, pages 24–29. Japan Society for Fuzzy Theory and Intelligent Informatics.

[Lorenz et al., 2013] Lorenz, T., Mörtl, A., and Hirche, S. (2013). Movement synchronization fails during non-adaptive human-robot interaction. In *Proceedings of the 8th ACM/IEEE international conference on Human-robot interaction*, pages 189–190. IEEE Press.

[Lotto et al., 2009] Lotto, A. J., Hickok, G. S., and Holt, L. L. (2009). Reflections on mirror neurons and speech perception. *Trends in cognitive sciences*, 13(3):110–114.

[Luft et al., 2004] Luft, A. R., McCombe-Waller, S., Whitall, J., Forrester, L. W., Macko, R. F., Sorkin, J. D., Schulz, J. B., Goldberg, A. P., and Hanley, D. F. (2004). Repetitive bilateral arm training and motor cortex activation in chronic stroke: a randomized controlled trial. *Journal of the American Medical Association (JAMA)*, 292 15:1853–61.

[Luo et al., 2013] Luo, R. C., Shih, B.-H., and Lin, T.-W. (2013). Real time human motion imitation of anthropomorphic dual arm robot based on cartesian impedance control. In *2013 IEEE international symposium on robotic and sensors environments (ROSE)*, pages 25–30. IEEE.

[MacDonald et al., 2014] MacDonald, M., Lord, C., and Ulrich, D. A. (2014). Motor skills and calibrated autism severity in young children with autism spectrum disorder. *Adapted physical activity quarterly*, 31(2):95–105.

[Macrae et al., 2008] Macrae, C. N., Duffy, O. K., Miles, L. K., and Lawrence, J. (2008). A case of hand waving: Action synchrony and person perception. *Cognition*, 109(1):152–156.

[Maeda et al., 2001] Maeda, Y., Takahashi, A., Hara, T., and Arai, T. (2001). Human-robot cooperation with mechanical interaction based on rhythm entrainment-realization of cooperative rope turning. In *Robotics and Automation, 2001. Proceedings 2001 ICRA. IEEE International Conference on*, volume 4, pages 3477–3482. IEEE.

[Manoonpong et al., 2008] Manoonpong, P., Pasemann, F., and Wörgötter, F. (2008). Sensor-driven neural control for omnidirectional locomotion and versatile reactive behaviors of walking machines. *Robotics and Autonomous Systems*, 56(3):265–288.

[Manwaring et al., 2017] Manwaring, S. S., Mead, D. L., Swineford, L., and Thurm, A. (2017). Modelling gesture use and early language development in autism spectrum disorder. *International Journal of Language & Communication Disorders*, 52(5):637–651.

[Marder and Bucher, 2001] Marder, E. and Bucher, D. (2001). Central pattern generators and the control of rhythmic movements. *Current biology*, 11(23):R986–R996.

[Marder et al., 2005] Marder, E., Bucher, D., Schulz, D. J., and Taylor, A. L. (2005). Invertebrate central pattern generation moves along. *Current Biology*, 15(17):R685–R699.

[Marin et al., 2009] Marin, L., Issartel, J., and Chaminade, T. (2009). Interpersonal motor coordination: From human–human to human–robot interactions. *Interaction Studies*, 10(3):479–504.

[Martin and Farnum, 2002] Martin, F. and Farnum, J. (2002). Animal-assisted therapy for children with pervasive developmental disorders. *Western journal of nursing research*, 24(6):657–670.

[Martinez et al., 2017] Martinez, J., Hossain, R., Romero, J., and Little, J. J. (2017). A simple yet effective baseline for 3d human pose estimation. In *Proceedings of the IEEE International Conference on Computer Vision*, pages 2640–2649.

[Masterton and Biederman, 1983] Masterton, B. and Biederman, G. (1983). Proprioceptive versus visual control in autistic children. *Journal of Autism and Developmental Disorders*, 13(2):141–152.

[Matos and Santos, 2010] Matos, V. and Santos, C. (2010). Omnidirectional locomotion in a quadruped robot: A cpg-based approach. In *The 2010 IEEE/RSJ International Conference on Intelligent Robots and Systems, IROS 2010*, pages 3392–3397.

[Matsuoka, 1985] Matsuoka, K. (1985). Sustained oscillations generated by mutually inhibiting neurons with adaptation. *Biological cybernetics*, 52(6):367–376.

[Matsuoka, 2011] Matsuoka, K. (2011). Analysis of a neural oscillator. *Biological cybernetics*, 104(4):297–304.

[Meltzoff, 1993] Meltzoff, A. (1993). The role of imitation in understanding persons and developing theory of mind. *Understanding other minds: Perspectives from autism*, pages 335–366.

[Meltzoff, 1988] Meltzoff, A. N. (1988). Infant imitation after a 1-week delay: long-term memory for novel acts and multiple stimuli. *Developmental psychology*, 24(4):470.

[Meltzoff and Prinz, 2002] Meltzoff, A. N. and Prinz, W. (2002). *The imitative mind: Development, evolution and brain bases*, volume 6. Cambridge University Press.

[Meuter et al., 2005] Meuter, M. L., Bitner, M. J., Ostrom, A. L., and Brown, S. W. (2005). Choosing among alternative service delivery modes: An investigation of customer trial of self-service technologies. *Journal of marketing*, 69(2):61–83.

[Michalowski et al., 2007] Michalowski, M. P., Sabanovic, S., and Kozima, H. (2007). A dancing robot for rhythmic social interaction. In *2007 2nd ACM/IEEE International Conference on Human-Robot Interaction (HRI)*, pages 89–96. IEEE.

[Ming et al., 2007] Ming, X., Brimacombe, M., and Wagner, G. C. (2007). Prevalence of motor impairment in autism spectrum disorders. *Brain and Development*, 29(9):565 – 570.

[Miyazaki et al., 2006] Miyazaki, F., Matsushima, M., and Takeuchi, M. (2006). Learning to dynamically manipulate: A table tennis robot controls a ball and rallies with a human being. In *Advances in Robot Control*, pages 317–341. Springer.

[Mizuno et al., 2006] Mizuno, A., Villalobos, M. E., Davies, M. M., Dahl, B. C., and Müller, R.-A. (2006). Partially enhanced thalamocortical functional connectivity in autism. *Brain research*, 1104(1):160–174.

[Molloy et al., 2003] Molloy, C. A., Dietrich, K. N., and Bhattacharya, A. (2003). Postural stability in children with autism spectrum disorder. *Journal of autism and developmental disorders*, 33(6):643–652.

[Monno et al., 2002] Monno, A., Temprado, J.-J., Zanone, P.-G., and Laurent, M. (2002). The interplay of attention and bimanual coordination dynamics. *Acta psychologica*, 110(2-3):187–211.

[Moorthy and Pugazhenthi, 2016] Moorthy, R. S. and Pugazhenthi, S. (2016). Imitation based training to enhance psychomotor skills in autistic children using a snatcher robot. In *Robotics and Automation for Humanitarian Applications (RAHA), 2016 International Conference on*, pages 1–6. IEEE.

[Moorthy et al., 2016] Moorthy, R. S., Vigneshwaran, G., Iyer, A. R., and Pugazhenthi, S. (2016). Mechatronic-shoe kit for training children with asd in enhancement of psychomotor and daily life skills. In *2016 International Conference on Robotics: Current Trends and Future Challenges (RCTFC)*, pages 1–6. IEEE.

[Mori et al., 2004] Mori, T., Nakamura, Y., Sato, M.-A., and Ishii, S. (2004). Reinforcement learning for cpg-driven biped robot. In *AAAI*, volume 4, pages 623–630.

[Mostofsky et al., 2009] Mostofsky, S. H., Powell, S. K., Simmonds, D. J., Goldberg, M. C., Caffo, B., and Pekar, J. J. (2009). Decreased connectivity and cerebellar activity in autism during motor task performance. *Brain*, 132(9):2413–2425.

[Mottet and Bootsma, 1999] Mottet, D. and Bootsma, R. J. (1999). The dynamics of goal-directed rhythmical aiming. *Biological cybernetics*, 80(4):235–245.

[Müller and Lindenberger, 2011] Müller, V. and Lindenberger, U. (2011). Cardiac and respiratory patterns synchronize between persons during choir singing. *PloS one*, 6(9):e24893.

[Mundy and Jarrold, 2010] Mundy, P. and Jarrold, W. (2010). Infant joint attention, neural networks and social cognition. *Neural Networks*, 23(8-9):985–997.

[Myers et al., 1981] Myers, A. K., Cotton, B., and Hilp, H. A. (1981). Matching the rate of concurrent tone bursts and light flashes as a function of flash surround luminance. *Perception & Psychophysics*, 30(1):33–38.

[Nadel, 2005] Nadel, J. (2005). Imitation: does it matter to children with autism. *Imitation and the development of the social mind. New York: Guilford Publications.*

[Nair et al., 2015] Nair, A., Carper, R. A., Abbott, A. E., Chen, C. P., Solders, S., Nakutin, S., Datko, M. C., Fishman, I., and Müller, R.-A. (2015). Regional specificity of aberrant thalamocortical connectivity in autism. *Human Brain Mapping*, 36(11):4497–4511.

[Nair et al., 2013] Nair, A., Treiber, J., Shukla, D. K., Shih, P., and Müller, R.-A. (2013). Impaired thalamocortical connectivity in autism spectrum disorder: a study of functional and anatomical connectivity. *Brain : a journal of neurology*, 136 Pt 6:1942–55.

[Nassour et al., 2014] Nassour, J., Hénaff, P., Benouezdou, F., and Cheng, G. (2014). Multi-layered multi-pattern cpg for adaptive locomotion of humanoid robots, biological cybernetics. *Biological cybernetics*, 108(3):291–303.

[Nassour et al., 2019] Nassour, J., Hoa, T. D., Atoofi, P., and Hamker, F. (2019). Concrete action representation model: from neuroscience to robotics. *IEEE Transactions on Cognitive and Developmental Systems.*

[Nazarali et al., 2009] Nazarali, N., Glazebrook, C. M., and Elliott, D. (2009). Movement planning and reprogramming in individuals with autism. *Journal of Autism and Developmental Disorders*, 39(10):1401–1411.

[Nehaniv and Dautenhahn, 2001] Nehaniv, C. L. and Dautenhahn, K. (2001). Like me?-measures of correspondence and imitation. *Cybernetics & Systems*, 32(1-2):11–51.

[Nehaniv et al., 2002] Nehaniv, C. L., Dautenhahn, K., et al. (2002). The correspondence problem. *Imitation in animals and artifacts*, 41.

[Nemeth et al., 2010] Nemeth, D., Janacsek, K., Balogh, V., Londe, Z., Mingesz, R., Fazekas, M., Jambori, S., Danyi, I., and Vetro, A. (2010). Learning in autism: implicitly superb. *PloS one*, 5(7):e11731.

[Nessler and Gilliland, 2009] Nessler, J. A. and Gilliland, S. J. (2009). Interpersonal synchronization during side by side treadmill walking is influenced by leg length differential and altered sensory feedback. *Human movement science*, 28(6):772–785.

[Nishitani et al., 2004] Nishitani, N., Avikainen, S., and Hari, R. (2004). Abnormal imitation-related cortical activation sequences in asperger's syndrome. *Annals of neurology*, 55(4):558–562.

[Nomura et al., 2004] Nomura, T., Suzuki, T., Kanda, T., and Kato, K. (2004). The relationship between the attitude toward robots and the response for robot. *The Japanese Journal of Psychology*.

[Oberman and Ramachandran, 2007] Oberman, L. M. and Ramachandran, V. S. (2007). The simulating social mind: the role of the mirror neuron system and simulation in the social and communicative deficits of autism spectrum disorders. *Psychological bulletin*, 133(2):310.

[O'Connor, 1971] O'Connor, N. (1971). Visual perception in autistic children. *Infantile autism: Concepts, characteristics and treatment. London: Churchill Livingstone*.

[O'Connor and Hermelin, 1965] O'Connor, N. and Hermelin, B. (1965). Sensory dominance: In autistic imbecile children and controls. *Archives of General Psychiatry*, 12(1):99–103.

[Ogawa et al., 1982] Ogawa, T., Sugiyama, A., Ishiwa, S., Suzuki, M., Ishihara, T., and Sato, K. (1982). Ontogenic development of eeg-asymmetry in early infantile autism. *Brain and Development*, 4(6):439–449.

[Okada et al., 2002] Okada, M., Tatani, K., and Nakamura, Y. (2002). Polynomial design of the nonlinear dynamics for the brain-like information processing of whole body motion. In *Proceedings 2002 IEEE International Conference on Robotics and Automation (Cat. No. 02CH37292)*, volume 2, pages 1410–1415. IEEE.

[Oldehinkel et al., 2018] Oldehinkel, M., Mennes, M., Marquand, A., Charman, T., Tillmann, J., Ecker, C., Dell'Acqua, F., Brandeis, D., Banaschewski, T., Baumeister, S., Moessnang, C., Baron-Cohen, S., Holt, R., Bölte, S., Durston, S., Kundu, P., Lombardo, M. V., Spooren, W., Loth, E., Murphy, D. G., Beckmann, C. F., Buitelaar, J. K., Ahmad, J., Ambrosino, S., Auyeung, B., Banaschewski, T., Baron-Cohen, S., Baumeister, S., Beckmann, C. F., Bölte, S., Bourgeron, T., Bours, C., Brammer, M., Brandeis, D., Brogna, C., de Bruijn, Y., Buitelaar, J. K., Chakrabarti, B., Charman, T., Cornelissen, I., Crawley, D., Dell'Acqua, F., Dumas, G., Durston, S., Ecker, C., Faulkner, J., Frouin, V., Garcés, P., Goyard, D., Ham, L., Hayward,

H., Hipp, J., Holt, R., Johnson, M. H., Jones, E. J., Kundu, P., Lai, M.-C., D'ardhuy, X. L., Lombardo, M. V., Loth, E., Lythgoe, D. J., Mandl, R., Marquand, A., Mason, L., Mennes, M., Meyer-Lindenberg, A., Moessnang, C., Mueller, N., Murphy, D. G., Oakley, B., O'Dwyer, L., Oldehinkel, M., Oranje, B., Pandina, G., Persico, A. M., Ruggeri, B., Ruigrok, A., Sabet, J., Sacco, R., Cáceres, A. S. J., Simonoff, E., Spooren, W., Tillmann, J., Toro, R., Tost, H., Waldman, J., Williams, S. C., Wooldridge, C., and Zwiers, M. P. (2018). Altered connectivity between cerebellum, visual, and sensory-motor networks in autism spectrum disorder: Results from the eu-aims longitudinal european autism project. *Biological Psychiatry: Cognitive Neuroscience and Neuroimaging*.

[Ornitz and Ritvo, 1968a] Ornitz, E. M. and Ritvo, E. R. (1968a). Neurophysiologic mechanisms underlying perceptual inconstancy in autistic and schizophrenic children. *Archives of General Psychiatry*, 19(1):22–27.

[Ornitz and Ritvo, 1968b] Ornitz, E. M. and Ritvo, E. R. (1968b). Perceptual inconstancy in early infantile autism: The syndrome of early infant autism and its variants including certain cases of childhood schizophrenia. *Archives of general psychiatry*, 18(1):76–98.

[Ott et al., 2008] Ott, C., Lee, D., and Nakamura, Y. (2008). Motion capture based human motion recognition and imitation by direct marker control. In *Humanoids 2008-8th IEEE-RAS International Conference on Humanoid Robots*, pages 399–405. IEEE.

[Oztop et al., 2005] Oztop, E., Franklin, D. W., Chaminade, T., and Cheng, G. (2005). Human–humanoid interaction: is a humanoid robot perceived as a human? *International Journal of Humanoid Robotics*, 2(04):537–559.

[Palsbo and Hood-Szivek, 2012] Palsbo, S. E. and Hood-Szivek, P. (2012). Effect of robotic-assisted three-dimensional repetitive motion to improve hand motor function and control in children with handwriting deficits: a nonrandomized phase 2 device trial. *American Journal of Occupational Therapy*, 66(6):682–690.

[Pandey and Gelin, 2018] Pandey, A. K. and Gelin, R. (2018). A mass-produced sociable humanoid robot: pepper: the first machine of its kind. *IEEE Robotics & Automation Magazine*, 25(3):40–48.

[Panwart and Kumar, 2012] Panwart, V. and Kumar, R. (2012). Stable biped locomotion using central pattern generators based on matsuoka neural oscillators.

[Paraschos et al., 2013] Paraschos, A., Daniel, C., Peters, J. R., and Neumann, G. (2013). Probabilistic movement primitives. In *Advances in neural information processing systems*, pages 2616–2624.

[Pascolo et al., 2009] Pascolo, P., Ragogna, P., and Rossi, R. (2009). The mirror-neuron system paradigm and its consistency. *Gait & posture*, (30):S65.

[Passingham, 1985] Passingham, R. (1985). Premotor cortex: sensory cues and movement. *Behavioural brain research*, 18(2):175–185.

[Paxton and Dale, 2017] Paxton, A. and Dale, R. (2017). Interpersonal movement synchrony responds to high-and low-level conversational constraints. *Frontiers in psychology*, 8:1135.

[Pelc et al., 2008] Pelc, E. H., Daley, M. A., and Ferris, D. P. (2008). Resonant hopping of a robot controlled by an artificial neural oscillator. *Bioinspiration & biomimetics*, 3(2):026001.

[Peña de Moraes et al., 2017] Peña de Moraes, Í. A., Massetti, T., Brusque Crocetta, T., Dias da Silva, T., Del Ciello de Menezes, L., Bandeira de Mello Monteiro, C., and Magalhães, F. H. (2017). Motor learning characterization in people with autism spectrum disorder. *Dementia and Neuropsychologia*, 11(3).

[Perry et al., 2010] Perry, A., Troje, N. F., and Bentin, S. (2010). Exploring motor system contributions to the perception of social information: Evidence from eeg activity in the mu/alpha frequency range. *Social neuroscience*, 5(3):272–284.

[Petrič et al., 2011] Petrič, T., Gams, A., Ijspeert, A. J., and Žlajpah, L. (2011). On-line frequency adaptation and movement imitation for rhythmic robotic tasks. *The International Journal of Robotics Research*, 30(14):1775–1788.

[Pierno et al., 2008] Pierno, A. C., Mari, M., Lusher, D., and Castiello, U. (2008). Robotic movement elicits visuomotor priming in children with autism. *Neuropsychologia*, 46(2):448–454.

[Pinto et al., 2012] Pinto, C. M., Rocha, D., and Santos, C. P. (2012). Hexapod robots: new cpg model for generation of trajectories. *J. Numer. Anal. Ind. Appl. Math*, 7(1-2):15–26.

[Poggi, 2007] Poggi, I. (2007). *Mind, hands, face and body: a goal and belief view of multimodal communication*. Weidler.

[Pollard et al., 2002] Pollard, N. S., Hodgins, J. K., Riley, M. J., and Atkeson, C. G. (2002). Adapting human motion for the control of a humanoid robot. In *Proceedings 2002 IEEE international conference on robotics and automation (Cat. No. 02CH37292)*, volume 2, pages 1390–1397. IEEE.

[Pomplun and Mataric, 2000] Pomplun, M. and Mataric, M. J. (2000). Evaluation metrics and results of human arm movement imitation. In *Proceedings, First IEEE-RAS International Conference on Humanoid Robotics (Humanoids-2000)*, pages 7–8.

[Pongas et al., 2005] Pongas, D., Billard, A., and Schaal, S. (2005). Rapid synchronization and accurate phase-locking of rhythmic motor primitives. In *Intelligent Robots and Systems, 2005.(IROS 2005). 2005 IEEE/RSJ International Conference on*, pages 2911–2916. IEEE.

[Pope et al., 1995] Pope, A. T., Bogart, E. H., and Bartolome, D. S. (1995). Biocybernetic system evaluates indices of operator engagement in automated task. *Biological psychology*, 40(1-2):187–195.

[Posner et al., 1976] Posner, M. I., Nissen, M. J., and Klein, R. M. (1976). Visual dominance: an information-processing account of its origins and significance. *Psychological review*, 83(2):157.

[Press et al., 2010] Press, C., Richardson, D., and Bird, G. (2010). Intact imitation of emotional facial actions in autism spectrum conditions. *Neuropsychologia*, 48(11):3291–3297.

[Provost et al., 2007] Provost, B., Lopez, B. R., and Heimerl, S. (2007). A comparison of motor delays in young children: autism spectrum disorder, developmental delay, and developmental concerns. *Journal of autism and developmental disorders*, 37(2):321–328.

[Purpura et al., 2016] Purpura, G., Fulceri, F., Puglisi, V., Masoni, P., and Contaldo, A. (2016). Motor coordination impairment in children with autism spectrum disorder: a pilot study using movement assessment battery for children-2 checklist. *Minerva Pediatrica*.

[Purves et al., 2001] Purves, D., Augustine, G. J., Fitzpatrick, D., Hall, W., LaMantia, A.-S., McNamara, J. O., and White, L. (2001). *Neuroscience - Chapter 16, Lower Motor Neuron Circuits and Motor Control*. Sunderland.

[Raub, 1981] Raub, A. C. (1981). Correlates of computer anxiety in college students.

[Redefer and Goodman, 1989] Redefer, L. A. and Goodman, J. F. (1989). Brief report: Pet-facilitated therapy with autistic children. *Journal of autism and developmental disorders*, 19(3):461–467.

[Renard et al., 2010] Renard, Y., Lotte, F., Gibert, G., Congedo, M., Maby, E., Delannoy, V., Bertrand, O., and Lécuyer, A. (2010). Openvibe: An open-source software platform to design, test, and use brain–computer interfaces in real and virtual environments. *Presence: teleoperators and virtual environments*, 19(1):35–53.

[Renshaw, 1930] Renshaw, S. (1930). The errors of cutaneous localization and the effect of practice on the localizing movement in children and adults. *The Pedagogical Seminary and Journal of Genetic Psychology*, 38(1-4):223–238.

[Repp and Penel, 2002] Repp, B. H. and Penel, A. (2002). Auditory dominance in temporal processing: new evidence from synchronization with simultaneous visual and auditory sequences. *Journal of Experimental Psychology: Human Perception and Performance*, 28(5):1085.

[Richardson and Dale, 2005] Richardson, D. C. and Dale, R. (2005). Looking to understand: The coupling between speakers' and listeners' eye movements and its relationship to discourse comprehension. *Cognitive science*, 29(6):1045–1060.

[Riek et al., 2010] Riek, L. D., Paul, P. C., and Robinson, P. (2010). When my robot smiles at me: Enabling human-robot rapport via real-time head gesture mimicry. *Journal on Multimodal User Interfaces*, 3(1-2):99–108.

[Righetti et al., 2006] Righetti, L., Buchli, J., and Ijspeert, A. J. (2006). Dynamic hebbian learning in adaptive frequency oscillators. *Physica D: Nonlinear Phenomena*, 216(2):269–281.

[Righetti and Ijspeert, 2006] Righetti, L. and Ijspeert, A. J. (2006). Programmable central pattern generators: an application to biped locomotion control. In *Robotics and Automation, 2006. ICRA 2006. Proceedings 2006 IEEE International Conference on*, pages 1585–1590. IEEE.

[Righetti and Ijspeert, 2008] Righetti, L. and Ijspeert, A. J. (2008). Pattern generators with sensory feedback for the control of quadruped locomotion. In *Robotics and Automation, 2008. ICRA 2008. IEEE International Conference on*, pages 819–824. IEEE.

[Rinehart et al., 2006a] Rinehart, N. J., Tonge, B. J., Bradshaw, J. L., Iansek, R., Enticott, P. G., and McGinley, J. (2006a). Gait function in high-functioning autism and asperger's disorder. *European child & adolescent psychiatry*, 15(5):256–264.

[Rinehart et al., 2006b] Rinehart, N. J., Tonge, B. J., Iansek, R., McGinley, J., Brereton, A. V., Enticott, P. G., and Bradshaw, J. L. (2006b). Gait function in newly diagnosed children with autism: cerebellar and basal ganglia related motor disorder. *Developmental medicine and child neurology*, 48(10):819–824.

[Riquelme et al., 2016] Riquelme, I., Hatem, S., and Montoya, P. (2016). Abnormal pressure pain, touch sensitivity, proprioception, and manual dexterity in children with autism spectrum disorders. *Neural Plasticity*, 2016(1723401):1–9.

[Risko and Kingstone, 2011] Risko, E. F. and Kingstone, A. (2011). Eyes wide shut: implied social presence, eye tracking and attention. *Attention, Perception, & Psychophysics*, 73(2):291–296.

[Ritvo et al., 1986] Ritvo, E. R., Freeman, B., Scheibel, A. B., Duong, T., Robinson, H., Guthrie, D., and Ritvo, A. (1986). Lower purkinje cell counts in the cerebella of four autistic subjects: Initial findings of the ucla-nsac research report. *The American journal of psychiatry*.

[Rizzolatti and Craighero, 2004] Rizzolatti, G. and Craighero, L. (2004). The mirror-neuron system. *Annu. Rev. Neurosci.*, 27:169–192.

[Rizzolatti et al., 1996] Rizzolatti, G., Fadiga, L., Gallese, V., and Fogassi, L. (1996). Premotor cortex and the recognition of motor actions. *Cognitive brain research*, 3(2):131–141.

[Robins and Dautenhahn, 2014] Robins, B. and Dautenhahn, K. (2014). Tactile interactions with a humanoid robot: novel play scenario implementations with children with autism. *International journal of social robotics*, 6(3):397–415.

[Robins et al., 2005a] Robins, B., Dautenhahn, K., and Dubowski, J. (2005a). Robots as isolators or mediators for children with autism a cautionary tale. In *Procs of the AISB 05 Symposium on Robot Companions*. AISB.

[Robins et al., 2005b] Robins, B., Dautenhahn, K., Te Boekhorst, R., and Billard, A. (2005b). Robotic assistants in therapy and education of children with autism: can a small humanoid robot help encourage social interaction skills? *Universal Access in the Information Society*, 4(2):105–120.

[Rodgers et al., 2019] Rodgers, R. A., Travers, B. G., and Mason, A. H. (2019). Bimanual reach to grasp movements in youth with and without autism spectrum disorder. *Frontiers in Psychology*, 9:2720.

[Rogers, 1999] Rogers, S. J. (1999). An examination of the imitation deficit in autism.

[Rogers and Pennington, 1991] Rogers, S. J. and Pennington, B. F. (1991). A theoretical approach to the deficits in infantile autism. *Development and psychopathology*, 3(2):137–162.

[Rogers et al., 2010] Rogers, S. J., Young, G. S., Cook, I., Giolzetti, A., and Ozonoff, S. (2010). Imitating actions on objects in early-onset and regressive autism: Effects and implications of task characteristics on performance. *Development and Psychopathology*, 22(1):71–85.

[Romero et al., 2016] Romero, V., Fitzpatrick, P., Schmidt, R., and Richardson, M. J. (2016). Using cross-recurrence quantification analysis to understand social motor coordination in children with autism spectrum disorder. In *Recurrence Plots and Their Quantifications: Expanding Horizons*, pages 227–240. Springer.

[Ronsse et al., 2010] Ronsse, R., Vitiello, N., Lenzi, T., Van Den Kieboom, J., Carrozza, M. C., and Ijspeert, A. J. (2010). Human–robot synchrony: flexible assistance using adaptive oscillators. *IEEE Transactions on Biomedical Engineering*, 58(4):1001–1012.

[Rosenblum et al., 1996] Rosenblum, M. G., Pikovsky, A. S., and Kurths, J. (1996). Phase synchronization of chaotic oscillators. *Physical review letters*, 76(11):1804.

[Rowat and Selverston, 1993] Rowat, P. F. and Selverston, A. I. (1993). Modeling the gastric mill central pattern generator of the lobster with a relaxation-oscillator network. *Journal of neurophysiology*, 70(3):1030–1053.

[Rybak et al., 2006] Rybak, I. A., Shevtsova, N. A., Lafreniere-Roula, M., and McCrea, D. A. (2006). Modelling spinal circuitry involved in locomotor pattern generation: insights from deletions during fictive locomotion. *The Journal of physiology*, 577(2):617–639.

[Sacrey et al., 2014] Sacrey, L.-A., Germani, T., Bryson, S., and Zwaigenbaum, L. (2014). Reaching and grasping in autism spectrum disorder: A review of recent literature. *Frontiers in Neurology*, 5:6.

[Salowitz et al., 2013] Salowitz, N. M., Eccarius, P., Karst, J., Carson, A., Schohl, K., Stevens, S., Van Hecke, A. V., and Scheidt, R. A. (2013). Brief report: visuo-spatial guidance of movement during gesture imitation and mirror drawing in children with autism spectrum disorders. *Journal of autism and developmental disorders*, 43(4):985–995.

[Sato et al., 2007] Sato, T., Hashimoto, M., and Tsukahara, M. (2007). Synchronization based control using online design of dynamics and its application to human-robot interaction. In *2007 IEEE International Conference on Robotics and Biomimetics (ROBIO)*, pages 652–657. IEEE.

[Saunders et al., 2006] Saunders, J., Nehaniv, C. L., and Dautenhahn, K. (2006). Teaching robots by moulding behavior and scaffolding the environment. In *Proceedings of the 1st ACM SIGCHI/SIGART conference on Human-robot interaction*, pages 118–125. ACM.

[Schaal, 2006] Schaal, S. (2006). Dynamic movement primitives-a framework for motor control in humans and humanoid robotics. In *Adaptive motion of animals and machines*, pages 261–280. Springer.

[Schaal et al., 2003] Schaal, S., Peters, J., Nakanishi, J., and Ijspeert, A. (2003). Control, planning, learning, and imitation with dynamic movement primitives. In *Workshop on bilateral paradigms on humans and humanoids, IEEE International Conference on Intelligent Robots and Systems*, pages 1–21.

[Schaal et al., 2004] Schaal, S., Sternad, D., Osu, R., and Kawato, M. (2004). Rhythmic arm movement is not discrete. *Nature neuroscience*, 7(10):1136.

[Schipul et al., 2011] Schipul, S. E., Keller, T. A., and Just, M. A. (2011). Inter-regional brain communication and its disturbance in autism. In *Frontiers in Systems Neuroscience*.

[Schmidt et al., 1990] Schmidt, R. C., Carello, C., and Turvey, M. T. (1990). Phase transitions and critical fluctuations in the visual coordination of rhythmic movements between people. *Journal of experimental psychology: human perception and performance*, 16(2):227.

[Schöner et al., 1986] Schöner, G., Haken, H., and Kelso, J. (1986). A stochastic theory of phase transitions in human hand movement. *Biological cybernetics*, 53(4):247–257.

[Schopler, 1965] Schopler, E. (1965). Early infantile autism and receptor processes. *Archives of General Psychiatry*, 13(4):327–335.

[Schopler, 1966] Schopler, E. (1966). Visual versus tactual receptor preference in normal and schizophrenic children. *Journal of Abnormal Psychology*, 71(2):108.

[Schopler, 2005] Schopler, E. (2005). *Psychoeducational Profile: PEP-3; TEACCH Individualized Psychoeducational Assessment for Children with Autism Spectrum Disorders*. Pro-ed.

[Selverston, 2005] Selverston, A. I. (2005). A neural infrastructure for rhythmic motor patterns. *Cellular and molecular neurobiology*, 25(2):223–244.

[Seo et al., 2010] Seo, K., Chung, S.-J., and Slotine, J.-J. E. (2010). Cpg-based control of a turtle-like underwater vehicle. *Autonomous Robots*, 28(3):247–269.

[Shan and Nagashima, 2002] Shan, J. and Nagashima, F. (2002). Neural locomotion controller design and implementation for humanoid robot hoap-1. In *20th annual conference of the robotics society of Japan*.

[Shipley, 1964] Shipley, T. (1964). Auditory flutter-driving of visual flicker. *Science*, 145(3638):1328–1330.

[Shockley et al., 2002] Shockley, K., Butwill, M., Zbilut, J. P., and Webber Jr, C. L. (2002). Cross recurrence quantification of coupled oscillators. *Physics Letters A*, 305(1-2):59–69.

[Sidner et al., 2005] Sidner, C. L., Lee, C., Kidd, C. D., Lesh, N., and Rich, C. (2005). Explorations in engagement for humans and robots. *Artificial Intelligence*, 166(1-2):140–164.

[Silva et al., 2018] Silva, K., Lima, M., Santos-Magalhaes, A., Fafiães, C., and de Sousa, L. (2018). Can dogs assist children with severe autism spectrum disorder in complying with challenging demands? an exploratory experiment with a live and a robotic dog. *The Journal of Alternative and Complementary Medicine*, 24(3):238–242.

[Sivaswamy et al., 2010] Sivaswamy, L., Kumar, A., Rajan, D., Behen, M., Muzik, O., Chugani, D., and Chugani, H. (2010). A diffusion tensor imaging study of the cerebellar pathways in children with autism spectrum disorder. *Journal of Child Neurology*, 25(10):1223–1231. PMID: 20179000.

[So et al., 2019] So, W.-C., Wong, M. K.-Y., Lam, W.-Y., Cheng, C.-H., Ku, S.-Y., Lam, K.-Y., Huang, Y., and Wong, W.-L. (2019). Who is a better teacher for children with autism? comparison of learning outcomes between robot-based and human-based interventions in gestural production and recognition. *Research in developmental disabilities*, 86:62–75.

[So et al., 2018] So, W.-C., Wong, M. K.-Y., Lam, W.-Y., Cheng, C.-H., Yang, J.-H., Huang, Y., Ng, P., Wong, W.-L., Ho, C.-L., Yeung, K.-L., et al. (2018). Robot-based intervention may reduce delay in the production of intransitive gestures in chinese-speaking preschoolers with autism spectrum disorder. *Molecular autism*, 9(1):34.

[Southgate and Hamilton, 2008] Southgate, V. and Hamilton, A. F. d. C. (2008). Unbroken mirrors: Challenging a theory of autism. *Trends in cognitive sciences*, 12(6):225–229.

[Sowden et al., 2016] Sowden, S., Koehne, S., Catmur, C., Dziobek, I., and Bird, G. (2016). Intact automatic imitation and typical spatial compatibility in autism spectrum disorder: Challenging the broken mirror theory. *Autism Research*, 9(2):292–300.

[Sprowitz et al., 2010] Sprowitz, A., Pouya, S., Bonardi, S., Van Den Kieboom, J., Mockel, R., Billard, A., Dillenbourg, P., and Ijspeert, A. J. (2010). Roombots: reconfigurable robots for adaptive furniture. *IEEE Computational Intelligence Magazine*, 5(3):20–32.

[Srinivasan et al., 2015] Srinivasan, S. M., Kaur, M., Park, I. K., Gifford, T. D., Marsh, K. L., and Bhat, A. N. (2015). The effects of rhythm and robotic interventions on the imitation/praxis, interpersonal synchrony, and motor performance of children with autism spectrum disorder (asd): a pilot randomized controlled trial. *Autism research and treatment*, 2015.

[Srinivasan et al., 2013] Srinivasan, S. M., Lynch, K. A., Bubela, D. J., Gifford, T. D., and Bhat, A. N. (2013). Effect of interactions between a child and a robot on the imitation and praxis performance of typically devloping children and a child with autism: A preliminary study. *Perceptual and Motor Skills*, 116(3):885–904.

[Stanton et al., 2012] Stanton, C., Bogdanovych, A., and Ratanasena, E. (2012). Teleoperation of a humanoid robot using full-body motion capture, example movements, and machine learning. In *Proc. Australasian Conference on Robotics and Automation*.

[Sternad, 2008] Sternad, D. (2008). Towards a unified theory of rhythmic and discrete movements—behavioral, modeling and imaging results. In *Coordination: Neural, behavioral and social dynamics*, pages 105–133. Springer.

[Sternad et al., 2000] Sternad, D., Dean, W. J., and Schaal, S. (2000). Interaction of rhythmic and discrete pattern generators in single-joint movements. *Human Movement Science*, 19(4):627–664.

[Stoit et al., 2013] Stoit, A. M., van Schie, H. T., Slaats-Willemse, D. I., and Buitelaar, J. K. (2013). Grasping motor impairments in autism: not action planning but movement execution is deficient. *Journal of autism and developmental disorders*, 43(12):2793–2806.

[Suleiman et al., 2008] Suleiman, W., Yoshida, E., Kanehiro, F., Laumond, J.-P., and Monin, A. (2008). On human motion imitation by humanoid robot. In *2008 IEEE International Conference on Robotics and Automation*, pages 2697–2704. IEEE.

[Suteerawattananon et al., 2004] Suteerawattananon, M., Morris, G., Etnyre, B., Jankovic, J., and Protas, E. (2004). Effects of visual and auditory cues on gait in individuals with parkinson's disease. *Journal of the neurological sciences*, 219(1-2):63–69.

[Taga, 1995] Taga, G. (1995). A model of the neuro-musculo-skeletal system for human locomotion. *Biological cybernetics*, 73(2):97–111.

[Taga et al., 1991] Taga, G., Yamaguchi, Y., and Shimizu, H. (1991). Self-organized control of bipedal locomotion by neural oscillators in unpredictable environment. *Biological cybernetics*, 65(3):147–159.

[Tagne et al., 2016] Tagne, G., Hénaff, P., and Gregori, N. (2016). Measurement and analysis of physical parameters of the handshake between two persons according to simple social contexts. In *Intelligent Robots and Systems (IROS), 2016 IEEE/RSJ International Conference on*, pages 674–679.

[Taheri et al., 2015] Taheri, A., Alemi, M., Meghdari, A., Pouretemad, H., and Holderread, S. (2015). Clinical application of humanoid robots in playing imitation games for autistic children in iran. *Procedia-Social and Behavioral Sciences*, 176:898–906.

[Tapus et al., 2012] Tapus, A., Peca, A., Aly, A., Pop, C., Jisa, L., Pintea, S., Rusu, A. S., and David, D. O. (2012). Children with autism social engagement in interaction with nao, an imitative robot: A series of single case experiments. *Interaction studies*, 13(3):315–347.

[Thach et al., 1992] Thach, W. T., Goodkin, H., and Keating, J. (1992). The cerebellum and the adaptive coordination of movement. *Annual review of neuroscience*, 15(1):403–442.

[Thaut et al., 1999] Thaut, M. H., Kenyon, G. P., Schauer, M. L., and McIntosh, G. C. (1999). The connection between rhythmicity and brain function. *IEEE Engineering in Medicine and Biology Magazine*, 18(2):101–108.

[Thompson, 2011] Thompson, C. J. (2011). Multi-sensory intervention observational research. *International Journal of Special Education*, 26(1):202–214.

[Thorpe, 1956] Thorpe, W. H. (1956). Learning and instinct in animals.

[Tognoli, 2008] Tognoli, E. (2008). Eeg coordination dynamics: neuromarkers of social coordination. In *Coordination: Neural, behavioral and social dynamics*, pages 309–323. Springer.

[Tognoli et al., 2007] Tognoli, E., Lagarde, J., DeGuzman, G. C., and Kelso, J. S. (2007). The phi complex as a neuromarker of human social coordination. *Proceedings of the National Academy of Sciences*, 104(19):8190–8195.

[Tomasello, 1999] Tomasello, M. (1999). The human adaptation for culture. *Annual review of anthropology*, 28(1):509–529.

[Traynor et al., 2018] Traynor, J., Doyle-Thomas, K., Hanford, L., Foster, N., Tryfon, A., Hyde, K., Anagnostou, E., Evans, A., Zwaigenbaum, L., Hall, G., et al. (2018). Indices of repetitive behaviour are correlated with patterns of intrinsic functional connectivity in youth with autism spectrum disorder. *Brain research*, 1685:79–90.

[Treffner and Turvey, 1996] Treffner, P. and Turvey, M. (1996). Symmetry, broken symmetry, and handedness in bimanual coordination dynamics. *Experimental Brain Research*, 107(3):463–478.

[Troje et al., 2006] Troje, N. F., Sadr, J., Geyer, H., and Nakayama, K. (2006). Adaptation aftereffects in the perception of gender from biological motion. *Journal of vision*, 6(8):7–7.

[Tryfon et al., 2017] Tryfon, A., Foster, N. E., Ouimet, T., Doyle-Thomas, K., Anagnostou, E., Sharda, M., and Hyde, K. L. (2017). Auditory-motor rhythm synchronization in children with autism spectrum disorder. *Research in Autism Spectrum Disorders*, 35:51 – 61.

[Turner et al., 2006] Turner, K. C., Frost, L., Linsenbardt, D., McIlroy, J. R., and Müller, R.-A. (2006). Atypically diffuse functional connectivity between caudate nuclei and cerebral cortex in autism. *Behavioral and Brain Functions*, 2(1):34.

[Turner and Desmurget, 2010] Turner, R. S. and Desmurget, M. (2010). Basal ganglia contributions to motor control: a vigorous tutor. *Current opinion in neurobiology*, 20(6):704–716.

[Ubukata et al., 2009] Ubukata, T., Kotosaka, S., and Ohtaki, H. (2009). Trajectory generation for adaptive motion by phase feedback–synchronization of multicycle human movement. *Journal of Robotics and Mechatronics*, 21(3):342.

[Umilta et al., 2001] Umilta, M. A., Kohler, E., Gallese, V., Fogassi, L., Fadiga, L., Keysers, C., and Rizzolatti, G. (2001). I know what you are doing: A neurophysiological study. *Neuron*, 31(1):155–165.

[Valdesolo et al., 2010] Valdesolo, P., Ouyang, J., and DeSteno, D. (2010). The rhythm of joint action: Synchrony promotes cooperative ability. *Journal of Experimental Social Psychology*, 46(4):693–695.

[Vanvuchelen et al., 2011] Vanvuchelen, M., Roeyers, H., and De Weerdt, W. (2011). Do imitation problems reflect a core characteristic in autism? evidence from a literature review. *Research in Autism Spectrum Disorders*, 5(1):89–95.

[Varni et al., 2008] Varni, G., Camurri, A., Coletta, P., and Volpe, G. (2008). Emotional entrainment in music performance. In *2008 8th IEEE International Conference on Automatic Face & Gesture Recognition*, pages 1–5. IEEE.

[Varni et al., 2009] Varni, G., Camurri, A., Coletta, P., and Volpe, G. (2009). Toward a real-time automated measure of empathy and dominance. In *2009 International Conference on Computational Science and Engineering*, volume 4, pages 843–848. IEEE.

[Vernazza-Martin et al., 2005] Vernazza-Martin, S., Martin, N., Vernazza, A., Lepellec-Muller, A., Rufo, M., Massion, J., and Assaiante, C. (2005). Goal directed locomotion and balance control in autistic children. *Journal of autism and developmental disorders*, 35(1):91–102.

[Villalobos et al., 2005] Villalobos, M. E., Mizuno, A., Dahl, B. C., Kemmotsu, N., and Müller, R.-A. (2005). Reduced functional connectivity between v1 and inferior frontal cortex associated with visuomotor performance in autism. *Neuroimage*, 25(3):916–925.

[Vivanti et al., 2011] Vivanti, G., McCormick, C., Young, G. S., Abucayan, F., Hatt, N., Nadig, A., Ozonoff, S., and Rogers, S. J. (2011). Intact and impaired mechanisms of action understanding in autism. *Developmental psychology*, 47(3):841.

[Vivanti et al., 2014] Vivanti, G., Trembath, D., and Dissanayake, C. (2014). Mechanisms of imitation impairment in autism spectrum disorder. *Journal of Abnormal Child Psychology*, 42(8):1395–1405.

[Von Holst, 1973] Von Holst, E. (1973). *The behavioural physiology of animals and man: the collected papers of Erich von Holst*, volume 1. University of Miami Press.

[Vroomen and Gelder, 2000] Vroomen, J. and Gelder, B. d. (2000). Sound enhances visual perception: cross-modal effects of auditory organization on vision. *Journal of experimental psychology: Human perception and performance*, 26(5):1583.

[Wainer et al., 2014] Wainer, J., Robins, B., Amirabdollahian, F., and Dautenhahn, K. (2014). Using the humanoid robot kaspar to autonomously play triadic games and facilitate collaborative play among children with autism. *IEEE Transactions on Autonomous Mental Development*, 6(3):183–199.

[Walker and Scott, 1981] Walker, J. T. and Scott, K. J. (1981). Auditory–visual conflicts in the perceived duration of lights, tones, and gaps. *Journal of Experimental Psychology: Human Perception and Performance*, 7(6):1327.

[Wang et al., 2013] Wang, T., Hu, Y., and Liang, J. (2013). Learning to swim: a dynamical systems approach to mimicking fish swimming with cpg. *Robotica*, 31(3):361–369.

[Watson, 1989] Watson, L. R. (1989). *Teaching spontaneous communication to autistic and developmentally handicapped children*. Pro-Ed.

[Webber Jr and Zbilut, 1994] Webber Jr, C. L. and Zbilut, J. P. (1994). Dynamical assessment of physiological systems and states using recurrence plot strategies. *Journal of applied physiology*, 76(2):965–973.

[Welch, 1999] Welch, R. B. (1999). Meaning, attention, and the "unity assumption" in the intersensory bias of spatial and temporal perceptions. In *Advances in psychology*, volume 129, pages 371–387. Elsevier.

[Whiten, 2017] Whiten, A. (2017). Social learning and culture in child and chimpanzee. *Annual Review of Psychology*, 68:129–154.

[Williams et al., 1980] Williams, R. S., Hauser, S. L., Purpura, D. P., DeLong, G. R., and Swisher, C. N. (1980). Autism and mental retardation: neuropathologic studies performed in four retarded persons with autistic behavior. *Archives of neurology*, 37(12):749–753.

[Williamson, 1998a] Williamson, M. M. (1998a). Neural control of rhythmic arm movements. *Neural networks*, 11(7-8):1379–1394.

[Williamson, 1998b] Williamson, M. M. (1998b). Rhythmic robot arm control using oscillators. In *Intelligent Robots and Systems, 1998. Proceedings., 1998 IEEE/RSJ International Conference on*, volume 1, pages 77–83. IEEE.

[Wu and Ma, 2010] Wu, X. and Ma, S. (2010). Adaptive creeping locomotion of a cpg-controlled snake-like robot to environment change. *Autonomous Robots*, 28(3):283–294.

[Xavier et al., 2015] Xavier, J., Bursztejn, C., Stiskin, M., Canitano, R., and Cohen, D. (2015). Autism spectrum disorders: An historical synthesis and a multidimensional assessment toward a tailored therapeutic program. *Research in Autism Spectrum Disorders*, 18:21–33.

[Xavier et al., 2018] Xavier, J., Gauthier, S., Cohen, D., Zahoui, M., Chetouani, M., Villa, F., Berthoz, A., and Anzalone, S. (2018). Interpersonal synchronization, motor coordination, and control are impaired during a dynamic imitation task in children with autism spectrum disorder. *Frontiers in Psychology*, 9:1467.

[Xu et al., 2009] Xu, W., Fang, F. C., Bronlund, J., and Potgieter, J. (2009). Generation of rhythmic and voluntary patterns of mastication using matsuoka oscillator for a humanoid chewing robot. *Mechatronics*, 19(2):205–217.

[Yang et al., 2010] Yang, W., Bae, J.-H., Oh, Y., Chong, N. Y., You, B.-J., and Oh, S.-R. (2010). Cpg based self-adapting multi-dof robotic arm control. In *Intelligent Robots and Systems (IROS), 2010 IEEE/RSJ International Conference on*, pages 4236–4243. IEEE.

[Yazdani et al., 2017] Yazdani, M., Salarieh, H., and Foumani, M. S. (2017). Decentralized control of rhythmic activities in fully–actuated/under–actuated robots. *Robotics and Autonomous Systems*.

[Yonekura et al., 2012] Yonekura, K., Kim, C. H., Nakadai, K., Tsujino, H., and Sugano, S. (2012). A role of multi-modal rhythms in physical interaction and cooperation. *EURASIP Journal on Audio, Speech, and Music Processing*, 2012(1):12.

[Yoo and Kim, 2018] Yoo, G. E. and Kim, S. J. (2018). Dyadic drum playing and social skills: Implications for rhythm-mediated intervention for children with autism spectrum disorder. *Journal of music therapy*, 55(3):340–375.

[Yu et al., 2014] Yu, J., Tan, M., Chen, J., and Zhang, J. (2014). A survey on cpg-inspired control models and system implementation. *IEEE Transactions on neural networks and learning systems*, 25(3):441–456.

[Zanone and Kostrubiec, 2004] Zanone, P.-G. and Kostrubiec, V. (2004). Searching for (dynamic) principles of learning. In *Coordination dynamics: Issues and trends*, pages 57–89. Springer.

[Zaporozhets, 1961] Zaporozhets, A. (1961). The origin and development of the conscious control of movements in man. In *Recent Soviet psychology.* Liveright New York.

[Zehr et al., 2004] Zehr, E. P., Carroll, T. J., Chua, R., Collins, D. F., Frigon, A., Haridas, C., Hundza, S. R., and Thompson, A. K. (2004). Possible contributions of cpg activity to the control of rhythmic human arm movement. *Canadian journal of physiology and pharmacology*, 82(8-9):556–568.

[Zhang and Hashimoto, 2009] Zhang, X. and Hashimoto, M. (2009). Sbc for motion assist using neural oscillator. In *2009 IEEE International Conference on Robotics and Automation*, pages 659–664. IEEE.

[Zheng et al., 2016] Zheng, Z., Young, E. M., Swanson, A. R., Weitlauf, A. S., Warren, Z. E., and Sarkar, N. (2016). Robot-mediated imitation skill training for children with autism. *IEEE Transactions on Neural Systems and Rehabilitation Engineering*, 24(6):682–691.

[Zhou and Low, 2012] Zhou, C. and Low, K. (2012). Design and locomotion control of a biomimetic underwater vehicle with fin propulsion. *IEEE/ASME Transactions on Mechatronics*, 17(1):25–35.

Résumé

La communication gestuelle est un aspect important de l'interaction humain-robot pour la robotique sociale, d'assistance et de réhabilitation. En effet, la synchronie sociale est un élément clé des interactions interpersonnelles, aussi bien sur le plan comportemental que sur le plan social. Il est essentiel pour les robots d'être capables de s'adapter à leur partenaire d'interaction. Dans les interactions sociales rythmiques, les humains sont soumis à deux phénomènes physiques qui peuvent également être observés dans les oscillateurs: l'effet *magnet* qui entraîne les deux systèmes jusqu'à ce qu'ils soient couplés et synchronisés; l'effet *maintenance* qui représente l'effort de chaque système pour conserver sa propre fréquence. Ces mécanismes jouent un rôle fondamental dans les interactions interpersonnelles physiques et sociales.

Afin de reproduire ce comportement, des contrôleurs bio-inspirés dotés de mécanismes de plasticité peuvent être employés. Le but principal consiste à rendre ces interactions aussi naturelles et agréables que possible en intégrant des propriétés adaptatives, ce qui mène à l'émergence d'une coordination motrice et par conséquent d'une synchronie sociale. Une partie non négligeable du travail de recherche consiste à étudier l'humain dans les interactions humain-robot pour comprendre le comportement humain et donc mieux penser les interactions.

La première partie de cette thèse focalisera sur l'interaction humain-robot avec et sans contact. Nous introduirons plusieurs études d'interaction humain-robot où nous observerons le comportement humain lors d'une interaction rythmique avec un robot.

Dans la seconde partie, nous tenterons de reproduire le comportement humain grâce à un contrôleur bio-inspiré. Nous allons également présenter le contrôleur CPG (Central Pattern Generator). Les CPGs sont des structures biologiques présentes dans la moelle épinière des vertébrés et responsables de la génération de mouvements rythmiques. Ils peuvent générer un mouvement sans aucun signal d'entrée et s'adapter à un signal extérieur. Nous avons également intégré de nouveaux mécanismes de plasticité et présentons les résultats d'une étude comparative avec d'autres modèles d'oscillateurs pour souligner les capacités du modèle.

Dans la troisième partie, nous testons le contrôleur lors d'interactions humain-robot pour évaluer la performance et la perception du contrôleur.

Finalement, la dernière partie dévoilera les applications et perspectives de cette thèse pour la thérapie assistée par robot et plus particulièrement avec des enfants autistes.

Mots-clés: interactions humain-robot, coordination motrice, contrôleur bio-inspiré

Abstract

Gestural communication is an important aspect of HRI in social, assistance and rehabilitation robotics. Indeed, social synchrony is a key component of interpersonal interactions which affects the interaction on the behavioural level, as well as on the social level. It is paramount for the robot to be able to adapt to its interaction partner. In rhythmic social interactions, humans experience two physical phenomena which can also be observed in oscillators: the *magnet* effect which entrains both systems until they are coupled and synchronised; the *maintenance* effect

which is the struggle of each system to conserve its own intrinsic frequency. These mechanisms could play a fundamental role in physical and social interpersonal interactions.

To reproduce this behaviour, bio-inspired controllers endowed with plasticity mechanisms can be employed. The main goal consists in making these interactions as natural and enjoyable as possible by integrating adaptive properties, which leads to the emergence of motor coordination and hence social synchrony. A non-negligible part of this research also consists in studying humans in HRI to understand human behaviour better and design better interactions.

In the first part of this thesis, we will introduce synchrony in interpersonal interactions but also in human-robot interactions. We will also observe and endeavour to understand human behaviour in rhythmic human-robot interactions.

The second part will present the bio-inspired controller. We will integrate some new plasticity mechanisms, develop its discrete functioning mode and extend the model so that it can adapt to any rhythmic or discrete movement. We also analyse the results of a comparison study with other oscillators and controllers to highlight the capabilities of this model. Moreover, we will validate the controller experimentally in two user studies on human-robot interactions with and without contact. This chapter will evaluate several aspects, such as robot power consumption, controller learning rate, human muscular effort, user perception, coordination performance and engagement.

Finally, the third part will focus on the applications and perspectives of this thesis in robot-assisted therapy for children with motor deficits, notably with autistic children.

Keywords: human-robot interactions, motor coordination, bio-inspired controller